

Insect physiology aspects of environmentally friendly strategies for crop pests and invertebrate vectors control, volume II

Edited by

Marcelo Salabert Gonzalez, Norman Arthur Ratcliffe,
Guenter Artur Schaub and Ana Claudia A. Melo

Published in

Frontiers in Physiology



FRONTIERS EBOOK COPYRIGHT STATEMENT

The copyright in the text of individual articles in this ebook is the property of their respective authors or their respective institutions or funders. The copyright in graphics and images within each article may be subject to copyright of other parties. In both cases this is subject to a license granted to Frontiers.

The compilation of articles constituting this ebook is the property of Frontiers.

Each article within this ebook, and the ebook itself, are published under the most recent version of the Creative Commons CC-BY licence. The version current at the date of publication of this ebook is CC-BY 4.0. If the CC-BY licence is updated, the licence granted by Frontiers is automatically updated to the new version.

When exercising any right under the CC-BY licence, Frontiers must be attributed as the original publisher of the article or ebook, as applicable.

Authors have the responsibility of ensuring that any graphics or other materials which are the property of others may be included in the CC-BY licence, but this should be checked before relying on the CC-BY licence to reproduce those materials. Any copyright notices relating to those materials must be complied with.

Copyright and source acknowledgement notices may not be removed and must be displayed in any copy, derivative work or partial copy which includes the elements in question.

All copyright, and all rights therein, are protected by national and international copyright laws. The above represents a summary only. For further information please read Frontiers' Conditions for Website Use and Copyright Statement, and the applicable CC-BY licence.

ISSN 1664-8714
ISBN 978-2-8325-6266-6
DOI 10.3389/978-2-8325-6266-6

About Frontiers

Frontiers is more than just an open access publisher of scholarly articles: it is a pioneering approach to the world of academia, radically improving the way scholarly research is managed. The grand vision of Frontiers is a world where all people have an equal opportunity to seek, share and generate knowledge. Frontiers provides immediate and permanent online open access to all its publications, but this alone is not enough to realize our grand goals.

Frontiers journal series

The Frontiers journal series is a multi-tier and interdisciplinary set of open-access, online journals, promising a paradigm shift from the current review, selection and dissemination processes in academic publishing. All Frontiers journals are driven by researchers for researchers; therefore, they constitute a service to the scholarly community. At the same time, the *Frontiers journal series* operates on a revolutionary invention, the tiered publishing system, initially addressing specific communities of scholars, and gradually climbing up to broader public understanding, thus serving the interests of the lay society, too.

Dedication to quality

Each Frontiers article is a landmark of the highest quality, thanks to genuinely collaborative interactions between authors and review editors, who include some of the world's best academicians. Research must be certified by peers before entering a stream of knowledge that may eventually reach the public - and shape society; therefore, Frontiers only applies the most rigorous and unbiased reviews. Frontiers revolutionizes research publishing by freely delivering the most outstanding research, evaluated with no bias from both the academic and social point of view. By applying the most advanced information technologies, Frontiers is catapulting scholarly publishing into a new generation.

What are Frontiers Research Topics?

Frontiers Research Topics are very popular trademarks of the *Frontiers journals series*: they are collections of at least ten articles, all centered on a particular subject. With their unique mix of varied contributions from Original Research to Review Articles, Frontiers Research Topics unify the most influential researchers, the latest key findings and historical advances in a hot research area.

Find out more on how to host your own Frontiers Research Topic or contribute to one as an author by contacting the Frontiers editorial office: frontiersin.org/about/contact

Insect physiology aspects of environmentally friendly strategies for crop pests and invertebrate vectors control, volume II

Topic editors

Marcelo Salabert Gonzalez — Fluminense Federal University, Brazil
Norman Arthur Ratcliffe — Swansea University, United Kingdom
Guenter Artur Schaub — Ruhr University Bochum, Germany
Ana Claudia A. Melo — Federal University of Rio de Janeiro, Brazil

Citation

Gonzalez, M. S., Ratcliffe, N. A., Schaub, G. A., Melo, A. C. A., eds. (2025). *Insect physiology aspects of environmentally friendly strategies for crop pests and invertebrate vectors control, volume II*. Lausanne: Frontiers Media SA.
doi: 10.3389/978-2-8325-6266-6

Table of contents

- 04 Editorial: Insect physiology aspects of environmentally friendly strategies for crop pests and invertebrate vector control, volume II
Marcelo Salabert Gonzalez, Guenter Artur Schaub, Norman Arthur Ratcliffe and Ana Claudia do Amaral Melo
- 06 Biocontrol efficacy of cajeput oil against *Anopheles stephensi* L. mosquito and its effect on non-target species
Perumal Vivekanandhan, Tahani Awad Alahmadi, Mohammad Javed Ansari and S. P. Subala
- 19 Transgenic line for characterizing GABA-receptor expression to study the neural basis of olfaction in the yellow-fever mosquito
Angela Rouyar, Anandrao A. Patil, Melissa Leon-Noreña, Ming Li, Iliano V. Coutinho-Abreu, Omar S. Akbari and Jeff A. Riffell
- 34 Attractant potential of *Enterobacter cloacae* and its metabolites to *Bactrocera dorsalis* (Hendel)
Yawen Duan, Anjuan Li, Lin Zhang, Chongwen Yin, Zhihong Li and Lijun Liu
- 48 Sugar feeding in triatomines: a new perspective for controlling the transmission of Chagas disease
Mariana C. Costa, Carlos J. C. Moreira, Pedro Lagerblad de Oliveira, José Juberg, Daniele Pereira de Castro and Fernando Ariel Genta
- 61 Erratum: Sugar feeding in triatomines: a new perspective for controlling the transmission of Chagas disease
Frontiers Production Office
- 62 Cry1Ac toxin binding in the velvetbean caterpillar *Anticarsia gemmatilis*: study of midgut aminopeptidases N
M. D. Lanzaro, I. Padilha, L. F. C. Ramos, A. P. G. Mendez, A. Menezes, Y. M. Silva, M. R. Martins, M. Junqueira, F. C. S. Nogueira, C. D. AnoBom, G. M. Dias, F. M. Gomes and D. M. P. Oliveira
- 75 Identification and odor exposure regulation of odorant-binding proteins in *Picromerus lewisi*
Shan-Cheng Yi, Jia-Ling Yu, Sara Taha Abdelkhalek, Zhi-Rong Sun and Man-Qun Wang
- 86 Evaluation of diflubenzuron–verapamil combination strategy for eco-safe management of *Aedes aegypti*
Manu Sankar, Divya Yadav and Sarita Kumar
- 98 Characterization of the ligand-binding properties of odorant-binding protein 38 from *Riptortus pedestris* when interacting with soybean volatiles
Jianglong Guo, Panjing Liu, Xiaofang Zhang, Jingjie An, Yaofa Li, Tao Zhang and Zhanlin Gao
- 110 Endocrine and enzymatic shifts during insect diapause: a review of regulatory mechanisms
Hamzeh Izadi



OPEN ACCESS

EDITED AND REVIEWED BY
Silke Sachse,
Max Planck Institute for Chemical
Ecology, Germany

*CORRESPONDENCE
Ana Claudia do Amaral Melo,
✉ anamelo@iq.ufrj.br

RECEIVED 27 March 2025
ACCEPTED 03 April 2025
PUBLISHED 15 April 2025

CITATION
Gonzalez MS, Schaub GA, Ratcliffe NA and
Melo ACdA (2025) Editorial: Insect physiology
aspects of environmentally friendly strategies
for crop pests and invertebrate vector control,
volume II.
Front. Physiol. 16:1601424.
doi: 10.3389/fphys.2025.1601424

COPYRIGHT
© 2025 Gonzalez, Schaub, Ratcliffe and Melo.
This is an open-access article distributed
under the terms of the [Creative Commons
Attribution License \(CC BY\)](#). The use,
distribution or reproduction in other forums is
permitted, provided the original author(s) and
the copyright owner(s) are credited and that
the original publication in this journal is cited,
in accordance with accepted academic
practice. No use, distribution or reproduction
is permitted which does not comply with
these terms.

Editorial: Insect physiology aspects of environmentally friendly strategies for crop pests and invertebrate vector control, volume II

Marcelo Salabert Gonzalez^{1,2,3,4}, Guenter Artur Schaub⁵,
Norman Arthur Ratcliffe^{3,6} and Ana Claudia do Amaral Melo^{1,7*}

¹National Institute of Science and Technology - Molecular Entomology, Rio de Janeiro, Brazil, ²Department of General Biology, Institute of Biology, Fluminense Federal University, Niterói, Brazil, ³Postgraduate Program in Science and Biotechnology, Fluminense Federal University, Niterói, Brazil, ⁴Postgraduate Program in Applied Physics, Institute of Physics, Federal University of Rio de Janeiro, Rio de Janeiro, Brazil, ⁵Chair of Evolutionary Ecology and Animal Biodiversity, Working Group for Zoology and Parasitology, Ruhr-Universität Bochum, Bochum, Germany, ⁶Department of Biosciences, Swansea University, Swansea, United Kingdom, ⁷Chemistry Institute, Federal University of Rio de Janeiro, Rio de Janeiro, Brazil

KEYWORDS

insect physiology, crop pests, insect vectors, environmentally friendly strategies, insect control

Editorial on the Research Topic

Insect physiology aspects of environmentally friendly strategies for crop pests and invertebrate vector control, volume II

The articles featured in this second volume explore innovative and sustainable strategies for controlling insect pests and disease vectors, drawing on a deep understanding of insect physiology. The studies presented here encompass a wide range of techniques, from the use of natural control agents (biocontrol) to advanced molecular tools aimed at managing insect populations. Each strategy explores aspects of the survival, morphology, behavior, and physiology of the insect models studied, intending to develop environmentally safe solutions that reduce reliance on chemical agents both in agriculture and in the control of disease vectors, thereby minimizing environmental impact.

The study by [Vivekanandhan et al.](#) demonstrates the effectiveness of the natural oil, Cajeput, as a control agent against *Anopheles stephensi*, one of the malaria vectors. The study revealed that Cajeput oil has larvicidal properties, acting by directly inhibiting the carboxylesterase and acetylcholinesterase enzyme systems of *A. stephensi* larvae. Furthermore, the authors demonstrated that there are no significant toxicity risks to non-target species, such as the earthworm *Eudrilus eugeniae*. Based on the results obtained, the authors suggest replacing the widely used chemical agents in malaria mosquito control with essential oils as a correct, natural, and eco-friendly alternative for controlling malaria incidence.

[Costa et al.](#) explore the ability of triatomine bugs, vectors of Chagas disease, to feed on sugar as a potential strategy for controlling transmission. Through artificial feeding experiments, researchers reported the ingestion of sugar solutions in several species of triatomines. They also showed that when first instar nymphs of *Rhodnius prolixus* ingested

different combinations of insecticides with sugar, survival was significantly reduced. This discovery supports the idea of using sugar-based traps combined with chemical agents to reduce triatomine populations and lower Chagas disease transmission.

This second volume also introduces research by Rouyar et al. on the neural mechanisms of olfaction in *Aedes aegypti*, a major vector of arboviruses worldwide. By developing a transgenic strain of *A. aegypti*, the authors investigated the role of GABA-type receptors in odor detection, shedding light on the genetic and neural processes underlying attraction to odors. The observed changes in attractiveness to fruit scents emphasize the importance of the GABA-B1 receptor in mosquito olfaction. These findings could help us create more targeted and effective strategies for mosquito control, making a real difference in managing these vectors.

Another study by Duan et al. featured here examines *Bactrocera dorsalis*, the oriental fruit fly, and the attraction effect of L-prolinamide, a metabolite isolated from *Enterobacter cloacae*, a gut bacterial strain from *B. dorsalis*. In contrast to most of the current attractants, there was no significant difference between the attraction effect of L-prolinamide on male and female adults. The attraction mechanism of *B. dorsalis* to *E. cloacae* and its metabolites provides new prospects for the development of novel green control technologies for this notorious pest.

Guo et al. present details of how *Riptortus pedestris* (Fabricius) (Hemiptera: Alydidae), a major soybean pest throughout East Asia, relies on its advanced odorant-binding proteins (OBPs) to detect plant-derived volatile compounds produced by soybeans. Understanding OBP interactions with specific volatile compounds could lead to new ecologically friendly pest management approaches, disrupting feeding and resulting in more targeted and efficient control methods for crop pests.

Another interesting study by Yi et al. also investigates OBPs, but in *Picromerus lewisi*, a natural predator of agricultural pests. Through transcriptomic analysis, the authors identified 15 OBPs from this species. They also observed sex-dependent differences in gene expression after exposure to odors from *Spodoptera litura*-infested tobacco plants. These results suggest that some OBPs play a pivotal role in detecting herbivore-induced plant volatiles. Based on this, it is possible to develop pest management strategies that attract beneficial predators.

Research by Sankar et al. reports on the combination of diflubenzuron, an insect growth regulator that interferes with chitin synthesis, with verapamil, a calcium channel blocker, in order to control *Aedes aegypti*. The results show that this combination enhances the effectiveness of diflubenzuron by reducing adult emergence while having no harmful effects on non-target organisms. This indicates a safer and more sustainable approach to mosquito population control by developing targeted and eco-friendly strategies for managing *Ae. aegypti* populations more effectively.

Lanzaro et al. present their results of a study on Cry1Ac toxin binding in the velvetbean caterpillar, *Anticarsia gemmatilis*, a soybean pest in Brazil. The study explored the role of midgut aminopeptidases N (APNs) as receptors for Cry1Ac, using immunohistochemistry, ligand blotting, and mass spectrometry to identify seven APNs involved in toxin interaction. The authors propose that these findings contribute to our understanding of Cry toxin mechanisms and resistance management in *A. gemmatilis*, supporting the development of more effective biopesticides.

A comprehensive review is also presented by Izadi of diapause regulation in insects, a key survival mechanism allowing them to endure stressful environmental conditions. Approximately 250 papers were analyzed to consolidate current knowledge on the enzymatic and hormonal regulation of diapause. The review also lays the groundwork for enhancing pest control strategies and ecological conservation by deepening our understanding of diapause mechanisms. By analyzing the hormonal and enzymatic pathways involved in diapause, the study provides valuable knowledge that could pave the way for novel pest control strategies.

The studies presented here reveal the growing body of knowledge related to environment friendly approaches that can be used for pest and vector management. By integrating innovative biocontrol techniques, molecular tools, and the physiological aspects of insect survival, this volume represents a significant step toward more effective and ecologically sound insect control strategies.

Research in the field of entomology and insect physiology must continue to be funded so that we can expand our knowledge and develop more sustainable methodologies for controlling pest insects and disease vectors, aiming to achieve ecological balance and the health of all living beings on Earth.

Author contributions

MG: Writing – review and editing, Writing – original draft. GS: Writing – original draft, Writing – review and editing. NR: Writing – original draft, Writing – review and editing. AM: Writing – original draft, Writing – review and editing.

Funding

The author(s) declare that financial support was received for the research and/or publication of this article. Fundação Carlos Chagas Filho de Amparo à Pesquisa do Estado do Rio de Janeiro, grant No. E-26/211.504/2021.

Conflict of interest

The authors declare that the research was conducted in the absence of any commercial or financial relationships that could be construed as a potential conflict of interest.

Generative AI statement

The author(s) declare that no Generative AI was used in the creation of this manuscript.

Publisher's note

All claims expressed in this article are solely those of the authors and do not necessarily represent those of their affiliated organizations, or those of the publisher, the editors and the reviewers. Any product that may be evaluated in this article, or claim that may be made by its manufacturer, is not guaranteed or endorsed by the publisher.



OPEN ACCESS

EDITED BY

Ana Claudia A. Melo,
Federal University of Rio de Janeiro, Brazil

REVIEWED BY

Nathália F. Brito,
National Cancer Institute (INCA), Brazil
Chandra Kanta Dash,
Sylhet Agricultural University, Bangladesh

*CORRESPONDENCE

Perumal Vivekanandhan,
✉ mosqvk@gmail.com

RECEIVED 18 December 2023

ACCEPTED 19 February 2024

PUBLISHED 01 March 2024

CITATION

Vivekanandhan P, Alahmadi TA, Ansari MJ and Subala SP (2024), Biocontrol efficacy of cajeput oil against *Anopheles stephensi* L. mosquito and its effect on non-target species. *Front. Physiol.* 15:1357411. doi: 10.3389/fphys.2024.1357411

COPYRIGHT

© 2024 Vivekanandhan, Alahmadi, Ansari and Subala. This is an open-access article distributed under the terms of the [Creative Commons Attribution License \(CC BY\)](#). The use, distribution or reproduction in other forums is permitted, provided the original author(s) and the copyright owner(s) are credited and that the original publication in this journal is cited, in accordance with accepted academic practice. No use, distribution or reproduction is permitted which does not comply with these terms.

Biocontrol efficacy of cajeput oil against *Anopheles stephensi* L. mosquito and its effect on non-target species

Perumal Vivekanandhan^{1*}, Tahani Awad Alahmadi²,
Mohammad Javed Ansari³ and S. P. Subala⁴

¹Department of General Pathology, Saveetha Dental College and Hospitals, Saveetha Institute of Medical and Technical Sciences (SIMATS), Saveetha University, Chennai, India, ²Department of Pediatrics, College of Medicine and King Khalid University Hospital, King Saud University, Riyadh, Saudi Arabia, ³Department of Botany, Hindu College Moradabad (Mahatma Jyotiba Phule Rohilkhand University Bareilly), Moradabad, India, ⁴Department of Biotechnology, Ayya Nadar Janaki Ammal College (Autonomous), Sivakasi, India

Chemical insecticides are effective at controlling mosquito populations, but their excessive use can pollute the environment and harm non-target organisms. Mosquitoes can also develop resistance to these chemicals over time, which makes long-term mosquito control efforts challenging. In this study, we assessed the phytochemical, biochemical, and insecticidal properties of the chemical constituents of cajeput oil. Results show that *Melaleuca cajuputi* essential oil may exhibit mosquito larvicidal properties against *Anopheles stephensi* larvae (second-fourth instar) at 24 h post-treatment. At 24 h post-exposure, the essential oil resulted in a significant decrease in detoxifying enzymes. All of these findings indicate that cajeput oil infects *An. stephensi* larvae directly affect the immune system, leading to decreased immune function. Cajeput oil significantly affects the second, third, and fourth instar larvae of *An. stephensi*, according to the bioassay results. Cajeput oil does not induce toxicity in non-target *Eudrilus eugeniae* earthworm species, as indicated by a histological study of earthworms. Phytochemical screening and GC-MS analysis of the essential oil revealed the presence of several major phytochemicals that contribute to mosquito larvicidal activity. The importance of cajeput oil as an effective candidate for biological control of the malarial vector *An. stephensi* is supported by this study.

KEYWORDS

botanical essential oil, *Anopheles stephensi*, *Eudrilus eugeniae*, acetylcholinesterase (AChE), α β -carboxylesterase

Highlights

- *M. cajuputi* essential oil shows high mosquito larvicidal properties against second to fourth instar *An. stephensi* larvae within 24 h post-treatment.
- *M. cajuputi* essential oil resulted in a decrease in larval detoxifying enzymes. All of these findings indicate that cajeput oil infects *An. stephensi* larvae directly affect the immune system, leading to decreased immune function.
- *M. cajuputi* does not cause toxicity in non-target *E. eugeniae* earthworm species, as indicated by a histological study of earthworms.

Introduction

When left uncontrolled, the malarial mosquito, *An. stephensi*, possess a serious threat to human health. This mosquito species is responsible for the spread of parasites that cause malaria in humans (Okoro et al., 2018; Vivekanandhan et al., 2021; Manikandan et al., 2023). Malaria remains a global public health issue, with an estimated 247 million cases and 619,000 deaths worldwide in 2022, primarily affecting children on the African continent. Malaria primarily affects the intertropical region, where climatic and geographical conditions are favorable for the spread of the disease's vector, the female Anopheles species. A variety of chemical insecticide modes of action have been demonstrated to be effective interventions for mosquito population reduction in the field (Manjarres-Suarez and Olivero-Verbel, 2013). However, repeated application of these chemicals may lead to the development of insecticide-resistant mosquito populations, causing product failures and reducing effectiveness (Vivekanandhan et al., 2021). It is critical to develop new alternative methods for reducing mosquito populations, which helps protect human health.

Chemical constituents derived from microbes, plant crude extract and essential oils (EOs) are promising for reducing mosquito populations (Vivekanandhan et al., 2018a; Vivekanandhan et al., 2018b; Vivekanandhan et al., 2018c; Balumahendhiran et al., 2019; Logeswaran et al., 2019; Vivekanandhan et al., 2020a; Vivekanandhan et al., 2020b; Perumal et al., 2023a; Perumal et al., 2023b; Perumal et al., 2023c). In the case of insecticide-resistant mosquitoes, EOs can act as biorational alternatives or synergist additives to existing insecticides. Recent studies have already reported on the insecticidal activities of essential oils (EOs) and their ability to enhance the effectiveness of insecticides (Amer and Mehlhorn, 2006a; Norris et al., 2018; O'Neal et al., 2019). Many species in the Myrtaceae family plants are being studied as potential bioinsecticides (Pratiwi and Nurlaeni, 2021). *Melaleuca leucadendron*, *Melaleuca quinquenervia*, and *M. cajuputi* have been reported as adulticides, repellents, and growth regulators for mosquitoes (Amer and Mehlhorn, 2006b; Noosidum et al., 2008; Bakar et al., 2012; Brophy et al., 2014; Leyva et al., 2016). *M. cajuputi* is a native of Southeast Asia and Australia. In Southeast Asia, it is considered a common household medicine with a few medicinal applications. Now, US Food and Drug Administration (FDA) approved cajuput oil has an edible use because it is non-toxic and non-sensitizing.

Insect acetylcholinesterase (AChE) is an important enzyme in the nervous system that facilitates nerve signal transmission by degrading acetylcholine. Pesticides frequently inhibit AChE activity and cause neurotoxic effects in insects (Vivekanandhan et al., 2022; Perumal et al., 2023a; Perumal et al., 2023b; Perumal et al., 2023c). Understanding AChE offers insights into insecticide mechanisms and aids in the development of pest control strategies. Insect α and β carboxylesterase enzymes play critical roles in the detoxification and metabolism of xenobiotics, especially insecticides. These enzymes are found in the digestive system and other tissues of insects and are used to catalyze the hydrolysis of ester-containing compounds. Insects can break down and eliminate a wide range of exogenous chemicals, including synthetic pesticides. The importance of these enzymes in insecticide resistance mechanisms, where increased expression or mutations in their genes can confer resistance to specific chemical agents. Understanding the biochemical pathways

involving α and β carboxylesterases is critical for developing long-term pest control strategies. Nowadays, Researchers perform AChE enzyme levels in order to decipher the mechanisms used by insects to counteract the effects of insecticides, which will ultimately aid in the design of more effective and environmentally friendly pest control approaches that reduce the risk of resistance development in target insect populations.

E. eugeniae, also known as the African nightcrawler, is a species of earthworm that is widely used in vermicomposting due to its efficient organic matter decomposition. Because of its sensitivity to environmental changes, *E. eugeniae* serves as an ecological indicator (Perumal et al., 2023a; Perumal et al., 2023b). Monitoring *E. eugeniae* populations helps assess soil quality because earthworms play an important role in soil health. Changes in behaviour can indicate ecological shifts, assisting in the assessment of environmental conditions (Vivekanandhan et al., 2023). The aim of this study was to extract essential oil and test the bio-insecticidal activity of cajuput oil against malarial mosquito larvae, *An. stephensi*, using toxicological, biochemical, and non-target species toxicity approaches. These findings shed light on cajuput oil's bio-insecticidal activity against malarial mosquito larvae, *An. stephensi*, and suggest that it could be used as a bioinsecticide to reduce mosquito populations and ultimately, prevent community transmission of mosquito-borne pathogens that cause human disease.

Materials and methods

Plant materials

M. cajuputi leaves (Figure 1) were collected in Tamil Nadu (11° 7' 37.6428" N and 78° 39' 24.8076" E). Plant taxonomists identified the botanical nomenclature of the plant, prepared the herbarium specimen (VK_325), and stored it in the entomological laboratory.

Plant materials preparation and essential oils extraction

Collected leaves of the *M. cajuputi* plant were washed with tap water to remove surface particles and debris before being ground into powder. The essential oil was then extracted using hydrodistillation methods with a modified Clevenger apparatus, as described by Vivekanandhan et al. (2018c). In each instance, 100 g of leaf powder was distilled for 3 h in a 500 mL flask containing 300 mL of distilled water. The essential oil was extracted from the leaves and collected in sterilized glass vials. To remove water traces, anhydrous sodium sulfate was used, and the *M. cajuputi* essential oil samples were stored at 4°C for future experiments.

Mosquito culture

The larvae of *An. stephensi* mosquitoes were obtained from the National Centre for Disease Control (NCDC) in Mettupalayam, Tamil Nadu, India. Mosquito larvae were reared and maintained in a laboratory at a temperature of 27°C \pm 2°C and a humidity of 75%. The larvae were fed a mixture of dog biscuits, millet powder, and

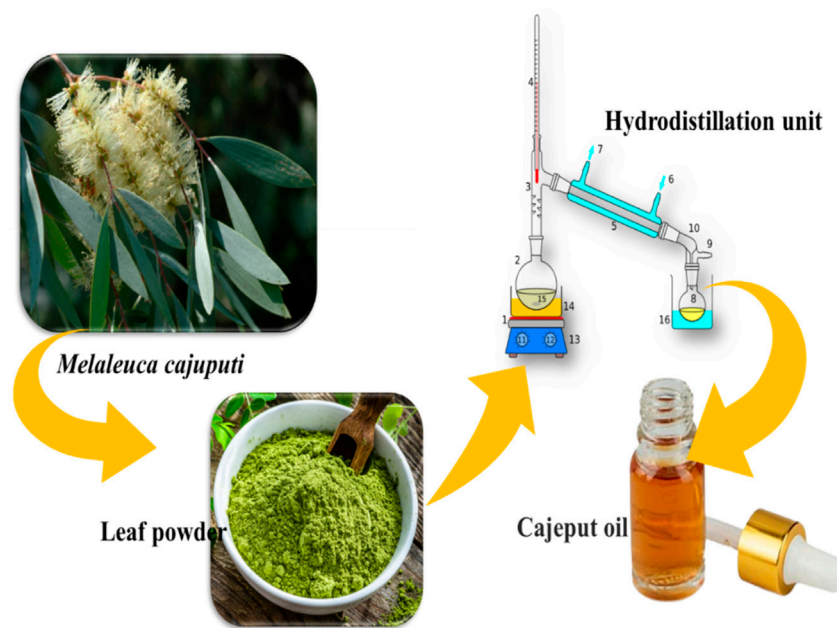


FIGURE 1
The schematic diagram illustrates the process of extracting essential oil from *Melaleuca cajuputi*.

yeast powder in a 3:3:1 ratio, as previously described (Vivekanandhan et al., 2018a).

Larvicidal bioassay

The larvicidal bioassay of *M. cajuputi* essential oils was conducted following the World Health Organization method (WHO, 2005; Pratheeba et al., 2019). About 30 s to fourth instar larvae were individually transferred into bioassay trays containing 249 mL of tap water and 1.0 mL of the specified plant essential oil at various concentrations (30, 50, 100, 150, and 200 ppm/mL) dissolved in 1 mL of 0.5% dimethyl sulfoxide (DMSO). Control groups were treated with DMSO alone. Larval mortality was calculated 24 h after treatment. Each concentration has five replicates, with 30 larvae in each replicate.

Larval enzyme preparation

An. stephensi larvae from both the control group and the group treated with essential oil were selected for studying detoxification enzyme activity 24 h after treatment, specifically in the fourth instar larvae. The larval midgut was dissected, homogenized using 2 mL of phosphate-buffered saline, and then centrifuged at 10,000 rpm for 15 min at 4 °C. The supernatant was then decanted into a clean Eppendorf tube, placed on ice, and used immediately for subsequent enzyme assays.

Acetylcholinesterase assay

Ellman et al. (1961) utilized acetylcholine iodide as a substrate to test the acetylcholinesterase activity of larval homogenate. 50 mL of larval tissues (pH 7.5) were mixed with 850 mL of 100 mM sodium phosphate buffer. Each reaction mixture consisted of 50 mL of 10 mM 5,5'-dithiobis-2-nitrobenzoic acid (DTNB) and 50 mL of 12.5 mM cholinergic iodide, both of which were kept at room temperature for 5 min. The sample's optical density was measured at 405 nm using an appropriate blank and a Multiskan EX (200–240 V) spectrophotometer.

Carboxylesterase assays

Alpha and beta-carboxylesterase enzyme activity was assessed using larval midgut homogenate as described by Van Asperen (1962). 30 mL of homogenate was mixed with 1 mL of sodium phosphate buffer (pH 7.0, 100 mM) containing 250 mM of α - and β -naphthyl acetate and incubated at room temperature for 30 min. To inhibit the enzymatic process, each reaction mixture was treated with 40 mL of 0.3% Fast Blue B in 3.3% sodium dodecyl sulfate (SDS). The mixture was left at room temperature for 15 min to develop its distinct color. The optical density was measured using a Multiskan EX-200–240 V spectrophotometer (Thermo Scientific) and the corresponding reagent or blank. α - and β -carboxylesterase enzyme activities were determined using a standard curve with naphthol as a control.

Earthworm non-target toxicity

E. eugeniae, also known as the “African nightcrawler,” was sustained in the laboratory by using cow dung. Vivekanandhan et al. (2023) cultured earthworms at a constant temperature of $26^{\circ}\text{C} \pm 2^{\circ}\text{C}$. The contact filter paper test involved placing a section of filter paper on a 5-cm petri plate and evaluating different concentrations of essential oils (30, 50, 100, 150, and 200 ppm), as well as monocrotophos (200 ppm; a commercial pesticide) using Sigma-Aldrich Pestanal[®] analytical standard. Earthworms were transferred individually onto the treated paper tissue, which was moistened with 2 mL of sterile distilled water (ddH₂O). The treatments were kept in the dark at $25^{\circ}\text{C} \pm 1^{\circ}\text{C}$ for 24 h, and the mortality rate was assessed. Similarly, artificial soil composed of 16% kaolinite clay, 72% fine sand, and 12% ground sphagnum peat was used in artificial soil tests (ASTs). The tests were then analyzed to determine the mortality rate at different time points, specifically 24 h. The control group of earthworms was administered with PBS saline alone, and the entire treatment was carried out with five replicates.

Gut histochemistry

The study investigated the impact of essential oils on the midgut tissues of earthworms and fourth-instar larvae at sub-lethal doses. Mosquito larvae and earthworm samples from the mid-gut control group and those treated with a sub-lethal dosage (200 ppm) were immobilized overnight in Bouin's chemical reagent. The sectioned blocks were then cooled to approximately $26^{\circ}\text{C} \pm 2^{\circ}\text{C}$ for 2 h before being cut into 1.5 mm portions using a cryo-microtome (Cryocut 1800; Leica, Germany). The entire mid-gut was sectioned for microscopic slides and observed under an Optika Fluo Series HBO (mercury short-arc lamp) light microscope (Murfadunnisa et al., 2019).

Phytochemical screening

Preliminary phytochemical analysis was conducted on essential oils extracted from *M. cajuputi* using methods slightly modified from Satheesh and Wesley, (2012).

Alkaloids

Mayer's/Bertrand's/Valser's test: One mL of essential oil was mixed with 1 mL of con. Add HCL, followed by two to three drops of Mayer's reagent. The presence of alkaloids is indicated by the formation of a creamy white or yellow precipitate (Auwal et al., 2014).

Flavonoid

Lead acetate test: The researchers utilized a colorimetric assay to quantify the overall flavonoid content (Auwal et al., 2014). They added 100 μL of extract to 4 mL of distilled water, followed by the addition of 0.3 mL of 5% sodium nitrite and 0.3 mL of 10% aluminum chloride after 5 min. Then, 2 mL of 1 M sodium hydroxide was added to the mixture after 6 min. The mixture was promptly diluted with 3.3 mL of

distilled water and thoroughly mixed. The absorbance was then measured at 510 nm against a blank using catechin as the standard for the calibration curve.

Phenol

Ferric chloride test: One mL of essential oil was combined with a 5% ferric chloride solution. The presence of phenol is confirmed by the formation of a reddish-brown precipitate (Pandey et al., 2014).

Saponin

Foam test: One mL of essential oils was mixed with 1 mL of distilled water. The solution was then vigorously shaken, and the formation of foam indicated the presence of saponin (Dhawan and Gupta, 2017).

Quinones

Conc. HCl test: One milliliter of essential oils was mixed with 0.5 mL of concentrated hydrochloric acid (HCl). The formation of a yellow precipitate indicates the existence of quinones (Maria et al., 2018).

Tannin

Lead sub acetate test: 3 drops of lead subacetate solution were mixed into 5 mL of plant essential oils dissolved in 45% ethanol. The presence of tannins is demonstrated by the appearance of a creamy, viscous precipitate (Sheel et al., 2014).

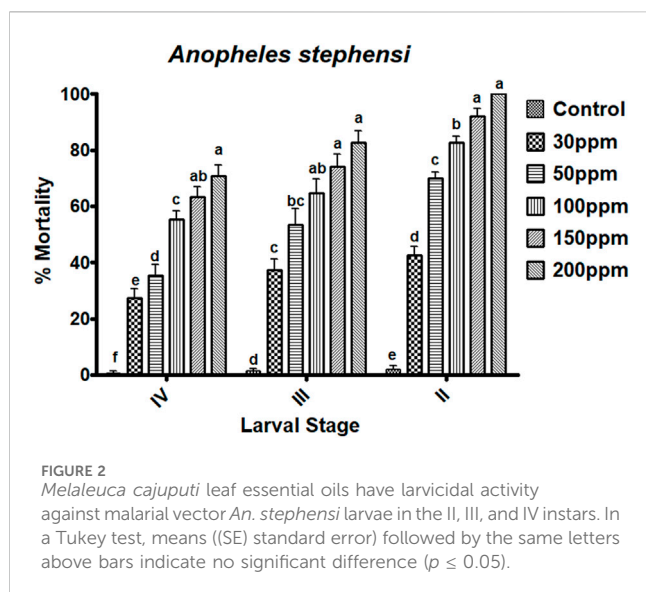
GC–MS analysis

GC-MS analysis was conducted to identify anti-ulcer compounds in the essential oil. For the sample preparation for GC-MS analysis, a 5 MSTG column (30 m \times 0.25 mm, 0.25 μm) and a THERMO TRACE 1300 gas chromatograph-mass spectrometer coupled with the TSQ-8000 mass spectrometer were utilized. As a carrier gas, helium was used at a flow rate of approximately 1 mL/min. The oven's temperature ranged from 60°C to 280°C , increasing at a rate of 10°C per minute. With a splitting ratio of 1:10 and a temperature of 250°C , the injection volume was set to 1.0 L. The mass spectrum was captured for 31 min at an ionizing energy of 70 eV, with the mass spectrometry transfer line temperature maintained at 280°C and the ion source temperature maintained at 230°C , respectively (Geetha et al., 2013).

Results

Larvicidal bioassay

The essential oils of *M. cajuputi* had a dose-dependent mortality rate against all instar stages of *An. stephensi* mosquito larvae



(second-fourth). The mortality percentage of *An. stephensi* was no significant across treatment and control, with the rate of mortality being prominent at the maximum dosage (200 ppm) in the second 100% ($F_{(5,12)} = 304.147$, $p \leq 0.01$), the third 82.66% ($F_{(5,24)} = 45.192$, $p \leq 0.01$), and the fourth instar 70.66% ($F_{(5,24)} = 62.229$, $p \leq 0.01$) (Figure 2; Figure 3). Furthermore, the lethal concentration (LC_{50} and LC_{90}) of essential oils on *An. stephensi* were determined at the

second instar (34.663 and 114.863 ppm/mL), third instar (48.848 and 392.088 ppm/mL), and fourth instar (84.226 and 671.625 ppm/mL) respectively (Figure 2; Figure 3).

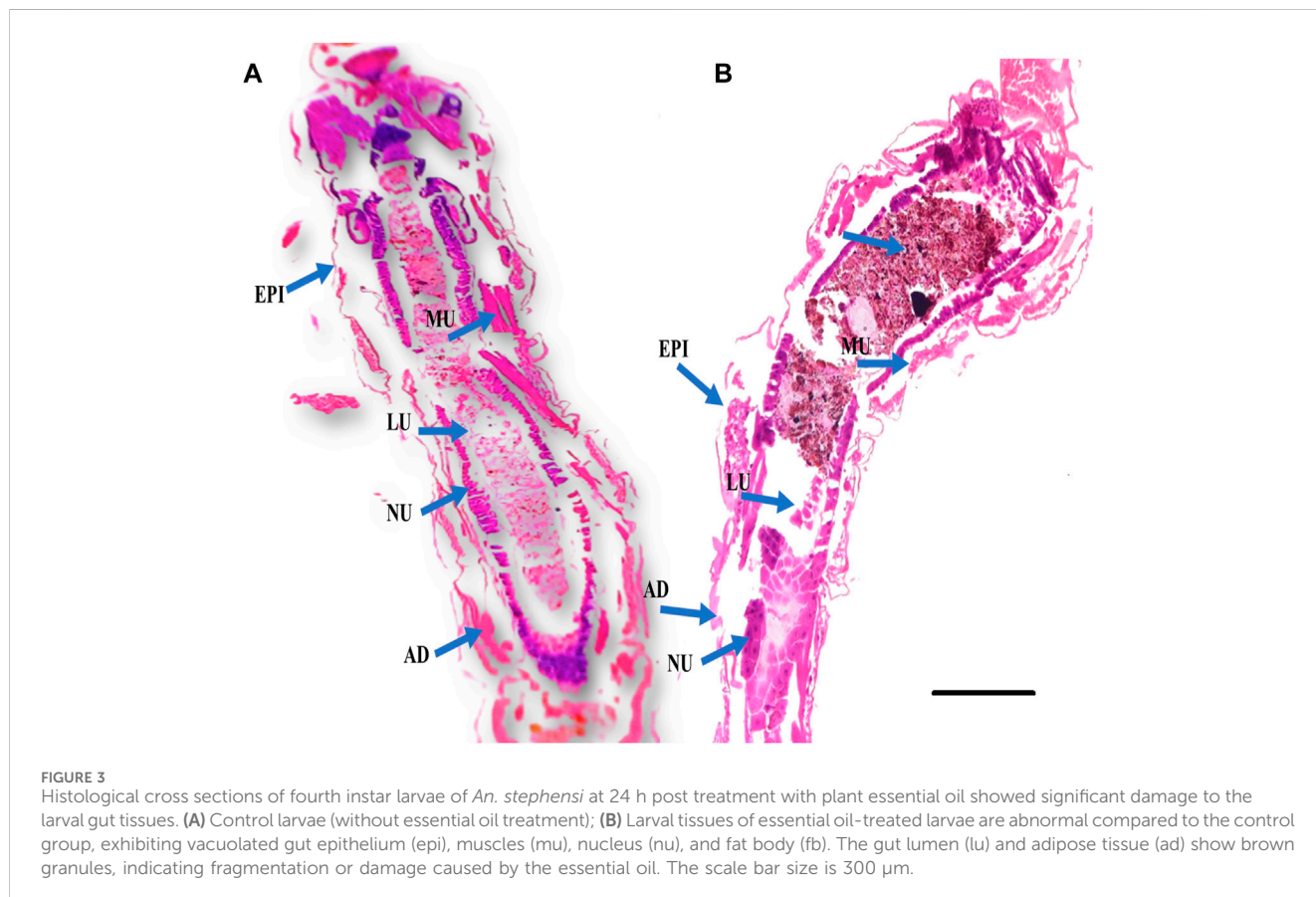
Larval biochemical assay

Acetylcholinesterase assay

The biochemical effects of essential oils from *M. cajuputi* on *An. stephensi* larvae were investigated. The lowest AchE enzyme activity was found to be in higher test concentration (200 ppm/mL). When larvae were exposed to essential oils from *M. cajuputi*, their acetylcholinesterase enzyme activity was significantly ($p < 0.05$) reduced compared to controls (12.33–7.0 mg protein/mL of homogenate) (df 5; $F_{(5,12)} = 0.728$; $p \leq 0.01$) (Figure 4A). The enzyme level was found to be normal in the control larvae. In the treatment the expression of AchE enzymes was primarily dose-dependent, with larvae exposed to essential oils from *M. cajuputi* exhibiting lower levels. The amount of AchE enzyme activity was decreased when essential oil concentrations are increased (Figure 4A).

α -carboxylesterase and β -carboxylesterase assay

Results showed that *M. cajuputi* essential oils on *An. stephensi* larvae resulted in lower levels of α and β -carboxylesterase enzyme activity (Figures 4B,C), after 24 h of treatment. The essential oils of *M. cajuputi* had a dose-dependent effect on the enzyme activity of α -



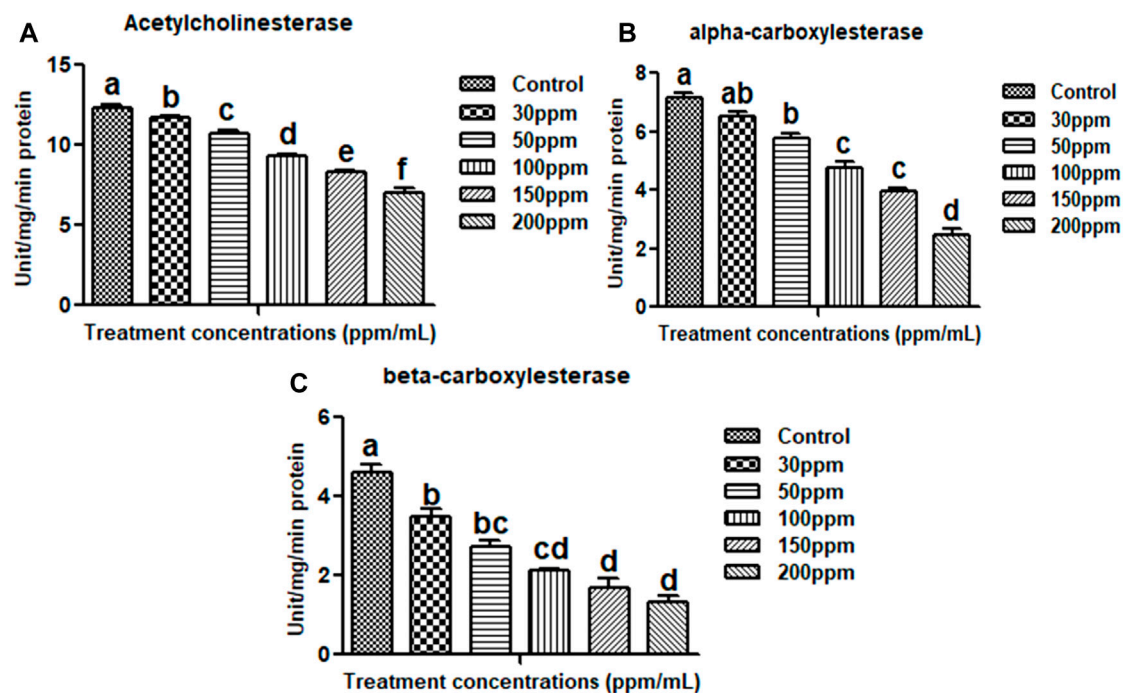


FIGURE 4 Acetylcholinesterase (A), alpha carboxylesterase (B), beta carboxylesterase (C). There is no statistically significant difference between values that follow the same letter (one-way ANOVA), as shown by the Tukey test at $p = 0.05$. Notes: the mid-gut tissues of larvae were stained with ehrlich's haematoxylin and viewed under a light microscope at $\times 100$ magnification.

carboxylesterase in larvae. When larvae were exposed to essential oils from *M. cajuputi*, their α -carboxylesterase activity was not significant compared to controls (7.16–2.45 mg protein/mL of homogenate) (df 5; $F_{(5,12)} = 99.947$; $p \leq 0.01$) (See [Figure 4B](#)). A similar finding was made with β -carboxylesterase, which showed a significant decrease in activity (from 5.0 to 1.1 mM/protein/mg/min) in *An. stephensi* larvae (df = 5; $F_{(5, 12)} = 56.278$; $p \leq 0.01$) (See [Figure 4C](#)).

Non-target toxicity assay

M. cajuputi essential oils had a minimal mortality rate were observed on *E. eugeniae* earthworm species. The toxicity of *M. cajuputi*-derived essential oils was less or minimal at the maximum dosage (200 ppm), which showed 4% mortality. This was similar to the control treatment as compared to the market-available chemical pesticide monocrotophos (200 ppm) showed 97.33% mortality ($F_{(1,8)} = 890$, $p \leq 0.01$) ([Figure 5](#); [Figure 6](#)). All treatment dosages are significant ($p < 0.05$) in comparison to the control, but there is no significant difference between the control and chemical pesticide treatments ([Figure 5](#); [Figure 6](#)).

Gut histochemistry

E. eugeniae is a suitable candidate as a bioindicator in soil toxicology. No deaths occurred within 24 h after essential oil treatment. There were no sublethal effects of essential oils on gut tissues, but the gut tissues of mosquito larvae were highly damaged by the botanical-derived essential oils (see [Figure 7](#)). Monocrotophos, a chemical pesticide used as a positive control, induced changes in earthworm gut cells and an irregular epithelial

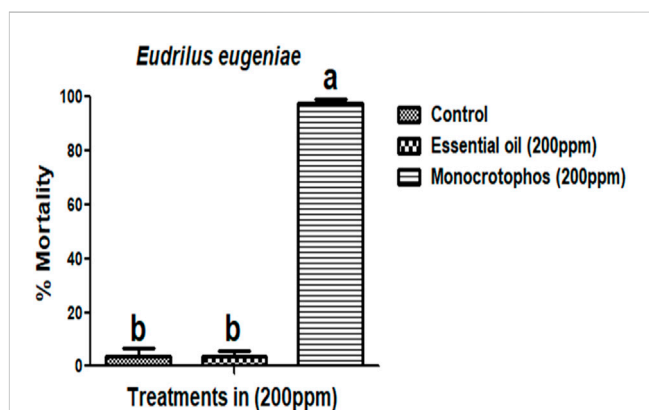


FIGURE 5 *Melaleuca cajuputi* essential oils minimal toxicity effects on *Eudrilus eugeniae* compared to chemical pesticide monocrotophos. In a Tukey test, means ((SE) standard error) followed by the same letters above bars indicate no significant difference ($p \leq 0.05$).

surface. Cellular debris was present, and the nuclei were not spherical (see [Figure 7](#)). [Figure 4](#) and [Figure 5](#) show that the essential oil treatment produced the same results as the control.

Essential oil phytochemicals

Phytochemical analysis of essential oils extracted from *M. cajuputi* indicates the presence of phenols, flavonoids, alkaloids, quinones, saponins, and tannins ([Table 1](#)). The phenols, flavonoids, alkaloids, quinones, saponins, and tannins extracted from *M.*

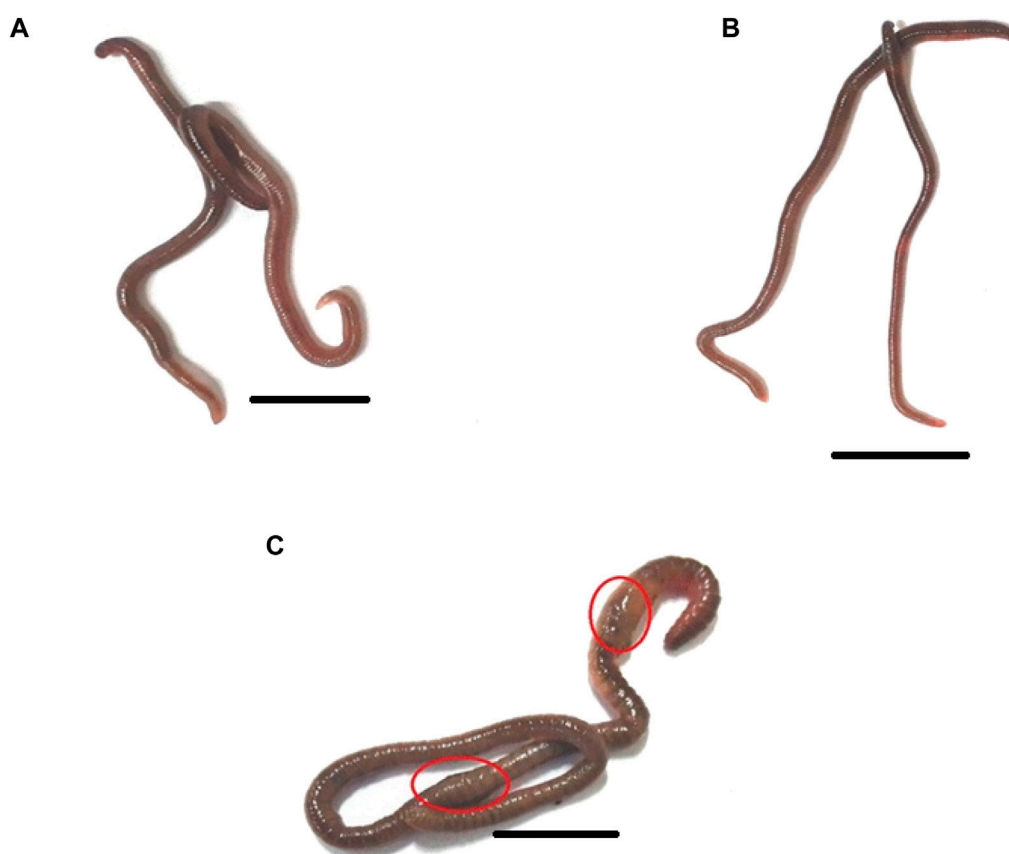


FIGURE 6

The morphology of the earthworm *Eudrilus eugeniae* in response to distilled water (negative control), essential oil, and Monocrotophos (positive control). Both the control (A) and essential oil treatments had normal external morphology (B). Monocrotophos-treated treatments have abnormal morphology (C). Chemical pesticide exposure altered the morphology of earthworms, affecting their body structure and size. The red circle indicates that chemical pesticides damaged the earthworm's epidermis. The scale bar size is 10 mm.

cajuputi essential oils may contribute to the mosquito larvicidal activity (see Table 1).

GC-MS chemical constituents' analysis

GC-MS analysis of *M. cajuputi* essential oils shows the presence of thirty-seven phytochemical constituents. Among the chemical constituents, the nine major are: 1,8-cineole (52.83%); limonene (13.50%); beta-pinene (5.43%); alpha-terpineol (4.65%); alpha-pinene (4.61%); gamma-terpinene (3.48); and beta-caryophyllene (3.11%). These major chemicals may have larvicidal activity (Table 2).

Discussion

In this study, we focused on the larvicidal properties of *M. cajuputi* plant essential oils against the malarial vector *An. stephensi*. Many researchers have conducted studies on the biological activities of plant essential oils. *M. cajuputi* is a native plant of Australia and belongs to the Myrtaceae family (Southwell and Lowe, 1999). It is commonly found in marshy areas near the coast of Malaysia. For centuries, the Aboriginal people of Australia have used the leaves for a variety of medicinal purposes.

Locals in Asia have traditionally used its oil to treat joint pain, stiffness, and rheumatism.

The essential oils of *M. cajuputi* had a dose-dependent mortality rate against all instar stages of *An. stephensi* mosquito larvae (second-fourth). The mortality percentage of *An. stephensi* was significant across treatment and control, with the rate of mortality being prominent at the maximum dosage (200 ppm) in the second 100%, the third 82.66%, and the fourth instar 70.66% (Figure 2; Figure 3). Researchers tested cajeput oil (*M. cajuputi*) on *Aedes* mosquito species, which showed high mosquitocidal activity against larvae and adult mosquitoes (Bakar et al., 2012; Bakar et al., 2019). A similar study by Jayakumar et al. (2016) found that eucalyptus essential oil was the most effective against *Cx. quinquefasciatus* larvae and pupae, with LC₅₀ values of 186.77 mg/L and 206.08 mg/L, respectively. Similarly, *M. cajuputi* essential oil has a lower LC₅₀ of 120.99 mg/L against *Ae. aegypti* larvae (Bakar et al., 2019). The present study clearly shows that *M. cajuputi*-derived essential oil had lower LC₅₀ and LC₉₀ values against larvae of *An. stephensi* were, 34.663 ppm/mL and 114.863 ppm/mL, respectively (Figure 2; Figure 3). Previous research on the effectiveness of *M. cajuputi* (Family: Myrtaceae) essential oil against dengue vectors revealed remarkable mosquito larvicidal and adulticidal activity (Bakar et al., 2012). In general, essential oil act as contact insecticides, with a neurotoxic mode of action that targets GABA

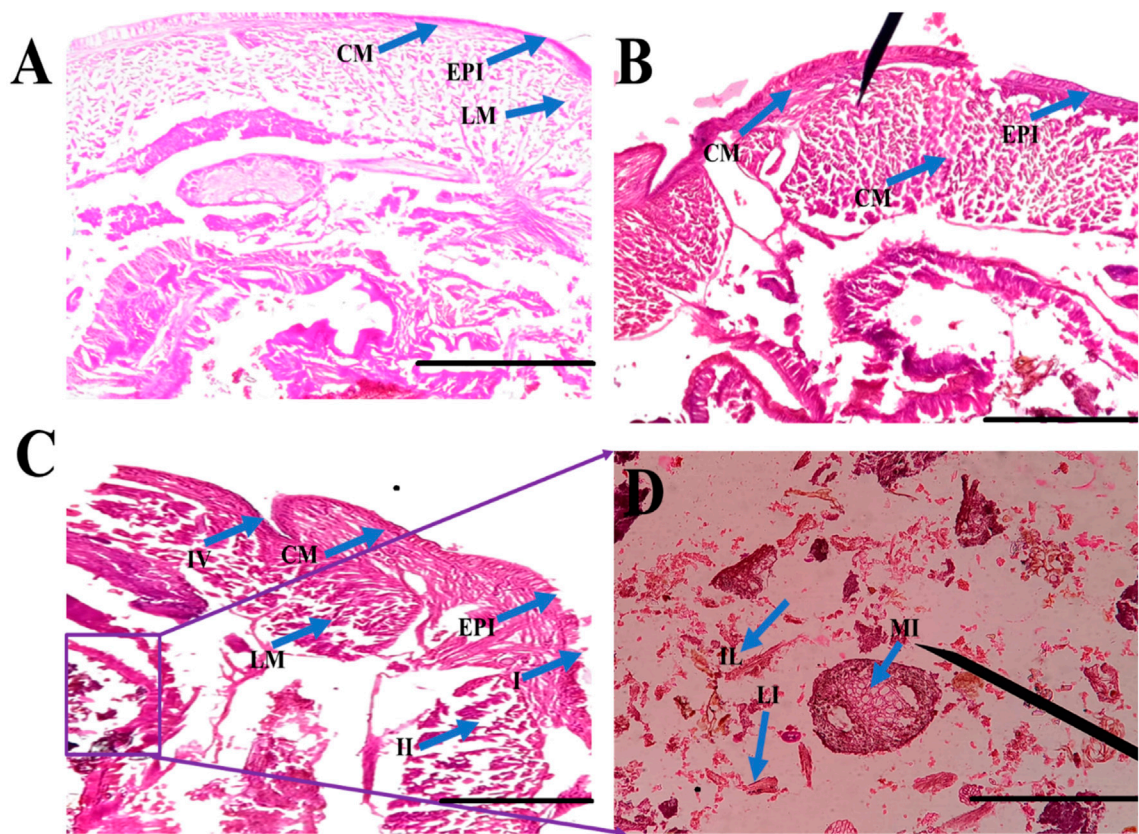


FIGURE 7
Histological studies of *Eudrilus eugeniae* after 24 h of essential oil treatment revealed that minimal toxicity effects was observed in the essential oil treatment. In gut tissues, no sublethal effects of oils were observed. The histological studies revealed essential oil-treated earthworm gut cells similar to the negative control. In the control and oil treated gut tissues there is no cellular debris in the earthworm gut tissues, and the nuclei are round in shape. Similar outcomes were seen in the control treatment as well. The chemical insecticide monocrotophos (positive control) caused significant damage to gut tissues. (EPI = epidermis, SE = setae, IL = intestinal lumen, LM = longitudinal muscle, CO = coelom, CM = circular muscle, MI = mitochondrion). The scale bar size is 0.1 mm.

TABLE 1 Qualitative Analysis of the phytoconstituents present in *Melaleuca cajuputi* derived essential oils.

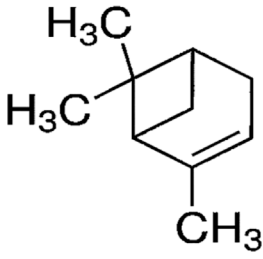
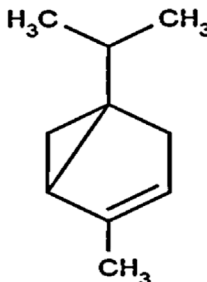
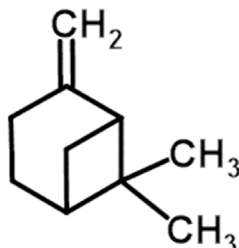
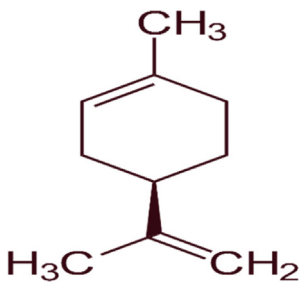
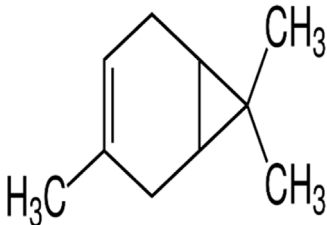
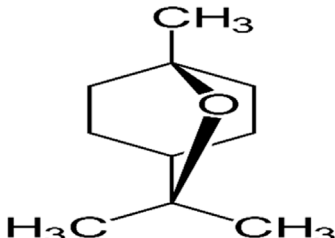
S.No	Phytoconstituents	Test method	Observation	Result
1	Alkaloids	Mayer's/Bertrand's/Valser's test	creamy white or yellow precipitate	Positive
2	Flavonoid	Lead acetate test	creamy white or yellow precipitate	Positive
3	Phenol	Ferric chloride test	formation of a reddish-brown precipitate	Positive
4	Saponin	Foam test	formation of foam	Positive
5	Quinones	Conc. HCl test	formation yellow precipitate	Positive
6	Tannin	Lead sub acetate test	appearance of a creamy, viscous precipitate	Positive

and octopamine synapses, as well as acetylcholinesterase (Regnault-Roger et al., 2012). Although the mode of action of essential oils in mosquito larvae is unknown, previous research has shown that plant chemical constituents initially affect the midgut epithelium, gastric caeca, and Malpighian tubules in mosquito larvae (Rey et al., 1999). Similarly, Myrtaceae plant essential oils have larvicidal properties against the dengue vector *Ae. aegypti* larvae (Dias et al., 2015). Sosan et al. (2001) found that essential oils of *Ocimum gratissimum*, *Cymbopogon citrus*, and *A. conyzoides* had 100% mortality against *Ae.*

aegypti at 120, 200, and 300 ppm concentrations, respectively. Many recent studies have identified plant extracts and essential oils as important sources of botanical insecticides. Plant compounds, rather than synthetic insecticides, may lead to the development of effective natural mosquitocidal products. Because of the volatile nature of plant essential oils, their insecticidal products degrade quickly, posing a lower environmental risk than synthetic insecticides.

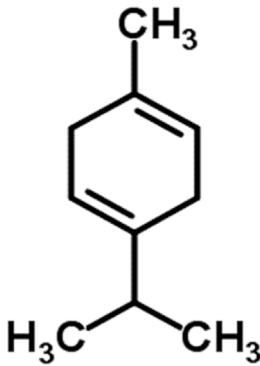
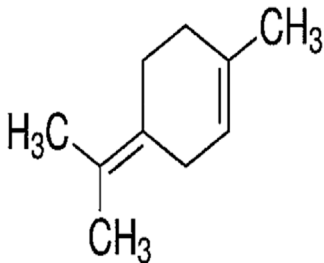
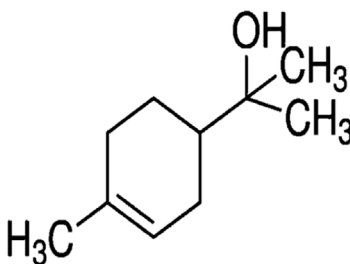
The results showed that the biochemical effects of essential oils derived from *M. cajuputi* leaves were tested against *An. stephensi*

TABLE 2 GC-MS analysis of *Melaleuca cajuputi* leaves derived essential oils.

S.No	RT mins	Area %	Compound Name	Structure	Biological activity
1	5.25	4.61	alpha-Pinene		Treatment of bladder, kidney stones, antimicrobial, anti-inflammatory
2	8.06	2.34	alpha-Thujene		Cosmetic and fragrance industries, inflammatory disorders such as osteoarthritis, bronchial asthma, chronic colitis
3	9.36	5.43	beta-Pinene		Antibacterial, antidepressant, cytotoxic, and antimicrobial
4	10.62	13.50	Limonene		Used in perfumes, household cleaners, foods, and medicines
5	21.49	2.86	delta-3-Carene		Relieve inflammation related to arthritis or fibromyalgia
6	24.50	52.51	1,8-Cineole		Acute bronchitis, asthma, COPD and sinusitis

(Continued on following page)

TABLE 2 (Continued) GC-MS analysis of *Melaleuca cajuputi* leaves derived essential oils.

S.No	RT mins	Area %	Compound Name	Structure	Biological activity
7	25.42	3.85	gamma-Terpinene		Used in food, flavours, soaps, cosmetics, pharmaceuticals, tobacco, confectionery, and perfume industries
8	32.13	2.52	Terpinolene		Used for these aromatic qualities in soaps, perfumes, and some insect repellents
9	36.25	4.23	alpha-Terpineol		Medicine to strengthen memory and treat dementia

larvae. The results clearly showed that the activity of the AchE enzyme decreased as the concentration of essential oil increased. The lowest activity of the AchE enzyme was found at a higher test concentration of 200 ppm/mL. When the larvae were exposed to essential oils, the activity of the acetylcholinesterase enzyme was not significant compared to the controls (from 12.33 to 7.0 mg protein/mL of homogenate) (Figure 4A). The enzyme level was found to be normal in the control larvae. In the treatment, the reduction of AchE enzymes in the larvae was primarily dose-dependent (see Figure 4A). Also, *M. cajuputi* essential oils treated *An. stephensi* larvae exhibited reduced levels of α and β -carboxylesterase enzyme activity (Figures 4B,C), reaching the lowest level within 24 h of treatment. The essential oils of *M. cajuputi* exhibited a dose-dependent effect on the enzyme activity of α -carboxylesterase in larvae. When the larvae were exposed to essential oils from *M. cajuputi*, their α -carboxylesterase activity was not significantly different compared to the controls (7.16–2.45 mg protein/mL of homogenate) (see Figure 4B). A similar finding was made with β -carboxylesterase, which showed a decrease in enzyme levels as the test concentration was increased (from 5.0 to 1.1 mM/protein/mg/min) in *An. stephensi* larvae (see Figure 4C). Similar to the present study, *Acacia nilotica* seed-derived essential oils showed not significant in acetylcholinesterase, α , and β -carboxylesterase (Perumal et al., 2023a).

According to the findings of the histological investigation, the larvae of *An. stephensi* were significantly impacted by their exposure to the essential oils derived from botanical sources. Cross-sections of *An. stephensi* larvae in their fourth instar that had been treated with essential oils caused lethal effects in the midgut tissues. The larval midgut of *An. stephensi* exhibited high damage, with distinct vacuolation within the epithelial cells of the midgut as well as in the adipose tissue and the muscles (Figure 3). These findings are comparable to *F. oxysporum* crude extracts is extremely toxic to the major disease mosquito vectors, which are *Aedes aegypti*, *An. stephensi*, and *Culex quinquefasciatus* (Vivekanandhan et al., 2018b).

Phytochemical analysis of essential oils derived from *M. cajuputi* reveals the presence of phenols, flavonoids, alkaloids, quinone, saponins, and tannins (Table 1). The phenols, flavonoids, alkaloids, quinone, saponins, and tannins derived from *M. cajuputi* essential oils may be involved in mosquito larvicidal activity (Table 1). Similar to the present study, Naringi crenulata (Rutaceae) plant extracts showed similar phytochemicals such as phenols, flavonoids, alkaloids, quinone, saponins, and tannins (Pratheeba et al., 2019). GC-MS analysis of *M. cajuputi* essential oils shows the presence of thirty-seven phytochemical constituents. Among the chemical constituents, the nine major are: 1,8-cineole

(52.83%); limonene (13.50%); beta-pinene (5.43%); alpha-terpineol (4.65%); alpha-pinene (4.61%); gamma-terpinene (3.48); and beta-caryophyllene (3.11%). These major chemicals may have larvicidal activity (Table 2). Similar to the present study reported that the main chemical constituents of cajuput oil used in this study are the terpenes eucalyptol (44.86%), D-limonene (22.03%), and o-cymene (14.51%). There are an additional 8 minor chemical constituents in the cajuput oil, including γ -terpinene (7.87%), cyclofenchene (4.85%), α -terpineol (1.41%), α -phellandrene (1.01%), terpine 4-acetate (0.67%), β -pinene (0.66%), β -myrcene (0.65%), and (+)-4-carene (0.63%) (Rault et al., 2022). Similarly, Bakar et al. (2019) reported the main constituents of cajuput oil showed high mosquito larvicidal activity against dengue mosquito vectors *Aedes aegypti*.

Following the results of the bioassay was showed that essential oils derived from botanical sources did not have any impact on the *E. eugeniae* species. In the present study, essential oils derived from botanical sources showed the lower mortality rate ranged from 0% to 4%. On the other hand, the monocrotophos treatment served as a positive control, and it resulted in the death of more than 97.33% mortality of the earthworms (Figure 5; Figure 6). According to the findings, essential oils derived from plants do not have a significant adverse effect on earthworms because of their lower toxicity of chemical composition. Similar findings presented here, it was discovered that *Metarhizium anisopliae* conidia or secondary metabolites did not have any impact on *E. eugeniae* earthworm species when they were exposed to soil conditions (Perumal et al., 2023b). In addition, the chemical constituents derived from *M. anisopliae* did not cause pathogenicity in *E. eugeniae* when tested in a laboratory setting (Perumal et al., 2023c). Histological findings provide additional evidence in support of the essential oils derived from botanical sources that, in comparison to chemical pesticides (Monocrotophos), do not pose a threat to earthworm species that live in the soil (Figure 7). The findings demonstrated that essential oils derived from botanical sources do not cause pathogenicity within the gut tissues of earthworms. Previous studies have shown that extracts and essential oils derived from botanical sources do not have any toxic effects on the gut tissues of earthworms (Vivekanandhan et al., 2018a; Pratheeba et al., 2019; Perumal et al., 2023a). This current result lends support to the findings of those earlier studies. The findings demonstrated that all of the earthworm tissues, including the epidermis, circular muscle, setae, mitochondrion, and intestinal lumen tissues, were normal and comparable to the control group. On the other hand, monocrotophos appeared to be completely toxic to the tissues of earthworms.

Conclusion

Plant essential oil compositions continue to be a promising source of natural product chemistries that have the potential to reduce populations of mosquitoes that transmit disease-causing pathogens and, ultimately, to mitigate the transmission of human diseases within and between communities. In order to develop and implement effective bioinsecticides, it is necessary to first determine the chemistries that interact with essential oils (EO) and the mechanism by which they exert their effects. This study is

the first-ever report on the biological insecticidal activity of cajuput oil against the mosquito vector *An. stephensi*, which is responsible for transmitting the malarial disease. It is necessary to conduct additional research in order to provide conclusive evidence that the essential oil receptor modulation is the mechanism of action that is responsible for the biological insecticidal activity of cajuput oil.

Data availability statement

The original contributions presented in the study are included in the article/Supplementary material, further inquiries can be directed to the corresponding author.

Ethics statement

The manuscript presents research on animals that do not require ethical approval for their study.

Author contributions

PV: Conceptualization, Data curation, Formal Analysis, Investigation, Methodology, Project administration, Resources, Software, Supervision, Validation, Visualization, Writing—original draft, Writing—review and editing. TA: Data curation, Formal Analysis, Funding acquisition, Resources, Software, Validation, Visualization, Writing—original draft, Writing—review and editing. MA: Data curation, Formal Analysis, Funding acquisition, Resources, Software, Validation, Visualization, Writing—original draft, Writing—review and editing. SS: Data curation, Formal Analysis, Resources, Software, Validation, Visualization, Writing—original draft, Writing—review and editing.

Funding

The author(s) declare that financial support was received for the research, authorship, and/or publication of this article.

Acknowledgments

We acknowledge the Department of General Pathology at Saveetha Dental College and Hospitals, Saveetha Institute of Medical and Technical Sciences, Saveetha University in Chennai, Tamil Nadu, India, for laboratory facilities. This project was supported by Researchers Supporting Project Number (RSP 2024R230) at King Saud University, Riyadh, Saudi Arabia.

Conflict of interest

The authors declare that the research was conducted in the absence of any commercial or financial relationships that could be construed as a potential conflict of interest.

Publisher's note

All claims expressed in this article are solely those of the authors and do not necessarily represent those of their affiliated

References

- Amer, A., and Mehlhorn, H. (2006a). Larvicidal effects of various essential oils against *Aedes*, *Anopheles*, and *Culex* larvae (Diptera, Culicidae). *Parasitol. Res.* 99, 466–472. doi:10.1007/s00436-006-0182-3
- Amer, A., and Mehlhorn, H. (2006b). Repellency effect of forty-one essential oils against *Aedes*, *Anopheles*, and *Culex* mosquitoes. *Parasitol. Res.* 99, 478–490. doi:10.1007/s00436-006-0184-1
- Auwal, M. S., Saka, S., Mairiga, I. A., Sanda, K. A., Shuaibu, A., and Ibrahim, A. (2014). Preliminary phytochemical and elemental analysis of aqueous and fractionated pod extracts of *Acacia nilotica* (Thorn mimosa). *Veterinary Res. forum Int. Q. J.* 5 (2), 95–100.
- Bakar, A. A., Ahmad, H., Sulaiman, S., Omar, B., and Ali, R. M. (2019). Evaluation of *in vitro* bioactivity of *Melaleuca cajuputi* powell essential oil against *Aedes aegypti* (L.) and *Aedes albopictus* (skuse). *Sains Malays.* 48 (9), 1919–1926. doi:10.17576/jsm-2019-4809-13
- Bakar, A. A., Sulaiman, S., Omar, B., and Ali, R. M. (2012). Evaluation of *Melaleuca cajuputi* (Family: Myrtaceae) essential oil in aerosol spray cans against dengue vectors in low cost housing flats. *J. Arthropod-Borne Dis.* 6 (1), 28–35.
- Balumahendhiran, K., Vivekanandhan, P., and Shivakumar, M. S. (2019). Mosquito control potential of secondary metabolites isolated from *Aspergillus flavus* and *Aspergillus fumigatus*. *Biocatal. Agric. Biotechnol.* 21, 101334. doi:10.1016/j.bcab.2019.101334
- Brophy, J. J., Hnawia, E., Lawes, D. J., Lebouvier, N., and Nour, M. (2014). An examination of the leaf essential oils of three *Eugenia* (Myrtaceae) species endemic to New Caledonia. *J. Essent. Oil Res.* 26 (2), 71–75. doi:10.1080/10412905.2013.871671
- Dhawan, D., and Gupta, J. (2017). Research article comparison of different solvents for phytochemical extraction potential from *Datura metel* plant leaves. *Int. J. Biol. Chem.* 11 (1), 17–22. doi:10.3923/ijbc.2017.17.22
- Dias, R. O., Via, A., Brandão, M. M., Tramontano, A., and Silva-Filho, M. C. (2015). Digestive peptidase evolution in holometabolous insects led to a divergent group of enzymes in Lepidoptera. *Insect Biochem. Mol. Biol.* 58, 1–11. doi:10.1016/j.ibmb.2014.12.009
- Ellman, G. L., Courtney, K. D., Andres, V., Jr, and Featherstone, R. M. (1961). A new and rapid colorimetric determination of acetylcholinesterase activity. *Biochem. Pharmacol.* 7 (2), 88–95. doi:10.1016/0006-2952(61)90145-9
- Geetha, A. R., George, E., Srinivasan, A., and Shaik, J. (2013). Optimization of green synthesis of silver nanoparticles from leaf extracts of *Pimenta dioica* (Allspice). *Sci. World J.* 2013, 362890. doi:10.1155/2013/362890
- Jayakumar, M., Arivoli, S., Raveen, R., and Samuel, T. (2016). Larvicidal and pupicidal efficacy of plant oils against *Culex quinquefasciatus* Say 1823 (Diptera: Culicidae). *J. Entomology Zoology Stud.* 4 (5), 449–456.
- Leyva, M., French-Pacheco, L., Quintana, F., Montada, D., Castex, M., Hernandez, A., et al. (2016). *Melaleuca quinquenervia* (cav.) ST blake (myrtales: Myrtaceae): natural alternative for mosquito control. *Asian Pac. J. Trop. Med.* 9 (10), 979–984. doi:10.1016/j.apjtm.2016.07.034
- Logeswaran, C., Vivekanandhan, P., and Shivakumar, M. S. (2019). Chemical constituents of thermal stress induced *Ganoderma* applanatum (Per.) secondary metabolites on larvae of *Anopheles stephensi*, *Aedes aegypti* and *Culex quinquefasciatus* and histopathological effects in mosquito larvae. *Biocatal. Agric. Biotechnol.* 20, 101253. doi:10.1016/j.bcab.2019.101253
- Manikandan, S., Mathivanan, A., Bora, B., Hemaladkshmi, P., Abhisubesh, V., and Poopathi, S. (2023). A review on vector borne disease transmission: current strategies of mosquito vector control. *Indian J. Entomology*, 503–513.
- Manjarres-Suarez, A., and Olivero-Verbel, J. (2013). Chemical control of *Aedes aegypti*: a historical perspective. *Rev. Costarric. Salud Pública* 22 (1), 68–75.
- Maria, R., Shirley, M., Xavier, C., Jaime, S., David, V., Rosa, S., et al. (2018). Preliminary phytochemical screening, total phenolic content and antibacterial activity of thirteen native species from *Guayas province* Ecuador. *J. King Saud University-Science* 30 (4), 500–505. doi:10.1016/j.jksus.2017.03.009
- Murfadunnisa, S., Vasantha-Srinivasan, P., Ganesan, R., Senthil-Nathan, S., Kim, T. J., Ponsankar, A., et al. (2019). Larvicidal and enzyme inhibition of essential oil from *Spheranthus amaranthoides* (Burm.) against lepidopteran pest *Spodoptera litura* (Fab.) and their impact on non-target earthworms. *Biocatal. Agric. Biotechnol.* 21, 101324. doi:10.1016/j.bcab.2019.101324
- Noosidum, A., Prabaripai, A., Chareonviriyaphap, T., and Chandrapatya, A. (2008). Excito-repellency properties of essential oils from *Melaleuca leucadendron* L., *Litsea cubeba* (Lour.) Persoon, and *Litsea salicifolia* (Nees) on *Aedes aegypti* (L.) mosquitoes. *J. Vector Ecol.* 33 (2), 305–312. doi:10.3376/1081-1710-33.2.305
- Norris, E. J., Johnson, J. B., Gross, A. D., Bartholomay, L. C., and Coats, J. R. (2018). Plant essential oils enhance diverse pyrethroids against multiple strains of mosquitoes and inhibit detoxification enzyme processes. *Insects* 9 (4), 132. doi:10.3390/insects9040132
- Okoro, O. J., Nnamonu, E. I., Ezewudo, B. I., and Okoye, I. C. (2018). Application of genetically modified mosquitoes (*Anopheles* species) in the control of malaria transmission. *Asian J. Biotechnol. Genet. Eng.* 1, 1–16.
- O'Neal, S. T., Johnson, E. J., Rault, L. C., and Anderson, T. D. (2019). Vapor delivery of plant essential oils alters pyrethroid efficacy and detoxification enzyme activity in mosquitoes. *Pesticide Biochem. Physiology* 157, 88–98. doi:10.1016/j.pestbp.2019.03.007
- Pandey, A. K., Mohan, M., Singh, P., Palni, U. T., and Tripathi, N. N. (2014). Chemical composition, antibacterial and antioxidant activity of essential oil of *Eupatorium adenophorum* Spreng. from Eastern Uttar Pradesh, India. *Food Biosci.* 7, 80–87. doi:10.1016/j.fbio.2014.06.001
- Perumal, V., Kannan, S., Alford, L., Pittarate, S., Geedi, R., Elangovan, D., et al. (2023a). First report on the enzymatic and immune response of *Metarhizium majus* bag formulated conidia against *Spodoptera frugiperda*: an ecofriendly microbial insecticide. *Front. Microbiol.* 14, 1104079. doi:10.3389/fmicb.2023.1104079
- Perumal, V., Kannan, S., Alford, L., Pittarate, S., Mekchay, S., Reddy, G. V., et al. (2023b). Biocontrol effect of entomopathogenic fungi *Metarhizium anisopliae* ethyl acetate-derived chemical molecules: an eco-friendly anti-malarial drug and insecticide. *Archives Insect Biochem. Physiology* 114 (2), 1–19. doi:10.1002/arch.22037
- Perumal, V., Kannan, S., Pittarate, S., Chinnaamy, R., and Krutmuang, P. (2023c). Essential oils from *Acacia nilotica* (Fabales: fabaceae) seeds: may have insecticidal effects? *Heliyon* 9 (4), e14808. doi:10.1016/j.heliyon.2023.e14808
- Pratheeba, T., Vivekanandhan, P., Faeza, A. N., and Natarajan, D. (2019). Chemical constituents and larvicidal efficacy of *Naringi crenulata* (Rutaceae) plant extracts and bioassay guided fractions against *Culex quinquefasciatus* mosquito (Diptera: Culicidae). *Biocatal. Agric. Biotechnol.* 19, 101137. doi:10.1016/j.bcab.2019.101137
- Pratiwi, R. A., and Nurlaeni, Y. (2021). The potency of Myrtaceae family from cibodas botanic gardens (cianjur, Indonesia) as botanical pesticide. *Biodiversitas J. Biol. Divers.* 22 (10). doi:10.13057/biodiv/d221058
- Rault, L. C., O'Neal, S. T., Johnson, E. J., and Anderson, T. D. (2022). Vaporous essential oils and isolates restore pyrethroid-treated netting efficacy to *Aedes aegypti* (Diptera: Culicidae). *bioRxiv*, 2022–2112.
- Regnault-Roger, C., Vincent, C., and Arnason, J. T. (2012). Essential oils in insect control: low-risk products in a high-stakes world. *Annu. Rev. Entomology* 57, 405–424. doi:10.1146/annurev-ento-120710-100554
- Rey, D., Cuany, A., Pautou, M. P., and Meyran, J. C. (1999). Differential sensitivity of mosquito taxa to vegetable tannins. *J. Chem. Ecol.* 25, 537–548. doi:10.1023/a:1020953804114
- Satheesh, S., and Wesley, S. G. (2012). Diversity and distribution of seaweeds in the Kudankulam coastal waters, south-eastern coast of India. *Biodivers. J.* 3 (1), 79–84.
- Sheel, R., Nisha, K., and Kumar, J. (2014). Preliminary phytochemical screening of methanolic extract of *Clerodendron infortunatum*. *IOSR J. Appl. Chem.* 7 (1), 10–13. doi:10.9790/5736-07121013
- Sosan, M. B., Adewoyin, F. B., and Adewunmi, C. O. (2001). Larvicidal properties of three indigenous plant oils on the mosquito *Aedes aegypti*. *Niger. J. Nat. Prod. Med.* 5, 30–33. doi:10.4314/njnp.v5i1.11719
- Southwell, I., and Lowe, R. (1999). *Tea tree: the genus Melaleuca*. Boca Raton, Florida, United States: CRC Press.
- Van Asperen, K. (1962). A study of housefly esterases by means of a sensitive colorimetric method. *J. Insect Physiology* 8 (4), 401–416. doi:10.1016/0022-1910(62)90074-4
- Vivekanandhan, P., Kavitha, T., Karthi, S., Senthil-Nathan, S., and Shivakumar, M. S. (2018a). Toxicity of *Beauveria bassiana*-28 mycelial extracts on larvae of *Culex quinquefasciatus* mosquito (Diptera: Culicidae). *Int. J. Environ. Res. public health* 15 (3), 440. doi:10.3390/ijerph15030440

- Vivekanandhan, P., Panikar, S., Sethuraman, V., Usha-Raja-Nanthini, A., and Shivakumar, M. S. (2023). Toxic and synergetic effect of plant essential oils along with nano-emulsion for control of three mosquito species. *J. Nat. Pesticide Res.* 5, 100045. doi:10.1016/j.napere.2023.100045
- Vivekanandhan, P., Senthil-Nathan, S., and Shivakumar, M. S. (2018b). Larvicidal, pupicidal and adult smoke toxic effects of *Acanthospermum hispidum* (DC) leaf crude extracts against mosquito vectors. *Physiological Mol. Plant Pathology* 101, 156–162. doi:10.1016/j.pmpp.2017.05.005
- Vivekanandhan, P., Swathy, K., Kalaimurugan, D., Ramachandran, M., Yuvaraj, A., Kumar, A. N., et al. (2020a). Larvicidal toxicity of *Metarhizium anisopliae* metabolites against three mosquito species and non-targeting organisms. *Plos one* 15 (5), e0232172. doi:10.1371/journal.pone.0232172
- Vivekanandhan, P., Thendralmanikandan, A., Kweka, E. J., and Mahande, A. M. (2021). Resistance to temephos in *Anopheles stephensi* larvae is associated with increased cytochrome P450 and α -esterase genes overexpression. *Int. J. Trop. Insect Sci.* 41, 2543–2548. doi:10.1007/s42690-021-00434-6
- Vivekanandhan, P., Usha-Raja-Nanthini, A., Valli, G., and Subramanian Shivakumar, M. (2020b). Comparative efficacy of *Eucalyptus globulus* (Labill) hydrodistilled essential oil and temephos as mosquito larvicide. *Nat. Prod. Res.* 34 (18), 2626–2629. doi:10.1080/14786419.2018.1547290
- Vivekanandhan, P., Venkatesan, R., Ramkumar, G., Karthi, S., Senthil-Nathan, S., and Shivakumar, M. S. (2018c). Comparative analysis of major mosquito vectors response to seed-derived essential oil and seed pod-derived extract from *Acacia nilotica*. *Int. J. Environ. Res. Public Health* 15 (2), 388. doi:10.3390/ijerph15020388
- World Health Organization (2005). *The World Health Report 2005: make every mother and child count*. Geneva, Switzerland: World Health Organization.



OPEN ACCESS

EDITED BY

Ana Claudia A. Melo,
Federal University of Rio de Janeiro, Brazil

REVIEWED BY

Matthieu Dacher,
Sorbonne Université, France
L. J. Zwiebel,
Vanderbilt University, United States

*CORRESPONDENCE

Jeff A. Riffell,
✉ jriffell@uw.edu

RECEIVED 02 February 2024

ACCEPTED 14 March 2024

PUBLISHED 28 March 2024

CITATION

Rouyar A, Patil AA, Leon-Noreña M, Li M,
Coutinho-Abreu IV, Akbari OS and Riffell JA
(2024), Transgenic line for characterizing
GABA-receptor expression to study the neural
basis of olfaction in the yellow-fever mosquito.
Front. Physiol. 15:1381164.
doi: 10.3389/fphys.2024.1381164

COPYRIGHT

© 2024 Rouyar, Patil, Leon-Noreña, Li,
Coutinho-Abreu, Akbari and Riffell. This is an
open-access article distributed under the terms
of the [Creative Commons Attribution License](#)
(CC BY). The use, distribution or reproduction in
other forums is permitted, provided the original
author(s) and the copyright owner(s) are
credited and that the original publication in this
journal is cited, in accordance with accepted
academic practice. No use, distribution or
reproduction is permitted which does not
comply with these terms.

Transgenic line for characterizing GABA-receptor expression to study the neural basis of olfaction in the yellow-fever mosquito

Angela Rouyar¹, Anandrao A. Patil¹, Melissa Leon-Noreña¹,
Ming Li², Iliano V. Coutinho-Abreu², Omar S. Akbari² and
Jeff A. Riffell^{1*}

¹Department of Biology, University of Washington, Seattle, WA, United States, ²Division of Biological Sciences, Section of Cell and Developmental Biology, University of California, San Diego, La Jolla, CA, United States

The mosquito *Aedes aegypti* is an important vector of diseases including dengue, Zika, chikungunya, and yellow fever. Olfaction is a critical modality for mosquitoes enabling them to locate hosts, sources of nectar, and sites for oviposition. GABA is an essential neurotransmitter in olfactory processing in the insect brain, including the primary olfactory center, the antennal lobe. Previous work with *Ae. aegypti* has suggested that antennal lobe inhibition via GABA may be involved in the processing of odors. However, little is known about GABA receptor expression in the mosquito brain, or how they may be involved in odor attraction. In this context, generating mutants that target the mosquito's olfactory responses, and particularly the GABAergic system, is essential to achieve a better understanding of these diverse processes and olfactory coding in these disease vectors. Here we demonstrate the potential of a transgenic line using the QF2 transcription factor, GABA-B1^{QF2-ECFP}, as a new neurogenetic tool to investigate the neural basis of olfaction in *Ae. aegypti*. Our results show that the gene insertion has a moderate impact on mosquito fitness. Moreover, the line presented here was crossed with a QUAS reporter line expressing the green fluorescent protein and used to determine the location of the metabotropic GABA-B1 receptor expression. We find high receptor expression in the antennal lobes, especially the cell bodies surrounding the antennal lobes. In the mushroom bodies, receptor expression was high in the Kenyon cells, but had low expression in the mushroom body lobes. Behavioral experiments testing the fruit odor attractants showed that the mutants lost their behavioral attraction. Together, these results show that the GABA-B1^{QF2-ECFP} line provides a new tool to characterize GABAergic systems in the mosquito nervous system.

KEYWORDS

GABA, mosquito, olfaction, GABA receptor, transgenic

1 Introduction

Neurotransmitters play essential roles in the insect motor and central nervous systems. Gamma-aminobutyric acid (GABA), an inhibitory neurotransmitter, is one of the most highly expressed neurotransmitters in the central nervous system of insects (Homberg, 2002; Rogers et al., 2004; Enell et al., 2007). It is highly expressed in many brain regions,

including the primary olfactory center, the antennal lobe (AL) (Okada et al., 2009), the optic lobe (Raghu et al., 2013), the mushroom bodies (MBs) (Yasuyama et al., 2002)—a site involved in learning and memory (Heisenberg et al., 1985; Davis, 1993), and the central complex (Enell et al., 2007). Accordingly, GABA is involved in many different sensory behaviors, including the processing of odors (Waldrop et al., 1987; Stopfer et al., 1997; Olsen and Wilson, 2008) and visual (Brotz et al., 2001; Freifeld et al., 2013) and auditory stimuli (Loh et al., 2023). The neuronal circuits and behaviors associated with learning and memory are also modulated by GABA, with GABAergic processes that broadly innervate the MBs (Liu and Davis, 2009). GABA is also involved in locomotion (Leal and Neckameyer, 2002), with many of the descending neurons from the brain being GABAergic (Hsu and Bhandawat, 2016) and are important for motor control and odor navigation (Tastekin et al., 2018).

GABA receptors—the membrane-bound receptor to which GABA binds—are important research foci in neurobiology and pest control (Hosie et al., 1997). GABA receptors occur in two types: 1) GABA_A type receptors, members of the ionotropic ligand-gated channel family, and 2) metabotropic GABA_B type receptors, members of the G-protein coupled receptor family. The GABA_A receptor have three subunit class encoded by three genes: *Rdl* (resistance to dieldrin; (Ffrench-Constant et al., 1991)); *Grd* (GABA and glycine-like receptor of *Drosophila*; (Harvey et al., 1994)) and *Lch3* (ligand-gated chloride channel homologue 3; (Henderson et al., 1993)), and the subunits named accordingly, RDL, GRD and LCCH3. The receptor can form a homomeric complex with the subunit RDL or a heteromeric association of RDL and LCCH3 subunits (Dupuis et al., 2010). Three GABA_B receptor subtypes, GABA-B1, -B2, and -B3, have also been identified in *Drosophila*. While GABA-B1 and -B2 exhibit significant sequence similarity to mammalian GABA_BR1 and R2, respectively, the receptor GABA-B3 appears to be an insect-specific subtype. While the GABA-B3 displays a unique expression pattern, the GABA-B1 and GABA-B2 subtypes coexpressed in the similar regions in central nervous system (Mezler et al., 2001). Together these subtypes form a heterodimer resulting to a functional GABA_B receptor (Galvez et al., 2001; Mezler et al., 2001).

The region- and cell-specific expression of these receptors can shape neural processing. For example, in the *Drosophila* AL, the inhibitory local interneurons (LNs) do not express either of the GABA receptor types; however, the projection neurons (PNs) express both receptors (Okada et al., 2009). The combined expression in the PNs is thought to modulate the neurons at the odor onset (via GABA_A) and inhibit the PNs at longer timescales by the metabotropic GABA_B receptors (Lei et al., 2002; Wilson and Laurent, 2005). Subtle region-specific differences in receptor expression can also occur. GABA_A and GABA_B receptors are highly expressed in the AL, mushroom body calyces, and regions in the optic lobe, and central complex, but may not overlap in subregions in the mushroom body calyces, which has been suggested as a spatial separation of slow and fast GABA transmission (Enell et al., 2007). Beyond cell- and region-specific expression, GABA receptors are targets of insecticides, including organochlorine, dieldrin, and fipronil insecticides that bind to the transmembrane regions and the resistant to dieldrin (Rdl) subunit to serve as receptor antagonists (Casida and Durkin, 2015; Ozoe, 2021). Antagonist binding of the GABA receptor blocks the activity of the GABA-gated chloride channels, increasing neuronal excitation.

A further example of the importance of the GABAergic system on mosquito behavior comes from the role of GABA receptors in processing olfactory information, including the odors of nectar sources and hosts. Inhibition in the antennal lobe, the primary olfactory system in the mosquito brain—mediated by GABAergic local interneurons—is critical for the enhancement of processing specific odors, including those that represent attractive odorants (Lei et al., 2002; Olsen and Wilson, 2008; Liou et al., 2018; Lahondère et al., 2020). This process can boost the signal of relatively weak, behaviorally important, odor input while suppressing the input from the background, or repellent, odors. In *Ae. aegypti*, inhibition is essential for processing odor mixtures, like those from flowers or hosts (Lahondère et al., 2020).

Despite the importance of GABA in mosquitoes, only a handful of studies have examined GABA expression in the mosquito brain (Lahondère et al., 2020; Loh et al., 2023; Singh et al., 2023), and none have examined GABA-receptor expression. In particular, the GABA-B1-receptors are involved in many vital physiological processes and constitutes a promising pharmacological target in insecticide development where resistance problems targeting GABA_A receptor subunit are now observed (Zulfa et al., 2022).

Here, we use the Q-system to characterize the GABA-B1-receptor expression in the mosquito brain. The Q-system is a binary expression system that has allowed the characterization of cell and circuit function in the mosquito (Riabinina et al., 2016) and consists of a transcription factor, QF, often inserted downstream of a gene of interest, which, when crossed with a QUAS reporter line, binds to the QUAS component that is upstream of genes coding for fluorescent proteins. This system was used to insert the QF2 transcription factor in the *GABA-receptor* gene locus, thereby knocking out the gene, and the resulting line was crossed to the QUAS-mCD8GFP reporter line to characterize GABA receptor expression of olfactory regions in the *Ae. aegypti* brain. Using this novel knock-in and knock-out approach, we asked the following questions: 1) How is the GABA-receptor expressed in olfactory regions of the mosquito brain, such as the AL and MB? 2) How does the knock-out of the receptor influence parameters of the mosquito life cycle?; and 3) How does the loss-of-function of the GABA-B1 receptor influence attraction to sources of nectar or fruit?

2 Materials and methods

2.1 Insect rearing

Ae. aegypti lines, from BEI Resources (Manassas, VA, United States) (*Ae. aegypti*: Rockefeller, Liverpool) were raised at the University of Washington campus. Mosquito lines provided were used in immunohistochemistry and behavioral experiments. The Liverpool line was used for transgenic lines as the genetic background. The mosquitoes were maintained in BSL2 insectary at 27°C, 70%–80% of relative humidity and at a photoperiod cycle of 12 h light/12 h dark. The eggs were hatched in plastic trays and in deoxygenated ultra-pure water. Larvae were maintained under the same conditions and fed with fish food (First Bites semi-buoyant granule, Hikari Tropical), and female mosquitoes were fed from heparinized bovine blood (Lampire Biologicals Laboratory Inc., Pipersville, PA 18947).

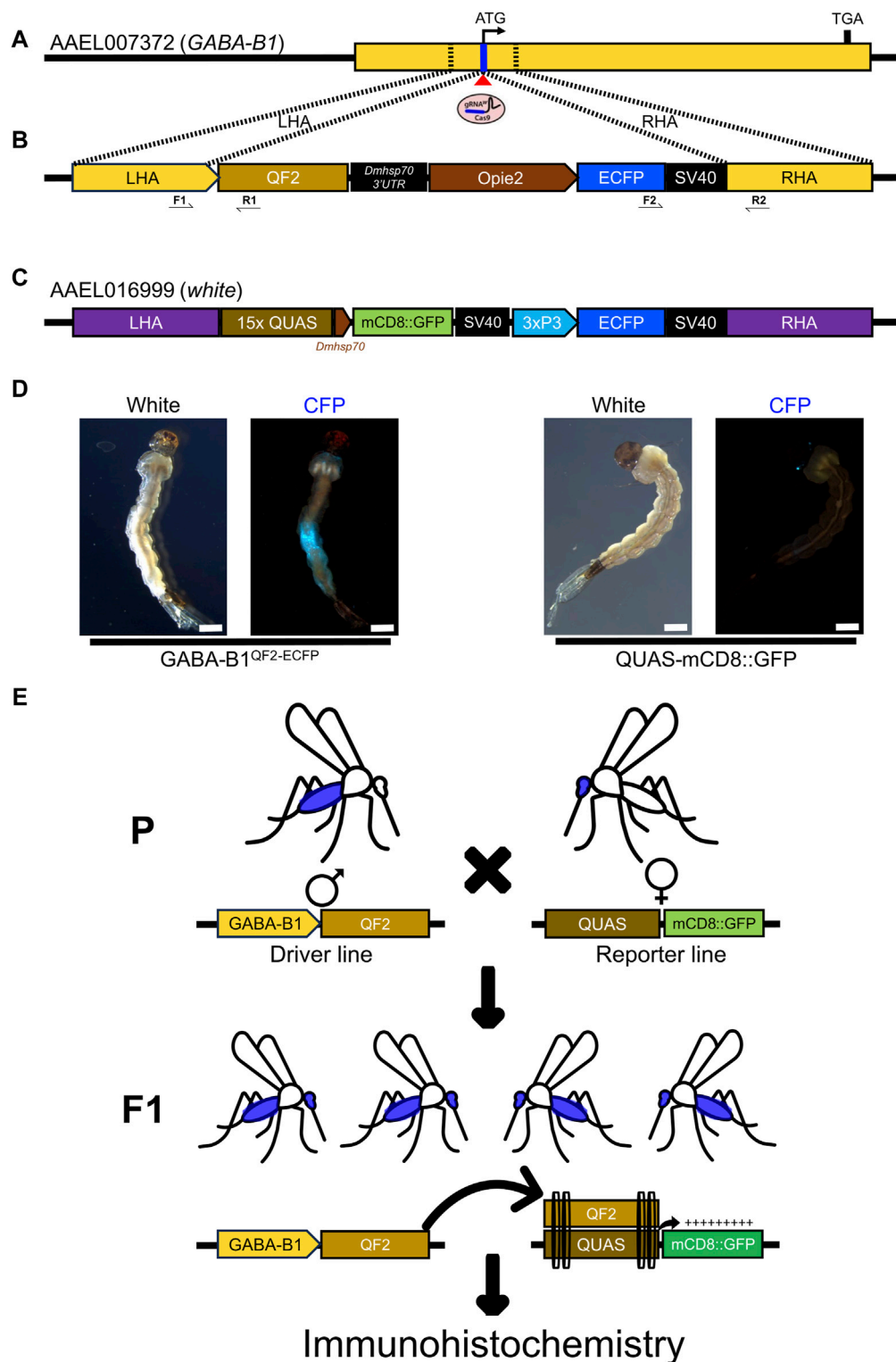


FIGURE 1

Generating *GABA-B1*^{QF2-ECFP} driver line. (A) The schematic representation of a *GABA-B1* gene structure and target gRNA location around the translational start codon (ATG). The Blue line represents the target gRNA location and the red triangle indicates a predicted Cas9 cleavage site. The dotted black lines represent the left and right homology arms from the genomic locus region selected to make a knock-in plasmid construct. (B) The schematic representation of the *GABA-B1* gene targeting homology-directed repair (HDR) knock-in construct flanked with left and right homology arms, the QF2 transcription factor expression cassette, and the Enhanced Cyan Fluorescent Protein (ECFP) screening marker expression cassette. Black arrow indicates genotyping primers to determine the left and right-side integration sites of knock-in. (C) Schematic representation of the sex-linked *white* gene targeting QUAS line components; *mCD8::GFP* reporter gene expression cassette and *3xP3* promoter driving ECFP screening marker. (D) The transgenic *GABA-B1*^{QF2-ECFP} and QUAS-mCD8GFP larvae showing presence of ECFP screening markers in the abdomen and eyes, respectively (Scale bar = 2 mm). The larvae were examined under the fluorescence microscope using cyan fluorescence protein (CFP) filter and white light. (E) Schematic representation (Continued)

FIGURE 1 (Continued)

of the QF2/QUAS binary expression system crossing scheme. The homozygous parents (♂) of driver line expressing QF2 transcription factor under the *GABA-B1* gene promoter crossed with the homozygous parents (♀) of QUAS reporter line. The F_1 progeny obtained from this crossing scheme will have both driver and reporter components. In the F_1 progeny, QF2 binds to QUAS enhancer to induce the expression of downstream reporter gene *mCD8::GFP* in *GABA-B1* gene-expressing cells or tissues, which was further visualized by immunohistochemistry.

2.2 Genetic construction

2.2.1 QF2 driver plasmid construction

In this research, we studied the role of G-protein coupled receptors (GPCR) family gene: *GABA-B1*. We have applied a CRISPR/Cas9 mediated homology-directed repair (HDR) knock-in approach to knockout *GABA-B1* gene and use its regulatory sequences to drive the expression of QF2 transcription factor. To make a HDR knock-in construct, first we retrieved the *Ae. aegypti* (LVP_AGWG strain) *GABA-B1* gene and transcript sequence from VectorBase [VectorBase (2022); *GABA-B1* (GPRGBB1: AAEL007372)]. Then, gene and transcript sequences were aligned to find the target gRNA sequence around the translational start codon using online tool CHOPCHOP [CHOPCHOP (2024); AAEL007372-gRNA: TAACCACGGTAGATCTTCAT]. Based on the predicted Cas9 cleavage site for the gRNA, homology arms were selected for knock-in plasmid construction. The nucleotide sequences (~1 kb) upstream of translation start codon (22 bp upstream of Cas9 cleavage site) was used as a left homology arm and the nucleotide sequences (~1 kb) downstream of Cas9 cleavage site was used as a right homology arm to build a knock-in construct (Figures 1A,B). The homology arm fragments, QF2 expression fragment (QF2-*Dmhs70*-3'UTR) and Opie2 promoter driving Enhanced Cyan Fluorescent Protein (ECFP) screening marker expression fragment (Opie2-ECFP-SV40), were synthesized commercially (GenScript) and assembled using Gibson enzymatic assembly (Gibson et al., 2009). Then, DNA assembly reaction mixture transformed into chemically competent *E. coli* cells (Zymo Research, JM109 Cat #T3005) and the plasmids were isolated from positive colonies (Zymo Research, Zippy plasmid miniprep kit, Cat. #D4036) and their nucleotide sequences were confirmed thoroughly using Oxford Nanopore Sequencing at Primordium Labs (Primordium Labs, 2023). For microinjection, plasmid was maxi-prepped (Zymo Research, ZymoPURE II Plasmid Maxiprep kit, Cat. #D4202).

2.2.2 Generating *GABA-B1*^{QF2-ECFP} transgenic lines

The QF2 driver transgenic strain was generated by microinjecting preblastoderm stage embryos (0.5–1 h old) with a mixture of the knock-in donor plasmid (100 ng/ul), sgRNA (100 ng/μL) and Cas9 protein (100 ng/μL). The embryo collection, microinjections, transgenic lines generation, and rearing were performed following previously established procedures (Bui et al., 2020; Li et al., 2020; 2021).

2.2.3 Genotyping and homozygosity of *GABA-B1*^{QF2-ECFP} line

To establish a homozygous QF2 line, ECFP screening markers expressing larvae (G_0) were maintained individually until they emerged as adults. To set up G_0 crosses, a single ECFP marker expressing virgin female or male was crossed with a wild type (WT)

single virgin female or male, and then females were blood-fed after 3 days of crossing and allowed to lay eggs on the wet paper (Figure 1E). Then, G_0 parents were collected for genomic DNA isolation to determine the insertion sites. To recover transgenic mosquitoes, G_1 larvae were screened under the Leica M165FC fluorescent stereomicroscope. Fluorescence was visualized using the CFP/YFP/mCherry triple filter, and the ECFP-positive larvae were selected from each cross and maintained separately. To determine the insertion sites for the knock-in construct, genomic DNA was isolated (Zymo Quick-DNA Miniprep Plus Kit Cat. No: D4068) from the G_0 parents whose progenies were ECFP positive. For genotyping PCR, primers were designed on both sides of the knock-in site (Figure 1B) and PCR was performed using the genomic DNA template, *OneTaq* DNA polymerase (NEB, Cat. No: M0484S), and primers listed in Supplementary Table S1. Then, amplified PCR fragments were gel analyzed, purified, and the nucleotide sequences were confirmed by Sanger sequencing (Supplementary Figure S1). The genotyping PCR insertion sites determined parents' ECFP positive progeny (G_1) were only maintained and used for further inbreeding to establish a homozygous line (Figure 1D).

2.2.4 QUAS reporter line

The QUAS-mCD8GFP reporter line (white-quas-mcd8-gfp) was generated (Craig Montell lab) by CRISPR/Cas9 mediated HDR knock-in of second coding-exon of the sex-linked *white* gene (AAEL016999), which is essential for eye pigmentation (Figure 1C). The QUAS line contains two expression cassettes; *mCD8::GFP* reporter gene expressed at basal level under the control of *D. melanogaster* heat shock protein 70 (*Dmhs70*) gene core promoter whereas the ECFP screening marker expressed in the eyes under 3xP3 promoter (Figure 1D). The QUAS enhancer copies (15x) are located upstream of the *Dmhs70* gene core promoter, which can induce the expression of downstream *mCD8::GFP* reporter gene upon binding of QF2 transcription factor.

2.3 Immunohistochemistry

2.3.1 Staining

For the immunostaining, *GABA-B1*^{QF2-ECFP} > QUAS-mCD8GFP females and males aged between 4 and 8 days old were used. Following an adapted protocol (Shankar and McMeniman, 2020), animals were anesthetized at 4°C and whole-body mosquitoes were fixed in Millonig's buffer: 4% paraformaldehyde in 0.1 M Millonig's Phosphate Buffer pH 7.4 (Electron Microscopy Sciences, 11582-10) with 0.25% Triton-X 100 for 3 h at 4°C. Brains were dissected in cool 0.1 M PBS pH 7.4 with fine forceps (Dumont #5, 100 nm tips) to carefully remove the head capsule as well as the pigmented ommatidia over the optic lobes and any floating air sacs connected to the brain. After

washing brains 3 times for 20 min each with 0.1 M PBS pH 7.4 with 0.25% Triton-X 100 (PBST) at room temperature, brains were incubated overnight at 4°C in a blocking solution consisting of 2% normal goat serum (NGS) and 4% Triton-X 100 in 0.1 M PBS pH 7.4. Then, brains were washed 3 times for 20 min each in PBST and incubated for 3 days at 4°C in the primary antibody solution containing mouse anti-Brp (DSHB, nc82-s, AB_2314866, 1:50 v/v) targeting the pre-synaptic active zone protein Bruchpilot (Brp) (Hofbauer et al., 2009) and rabbit anti-GFP (Invitrogen, A-6455, 1:100 v/v) targeting mCD8GFP. Following another 3 washes with PBST, the brains were exposed to a secondary antibody solution for 3 days at 4°C. The secondary antibody solution consisted of goat anti-mouse Cy3 (Jackson ImmunoResearch, AB_2338680, 1:200 v/v) and goat anti-rabbit Alexa Fluor 488 (Invitrogen, A-11008, 1:10200 v/v). Finally, the brains were washed 3 times for 20 min each with PBST at room temperature, incubated in SlowFade Diamond Antifade Mountant solution (Invitrogen, S36936) overnight at 4°C and mounted between glass slides and raised coverslip to avoid tissue distortion.

To test the specificity of this green fluorescent protein (GFP) antibody, we performed a preabsorption control where the primary antibody was preabsorbed with 1 mg/mL GFP protein overnight at 4°C before being used to incubate brains in the primary antibody solution. As the GFP protein and the Alexa Fluor 488 have the same emission spectrum and to ensure that the fluorescence observed on the brains is not due to GFP protein residues remaining despite washing, the Alexa Fluor 488 was replaced with Alexa Fluor 405. Controls where the primary antibody alone and the secondary antibody alone were also performed to confirm the specificity of the GFP antibody labeling (Figure 2F1, F2, F3).

2.3.2 Immunohistochemistry image acquisition settings

Brain tissue was imaged using A1R HD25 laser scanning confocal microscope. A $\times 20$ objective lens (0.75 NA, Plan-Apochromat) was used to capture the whole brain and AL and MB areas. Excitation of Cy3 signal was achieved with a 561 nm solid-state laser line between 0.5% and 2% laser power, a detector offset at 40 and a GaAsP PMT detector gain between 10 and 20. A 488 nm laser line was used to excite Alexa Fluor 488 with the same laser setting used for the Cy3 signal. The images were acquired with 2048 \times 2048-pixel resolution.

2.4 Bioassays

The fitness experiments were performed using GABA-B1^{QF2-ECFP} female and male mosquitoes. Larvae were screened at stage 4 of larval development using an epifluorescence microscope to ensure that all mosquitoes had the genetic insertion.

2.4.1 Wing size

To prepare the wings for size measurements, 1-day-old mosquitoes were anesthetized using a cooling method. Both left and right wings of each mosquito were removed using fine forceps. Then, the wings were mounted on microscope slides under dry conditions, ensuring a flat position without any folds or distortions. To capture images of the wings, a digital camera (Nikon model

D3400) mounted with an adapter on a Leica binocular microscope with a $\times 20$ objective and adjusted to $\times 4$ magnification was used. The length of each wing was measured directly on the captured wing images using ImageJ software. Measurements were taken from the apex of the wing to the axillary incision, excluding the marginal fringe (Packer and Corbet, 1989; Pelizza et al., 2013) (Figure 3A). To convert the wing length from pixel units to millimeters, a picture of an eyepiece graticule taken under the same conditions as the wing slides was utilized. The left wing was chosen at random in each mosquito for analysis because the differences between the length of right and left wings were not significant (Figure 3B).

2.4.2 Dry weight

To determine the dry weight of the WT and the GABA-B1^{QF2-ECFP} lines, mosquitoes from each line were collected within 24 h of emerging and killed by placing them at 4°C for 1 day. The mosquitoes were sorted by sex and grouped within Petri dishes. The number of mosquitoes per group ranged between 12 and 37 mosquitoes. These Petri dishes were then placed inside a lidded box containing anhydrous calcium sulfate desiccant granules at room temperature. The mosquitoes remained in this condition for 10 days, allowing the desiccant to dehydrate and remove the moisture from the specimens. Once the desiccation period was complete, the dry weight of each group of mosquitoes was measured using a precise scale (Figure 4A). The estimated dry weight of one mosquito was determined by the total dry weight of the group divided by the number of mosquitoes in each group.

2.4.3 Number of eggs laid

In order to limit the effects of various physiological processes and external factors that can impact fertility, we have chosen to compare only fecundity between the WT and GABA-B1^{QF2-ECFP} lines. For this, 1 to 2-day-old female and male mosquitoes from the same line were placed together in a rearing cage (Bugdorm-1, MegaView Science Co., Ltd. Taichung 407008, Taiwan) for a period of 6 days and were fed 10% sucrose. The sex ratio within the cage was maintained at 1 female for every 3 males. After the 6-day period, the female mosquitoes were blood-fed and the following day fed females were individually transferred to 50 mL plastic tubes containing moist filter paper placed along the inner perimeter to allow the females to lay their eggs on the moist paper. 3–4 days after the ingestion of blood, once oviposition had occurred, the filter papers with the eggs were removed. A digital camera (Nikon model D3400) was used to capture images of the flat filter papers, and the software ImageJ was utilized to count the number of eggs laid by individual females (Figure 5A).

2.4.4 Longevity

Following an adapted protocol (Reiskind and Lounibos, 2009), within 24 h of emergence, female and male mosquitoes were sorted into different rearing cages (Bugdorm-1, MegaView Science Co., Ltd. Taichung 407008, Taiwan) and stored within a climatic chamber at 27°C, 70%–80% relative humidity, and a photoperiod cycle of 12 h light/12 h dark. Each experiment was replicated three to five times. After the initial 3-day holding period where the mosquitoes were fed on 10% sucrose, and any dead adults were removed, the food was removed. The number of dead mosquitoes was then checked twice a day, both in the morning and evening, until

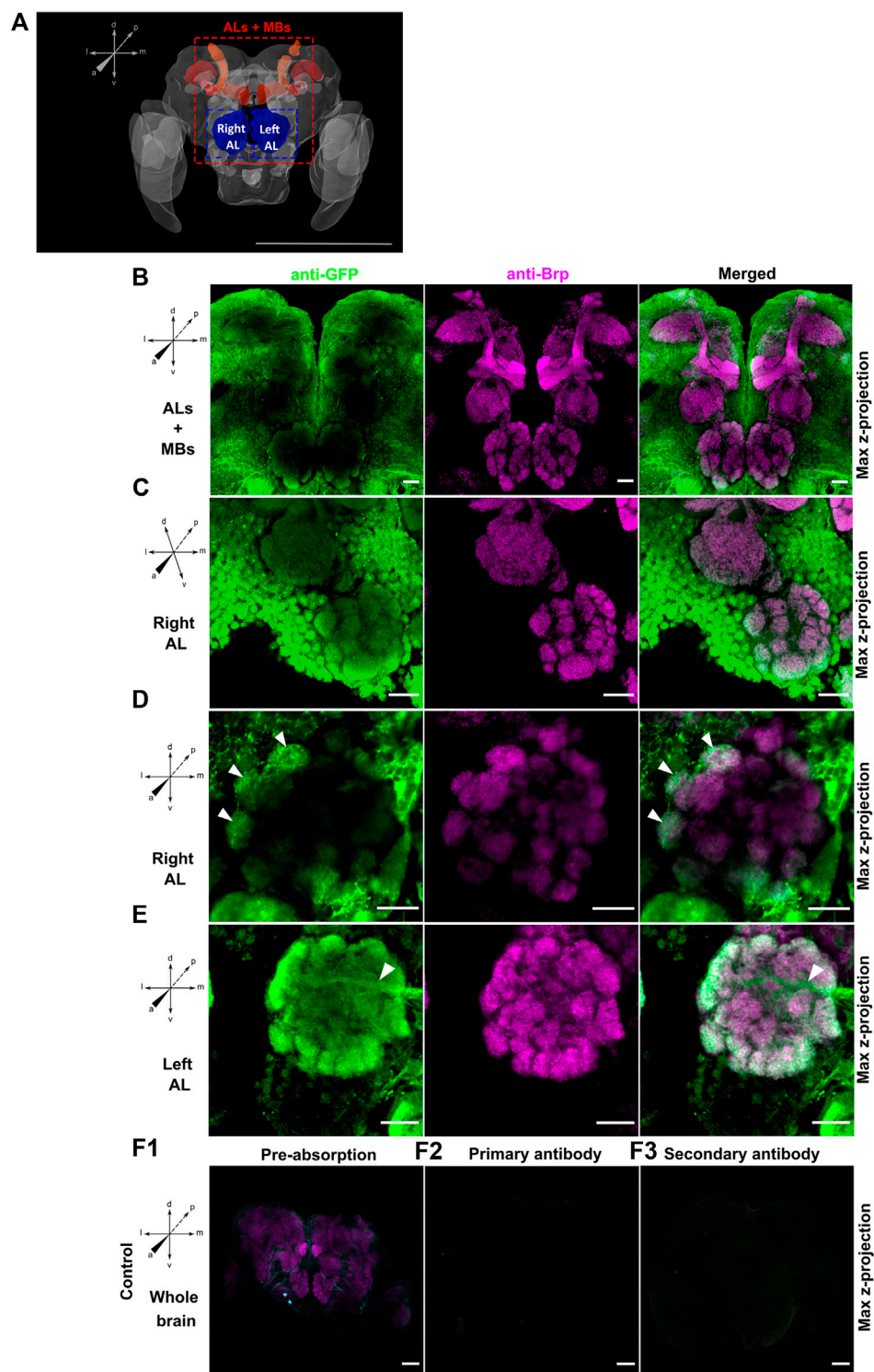


FIGURE 2
(A) Adapted schema of the *Ae. aegypti* brain from Insect Brain Database (Database, 2024) representing in red the mushroom bodies (MBs) and in blue the antennal lobes (ALs). Maximal projection view of confocal image stacks from male **(A,B,D and E)** and female **(C)** GABA-B1^{OF2-ECFP} > QUAS-mCD8GFP mosquito brains stained with anti-GFP antibody (green) and anti-Brp antibody (magenta). **(B)** View of antennal lobes (ALs) and mushroom bodies (MBs) area reveals that green fluorescent protein (GFP) expression is mainly present around the ALs while no expression is observed in the MBs. **(C)** Right antennal lobe (Right AL). GFP immunofluorescence shows expression of GABA-B1 in lateral and middle cell body clusters. **(D)** Right antennal lobe (Right AL). Neurons expressing the GABA-B1 receptor ramify multiple glomeruli (arrows). **(E)** Left antennal lobe (Left AL). GFP immunostaining overlaps with the presynaptic staining background in the peripheral glomeruli of ALs. A tract of GABA-B1-positive fiber entering the AL from the lateral side can be also seen (arrow). Different controls using different GABA-B1^{OF2-ECFP} > QUAS-mCD8GFP adult male brains were performed to test labeling specificity. **(F1)** The brain was preabsorbed with GFP protein. The preabsorption had almost abolished the GFP labeling without affecting the Bruchpilot (Brp) labeling. For the two other controls, either **(F2)** secondary antibodies or **(F3)** primary antibodies were omitted. Both controls showed no tissue labeling. Scale bars, 500 μ m **(A)** and 20 μ m **(B–F)**.

all mosquitoes in the population died. Longevity was defined by the most recent previous time-point at which the individual had been observed alive. Longevity is given in days after the initial 3-day holding period. (Figure 6A).

2.5 Olfactory preferences to attractive odors

A custom-made two-choice behavior assay was created to test the response of male and female GABA-B1^{QF2-ECFP} mosquitoes toward a known attractant. To prepare for the experiment, mosquitoes (3–5 day old) were starved overnight, placed inside cages (Bugdorm, 60 cm × 60 cm × 60 cm), and maintained on an inverted light/dark cycle. Our results showed that both males and females were strongly attracted to the trap with the banana odor (exact binomial test, for male $p = 1.943 \times 10^{-5}$; for female $p = 0.0009122$) and were not statistically different (Fisher's exact test, $p = 0.2564$)—we thus included both male and female mosquitoes in our trials. Environmental conditions in the behavior room were 25°C with a relative humidity of 70%–80%. The two-choice behavior assay consisted of a cage (55 × 55 cm) with two smaller traps that had a port in which mosquitoes could enter but not leave. The first container contained the attractant, and the second container contained the control (10% sucrose cotton ball). As an attractant, a banana was chosen as the fruit since it was easy to acquire throughout the year and elicited robust behavioral attraction. Both traps were laid on opposite sides of the cage and the mosquitoes were allowed to choose either the control or experimental trap for 48 h (Figure 7A). Mosquitoes that did not choose either trap were considered as not responsive and not included in the analysis. The placement of the traps was randomized to control for placement biases. The relative humidity difference between each pair of traps was observed to be within 5% of the absolute humidity and, therefore not considered to be attracting the animals. Each experiment was replicated 9 and 7 times for WT and GABA-B1^{QF2-ECFP} lines, respectively. The number of mosquitoes in each trap were counted and included in a Preference Index Assay. The Preference Index (PI) was calculated as $(E - C) / (E + C)$, where E is the number of mosquitoes inside the experimental trap, and C is the number of mosquitoes in the control trap.

2.6 Statistical analysis

Analyses were performed in R (version 4.3.0). For the wing size, the dry weight and the egg laying size data, the normal distribution of data was evaluated by the Shapiro-Wilk normality test. Following these results, to compare the wing size between GABA-B1^{QF2-ECFP} and WT line, we used the Student's t-test while to compare the dry weight and the egg laying size between both lines, we used the Mann-Whitney U test. For longevity, Kaplan-Meier analysis of survival with the log-rank test was made on pooled data according to sex and the line and used to do a pairwise comparison between the 2 lines. For the olfactory preference test, a binomial exact test was used to compare the choice of the mosquitoes in the cage between the both traps to a random distribution of 50% of each trap. A Fisher's exact test was also performed to make a direct comparison between both lines.

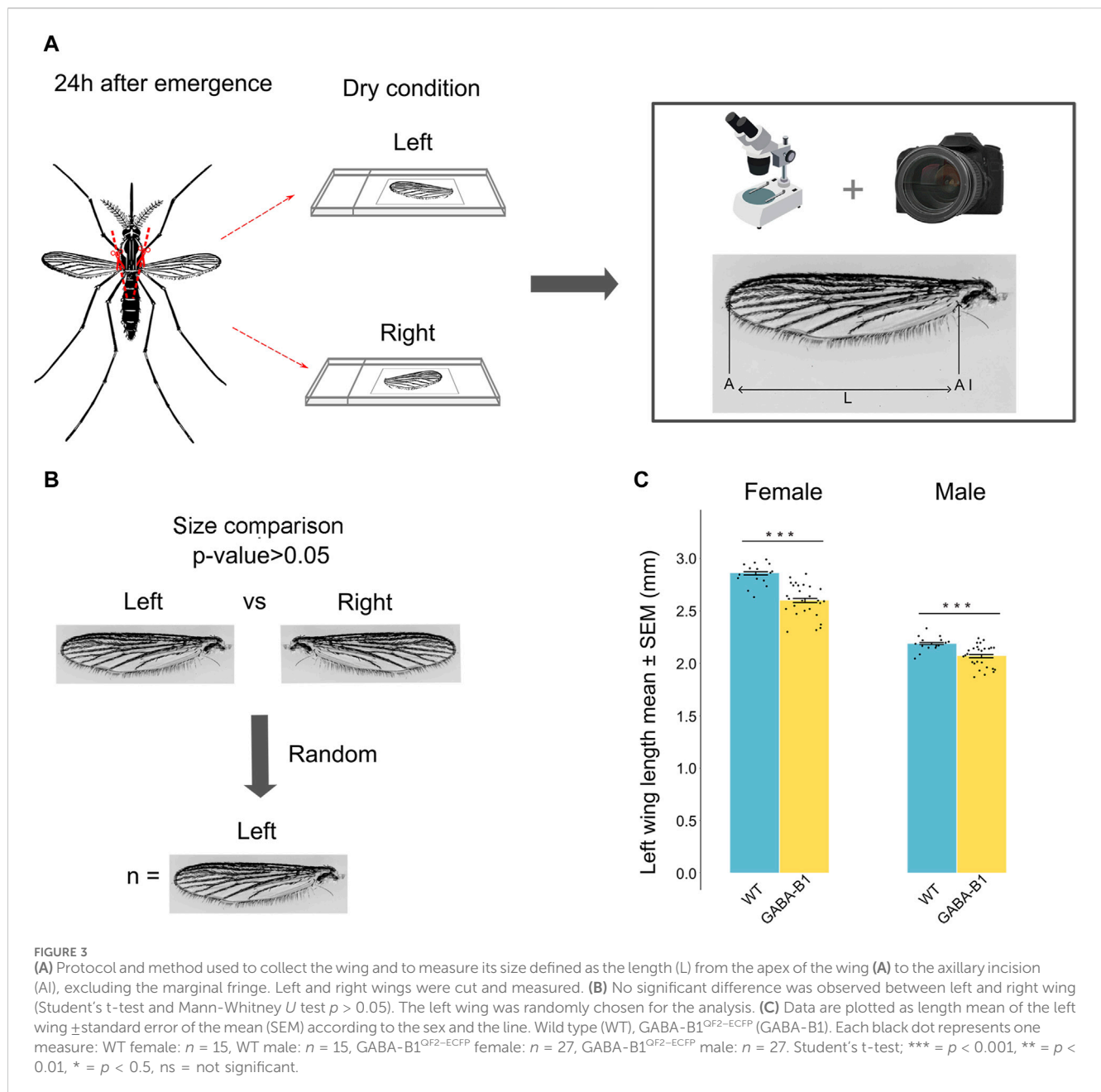
3 Results

3.1 Generating GABA-B1^{QF2-ECFP} transgenic line

To generate a CRISPR/Cas9 mediated HDR knock-in line, *GABA-B1* gene sequence was retrieved from Vectorbase. The *GABA-B1* gene is located on chromosome 2 and spans approximately 473 kb in length [AaegL5_2: 233,902,013.234,375,276 (–)], and is composed of a total of 16 protein-coding exons, and two non-coding exons which are located upstream of translational start codon (ATG). The target gRNA sequence is located on protein-coding exon-1 and was selected to undergo HDR and knock-in the DNA cassette downstream of 5'UTR and upstream of the translational start codon. The WT *Ae. aegypti* preblastoderm embryos ($n = 500$) were injected with an equal concentration of Cas9 protein, sgRNA, and knock-in donor plasmid (Figures 1A,B). A total of 337 adults (G_0) were recovered after the injection and were crossed with WT individuals, and G_1 eggs were collected. The genomic DNA PCR and Sanger sequencing from G_0 parents confirmed the integration site for the *GABA-B1* knock-in construct (Supplementary Figure S1). The left-side integration PCR confirmed that the knock-in construct integrated downstream of the 5'UTR sequence and upstream of the translational start codon, whereas the right-side integration PCR confirmed that the knock-in construct integrated 28 base pairs downstream of the translational start codon on coding exon-1 (Supplementary Figure S1). ECFP marker-expressing larvae (Figure 1D) were selected from every generation for inbreeding to establish a homozygous line.

3.2 GABA-B1 receptor localization in the mosquito olfactory system

To characterize the GABA-B1 receptor expression within the olfactory region of the *Ae. aegypti* brain, the driver QF2 line was first crossed with the QUAS-mCD8GFP reporter line to allow immunohistochemical localization of the receptor expression. The GFP immunofluorescence revealed low GABA-B1 receptor expression in the calyces and medial and vertical lobes of the MBs compared to outer regions, including the cell bodies. By contrast, the Brp staining clearly showed the different MB structures (Figure 2B). The GABA-B1 receptors were strongly expressed in the AL region. The strongest expression was observed in the lateral and middle cell body clusters surrounding the AL (Figure 2C). These results were consistent and found in male and female mosquitoes, and in both ALs (right and left). Within the AL glomeruli, GABA-B1-expressing neurons showed dendritic bleb-like processes. The GABAergic receptor expression appeared heterogeneous in the AL glomeruli, with higher expression in the outer regions of glomeruli where they receive input from olfactory sensory neurons. In addition, the glomeruli localized in the periphery of the AL show axial projections of neurons expressing GABA-B1 receptors (Figures 2D,E). These neurons do not emanate from the lateral and middle cell clusters but instead originate from a more central or medial area of the brain.



3.3 Bioassay

To evaluate the impact of the gene insertion on the fitness of GABA-B1^{QF2-ECFP} transgenic mosquitoes, we performed experiments comparing the size, weight, longevity, and female fecundity with WT mosquitoes.

3.3.1 Transgene insertion correlates with reduced wing size

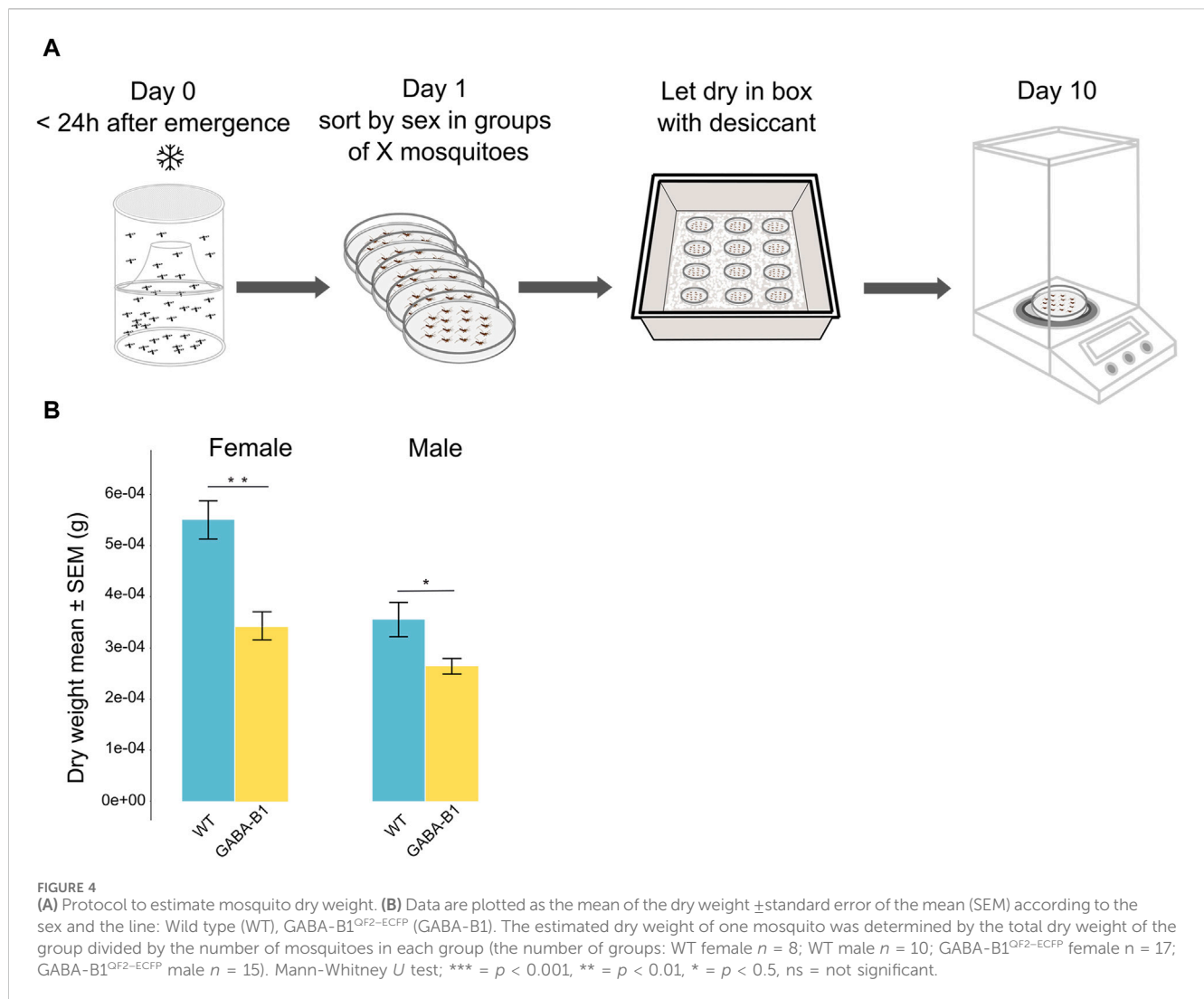
We examined the effects of transgene insertion on the wing size. For both mutants and WT, the wing size was longer in females than males. In GABA-B1^{QF2-ECFP} females and males, however, the transgene insertion significantly correlated with a reduced wing size compared to WT (for female and male: $p < 0.001$) (Figure 3C).

3.3.2 Transgene insertion correlates with reduced mass

Similar to what was observed for the wing size, males were still smaller than the females in both the WT and GABA-B1^{QF2-ECFP} lines. In addition, the GABA-B1^{QF2-ECFP} line showed significantly lower dry weight in both females and males compared to WT (for female: $p = 0.004$ and for male: $p = 0.05$) (Figure 4B).

3.3.3 Transgene insertion of GABA-B1^{QF2-ECFP} does not impact fecundity

On average, the WT females ($n = 10$) laid 49.6 ± 2.7 eggs while the GABA-B1^{QF2-ECFP} females ($n = 24$) laid 57.9 ± 3.7 eggs. This difference between the WT and the mutant lines was not significantly different ($p = 0.416$) (Figure 5B).



3.3.4 Transgene insertion has an impact on longevity

We compared the longevity of the mutant with WT. For the WT line, the survival probability of males was lower than the survival probability of females, while the survival probability is the same for GABA-B1^{QF2-ECFP} females and males. For the GABA-B1^{QF2-ECFP} females, longevity was significantly shorter compared with the WT females. (WT female vs. GABA-B1^{QF2-ECFP} female: $\chi^2 = 8.10$, $p = 0.004$). The median survival probability for GABA-B1^{QF2-ECFP} and WT females was 2 and 2.5 days, respectively. For the GABA-B1^{QF2-ECFP} males, longevity was significantly longer than the WT males, with a median survival probability at 2 and 1.5 days for GABA-B1^{QF2-ECFP} and WT males, respectively (WT male vs. GABA-B1^{QF2-ECFP} male: $\chi^2 = 40.20$, $p < 0.001$) (Figure 6B).

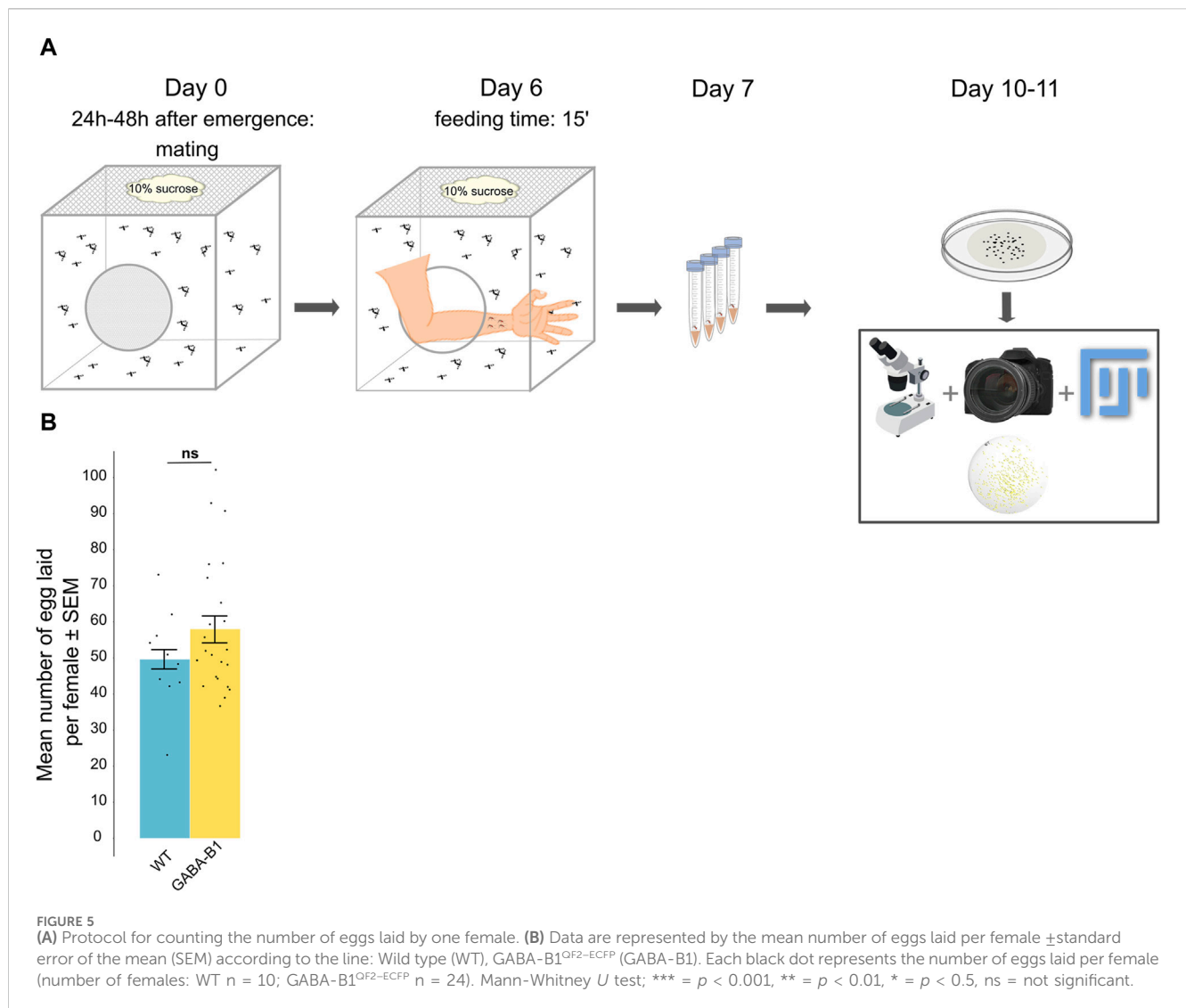
3.4 Olfactory preferences to attractive odors

The ability of mutant to respond to attractive odors, such as fruit, was evaluated by two-choice behavior assay where the mosquitoes are released in a cage and can choose between 2 traps

containing either an attractive odor or no odor (control). WT mosquitoes exhibited a strong attraction for the banana (exact binomial test $p < 0.001$). By contrast, the mutant mosquitoes did not show any preference for banana (exact binomial test $p = 1$) and exhibited the same behavior as mosquitoes exposed to the no-odor control (exact binomial test $p = 0.6208$) (Figure 7B). When comparing between treatments, the preference observed between WT and GABA-B1^{QF2-ECFP} groups and the WT and control groups were both significant (Fisher's exact test, WT vs. GABA-B1^{QF2-ECFP}: $p = 4.518 \times 10^{-5}$; WT vs. control: $p = 7.719 \times 10^{-10}$), while the preference was similar between the GABA-B1^{QF2-ECFP} and the control groups (Fisher's exact test, GABA-B1^{QF2-ECFP} vs. control: $p = 1$)

4 Discussion

We have developed a new transgenic line in one of the main disease vectors, *Ae. aegypti*. Using the CRISPR/Cas9 mediated HDR knock-in approach, the QF2 transcription factor was inserted in the GABA-B1 receptor gene locus, disrupting the coding sequence of the gene. The GABA-B1^{QF2-ECFP} mutant, expressing the ECFP marker



visible in the abdomen at the larval stage, survived and bred in the laboratory over multiple generations without any visible fitness issues, enabling us to establish a homozygous line. This knock-out line phenotype is phenotypically still quite similar to the WT one. The GABA-B1^{QF2-ECFP} individuals show a moderate reduction in size and mass, but not the number of eggs laid. There is a positive correlation between the size and the weight (Packer and Corbet, 1989). Although females of the GABA-B1^{QF2-ECFP} line showed greater variability in survival compared to the WT, male mutant, and WT lines exhibited similar trends in longevity, with the survival probability approaching 0% at approximately 4–5 days. The GABA-B1^{QF2-ECFP} line showed reduced attractiveness to scent emitted from banana fruit odor, which is shown to be attractive to mosquitoes (Paskewitz et al., 2018; Musunzaji et al., 2023).

The reduced attraction to the fruit scent may reflect the importance of GABAergic inhibition in the mosquito olfactory system. The GABA-B1's heterodimerization with the GABA-B2 subunit is critical for protein structure and function (Galvez et al., 2001; Mezler et al., 2001). In the *Ae. aegypti* mosquito, the antennae have abundant GABA_B receptors (Tallon et al., 2019). In *Drosophila*, olfactory receptor neurons (ORNs) express GABA_B receptors involved in presynaptic inhibition and reducing the

GABA_B receptor expression at the presynaptic terminals of ORNs impairs the capability of *Drosophila* flies to locate potential mates (Root et al., 2008). Additionally, the presynaptic inhibition mediated by GABA_B receptors offers a mechanism for adjusting olfactory gain. It was demonstrated that the expression of GABA_B receptors in ORNs scales the gain of PN responses (Olsen and Wilson, 2008). The work in *Drosophila* is reflected in results from the *Ae. aegypti* mosquito, where GABAergic inhibition in the AL was critical for the processing and the discrimination between attractive and repellent odors. Pharmacological interventions using GABA_B receptor antagonists prevented lateral inhibition of specific glomeruli that encoded attractive floral odors (Lahondère et al., 2020).

The GABA-B1^{QF2-ECFP} line was successfully used with the Q-system to drive mCD8GFP expression, allowing characterization of the GABA-B1 receptor expression in the *Ae. aegypti* brain, specifically focusing on loci involved in olfactory processing. The GABA-B1 receptor was not strongly expressed in all brain structures involved in olfactory processing. The receptors showed reduced expression in the MB lobes, although strongly expressed in the MB calyces (Figure 2). The receptors were also strongly expressed in lateral and middle cell body clusters surrounding AL. The peripheral AL glomeruli receive axial

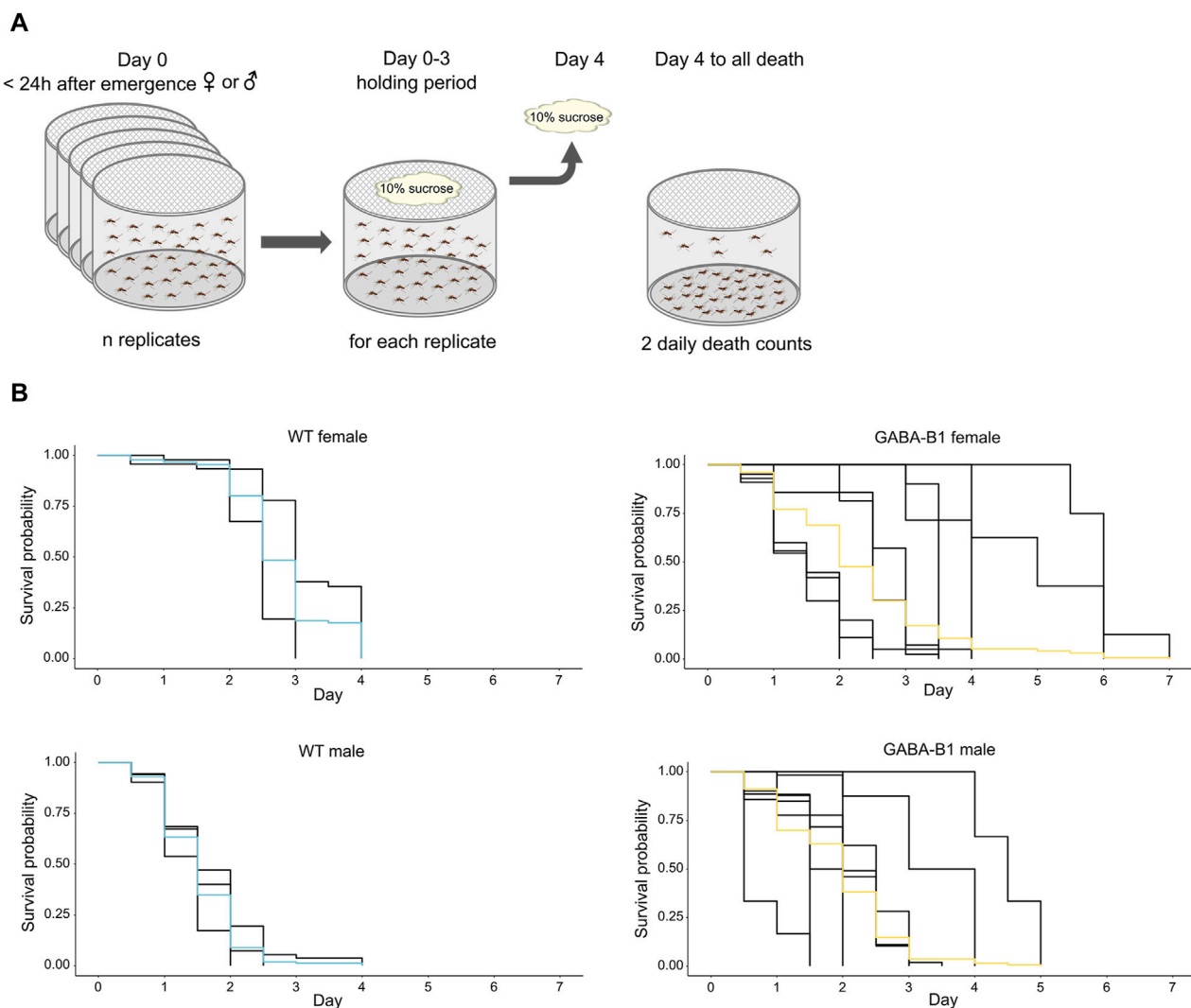
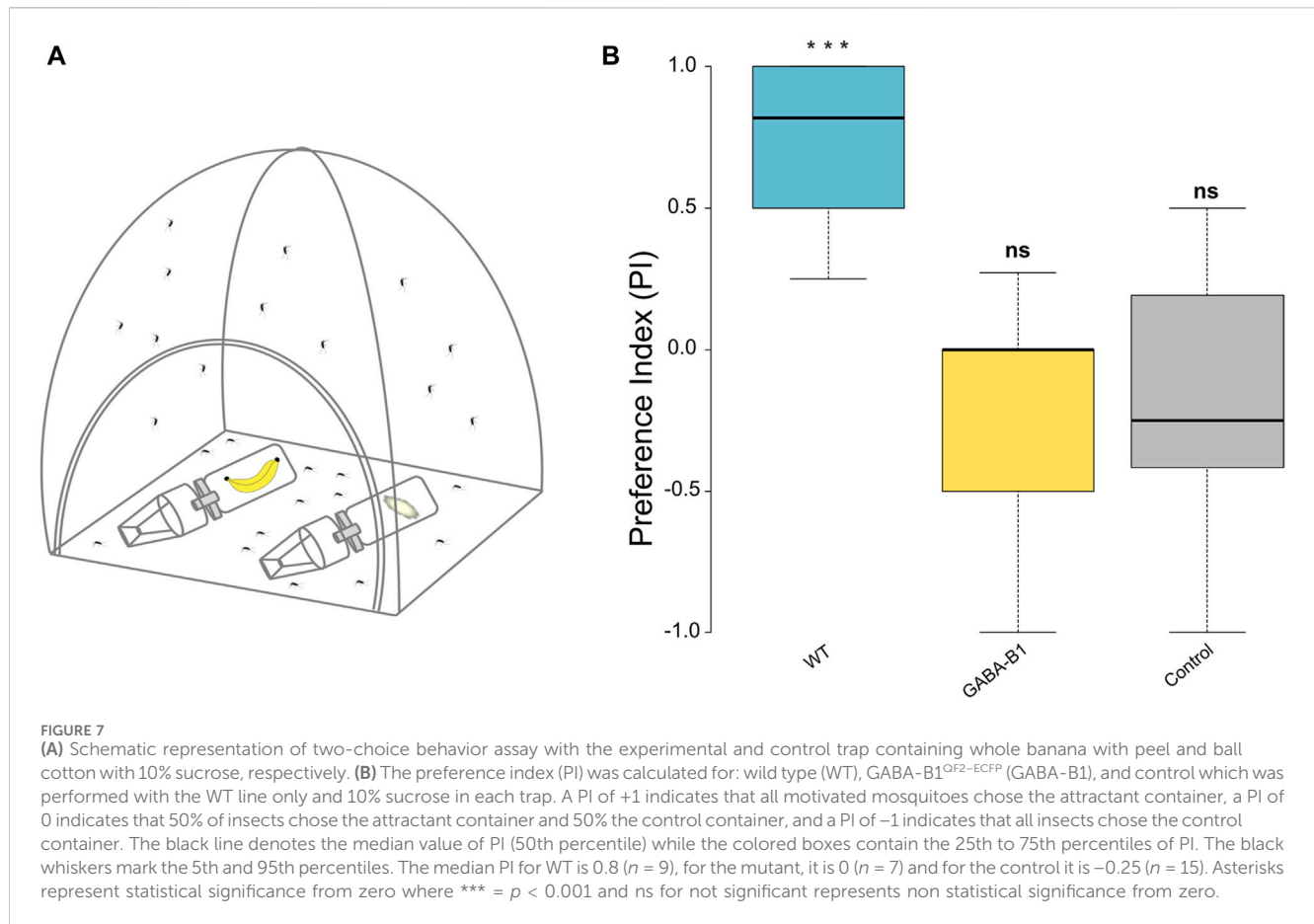


FIGURE 6

(A) Protocol to collect survival data. (B) Survival probability over time for each mosquito line after the 10% sucrose is removed. Differences in longevity is compared using Kaplan-Meier analysis. Each black trace corresponds to an individual replicate, and colored curves represent the overall survival probability.

projections from neurons expressing GABA receptors localized in central and medial areas of the brain. These results are consistent with earlier studies in *Ae. aegypti*, where the GABA-positive cell bodies are observed in the lateral and ventral clusters around the ALs and in the tracts from the lateral area going into the ALs (Singh et al., 2023). These lateral cell clusters probably correspond to LN clusters as previously found in *Ae. aegypti*. LNs typically project ipsilaterally, and in most of case, their innervation extends to the entire glomerulus. But there is also a small proportion of them which can exhibit a selective innervation to glomeruli. In *Drosophila*, similar to *Ae. aegypti*, many GABA-positive somata are observed in the lateral area of the AL neuropil (Wilson and Laurent, 2005). Among cell bodies bordering the ALs, the dorsolateral cluster contains cell bodies of both PNs and LNs, while anterodorsal cluster contains cell bodies of PNs (Wong et al., 2002; Das et al., 2008; Lai et al., 2008). PNs project from AL to the calyx of MB via the medial antennal lobe tract (mALT), while LNs, showing an ipsilateral projection in the AL, spread their neurites into most glomeruli

which contain both presynaptic and postsynaptic connections (Wilson and Laurent, 2005). As mALT neurons have limited presynaptic sites in the AL, LNs are the primary source of GABA signal in this specific *Drosophila* brain region. Moreover, both GABAergic mALT PNs and LNs and non-GABAergic lateral antennal lobe tract (lALT) PNs, projecting from AL to Lateral Horn, express genes of various ionotropic and metabotropic GABA receptor subunits. In addition, metabotropic receptors are expressed in the whole brain with a narrower population of cell bodies around the MB calyx, unlike ionotropic receptors, which are more widely presented in this part of the brain (Okada et al., 2009). In addition, both subunits of GABA_B receptors, GABA-B1 and GABA-B2 are co-expressed in similar regions (Okada et al., 2009). GABA receptors are also expressed in the ALs (Enell et al., 2007). The anatomical expression of the GABA_B receptor observed in our study also presents similarities with moths. In different moth species, LNs are always situated in the lateral cell clusters and the most multiglomerular LNs in the AL are GABA-positive



(Hoskins et al., 1986; Christensen et al., 1993; Anton and Hansson, 1994). In *Bombyx mori*, around 30% of lateral cell body clusters are GABAergic and, like *Ae. aegypti* and *Drosophila*, some of them are LNs that arborize in all AL glomeruli. Axonal PN tracts are also GABA-positive (Hoskins et al., 1986).

The development of the GABA-B1^{QF2-ECFP} mutant line also offers the future ability to characterize and manipulate neuronal functioning. For example, recently developed reporter lines (QUAS-GCaMP7s, QUAS-Crimson, and QUAS-Kir) may allow the characterization of GABA-B1-expressing neurons during odor activation (via QUAS-GCaMP7s), or manipulation of the neuronal activity by crossing the GABA-B1^{QF2-ECFP} line with QUAS-Crimson or QUAS-Kir. The GABA-B1^{QF2-ECFP} mutant line also is a promising tool for examining the neuronal mechanisms of odor representation mediated by GABA inhibition. Indeed, while GABA_A receptors shape and synchronize PN activity during the early phase of odor response, GABA_B receptors mediate odor-evoked inhibition on the longer time scales (>300 ms) relevant for encoding fluctuating odors that occur in odor plumes (Lei et al., 2002; Wilson and Laurent, 2005). In *Drosophila*, pre-synaptic inhibition of glomeruli encoding attractants (DM2 and DM3) via GABA_B receptors has been shown to be important for behavior (Mohamed et al., 2019), although both GABA_B and GABA_A receptor types are involved in mixture processing. Moreover, the modulation exerted by GABA_B receptors is wider, because it involves both pre- and postsynaptic mechanisms (Ozoe, 2013).

Beyond their importance in neural circuit functioning, GABA receptor types are pharmacological targets in insects. The GABA_A receptor contains subunits encoded by *Rdl*, which is the site of action for many insecticides. But serious problems of insecticide resistance have been observed, in particular in *Ae. aegypti* populations (Zulfa et al., 2022). As a vector of the pathogens of diseases causing 96 million new cases and around 40,000 deaths every year in the case of dengue alone (World Health Organization, 2020), there is an urgent need to investigate other insecticide targets. The GABA-B1 receptor is a promising target as it is involved in vital physiological mechanisms. In *Drosophila*, the developmental role of GABA-B1 receptors was demonstrated using an injectable RNAi method. Initially designed for selective gene suppression in adult flies, the method was adapted for embryos. Injections of double-stranded RNA targeting GABA-B1 or a GABA_B antagonist CGP54626 resulted in lethality by the third larval stage. The affected larvae were smaller, with compressed and folded tracheae, suggesting that GABA_B receptor antagonism disrupts the molting process during development (Dzitoyeva et al., 2005). GABA_B receptors also play a role in regulating circadian rhythms through the clock neurons and neuronal circuits of the circadian system. It was demonstrated that the master clock neurons, s-LN(v)s, utilize GABA as a slow inhibitory neurotransmitter that can be blocked by a GABA_B antagonist (Hamasaka et al., 2005). GABA_B receptors have been identified as pharmacological targets (Bowery, 2006) and could bring new solutions to manage vector populations.

In conclusion, the development of the GABA-B1^{QF2-ECFP} mutant line in *Ae. aegypti*, achieved through CRISPR/Cas9-mediated HDR knock-in, offers a valuable new neurogenetic tool for investigating the role of the GABAergic systems within the central olfactory system and will help us to investigate its role in the processing of attractive odors. The observed changes in attractiveness to fruit scents emphasize the importance of the GABA-B1 receptor in mosquito olfaction. Consequently, GABA-B1 receptors can be considered as potential pharmacological targets that present promising prospects for addressing insecticide resistance and developing novel strategies for vector population control.

Data availability statement

The original contributions presented in the study are included in the article/**Supplementary Material**, further inquiries can be directed to the corresponding author.

Ethics statement

The manuscript presents research on animals that do not require ethical approval for their study.

Author contributions

AR: Conceptualization, Data curation, Formal Analysis, Investigation, Methodology, Visualization, Writing—original draft, Writing—review and editing. AP: Investigation, Visualization, Writing—original draft. ML-N: Investigation, Methodology, Writing—original draft. ML: Investigation, Methodology, Writing—review and editing. IC-A: Investigation, Methodology, Writing—review and editing. OA: Conceptualization, Funding acquisition, Supervision, Writing—review and editing. JR: Conceptualization, Funding acquisition, Supervision, Writing—original draft, Writing—review and editing.

Funding

The author(s) declare that financial support was received for the research, authorship, and/or publication of this article. This study was supported by the National Science Foundation under grant 2124777; and the National Institutes of Health under grants R01AI148300 and R01AI175152.

References

- Anton, S., and Hansson, B. S. (1994). Central processing of sex pheromone, host odour, and oviposition deterrent information by interneurons in the antennal lobe of female *Spodoptera littoralis* (Lepidoptera: noctuidae). *J. Comp. Neurology* 350, 199–214. doi:10.1002/cne.903500205
- Bowery, N. G. (2006). GABAB receptor: a site of therapeutic benefit. *Curr. Opin. Pharmacol.* 6, 37–43. doi:10.1016/j.coph.2005.10.002
- Brotz, T. M., Gundelfinger, E. D., and Borst, A. (2001). Cholinergic and GABAergic pathways in fly motion vision. *BMC Neurosci.* 2, 1. doi:10.1186/1471-2202-2-1
- Bui, M.A.-, Li, M.A.-, Raban, R. R. A.-, Liu, N.A.-, and Akbari, O. S. A.- (2020). Embryo microinjection techniques for efficient site-specific mutagenesis in *Culex quinquefasciatus*. *JoVE*, e61375. doi:10.3791/61375

Acknowledgments

We thank Binh Nguyen for taking care of the mosquito colony, Pramod KC for his help in the brain orientation and Wai Pang Chan for his advice on imaging. We would like to thank Jason Pitts, Dan Kline for their helpful discussion. We thank Judy Ishikawa for helping with mosquito husbandry and microinjections at University of California, San Diego.

Conflict of interest

OA is a founder of Agragene, Inc. and Synvect, Inc. with equity interest. The terms of this arrangement have been reviewed and approved by the University of California, San Diego in accordance with its conflict-of-interest policies. The remaining authors declare that the research was conducted in the absence of any commercial or financial relationships that could be construed as a potential conflict of interest.

Publisher's note

All claims expressed in this article are solely those of the authors and do not necessarily represent those of their affiliated organizations, or those of the publisher, the editors and the reviewers. Any product that may be evaluated in this article, or claim that may be made by its manufacturer, is not guaranteed or endorsed by the publisher.

Supplementary material

The Supplementary Material for this article can be found online at: <https://www.frontiersin.org/articles/10.3389/fphys.2024.1381164/full#supplementary-material>

SUPPLEMENTARY TABLE S1

List of oligos used in this study.

SUPPLEMENTARY FIGURE S1

Genotyping of GABA-B1^{QF2-ECFP} line. **(A and B)** The schematic representation of the GABA-B1 gene structure and homology-directed repair (HDR) knock-in construct. The black arrow with F1-R1 and F2-R2 represents the primers used for genotyping PCR to determine the left and right-side integration of knock-in. **(C)** PCR products obtained from genotyping PCR were analyzed on 1% agarose gel and their nucleotide sequences were confirmed by Sanger sequencing. Left and right-side integration PCR performed using the GABA-B1^{QF2-ECFP} line genomic DNA template, whereas negative control PCR was performed using wild type genomic DNA template or no template. **(D)** The nucleotide sequence alignment of the left and right-side integration PCR confirmed the precise genomic insertion of the knock-in construct. The knock-in construct (top nucleotide sequences) is used as a reference sequence to align with the left and right site integration PCR sequence (bottom nucleotide sequences and chromatograms).

- Casida, J. E., and Durkin, K. A. (2015). Novel GABA receptor pesticide targets. *Pesticide Biochem. Physiology* 121, 22–30. doi:10.1016/j.pestbp.2014.11.006
- CHOPCHOP (2024). CHOPCHOP. Available at: <https://chopchop.cbu.uib.no/> (Accessed January 23, 2024).
- Christensen, T. A., Waldrop, B. R., Harrow, I. D., and Hildebrand, J. G. (1993). Local interneurons and information processing in the olfactory glomeruli of the moth *Manduca sexta*. *J. Comp. Physiology A* 173, 385–399. doi:10.1007/BF00193512
- Das, A., Sen, S., Lichtneckert, R., Okada, R., Ito, K., Rodrigues, V., et al. (2008). *Drosophila* olfactory local interneurons and projection neurons derive from a common neuroblast lineage specified by the empty spiracles gene. *Neural Dev.* 3, 33. doi:10.1186/1749-8104-3-33
- Database (2024). Insect brain Database. Available at: <https://insectbraindb.org/app/> (Accessed January 23, 2024).
- Davis, R. L. (1993). Mushroom bodies and *drosophila* learning. *Neuron* 11, 1–14. doi:10.1016/0896-6273(93)90266-T
- Dupuis, J. P., Bazet, M., Barbara, G. S., Pauter, S., Gauthier, M., and Raymond-Delpéch, V. (2010). Homomeric RDL and heteromeric RDL/LCCH3 GABA receptors in the honeybee antennal lobes: Two candidates for inhibitory transmission in olfactory processing. *J. of Neurophys.* 103, 458–468. doi:10.1152/jn.00798.2009
- Dzitoyeva, S., Gutnov, A., Imbesi, M., Dimitrijevic, N., and Manev, H. (2005). Developmental role of GABAB(1) receptors in *Drosophila*. *Dev. Brain Res.* 158, 111–114. doi:10.1016/j.devbrainres.2005.06.005
- Enell, L., Hamasaka, Y., Kolodziejczyk, A., and Nässel, D. R. (2007). gamma-Aminobutyric acid (GABA) signaling components in *Drosophila*: immunocytochemical localization of GABA(B) receptors in relation to the GABA(A) receptor subunit RDL and a vesicular GABA transporter. *J. Comp. Neurology* 505, 18–31. doi:10.1002/cne.21472
- French-Constant, R. H., Mortlock, D. P., Shaffer, C. D., MacIntyre, R. J., and Roush, R. T. (1991). Molecular cloning and transformation of cyclodiene resistance in *Drosophila*: an invertebrate gamma-aminobutyric acid subtype A receptor locus. *Proc. Natl. Acad. Sci.* 88, 7209–7213. doi:10.1073/pnas.88.16.7209
- Freifeld, L., Clark, D. A., Schnitzer, M. J., Horowitz, M. A., and Clandinin, T. R. (2013). GABAergic lateral interactions tune the early stages of visual processing in *Drosophila*. *Neuron* 78, 1075–1089. doi:10.1016/j.neuron.2013.04.024
- Galvez, T., Duthey, B., Kniazef, J., Blahos, J., Rovelli, G., Bettler, B., et al. (2001). Allosteric interactions between GB1 and GB2 subunits are required for optimal GABAB receptor function. *EMBO J.* 20, 2152–2159. doi:10.1093/emboj/20.9.2152
- Gibson, D. G., Young, L., Chuang, R.-Y., Venter, J. C., Hutchison, C. A., and Smith, H. O. (2009). Enzymatic assembly of DNA molecules up to several hundred kilobases. *Nat. Methods* 6, 343–345. doi:10.1038/nmeth.1318
- Hamasaka, Y., Wegener, C., and Nässel, D. R. (2005). GABA modulates *Drosophila* circadian clock neurons via GABAB receptors and decreases in calcium. *J. Neurobiol.* 65, 225–240. doi:10.1002/neu.20184
- Harvey, R. J., Schmitt, B., Hermans-Borgmeyer, I., Gundelfinger, E. D., Betz, H., and Darlison, M. G. (1994). Sequence of a *Drosophila* ligand-gated ion-channel polypeptide with an unusual amino-terminal extracellular domain. *J. Neurochem.* 62, 2480–2483. doi:10.1046/j.1471-4159.1994.62062480.x
- Heisenberg, M., Borst, A., Wagner, S., and Byers, D. (1985). *Drosophila* mushroom body mutants are deficient in olfactory learning. *J. Neurogenetics* 2, 1–30. doi:10.3109/01677068509100140
- Henderson, J. E., Soderlund, D. M., and Knipple, D. C. (1993). Characterization of a putative gamma-aminobutyric acid (GABA) receptor beta subunit gene from *Drosophila melanogaster*. *Biochem. Biophysical Res. Commun.* 193, 474–482. doi:10.1006/bbrc.1993.1648
- Hofbauer, A., Ebel, T., Waltenspiel, B., Oswald, P., Chen, Y., Halder, P., et al. (2009). The wuerzburg hybridoma library against *Drosophila* brain. *J. Neurogenetics* 23, 78–91. doi:10.1080/01677060802471627
- Homberg, U. (2002). Neurotransmitters and neuropeptides in the brain of the locust. *Microsc. Res. Tech.* 56, 189–209. doi:10.1002/jemt.10024
- Hosie, A., Sattelle, D., Aronstein, K., and French-Constant, R. (1997). Molecular biology of insect neuronal GABA receptors. *Trends Neurosci.* 20, 578–583. doi:10.1016/S0166-2236(97)01127-2
- Hoskins, S. G., Homberg, U., Kingan, T. G., Christensen, T. A., and Hildebrand, J. G. (1986). Immunocytochemistry of GABA in the antennal lobes of the sphinx moth *Manduca sexta*. *Cell. Tissue Res.* 244, 243–252. doi:10.1007/BF00219199
- Hsu, C. T., and Bhandawat, V. (2016). Organization of descending neurons in *Drosophila melanogaster*. *Sci. Rep.* 6, 20259. doi:10.1038/srep20259
- Lahondère, C., Vinauger, C., Okubo, R. P., Wolff, G. H., Chan, J. K., Akbari, O. S., et al. (2020). The olfactory basis of orchid pollination by mosquitoes. *Proc. Natl. Acad. Sci.* 117, 708–716. doi:10.1073/pnas.1910589117
- Lai, S.-L., Awasaki, T., Ito, K., and Lee, T. (2008). Clonal analysis of *Drosophila* antennal lobe neurons: diverse neuronal architectures in the lateral neuroblast lineage. *Development* 135, 2883–2893. doi:10.1242/dev.024380
- Leal, S. M., and Neckameyer, W. S. (2002). Pharmacological evidence for GABAergic regulation of specific behaviors in *Drosophila melanogaster*. *J. Neurobiol.* 50, 245–261. doi:10.1002/neu.10030
- Lei, H., Christensen, T. A., and Hildebrand, J. G. (2002). Local inhibition modulates odor-evoked synchronization of glomerulus-specific output neurons. *Nat. Neurosci.* 5, 557–565. doi:10.1038/nn0602-859
- Li, M., Yang, T., Bui, M., Gamez, S., Wise, T., Kandul, N. P., et al. (2021). Suppressing mosquito populations with precision guided sterile males. *Nat. Commun.* 12, 5374. doi:10.1038/s41467-021-25421-w
- Li, M., Yang, T., Kandul, N. P., Bui, M., Gamez, S., Raban, R., et al. (2020). Development of a confinable gene drive system in the human disease vector *Aedes aegypti*. *eLife* 9, e51701. doi:10.7554/eLife.51701
- Liou, N.-F., Lin, S.-H., Chen, Y.-J., Tsai, K.-T., Yang, C.-J., Lin, T.-Y., et al. (2018). Diverse populations of local interneurons integrate into the *Drosophila* adult olfactory circuit. *Nat. Commun.* 9, 2232. doi:10.1038/s41467-018-04675-x
- Liu, X., and Davis, R. L. (2009). The GABAergic anterior paired lateral neuron suppresses and is suppressed by olfactory learning. *Nat. Neurosci.* 12, 53–59. doi:10.1038/nn.2235
- Loh, Y. M., Su, M. P., Ellis, D. A., and Andrés, M. (2023). The auditory efferent system in mosquitoes. *Front. Cell. Dev. Biol.* 11, 1123738. doi:10.3389/fcell.2023.1123738
- Mezler, M., Müller, T., and Raming, K. (2001). Cloning and functional expression of GABAB receptors from *Drosophila*. *Eur. J. Neurosci.* 13, 477–486. doi:10.1046/j.1460-9568.2001.01410.x
- Mohamed, A. A. M., Retzke, T., Das Chakraborty, S., Fabian, B., Hansson, B. S., Knaden, M., et al. (2019). Odor mixtures of opposing valence unveil inter-glomerular crosstalk in the *Drosophila* antennal lobe. *Nat. Commun.* 10, 1201. doi:10.1038/s41467-019-09069-1
- Musunzaji, P. S., Ndenga, B. A., Mzee, S., Abubakar, L. U., Kitron, U. D., Labeaud, A. D., et al. (2023). Oviposition preferences of *Aedes aegypti* in msambweni, kwale county, Kenya. *J. Am. Mosquito Control Assoc.* 39, 85–95. doi:10.2987/22-7103
- Okada, R., Awasaki, T., and Ito, K. (2009). Gamma-aminobutyric acid (GABA)-mediated neural connections in the *Drosophila* antennal lobe. *J. Comp. Neurology* 514, 74–91. doi:10.1002/cne.21971
- Olsen, S. R., and Wilson, R. I. (2008). Lateral presynaptic inhibition mediates gain control in an olfactory circuit. *Nature* 452, 956–960. doi:10.1038/nature06864
- Ozoe, Y. (2013). “Chapter four - γ -aminobutyrate- and glutamate-gated chloride channels as targets of insecticides,” in *Advances in insect Physiology*. Editor E. Cohen (Germany: Academic Press), 211–286. doi:10.1016/B978-0-12-394389-7.00004-1
- Ozoe, Y. (2021). Ion channels and G protein-coupled receptors as targets for invertebrate pest control: from past challenges to practical insecticides. *Biosci. Biotechnol. Biochem.* 85, 1563–1571. doi:10.1093/bbb/zbab089
- Packer, M. J., and Corbet, P. S. (1989). Size variation and reproductive success of female *Aedes punctator* (Diptera: Culicidae). *Ecol. Entomol.* 14, 297–309. doi:10.1111/j.1365-2311.1989.tb00960.x
- Paskewitz, S., Irwin, P., Konwinski, N., and Larson, S. (2018). Impact of consumption of bananas on attraction of *Anopheles stephensi* to humans. *Insects* 9, 129. doi:10.3390/insects9040129
- Pelizza, S. A., Scorsetti, A. C., and Tranchida, M. C. (2013). The sublethal effects of the entomopathogenic fungus *Leptoglyphia chapmanii* on some biological parameters of the dengue vector *Aedes aegypti*. *J. Insect Sci.* 13, 22. doi:10.1673/031.013.2201
- Primordium (2023). Primordium labs. Available at: <https://www.primordiumlabs.com/> (Accessed January 23, 2024).
- Raghu, S. V., Claussen, J., and Borst, A. (2013). Neurons with GABAergic phenotype in the visual system of *Drosophila*. *J. Comp. Neurology* 521, 252–265. doi:10.1002/cne.23208
- Reiskind, M. H., and Lounibos, L. P. (2009). Effects of intraspecific larval competition on adult longevity in the mosquitoes *Aedes aegypti* and *Aedes albopictus*. *Med. Veterinary Entomology* 23, 62–68. doi:10.1111/j.1365-2915.2008.00782.x
- Riabina, O., Task, D., Marr, E., Lin, C.-C., Alford, R., O’Brochta, D. A., et al. (2016). Organization of olfactory centres in the malaria mosquito *Anopheles gambiae*. *Nat. Commun.* 7, 13010. doi:10.1038/ncomms13010
- Rogers, S. M., Matheson, T., Sasaki, K., Kendrick, K., Simpson, S. J., and Burrows, M. (2004). Substantial changes in central nervous system neurotransmitters and neuromodulators accompany phase change in the locust. *J. Exp. Biol.* 207, 3603–3617. doi:10.1242/jeb.01183
- Root, C. M., Masuyama, K., Green, D. S., Enell, L. E., Nässel, D. R., Lee, C.-H., et al. (2008). A presynaptic gain control mechanism fine-tunes olfactory behavior. *Neuron* 59, 311–321. doi:10.1016/j.neuron.2008.07.003
- Shankar, S., and McMeniman, C. J. (2020). An updated antennal lobe atlas for the yellow fever mosquito *Aedes aegypti*. *PLOS Neglected Trop. Dis.* 14, e0008729. doi:10.1371/journal.pntd.0008729
- Singh, P., Goyal, S., Gupta, S., Garg, S., Tiwari, A., Rajput, V., et al. (2023). Combinatorial encoding of odors in the mosquito antennal lobe. *Nat. Commun.* 14, 3539. doi:10.1038/s41467-023-39303-w

- Stopfer, M., Bhagavan, S., Smith, B., and Laurent, G. (1997). Impaired odour discrimination on desynchronization of odour-encoding neural assemblies. *Nature* 390, 70–74. doi:10.1038/36335
- Tallon, A. K., Hill, S. R., and Ignell, R. (2019). Sex and age modulate antennal chemosensory-related genes linked to the onset of host seeking in the yellow-fever mosquito, *Aedes aegypti*. *Sci. Rep.* 9, 43. doi:10.1038/s41598-018-36550-6
- Tastekin, I., Khandelwal, A., Tadres, D., Fessner, N. D., Truman, J. W., Zlatić, M., et al. (2018). Sensorimotor pathway controlling stopping behavior during chemotaxis in the *Drosophila melanogaster* larva. *eLife* 7, e38740. doi:10.7554/eLife.38740
- VectorBase (2022). VectorBase. Available at: <https://vectorbase.org/vectorbase/app> (Accessed January 23, 2024).
- Waldrop, B., Christensen, T., and Hildebrand, J. (1987). GABA-mediated synaptic inhibition of projection neurons in the antennal lobes of the sphinx moth, *Manduca sexta*. *J. Comp. physiology. A, Sens. neural, Behav. physiology* 161, 23–32. doi:10.1007/bf00609452
- Wilson, R. I., and Laurent, G. (2005). Role of GABAergic inhibition in shaping odor-evoked spatiotemporal patterns in the *Drosophila* antennal lobe. *J. Neurosci.* 25, 9069–9079. doi:10.1523/JNEUROSCI.2070-05.2005
- Wong, A. M., Wang, J. W., and Axel, R. (2002). Spatial representation of the glomerular map in the *Drosophila* protocerebrum. *Cell* 109, 229–241. doi:10.1016/S0092-8674(02)00707-9
- World Health Organization (2020). Vector-borne diseases. Available at: <https://www.who.int/news-room/factsheets/>.
- Yasuyama, K., Meinertzhagen, I. A., and Schürmann, F.-W. (2002). Synaptic organization of the mushroom body calyx in *Drosophila melanogaster*. *J. Comp. Neurology* 445, 211–226. doi:10.1002/cne.10155
- Zulfa, R., Lo, W.-C., Cheng, P.-C., Martini, M., and Chuang, T.-W. (2022). Updating the insecticide resistance status of *Aedes aegypti* and *Aedes albopictus* in asia: a systematic review and meta-analysis. *Trop. Med. Infect. Dis.* 7, 306. doi:10.3390/tropicalmed7100306



OPEN ACCESS

EDITED BY

Ana Claudia A. Melo,
Federal University of Rio de Janeiro, Brazil

REVIEWED BY

Junaid Ali Siddiqui,
Guizhou University, China
Bamisope Steve Bamisile,
South China Agricultural University, China

*CORRESPONDENCE

Lijun Liu,
✉ ljliu@cau.edu.cn

[†]These authors have contributed equally to this work and share first authorship

RECEIVED 17 July 2024

ACCEPTED 03 September 2024

PUBLISHED 03 October 2024

CITATION

Duan Y, Li A, Zhang L, Yin C, Li Z and Liu L (2024) Attractant potential of *Enterobacter cloacae* and its metabolites to *Bactrocera dorsalis* (Hendel). *Front. Physiol.* 15:1465946. doi: 10.3389/fphys.2024.1465946

COPYRIGHT

© 2024 Duan, Li, Zhang, Yin, Li and Liu. This is an open-access article distributed under the terms of the [Creative Commons Attribution License \(CC BY\)](#). The use, distribution or reproduction in other forums is permitted, provided the original author(s) and the copyright owner(s) are credited and that the original publication in this journal is cited, in accordance with accepted academic practice. No use, distribution or reproduction is permitted which does not comply with these terms.

Attractant potential of *Enterobacter cloacae* and its metabolites to *Bactrocera dorsalis* (Hendel)

Yawen Duan^{1,2†}, Anjuan Li^{1,2†}, Lin Zhang³, Chongwen Yin³, Zhihong Li^{1,2} and Lijun Liu^{1,2*}

¹College of Plant Protection, China Agricultural University, Beijing, China, ²Key Laboratory of Surveillance and Management for Plant Quarantine Pests, Ministry of Agriculture and Rural Affairs, Beijing, China, ³Institute of Sanya, China Agricultural University, Sanya, China

Objective: *Bactrocera dorsalis* (Hendel) has a wide host range. It has been the most important quarantine pest in many countries or regions. Currently, chemical control and bait trapping are mainly used in the monitoring, prevention, and control of *B. dorsalis*. However, chemical control will cause pollution of the environment and drug resistance of insects. Methyl eugenol, the main attractant currently used, can only attract males of *B. dorsalis*.

Methods: This study focused on the attractant function and active substances of one key intestinal bacterium, *Enterobacter cloacae*, which was isolated from *B. dorsalis*.

Results: First, the attraction of the *E. cloacae* autoclaved supernatant to male and female adults of 0, 6, and 15 days post-emergence was confirmed using a Y-type olfactometer. Subsequently, through metabolome sequencing and bioassays, L-prolinamide was identified and confirmed as the most effective attractant for *B. dorsalis*. Finally, the synergistic effect of L-prolinamide with the sex attractant ME was validated through field experiments. This study confirmed the attraction effect of *E. cloacae* on *B. dorsalis* and also proved the attraction effect of L-prolinamide, the metabolite of *E. cloacae*, on *B. dorsalis*. This laid a theoretical foundation for the development of a new attractant and safe, green, and efficient prevention and control technology of *B. dorsalis*.

KEYWORDS

oriental fruit fly, gut microorganism, *Enterobacter cloacae*, attractant effect, L-prolinamide, synergistic effect

1 Introduction

Bactrocera dorsalis (Hendel) belongs to the Diptera (Tephritidae) family. Due to the direct damage it causes to fruits and vegetables and its negative effect on imports and exports, *B. dorsalis* has become one of the world's most destructive agricultural pests and a major impediment to international fresh commodity trade (Qin et al., 2018). It has caused massive economic losses to agricultural production in tropical and subtropical countries or regions. *Bactrocera dorsalis* can damage over 40 families and 250 genera of fruits and vegetables due to its extensive host range (Liu et al., 2017). It causes fruit rot and premature fruit drop due to female adults laying eggs in the fruits and larvae eating the fruits before pupating (Qin et al., 2018; Vergheze et al., 2012; Chen and Ye, 2007). Therefore, the

prevention and management of this notorious pest are of great significance. At present, chemical, biological, and agricultural methods are employed, with chemical control prevailing due to its higher efficiency. Trapping males using methyl eugenol (ME), the main sexual attractant used currently, is also an effective method for population control. However, chemical control can also cause pollution to the environment and induce a high level of drug resistance in insects. Moreover, attractants can only attract males. Therefore, it is necessary to explore new environmentally friendly control methods and new efficient attractants.

Many microbes play a critical role in the growth and evolution of insects (Genta et al., 2006; Wang et al., 2011). Many studies have shown that four major phyla of intestinal bacteria, namely, Bacteroidetes, Actinobacteria, Firmicutes, and Proteobacteria, were found in the intestine of *B. dorsalis* (Hadapad et al., 2019; Colman et al., 2012; Liu et al., 2016). Several gut microbes have an attractive effect on fruit flies and play an essential role in the chemical exchange between individuals. Wang et al. (2014) have identified the intestinal bacteria of *B. dorsalis* adults by the PCR-DGGE method and confirmed the attraction effect of these bacteria on *B. dorsalis*. Their results indicated that Enterobacteriaceae, Enterococcaceae, and Bacillariophyceae had attraction effects on *B. dorsalis*, among which *Enterobacter cloacae* had a better attraction for *B. dorsalis*. It has been reported that the volatile substance 2-butanone produced by *Klebsiella pneumoniae*, *Citrobacter fumigatus*, and *E. cloacae* can attract *B. dorsalis* (Jang and Nishijima, 1990). It has also been found that metabolites of *K. pneumoniae*, *K. oxytoca*, and *Raoultella terrigena* isolated from the reproductive system of female *B. dorsalis* had an attraction effect on *B. dorsalis*, but the active substance responsible has not yet been confirmed (Shi et al., 2012; Shi et al., 2012).

Using attractants to control and prevent fruit flies can reduce the use of chemicals and, hence, alleviate the problems caused by pesticide resistance. Based on different attracting targets, attractants include male, female, and bisexual attractants. Most of the current male attractants are plant-derived volatiles or paraphylactones, which are usually used to attract males in the field or to monitor populations (Vargas et al., 2010), among which ME, ME analogs, Capilure, trimedlure, Zingerone [4-(4-hydroxy-3-methoxyphenyl)-2-butanone], and cuelure (CL) are the main known species (Zhang, 1991; Park et al., 2020). Until now, ME can be obtained from more than 450 kinds of plant releases, and it has been the most widely used *B. dorsalis* sex attractant (Tan et al., 2011). More than 80 species of fruit fly males, including *B. carambolae*, *B. correcta*, *B. invadens*, and *B. dorsalis*, are strongly attracted to ME (Tan et al., 2011; Shelly, 2010). A study has shown that the ME ingested by males can be converted into several metabolites, which are stored in their glands and act as components of the male sex pheromone (Nishida et al., 1988). In addition, ME plays an important role in enhancing the mating ability and total protein content of *B. dorsalis* males (Ji et al., 2013; Reyes-Hernández et al., 2019). Intake of ME by *B. carambolae* males will strengthen the sexual selection of poplar fruit flies (Wee et al., 2007). CL was initially noted to have a significant attraction effect on *Zeugodacus cucurbitae*, and the subsequent test revealed that raspberry ketone was not as effective as CL (Beroza et al., 1960; Keiser et al., 1973; Drew, 2010). However, ME and CL poorly attract some fruit fly males, such as *B. xanthodes* (Broun) and *B. halfordiae*

(Royer et al., 2019a; Royer et al., 2019b). It was also demonstrated that some eugenol analogs (isoeugenol, ME, and dihydroeugenol) and zinc ketone were more effective male attractants than CL or ME for some fruit flies, with ME showing an effective attraction more than 50 times higher than ME in attracting *Bactrocera xanthodes* (Royer et al., 2019b; Royer et al., 2018). The United States Department of Agriculture has developed trimedlure (TML), which has been widely used as an attractant for *Ceratitis capitata*. TML is an isomeric mixture of 4-(and 5-) chloro-2-methylcyclo-hexane-1-carboxylate. Among them, (1R,2R,4S) tert-butyl 4-chloro-2-methylcyclohexane-1-carboxylate was considered to be the most effective attractant (Jang et al., 2005), and its analog ceralure has also been found to be effective in attracting *C. capitata*. However, due to the difficulty of its synthesis, the most widely used attractant for Mediterranean fruit fly is still TML (Jang et al., 2005). However, most of these attractants are male attractants and can only attract males. There are also some female or bisexual attractants that can attract females or both males and females. These attractants are usually intraspecific pheromones, host volatiles (Fein et al., 1982), food source attractants (Heath et al., 1995), associated bacterial ferments, and secondary metabolites (Drew et al., 1983). Most of the reported intraspecific pheromones with female attraction potential were sex pheromones, which were obtained by extracting rectal gland isolates and were usually composed of pheromones released by male adults (Zhang et al., 2019). The role of female fruit flies is critical for population growth. Hence, despite the effectiveness of ME in attracting male fruit flies, a need exists for attractants that can target both sexes and reduce the environmental impact. *Enterobacter cloacae* and its metabolites may offer advantages in the attractant market by providing a stronger and longer-lasting attractant effect with lower environmental impact and production costs. Additionally, the natural sources and unique mechanisms of action of these metabolites could make them an effective and sustainable alternative. Thus, research on female or bisexual attractants is very important for the development of new green environment-friendly control technology of fruit flies.

In this study, a laboratory-reared population was utilized to investigate the attraction effect of *E. cloacae*, a key intestinal bacterium isolated from *B. dorsalis*, on host fruit flies at various developmental stages. Active substances with attraction properties were screened through metabolome analysis of the supernatant from *E. cloacae*. Synergistic effect of the active substances on ME was also investigated through a field experiment. This study reported for the first time that L-prolinamide has an attraction effect on *B. dorsalis*, and it has a synergistic effect on the sexual attractant named ME, which is important for further development of green and efficient attractants.

2 Materials and methods

2.1 Insects

Adults of *B. dorsalis* were initially collected from Guangzhou, Guangdong province, and the populations have been reared in the laboratory for more than 15 generations. Larvae were fed with artificial diets following the description of Bai et al. (2019). The adults were fed with a powdered diet (peptone: sucrose = 1: 3) after

TABLE 1 16S common primers.

Name	Sequence
27F	AGAGTTTGATCCTGGCTCAG
1492R	GGTACCTTGTTACGACTT

TABLE 2 Samples of attractor test on larvae.

Ingredient	A	B	C	D
Sucrose (g)	62.5	62.5	62.5	62.5
Brewer's yeast powder(g)	15.5	15.5	15.5	15.5
Wheat bran(g)	117.5	117.5	117.5	117.5
Sorbic acid(g)	0.5	0.5	0.5	0.5
Ascorbic acid(g)	0.25	0.25	0.25	0.25
Methylparaben(g)	0.3	0.3	0.3	0.3
Double-distilled water (mL)	300	300	300	—
<i>E. cloacae</i> supernatant (mL)	—	—	—	300
Fed by the larvae (themselves)	Yes	No	No	No
Fed by the larvae (other than themselves)	No	Yes	No	No

emergence and provided with deionized water using moist cotton balls. The larvae (4-day-old) and adult males and females (0, 6, and 15 days post-emergence) of laboratory-reared *B. dorsalis* were collected for this experiment.

2.2 Bacteria

Bactrocera dorsalis adults at 10 days post-eclosion were selected and washed with sterile enzyme-free water to clean their body surfaces. Sequentially, surface disinfection was performed using the 1% sodium hypochlorite solution and 75% ethanol solution, each for 1 min, followed by three washes with enzyme-free sterile water to remove residual solutions. The flies were then placed on ice for storage. In a sterile Petri dish, PBS buffer solution was added, and the midgut was dissected using dissecting forceps. The gut and remaining tissues were placed in separate sterile centrifuge tubes, with five guts combined as one biological replicate. After grinding in liquid nitrogen, PBS was added to create a grinding solution. Subsequently, 100 μL of the gut-grinding solution was pipetted onto NA culture medium and spread evenly. Following incubation at 37°C for 2 days, single bacterial colonies on the plates were purified. After two rounds of purification, single colonies were selected and cultured in the NB liquid medium. Bacterial DNA was extracted using a bacterial genome DNA extraction kit (Tiangen, Beijing, China), amplified using universal bacterial 16S rDNA primers (Table 1), and aligned with NCBI sequences. Physiological and biochemical identification kits specific to Enterobacteriaceae (SHBG08, Qingdao Hope Bio-Technology Co., Ltd., China) confirmed the strain as *E. cloacae*. *Enterobacter cloacae* was mixed with glycerin and stored at −80°C until reused. The strain

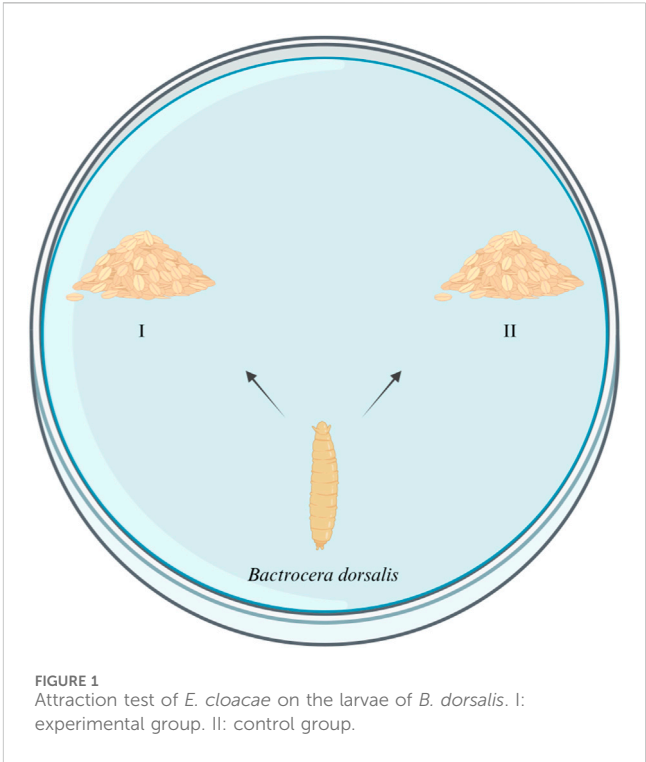


FIGURE 1 Attraction test of *E. cloacae* on the larvae of *B. dorsalis*. I: experimental group. II: control group.

2.3 Attracting ability of *E. cloacae* on larvae of *B. dorsalis*

Four kinds of artificial food were used for this experiment, including food which has been eaten by the same group of larvae (A), food which has been eaten by another group of larvae (B), fresh food with the *E. cloacae* supernatant added (C), and fresh food with nothing added as control (D). The formula and the condition of the food are listed in Table 2. A, B, and C are the experimental groups, and D is the control group. Five grams of food from the experiment group (A, B, or C) and control group (D) were put in the two sides of a 9-cm culture dish, respectively. Five 4-day-old larvae were placed at the mid-point between the two kinds of food each time, while their feeding choices were recorded. The condition that the larvae arrive at one group and feed, without secondary selection, can be recorded as a valid selection. Ten replicates were set up for each group (Figure 1).

2.4 Attracting ability of *E. cloacae* on adults of *B. dorsalis* with different developing periods

Two kinds of attractant and double-distilled water were used for this test, including the *E. cloacae* supernatant (A), autoclave sterilized *E. cloacae* supernatant (B), and double-distilled water as control (C). The detailed composition of these attractants are listed in Table 3. A self-made Y-type olfactometer was used to test the

TABLE 3 Samples of attractor test on adults.

Component	A	B	C
<i>E. cloacae</i> supernatant (mL)	50	—	—
Autoclaved supernatant of <i>E. cloacae</i> (mL)	—	50	—
Double-distilled water (mL)	—	—	50

attraction effect on male and female *B. dorsalis* at 0, 6, and 15 days post-emergence. The self-made Y-type olfactory instrument is composed of an air pump, a pressure regulator tank (Outstanding, China), a gas flowmeter (Shuanghuan, China), an activated carbon tube, a sample bottle, and a Y-type tube (Crystal Technical, China). The Y-type tube has a handle length of 20 cm, an arm length of 10 cm, and an angle of 60°. The two arms of the Y-type tube are equipped with fluorescent lamps. It was ensured that both arms have the same light intensity. The protocol is shown in [Figure 2](#), and the airflow rate was maintained at 100 mL/min. The condition that the adult entered the Y-tube for more than 1 cm and stayed for more than 15 s was recorded as a valid selection. After 30 valid selections in each group, the device was disassembled and rinsed with anhydrous ethanol and 75% alcohol and dried. Then, the sample bottles were switched, and the test was repeated. There were three replicates recorded for each developing period and sex. This part of the study involved the use of larvae (4-day-old) and adult males and females (0, 6, and 15 days post-emergence) of *B. dorsalis*. Each group had 30 valid samples.

2.5 Preparation of metabolome samples of *E. cloacae*

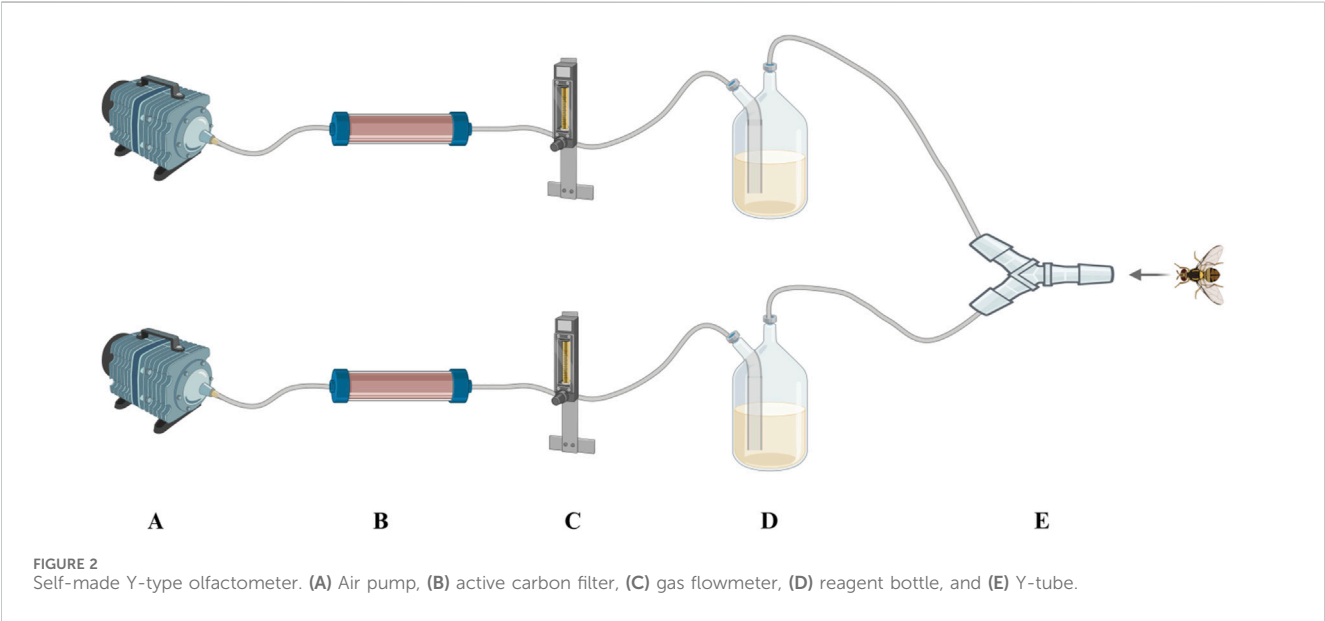
The bacteria solution, after being cultured for 48 h (37°C, 220 r/min) using LB liquid media, was centrifuged at 10,000 r/min for 15 min, and 200 mL of the supernatant was used as sample 1. An additional 200 mL

of the supernatant was autoclaved at 121°C for 20 min and used as sample 2. There were six replicates for each sample. Finally, the processed samples were used for the LC–MS non-targeted metabolomics study (Shanghai Majorbio Bio-Pharm Technology Co., Ltd.). A measure of 25 mg of solid sample was added to a 2-mL centrifuge tube, and a 6-mm-diameter grinding bead was added. An amount of 400 µL of the extraction solution [methanol: water = 4:1 (v:v)] containing 0.02 mg/mL of the internal standard (L-2-chlorophenylalanine) was used for metabolite extraction. Samples were ground by the Wonbio-96c (Shanghai Wanbo biotechnology co., Ltd.) frozen tissue grinder for 6 min (–10°C, 50 Hz), followed by low-temperature ultrasonic extraction for 30 min (5°C, 40 kHz). The samples were left at –20°C for 30 min, centrifuged for 15 min (4°C, 13,000 g), and the supernatant was transferred to the injection vial for LC–MS/MS analysis. An amount of 20 µL of the supernatant was removed from each sample and mixed as a quality control sample (QC) with the same volume as the sample. The QC samples were disposed and tested in the same manner as the analytic samples. It helped represent the whole sample set, which would be injected at regular intervals (every 5–15 samples) in order to monitor the stability of the analysis.

2.6 Analysis of the metabolome of *Enterobacter cloacae*

2.6.1 Liquid chromatography (LC)–mass spectrometry (MS)/MS analysis

The LC–MS/MS analysis of the sample was conducted on a Thermo UHPLC-Q Exactive HF-X system equipped with an ACQUITY HSS T3 column (100 mm × 2.1 mm i.d., 1.8 µm; Waters, United States) at Majorbio Bio-Pharm Technology Co. Ltd. (Shanghai, China). The mobile phases consisted of 0.1% formic acid in water: acetonitrile (95:5, v/v) (solvent A) and 0.1% formic acid in acetonitrile: isopropanol: water (47.5:47.5, v/v) (solvent B). The flow rate was 0.40 mL/min, and the column temperature was 40°C. The injection volume was 3 µL.



The mass spectrometric data were collected using a Thermo UHPLC-Q Exactive HF-X Mass Spectrometer equipped with an electrospray ionization (ESI) source operating in the positive mode and negative mode. The optimal conditions were set as follows: aux gas heating temperature at 425°C; capillary temp at 325°C; sheath gas flow rate at 50 psi; aux gas flow rate at 13 psi; ion-spray voltage floating (ISVF) at −3,500 V in negative mode and 3,500 V in positive mode; normalized collision energy, 20–40–60 eV rolling for MS/MS. The full MS resolution was 60,000, and the MS/MS resolution was 7,500. Data acquisition was performed in the data-dependent acquisition (DDA) mode. The detection was carried out over a mass range of 70–1,050 m/z.

2.6.2 Substance identification and analysis

The UHPLC-MS raw data were converted into the common format by Progenesis QI software (Waters, Milford, United States) through baseline filtering, peak identification, peak integral, retention time correction, and peak alignment. Then, the data matrix containing sample names, m/z, retention time, and peak intensities was exported for further analyses. At the same time, the metabolites were identified by searching the databases, and the main databases were the HMDB (<http://www.hmdb.ca/>), Metlin (<https://metlin.scripps.edu/>), and the self-compiled Majorbio Database (MJDB) of Majorbio Biotechnology Co., Ltd. (Shanghai, China).

The data matrix obtained by searching databases was uploaded to the Majorbio cloud platform (<https://cloud.majorbio.com>) for data analysis. First, the data matrix was pre-processed as follows: at least 80% of the metabolic features detected in any set of samples was retained. After filtering, the minimum value in the data matrix was selected to fill the missing value, and each metabolic signature was normalized to the sum. To reduce the errors caused by sample preparation and instrument instability, the response intensities of the sample mass spectrometry peaks were normalized using the sum normalization method to obtain the normalized data matrix. Meanwhile, the variables of QC samples with relative standard deviation (RSD) > 30% were excluded and log10 logarithmized to obtain the final data matrix for subsequent analysis. Then, through R software ropls tools, the data matrix of input samples was used for PCA analysis, which generally reflected the metabolic differences among samples in each group and the variation degree among samples in the group (Cala et al., 2018). OPLS-DA analysis was used to eliminate noise information that is not relevant to classification and also obtain relevant metabolite information that causes significant differences between the two groups (Cala et al., 2018). To visualize the content of metabolites, metabolites were clustered according to their content in each sample. At the same time, metabolites were classified according to their participation in the pathway or the function they perform using the KEGG database. The metabolically concentrated metabolites are displayed on the KEGG pathway map (Li et al., 2018).

2.7 Field experiment

The field experiment was conducted in Yazhou, Sanya City, Hainan Province, from October to November of 2023. A total of eight traps, where four traps were the control group and another four traps were the treatment group, were randomly hung on one of the

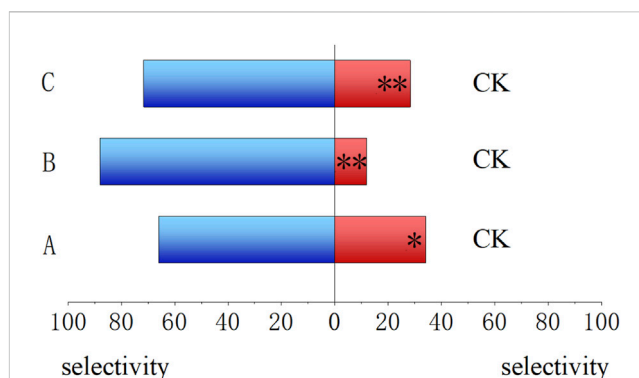


FIGURE 3

Feeding trend of *Bactrocera dorsalis* larvae for different larval feeds. (A) Food that has been fed by themselves for 4 days. (B) Food that has been fed by the larvae other than themselves for 4 days. (C) Fresh food prepared using the *Enterobacter cloacae* solution. (CK) Fresh food prepared using ddH₂O. *: $P < 0.05$; **: $P < 0.01$.

branches in the sunshade side of the green canopy. The hanging height was between 1 m and 1.5 m from the ground. For control groups, only the absorbent cotton, in which 3 mL ME was added, was placed in the small tank. However, for the treatment group, in addition to absorbent cotton with 3 mL ME, the bottom was filled with 100 mL L-prolinamide solution with a final concentration of 3%. The traps were hung on the same branch, and the distance between the control and treatment group was approximately 0.5 m. The numbers, species, and the sex ratio of flies were investigated every 7 days, and the traps were changed. There were four biological replications for this experiment, and the experiment was repeated four times.

2.8 Statistical analysis

SPSS statistical analysis software was used to analyze the relevant experimental data using nonparametric tests. S was used as the selection rate, and the calculation method is explained herein. The term “average number of *B. dorsalis* attracted” refers to the number of adults who enter the Y-tube side for more than 1 cm and stay for more than 15 s. The term “total number of *B. dorsalis*” refers to the 30 valid selections of the adult in each group.

$$S(\%) = \frac{\text{Average number of } B. \text{ dorsalis attracted to the treatment group (or control group)}}{\text{Total number of } B. \text{ dorsalis}} \times 100.$$

3 Results

3.1 Response of 4-day-old *B. dorsalis* larvae to various types of artificial food

As shown in Figure 3, compared to CK, the 4-day-old larvae preferred to feed on treated artificial food. The food that has been fed by other insects for 4 days showed the highest selectivity (88.00%, $P < 0.01$), followed by the fresh food prepared with *E. cloacae* solution (72%, $P < 0.01$) and the food that has been fed by themselves for 4 days (66.00%, $p = 0.015 < 0.05$).

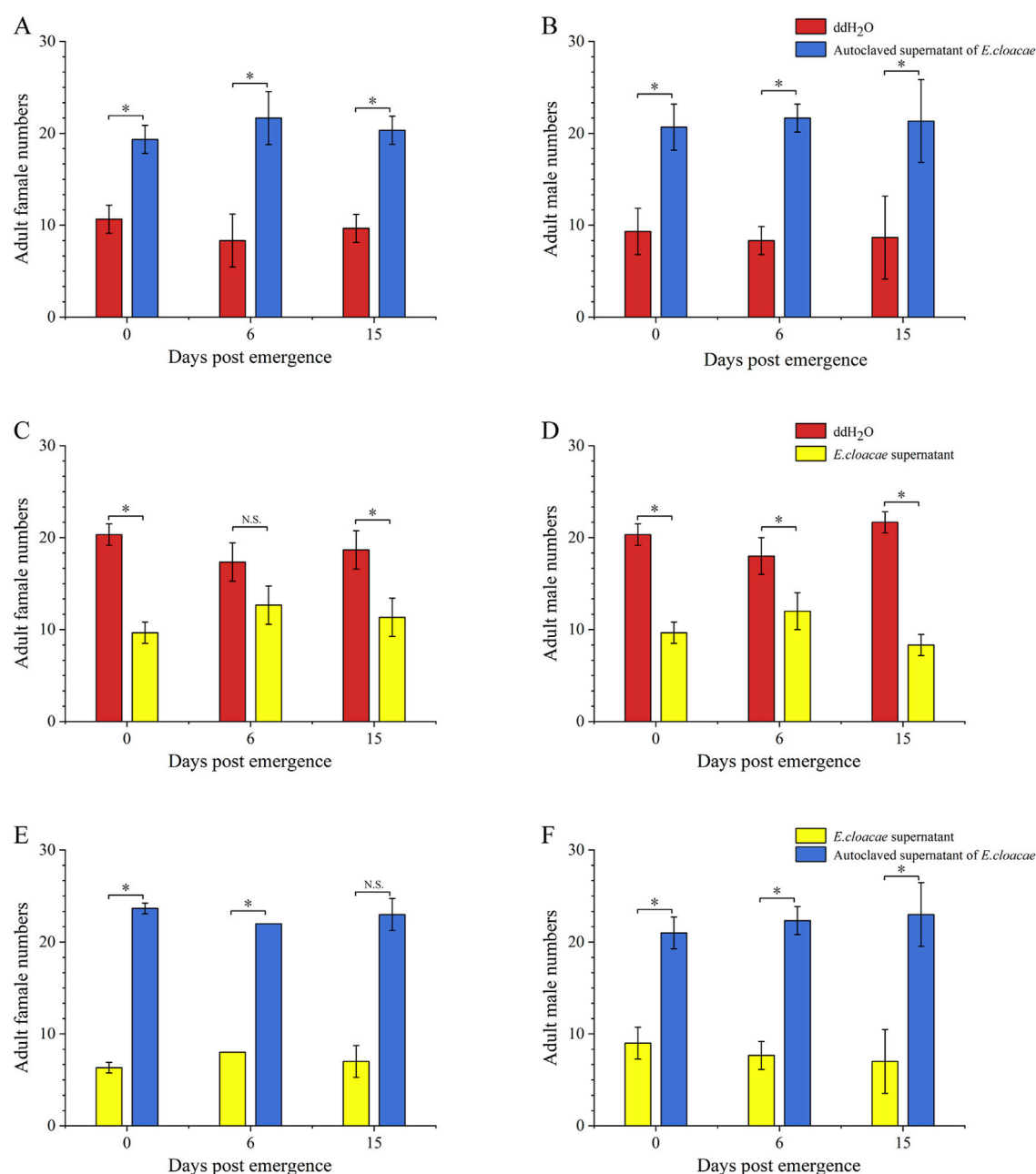


FIGURE 4

Attractant of *Enterobacter cloacae* to adults of *Bactrocera dorsalis*. Red: ddH₂O; yellow: supernatant of *Enterobacter cloacae*; blue: autoclaved supernatant of *E. cloacae*. (A): attraction of *Enterobacter cloacae* supernatant which has been autoclave sterilized to female *B. dorsalis*. (B): attraction of *E. cloacae* supernatant which has been autoclave sterilized to male *B. dorsalis*. (C): attraction of *E. cloacae* supernatant to female *B. dorsalis*. (D): attraction of *E. cloacae* supernatant male *B. dorsalis*. (E): attraction of *E. cloacae* supernatant which has been autoclave sterilized and *E. cloacae* supernatant to female *B. dorsalis*. (F): attraction of *E. cloacae* supernatant which has been autoclave sterilized and *E. cloacae* supernatant to male of *B. dorsalis*. *: $P < 0.05$; **: $P < 0.01$.

3.2 Attraction effect of *E. cloacae* on adult *B. dorsalis*

Compared to double-distilled water and the *E. cloacae* supernatant, the autoclaved supernatant of *E. cloacae* showed a significantly increased attraction ability for adults of *B. dorsalis*

at 0, 6, and 15 days post-emergence, including females (Figures 4A, E) and males (Figures 4B, F). Additionally, the number of *B. dorsalis* attracted by double-distilled water was significantly higher than that attracted by the supernatant of bacteria, except for 6-day-old females (Figures 4C, D).

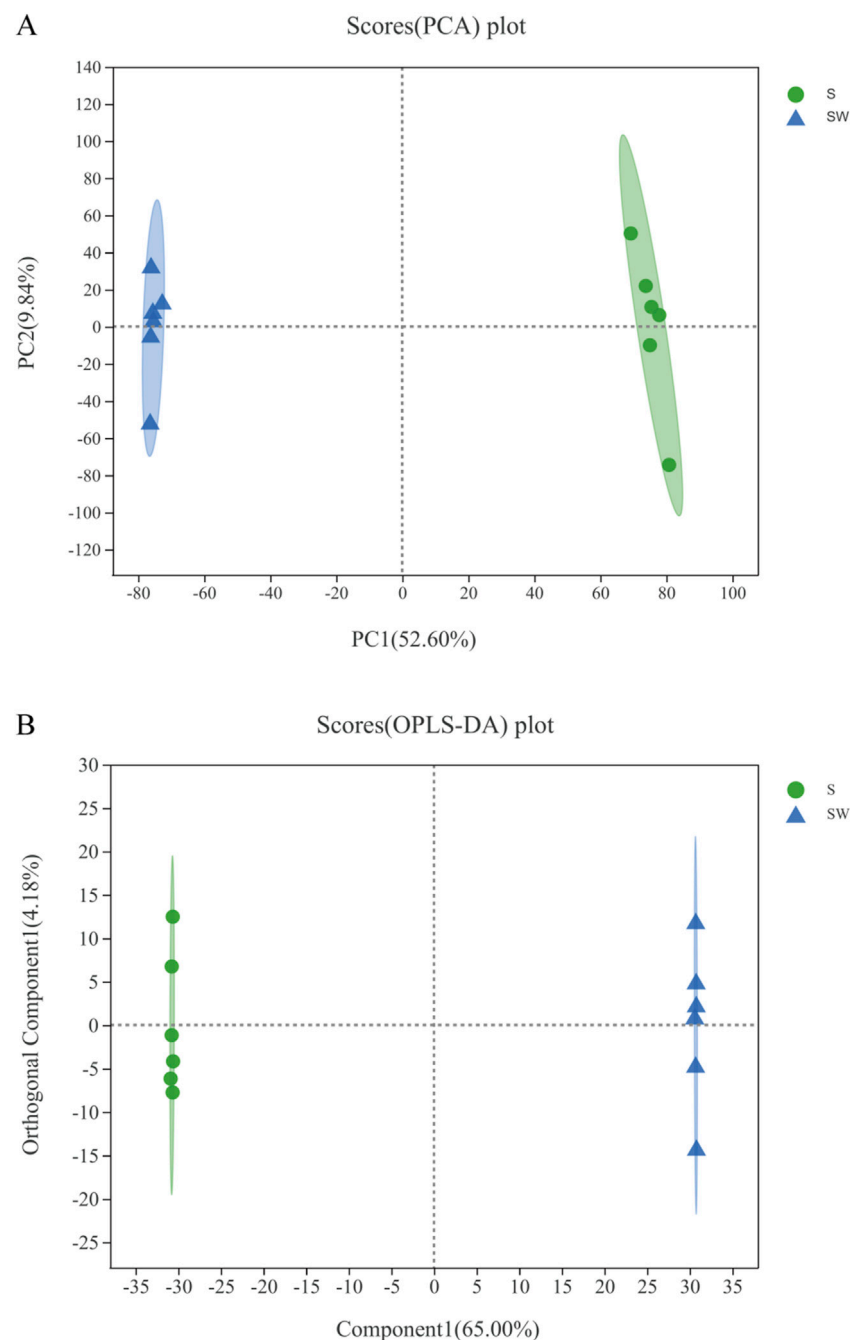


FIGURE 5

Scatter points of PCA (A). Dispersion points of OPLS-DA (B). (S) Experimental group: *Enterobacter cloaca* supernatant that has been autoclave sterilized. (SW) Control group: *Enterobacter cloaca* supernatant. The confidence ellipse represents the group of “true” samples with 95% confidence, and the samples beyond this region can be considered as possible abnormal samples.

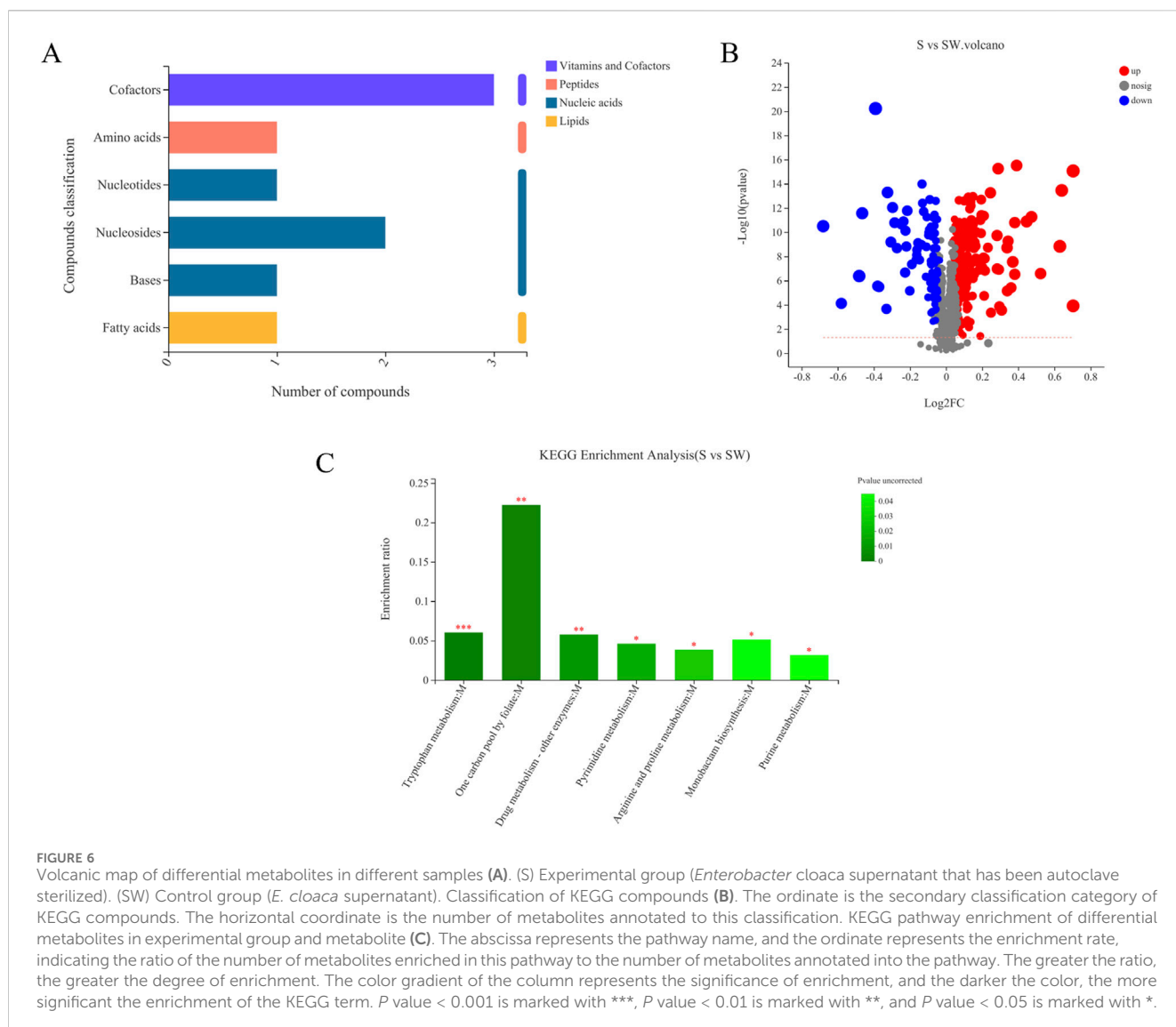
3.3 Comparative metabolome analysis of the supernatant and autoclaved supernatant of *E. cloacae*

3.3.1 PCA and orthogonal partial least-squares discrimination (OPLS-DA) analysis

As shown in [Supplementary Figure S1](#), the total ion overlap chromatograms of the quality control samples in the positive and negative ion modes had good peak shapes and relatively uniform

distribution, which represent a high quality of the metabolome. The PCA analysis allows us to observe the separation trend between groups and the presence of outliers in the experimental model and reflects the inter- and intra-group variability from the raw data. The treated group was farther apart from the control, and the biological repetitions in the treated or control group are closer together ([Figure 5A](#)).

The OPLS-DA method can distinguish the test group from the control group ($R^2X = 0.65$, $R^2Y = 1$, $Q^2 = 0.995$) with good stability,



as shown in Figure 5B. All samples in the test and control groups were within the 95% confidence interval, indicating that the accuracy of these data is relatively high. Both PCA and OPLS-DA analysis showed that the differences between the test and control groups are more pronounced and the intra-group replicates are more stable.

3.3.2 Heatmap analysis of differential metabolites

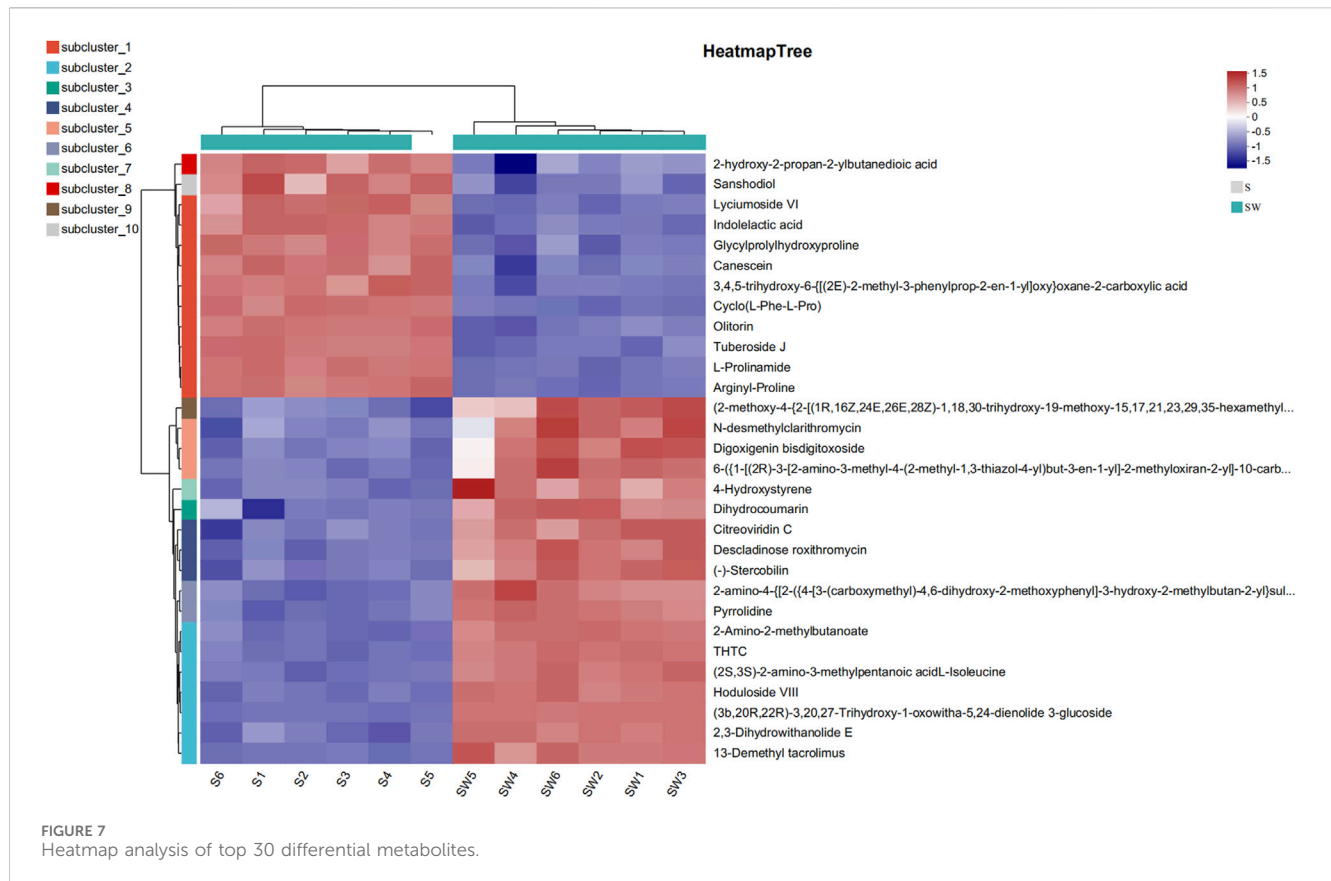
Differential metabolites between the autoclaved supernatant and supernatant of *E. cloacae* were screened based on univariate statistical analysis and VIP values. A total of 302 differential metabolites were screened ($P < 0.05$ and VIP values > 1), of which 208 were upregulated (VIP > 1 and fold change > 1) and 94 were downregulated (VIP > 1 and $0 < \text{fold change} < 1$) (Figure 6A). Among them, FC > 1 and the metabolites with clear species are provided in Supplementary Table S1.

Among the 81 upregulated metabolites, carboxylic acids and their derivatives were the most abundant, accounting for 18 species. The following were pregnenolone lipids, accounting for 14 species. The others were triterpenoids, sphingolipids,

peptides, nitrogen-containing carboxylic acid derivatives, and amides, respectively (Supplementary Table S1). KEGG compound is a collection of small molecules, biopolymers, and other chemicals associated with biological systems. As shown in Figure 6B, the differential metabolites can be classified into four kinds of metabolites, including lipids, nucleic acids, peptides, vitamins, and cofactors. Myristic acid was present in the lipids. There were four nucleic acids, among which were thymidine, deoxyuridine, 5'-CMP, and (2R,3R,4S,5R)-2-(6-aminopurin-9-yl)-5-(hydroxymethyl) oxolane-3,4-diol. There was one peptide, L-tyrosine. There were three vitamins and coenzyme factors, namely, S-adenosylmethionine, pyrroloquinoline quinone, and tetrahydrofolate (Figure 7; Supplementary Table S2).

3.3.3 KEGG enrichment analysis of differential metabolites

Based on the KEGG enrichment analysis, it was found that the different metabolites in the test and control groups were mainly enriched in the following pathways: tryptophan metabolism, one



carbon pool by folate, drug metabolism—other enzymes (pyrimidine metabolism), purine metabolism, monobactam biosynthesis, and arginine and proline metabolism pathways. The one carbon pool by folate pathway was the most enriched (Figure 6C).

3.3.4 Heatmap analysis of differential metabolites

Heatmaps constructed based on differential metabolites between the supernatant and autoclaved supernatant of *E. cloacae* showed a clear clustering (Supplementary Figure S2). The autoclaved supernatant showed a higher attracting ability than the *E. cloacae* supernatant, which helped us focus on the upregulated differential metabolite. Figure 6D shows the top 30 differential metabolites, which contain L-prolinamide.

3.4 Screening and identification of the attractive active substance of *E. cloacae* against *B. dorsalis*

Based on previous studies, most of the substances found to have attractive activity are pyrazines, amines, ammonia, alcohols, ketones, acids, and phenols. Three different metabolites, namely, 3-indoleacetic acid, 2-hydroxycinnamic acid, and L-prolinamide, were selected for the attractive ability test. These three substances had similar functional groups to methyl salicylate, ME, and N-(3-methylbutyl) acetamide (Table 4), whose attractive ability to *B. dorsalis* has been confirmed.

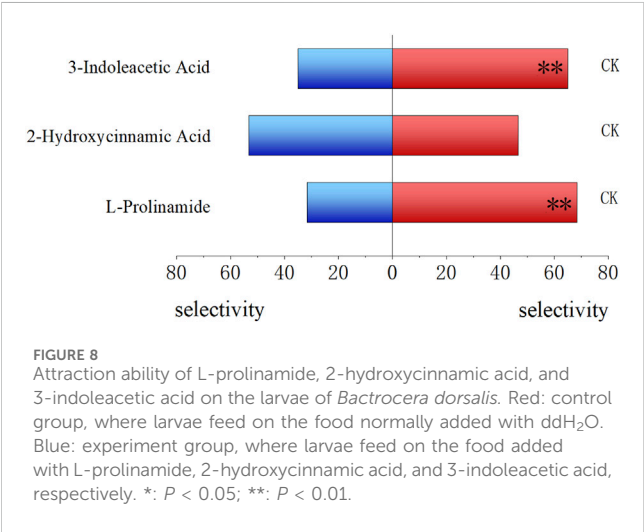
Compared to untreated fresh food, 3-indoleacetic acid-treated food and L-prolinamide-treated food showed a significantly lower attractive ability to the 4-day-old larvae, with an attraction rate of 35.00% ($P < 0.01$) and 31.77% ($P < 0.01$), respectively. The selection rate of 2-hydroxycinnamic acid-treated food (53.33%) and untreated fresh food (46.67%) by 4-day-old larvae had no significant difference (Figure 8). Meanwhile, for the attraction ability of these three substances on female and male adults, L-prolinamide was effective in attracting both newly emerged, 6-day, and 15-day-old males and females, and the number of *B. dorsalis* attracted in the treatment group was significantly higher than that in the control group (Figures 9A, B). 3-Indoleacetic acid showed attractive ability to 15-day-old males (Figures 9C, D), while 2-hydroxycinnamic acid only showed attractive ability to 6-day-old females (Figures 9E, F).

3.5 Potential use of L-prolinamide as the synergistic agents of sexual attractants in the field

As shown in Figure 10, the trapping rate of L-prolinamide with a concentration of 3% was significantly higher than that of the control group ($n = 16$, $P < 0.05$). Therefore, L-prolinamide with 3% concentration had a synergistic effect on ME for the attraction of *B. dorsalis*. A few females were trapped in the treatment group for our pre-experiment, which was constructed in Sanya, Hainan province, in July 2022. However, only 2–7 females were trapped, and it did not display a significant difference.

TABLE 4 CAS ID of the metabolite.

Metabolite	CAS ID	Molecular formula	Similar functional groups (the compound with an attractive effect)
L-Prolinamide	7,531-52-4	C ₅ H ₁₀ N ₂ O	Amidogen, acylamino
3-Indoleacetic acid	87-51-4	C ₁₀ H ₉ NO ₂	Benzene ring, imino
2-Hydroxycinnamic acid	614-60-8	C ₉ H ₈ O ₃	Benzene ring, hydroxy



4 Discussion

Wang et al. (2014) identified the attracting ability of gut microbes in adult *B. dorsalis*, and the results showed that Enterobacteraceae, Enterococcaceae, and Bacillaceae have attracting effects on adult *B. dorsalis*, among which *E. cloacae* has a better effect on host fruit fly. In addition, *Bacillus cereus*, *Enterococcus faecalis*, *Citrobacter fumigatus*, *Klebsiella oxytoca*, and *K. pneumoniae* have been reported to be effective in attracting *B. dorsalis* (Jang and Nishijima, 1990; Shi et al., 2012; Shi et al., 2012). *Enterobacter cloacae* also has an attractive effect on other fruit flies. Lauzon et al. showed that *E. cloacae*, isolated from the feces of *Rhagoletis pomonella*, has a strong attraction effect on *R. pomonella* (Lauzon et al., 1998). In addition, *E. cloacae* has an attractive effect on *Zeugodacus cucurbitae*, *B. papayae*, and *B. zonata* (Narit and Anuchit, 2011; Reddy et al., 2014). Although the attraction ability of many gut bacteria has been confirmed, the difference of attraction ability among different bacteria species and the specific substances that play a role are unknown. In our research, the results of the larval feeding tendency experiment showed that the 4-day-old larvae were more likely to feed on food that has been fed by themselves or other insects for 4 days, and they also liked the food prepared by the *E. cloacae* solution. Therefore, we speculated that *B. dorsalis* larvae may secrete a substance or pheromone during feeding, which attracted other larvae or themselves to feed. For the attraction to the adult females and males at 0, 6, and 15 days post-emergence, the autoclaved supernatant of *E. cloacae* displayed the highest attraction efficiency. Like our study, it has been shown that *E. cloacae* has a strong attraction effect on 8-day-old and sexually mature South Asian fruit flies. Additionally, research has

demonstrated that the autoclaved supernatant is more effective at attracting the flies than the fermentation stock (Luo, 2016).

It has been reported that ammonia, several amines, imines, pyrazines, and acetic acid in the headspace above the filtrate of the bacterial cultures were determined to be attractive to *Anastrepha ludens* (Robacker and Garcia, 1993; Robacker and Flath, 1995). Hereby, we speculated that the fermentation broth of *E. cloacae* can produce a stable secondary metabolite that has an attraction activity on *B. dorsalis* after being autoclaved. Meanwhile, our results showed that there was no significant difference in the attraction effect of the autoclaved supernatant of *E. cloacae* on female and male adults of different ages. This suggests that the active substances responsible for attraction produced by autoclaved *E. cloacae* are not linked to egg laying, sexual maturation, or sex pheromone synthesis. It has been demonstrated that the bacterial medium can provide the fruit flies with carbohydrates and, in turn, can affect the attractiveness of bacteria to fruit flies (Reddy et al., 2014). Meanwhile, the protein-fed or mated fruit flies respond similarly to associated bacterial odors, regardless of the presence or absence of the host fruit (Narit and Anuchit, 2011). Therefore, the attractive substances produced by *E. cloacae* may be some kind of protein or amino acid needed for the growth and development of *B. dorsalis* rather than substances related to sexual maturation and egg production. Therefore, when screening metabolites, combined with previous studies, we guessed that the attractant is the amine-containing substance. Studies of such substances provide a potential use of them as attractants or attractants synergist in the field, which can avoid the disadvantage that some attractants used now only attract males.

Related studies have indicated that most of the substances that have an attraction effect on *B. dorsalis* are substances containing ammonia, pyrazine, amines, alcohols, and phenols. Furthermore, sulfides, ketones, and acids have been reported to be able to attract some fruit fly's adults (Hadapad et al., 2016). The bacterial volatile components contained in *Anastrepha ludens* also showed significant attraction and were confirmed to contain mainly ammonia, amines, pyrazines, and acids (Robacker and Flath, 1995; Lee et al., 1995; DeMilo et al., 1996; Robacker and Bartelt, 1997; Robacker et al., 1998). Meanwhile, a related study has suggested that the reason some bacteria can have an attraction effect on fruit flies may be due to the production of ammonia by bacterial metabolisms. Meanwhile, amide, as a derivative of ammonia, may have an attraction effect because adult *B. dorsalis* feeds on it as a nitrogen source. Our results were consistent with these reports and findings. Among the three substances we chose, none of them showed attractive ability on larvae, and only L-prolinamide, a kind of amide, showed significantly higher attractive ability on the adult females and males, regardless the development stage.

Although previous studies have shown that most of the substances with an attractive effect on insects are alcohols,

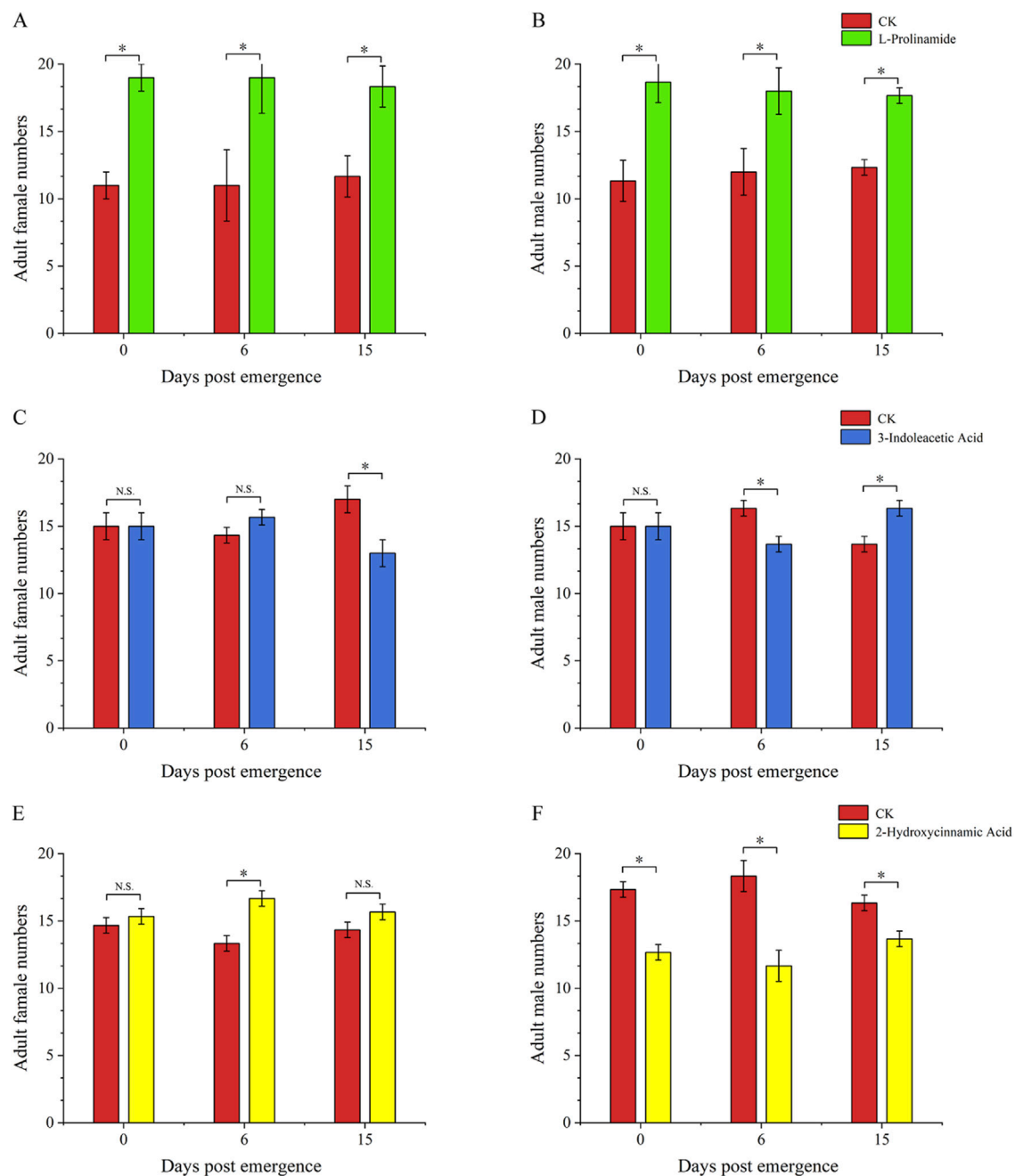


FIGURE 9

Attraction ability of L-prolinamide, 2-hydroxycinnamic acid, and 3-indoleacetic acid to adult *Bactrocera dorsalis*. Red: control group, where larvae feed on the food normally added with ddH₂O. Blue: experiment group, where larvae feed on the food normally added with L-prolinamide. Yellow: experiment group, where larvae feed on the food normally added with 2-hydroxycinnamic acid. (A) Attraction results of L-Prolinamide to female *Bactrocera dorsalis* at different ages; (B) Attraction results of L-Prolinamide to male *Bactrocera dorsalis* at different ages; (C) Attraction ability of 3-Indoleacetic Acid to female *Bactrocera dorsalis* at different; (D) Attraction ability of 3-Indoleacetic Acid to male *Bactrocera dorsalis* at different; (E) Attraction ability of 2-Hydroxycinnamic acid to female *Bactrocera dorsalis* at different ages; (F) Attraction ability of 2-Hydroxycinnamic acid to male *Bactrocera dorsalis* at different ages. *: $P < 0.05$. **: $P < 0.01$.

phenols, alkanes, and ketones, L-prolinamide has been less studied. Currently, studies have focused on the attraction effect of some other amides, such as *N*-(3-methylbutyl) acetamide and oleamide. It was evident that *N*-(3-methyl-butyl) acetamide induces electroantennographical response in different stages and sex combinations in *B. minax* by measuring citrus fruit volatiles and the electroantennographical response of *B. minax* (Li,

2020). A study found that the compound *N*-(3-methylbutyl) acetamide was the main volatile component in the venom of many female vespid wasps. The attraction ability of *N*-(3-methylbutyl) to *Polistes* genera has also been verified by field tests. The acetamide attracted male and female *P. aurifer* and *P. metricus*, as well as male *P. dorsalis* and *P. bellicosus* (Elmqvist et al., 2020). The endogenous components of *B. carambolae* males were

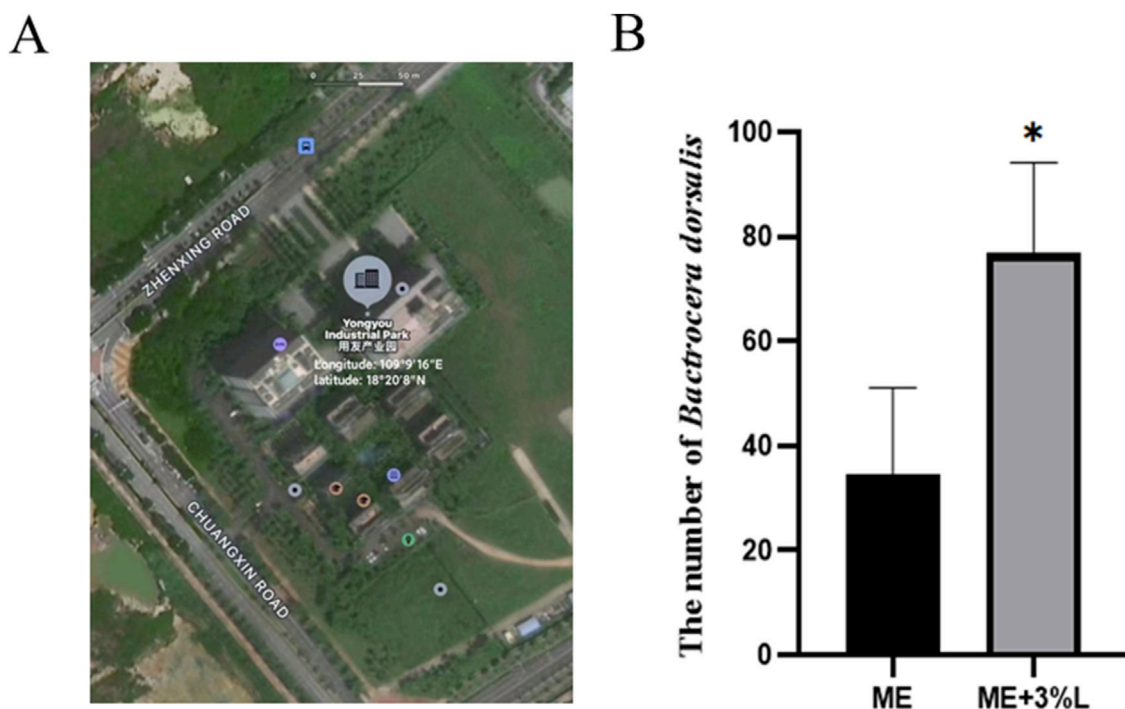


FIGURE 10

Synergistic effect of L-prolinamide on ME. (A) Geographical distribution of the site for field experiment: Yongyou Industrial Park (Longitude: 109°9'16"E; latitude: 18°20'8"N); (B) the number of *B. dorsalis* that were trapped using ME and ME mixed with L-prolinamide at a concentration of 3%, respectively. ME, methyl eugenol. ME, control group, only the absorbent cotton, in which 3 mL ME was added, was placed in the small tank for trapping. ME + 3% L: treatment group, besides absorbent cotton with 3 mL ME, the bottom was filled with 100 mL L-prolinamide solution with a final concentration of 3%. The traps were hung on the same branch, and the distance between the control and treatment group was approximately 15 m. N = 16. *: $P < 0.05$.

identified and analyzed for 6-oxo-1-nonanol and *N*-3-methylbutylacetamide, and subsequent studies showed that these endogenous components were able to attract a large number of females when released into the air as visible smoke (Wee and Tan, 2005). It was also found that 1 ng/ μ L of oleamide had a strong priming effect on the *Curculio chinensis* and identified a regulatory effect of oleamide on its behavior (Yan et al., 2023). In addition to attracting both males and females, L-prolinamide showed a high synergistic effect on the attraction ability of ME by a field test. Its potential use as attractants will be evaluated in the future. This laid a theoretical foundation for the development of new attractants and safe, green, and efficient prevention and control technology of *B. dorsalis*.

Guo et al. (2021) identified the volatile compounds of *Klebsiella oxytoca* and found that 3-methyl-1-butanol only attracted male *Drosophila suzukii*. In contrast, this study has identified a bacterium and its active compound that attract both male and female flies, addressing the current limitation where most attractants only lure males. Additionally, exploring the potential mechanism of *E. cloacae* and L-prolinamide in attracting *B. dorsalis* is critical for pest control. In *Drosophila melanogaster*, the sexually dimorphic central neural pathways associated with the odorant receptor DmelOR67d, which detects cVA, illustrate how olfactory sensory neurons and their projection neurons shape behavior (Datta et al., 2008; Ruta et al., 2010). Zhang et al. (2024) proposed a working model in which ME enhances the attractiveness of leks in attracting females to an arena to control *B. dorsalis* mating

behavior, providing a scientific foundation for understanding the mechanisms of the male annihilation technique and future improvements. Given that ME are currently primarily used for managing adult male pests, investigating the potential mechanisms by which *E. cloacae* and L-prolinamide attract female *B. dorsalis* can provide valuable insights for developing pest management strategies. Therefore, further research into these mechanisms could establish a theoretical basis for developing new, environmentally friendly attractants and improving overall control efficacy. In the future, integrating research on *E. cloacae* and its metabolites into current pest management strategies should focus on their broader ecological and pest control impacts. These metabolites demonstrate significant environmental friendliness and protect ecosystem biodiversity compared to traditional chemical attractants. Furthermore, combining these with existing attractants like ME could achieve more effective pest control measures (Cai et al., 2018).

In summary, in this study, the attraction effect of *E. cloacae*, a gut bacterial strain isolated from *B. dorsalis*, and one of its metabolites, L-prolinamide, on host fruit fly was demonstrated. It was confirmed that there was no significant difference between the attraction effect of L-prolinamide on male and female adults, which can compensate for the weakness that most of the current attractants, such as ME, can only attract males, and it can provide a new view for environmental protection and efficient control of *B. dorsalis*. However, among so many differential metabolites, only three substances have been selected to investigate the attraction ability; more differential metabolites should be selected for attraction effect

verification, and the comparison among these substances and their synergistic effect of existing attractants still need to be confirmed. Additionally, it is necessary to further investigate the mechanism of the attraction effect of *E. cloacae* and its metabolites on *B. dorsalis* to provide a theoretical basis for the development of novel green control technologies for this notorious pest.

Data availability statement

The original contributions presented in the study are included in the article/supplementary material, further inquiries can be directed to the corresponding author.

Author contributions

LL: conceptualization, funding acquisition, methodology, project administration, validation, visualization, and writing–review and editing. YD: conceptualization, formal analysis, methodology, software, validation, writing–original draft, and writing–review and editing. AL: software, writing–original draft, and writing–review and editing. LZ: validation and writing–original draft. CY: validation and writing–original draft. ZL: writing–review and editing.

Funding

The authors declare financial support was received for the research, authorship, and/or publication of this article. This study received financial support from the National Key Research and Development Project (2022YFC2601500; 2022YFC2601503).

References

- Bai, Z., Liu, L., Noman, M. S., Zeng, L., Luo, M., and Li, Z. (2019). The influence of antibiotics on gut bacteria diversity associated with laboratory-reared *Bactrocera dorsalis*. *B. Entomol. Res.* 5, 500–509. doi:10.1017/S0007485318000834
- Beroza, M., Alexander, B. H., Steiner, L. F., Mitchell, W. T., and Miyashita, D. H. (1960). New synthetic lures for the male melon fly. *Science* 131, 1044–1045. doi:10.1126/science.131.3406.1044
- Cai, X. M., Li, Z. Q., Pan, H. S., and Lu, Y. H. (2018). Research and application of food-based attractants of herbivorous insect pests. *Chin. J. Biol. Contr.* 34, 8–35. doi:10.16409/j.cnki.2095-039x.2018.01.002
- Cala, M. P., Agulló-Ortuño, M. T., Prieto-García, E., González-Riano, C., Parrilla-Rubio, L., Barbas, C., et al. (2018). Multiplatform plasma fingerprinting in cancer cachexia: a pilot observational and translational study. *Multiplatform plasma fingerprinting cancer cachexia. J. Cachexia Sarcopeni.* 9, 348–357. doi:10.1002/jcsm.12270
- Chen, P., and Ye, H. (2007). Population dynamics of *Bactrocera dorsalis* (Diptera: tephritidae) and analysis of factors influencing populations in Baoshanba, Yunnan, China. *Entomol. Sci.* 10, 141–147. doi:10.1111/j.1479-8298.2007.00208.x
- Colman, D. R., Toolson, E. C., and Takacs-Vesbach, C. D. (2012). Do diet and taxonomy influence insect gut bacterial communities? *Mol. Ecol.* 21, 5124–5137. doi:10.1111/j.1365-294X.2012.05752.x
- Datta, S. R., Vasconcelos, M. L., Ruta, V., Luo, S., Wong, A., Demir, E., et al. (2008). The *Drosophila* pheromone cVA activates a sexually dimorphic neural circuit. *Nature* 452, 473–477. doi:10.1038/nature06808
- DeMilo, A. B., Lee, C. J., Moreno, D. S., and Martinez, A. J. (1996). Identification of volatiles derived from *Citrobacter freundii* fermentation of a trypticase soy broth. *J. Agr. Food Chem.* 44, 607–612. doi:10.1021/jf950525o
- Drew, R. A. I. (2010). The responses of fruit fly species (Diptera: tephritidae) in the south pacific area to male attractants. *Aust. J. Entomol.* 13, 267–270. doi:10.1111/j.1440-6055.1974.tb.02206.x
- Drew, R. A. I., Courtice, A. C., and Teakle, D. S. (1983). Bacteria as a natural source of food for adult fruit flies (Diptera: tephritidae). *Oecologia* 60, 279–284. doi:10.1007/BF00376839
- Elmqvist, D. C., Landolt, P. J., Cooper, W. R., Reed, H., Foutz, J., Clepper, T., et al. (2020). The venom compound N-(3-methylbutyl) acetamide attracts several *Polistes* (fuscolistes) species (hymenoptera: vespidae). *J. Econ. Entomol.* 113, 1073–1079. doi:10.1093/jee/toaa065
- Fein, B. L., Reissig, W. H., and Roelofs, W. L. (1982). Identification of apple volatiles attractive to the apple maggot, *Rhagoletis pomonella*. *J. Chem. Ecol.* 8, 1473–1487. doi:10.1007/BF00989104
- Genta, F. A., Dillon, R. J., Terra, W. R., and Ferreira, C. (2006). Potential role for gut microbiota in cell wall digestion and glucoside detoxification in *Tenebrio molitor* larvae. *J. Insect Physiol.* 52, 593–601. doi:10.1016/j.jinsphys.2006.02.007
- Guo, Y. Y., Tan, D. Y., Shi, H. M., Wu, X. Y., Yu, Y., Li, T. G., et al. (2021). Attractiveness of intestinal bacterium *Klebsiella oxytoca* and its volatile substances to *Drosophila suzukii* adults. *Acta Entomol. Sin.* 64, 1161–1167. doi:10.16380/j.kcxb.2021.10.005
- Hadapad, A. B., Prabhakar, C. S., Chandekar, S. C., Tripathi, J., and Hire, R. S. (2016). Diversity of bacterial communities in the midgut of *Bactrocera cucurbitae* (Diptera: tephritidae) populations and their potential use as attractants. *Pest Manag. Sci.* 72, 1222–1230. doi:10.1002/ps.4102
- Hadapad, A. B., Shettigar, S. K., and Hire, R. S. (2019). Bacterial communities in the gut of wild and mass-reared *Zeugodacus cucurbitae* and *Bactrocera dorsalis* revealed by metagenomic sequencing. *BMC Microbiol.* 19, 282–311. doi:10.1186/s12866-019-1647-8
- Heath, R. R., Epsky, N. D., Guzman, A., Dueben, B. D., Manukian, A., and Meyer, W. L. (1995). Development of a dry plastic insect trap with food-based synthetic attractant for the Mediterranean and Mexican fruit flies (Diptera: tephritidae). *J. Econ. Entomol.* 88, 1307–1315. doi:10.1093/jee/88.5.1307

Acknowledgments

The authors would like to thank all the members of the Plant Quarantine Laboratory of China Agricultural University (CAUPQL). The data were analyzed through the free online platform of Majorbio cloud platform (<http://cloud.majorbio.com>). The authors also thank all reviewers for their comments on this manuscript.

Conflict of interest

The authors declare that the research was conducted in the absence of any commercial or financial relationships that could be construed as a potential conflict of interest.

Publisher's note

All claims expressed in this article are solely those of the authors and do not necessarily represent those of their affiliated organizations, or those of the publisher, the editors, and the reviewers. Any product that may be evaluated in this article, or claim that may be made by its manufacturer, is not guaranteed or endorsed by the publisher.

Supplementary material

The Supplementary Material for this article can be found online at: <https://www.frontiersin.org/articles/10.3389/fphys.2024.1465946/full#supplementary-material>

- Jang, E. B., Khirman, A., Holler, T. C., Casana-Giner, V., Lux, S., and Carvalho, L. A. (2005). Field response of Mediterranean fruit fly (Diptera: tephritidae) to ceralure B1: evaluations of enantiomeric B1 ratios on fly captures. *J. Econ. Entomol.* 98, 1139–1143. doi:10.1603/0022-0493-98.4.1139
- Jang, E. B., and Nishijima, K. A. (1990). Identification and attractancy of bacteria associated with *dacus-dorsalis* (Diptera: tephritidae). *Environ. Entomol.* 19, 1726–1731. doi:10.1093/ee/19.6.1726
- Ji, Q. E., Chen, J. H., McInnis, D. O., and Guo, Q. L. (2013). The effect of methyl eugenol exposure on subsequent mating performance of sterile males of *Bactrocera dorsalis*. *J. Appl. Entomol.* 137, 238–243. doi:10.1111/j.1439-0418.2011.01686.x
- Keiser, I., Nakagawa, S., Kobayashi, R. M., Chambers, D. L., Uraco, T., and Doolittle, R. E. (1973). Attractiveness of cue-lure and the degradation product 4-(p-hydroxyphenyl)-2-butanone to male melon flies in the field in Hawaii. *J. Econ. Entomol.* 66, 112–114. doi:10.1093/jee/66.1.112
- Lauson, C. R., Sjogren, R. E., Wright, S. E., and Prokopy, R. J. (1998). Attraction of *Rhagoletis pomonella* (Diptera: tephritidae) flies to odor of bacteria: apparent confinement to specialized members of Enterobacteriaceae. *Environ. Entomol.* 27, 853–857. doi:10.1093/ee/27.4.853
- Lee, C. J., DeMilo, A. B., Moreno, D. S., and Martinez, A. J. (1995). Analysis of the volatile components of a bacterial fermentation that is attractive to the Mexican fruit-fly, *Anastrepha ludens*. *J. Agr. Food Chem.* 43, 1348–1351. doi:10.1021/jf00053a041
- Li, k. (2020). Identification of host plant volatiles and pheromones and their electroantennogram responses of *Bactrocera minax*. Northwest A&F University. MA Thesis.
- Li, Y., Fang, J., Qi, X., Lin, M., Zhong, Y., Sun, L., et al. (2018). Combined analysis of the fruit metabolome and transcriptome reveals candidate genes involved in flavonoid biosynthesis in *actinidia arguta*. *J. Mol. Sci.* 9, 1471. doi:10.3390/jms19051471
- Liu, H., Zhao, X. F., Fu, L., Han, Y. Y., Chen, J., and Lu, Y. Y. (2017). *BdorOBP2* plays an indispensable role in the perception of methyl eugenol by mature males of *Bactrocera dorsalis* (Hendel). *Sci. Rep.* 7, 15894–15914. doi:10.1038/s41598-017-15893-6
- Liu, L. J., Martinez-Sañudo, I., Mazzon, L., Prabhakar, C. S., Girolami, V., Deng, Y. L., et al. (2016). Bacterial communities associated with invasive populations of *Bactrocera dorsalis* (Diptera: tephritidae) in China. *B. Entomol. Res.* 106, 718–728. doi:10.1017/S0007485316000390
- Luo, M. J. (2016). Molecular diversity analysis of the intestinal bacterial communities from adult *Bactrocera tau* (Walker) and their trapping effect. Thesis FAFU's master student.
- Narit, T., and Anuchit, C. (2011). Attraction of *Bactrocera cucurbitae* and *B. papayae* (Diptera: tephritidae) to the odor of the bacterium *Enterobacter cloacae*. *Philipp. Agric. Sci.* 94, 1–6. doi:10.5423/PPJ.2011.27.1.044
- Nishida, R., Tan, K. H., and Fukami, H. (1988). Cis-3,4-dimethoxycinnamyl alcohol from the rectal glands of male Oriental fruit fly, *Dacus dorsalis*. *Chem. Express* 3, 207–210.
- Park, S. J., De Faveri, S. G., Cheesman, J., Hanssen, B. L., Cameron, D. N., Jamie, I. M., et al. (2020). Zingerone in the flower of *Passiflora maliformis* attracts an Australian fruit fly, *Bactrocera jarvisi* (Tryon). *Molecules* 25, 2877. doi:10.3390/molecules25122877
- Qin, Y. J., Krosch, M. N., Schutze, M. K., Zhang, Y., Wang, X. X., Prabhakar, C. S., et al. (2018). Population structure of a global agricultural invasive pest, *Bactrocera dorsalis* (Diptera: tephritidae). *Evol. Appl.* 11, 1990–2003. doi:10.1111/eva.12701
- Reddy, K., Sharma, K., and Singh, S. (2014). Attractancy potential of culturable bacteria from the gut of peach fruit fly, *Bactrocera zonata* (Saunders). *Phytoparasitica* 42, 691–698. doi:10.1007/s12600-014-0410-9
- Reyes-Hernández, M., Thimmappa, R., Abraham, S., Pagadala Damodaram, K. J., and Pérez-Staples, D. (2019). Methyl eugenol effects on *Bactrocera dorsalis* male total body protein, reproductive organs and ejaculate. *J. Appl. Entomol.* 143, 177–186. doi:10.1111/jen.12576
- Robacker, D. C., and Bartelt, R. J. (1997). Chemicals attractive to Mexican fruit fly from *Klebsiella pneumoniae* and *Citrobacter freundii* cultures sampled by solid-phase microextraction. *J. Chem. Ecol.* 23, 2897–2915. doi:10.1023/A:1022579414233
- Robacker, D. C., and Flath, R. A. (1995). Attractants from *Staphylococcus aureus* cultures for Mexican fruit fly, *Anastrepha ludens*. *J. Chem. Ecol.* 21, 1861–1874. doi:10.1007/BF02033682
- Robacker, D. C., and Garcia, J. A. (1993). Effects of age, time of day, feeding history, and gamma irradiation on attraction of Mexican fruit flies (Diptera: tephritidae), to bacterial odor in laboratory experiments. *Environ. Entomol.* 22, 1367–1374. doi:10.1093/ee/22.6.1367
- Robacker, D. C., Martinez, A. J., Garcia, J. A., and Bartelt, R. J. (1998). Volatiles attractive to the Mexican fruit fly (Diptera: tephritidae) from eleven bacteria taxa. *Fla. Entomol.* 81, 497–508. doi:10.2307/3495948
- Royer, J. E., Khan, M., and Mayer, D. G. (2018). Methyl-isoeugenol, a highly attractive male lure for the cucurbit flower pest *Zeugodacus diversus* (Coquillett) (syn. *Bactrocera diversa*) (Diptera: tephritidae: Dacinae). *J. Econ. Entomol.* 111, 1197–1201. doi:10.1093/jee/toy068
- Royer, J. E., Mille, C., Cazerres, S., Brinon, J., and Mayer, D. G. (2019a). Isoeugenol, a more attractive male lure for the cue-lure-responsive pest fruit fly *Bactrocera curvipennis* (Diptera: tephritidae: Dacinae), and new records of species responding to zingerone in New Caledonia. *J. Econ. Entomol.* 112, 1502–1507. doi:10.1093/jee/toz034
- Royer, J. E., Teagle, G. E., Ahoafi, E., and Mayer, D. G. (2019b). Methyl-isoeugenol, a significantly more attractive male lure for the methyl eugenol-responsive Pacific fruit fly, *Bactrocera xanthodes* (Diptera: tephritidae). *Austral. Entomol.* 58, 800–804. doi:10.1111/aen.12398
- Ruta, V., Datta, S. R., Vasconcelos, M. L., Freeland, J., Looger, L. L., and Axel, R. (2010). A dimorphic pheromone circuit in *Drosophila* from sensory input to descending output. *Nature* 468, 686–690. doi:10.1038/nature09554
- Shelly, T. (2010). Effects of methyl eugenol and raspberry ketone/cue lure on the sexual behavior of *Bactrocera* species (Diptera: tephritidae). *Appl. Entomol. Zool.* 45, 349–361. doi:10.1303/aez.2010.349
- Shi, W., Kerdelhué, C., and Ye, H. (2012a). Genetic structure and inferences on potential source areas for *Bactrocera dorsalis* (Hendel) based on mitochondrial and microsatellite markers. *Plos One* 7, e37083. doi:10.1371/journal.pone.0037083
- Shi, Z., Wang, L., and Zhang, H. (2012b). Low diversity bacterial community and the trapping activity of metabolites from cultivable bacteria species in the female reproductive system of the oriental fruit fly, *Bactrocera dorsalis* Hendel (Diptera: tephritidae). *Int. J. Mol. Sci.* 13, 6266–6278. doi:10.3390/jms13056266
- Tan, K. H., Tokushima, I., Ono, H., and Nishida, R. (2011). Comparison of phenylpropanoid volatiles in male rectal pheromone gland after methyl eugenol consumption, and molecular phylogenetic relationship of four global pest fruit fly species: *Bactrocera invadens*, *B. dorsalis*, *B. correcta* and *B. zonata*. *Chemoecology* 21, 25–33. doi:10.1007/s00049-010-0063-1
- Vargas, R. L., Shelly, T. E., Leblanc, L., and Pinero, J. C. (2010). Recent advances in methyl eugenol and cue-lure technologies for fruit fly detection, monitoring, and control in Hawaii. *Vitamins Hormones* 83, 575–595. doi:10.1016/S00083-6729(10)83023-7
- Verghese, A., Soumya, C. B., Shivashankar, S., Manivannan, S., and Krishnamurthy, S. V. (2012). Phenolics as chemical barriers to female fruit fly, *Bactrocera dorsalis* (Hendel) in mango. *Curr. Sci.* 103, 563–566.
- Wang, H., Jin, L., Peng, T., Zhang, H., Chen, Q., and Hua, Y. (2014). Identification of cultivable bacteria in the intestinal tract of *Bactrocera dorsalis* from three different populations and determination of their attractive potential. *Pest Manag. Sci.* 70, 80–87. doi:10.1002/ps.3528
- Wang, H., Jin, L., and Zhang, H. (2011). Comparison of the diversity of the bacterial communities in the intestinal tract of adult *Bactrocera dorsalis* from three different populations. *J. Appl. Microbiol.* 110, 1390–1401. doi:10.1111/j.1365-2672.2011.05001.x
- Wee, S. L., and Tan, K. H. (2005). Female sexual response to male rectal volatile constituents in the fruit fly, *Bactrocera carambolae* (Diptera: tephritidae). *Appl. Entomol. Zool.* 40, 365–372. doi:10.1303/aez.2005.365
- Wee, S. L., Tan, K. H., and Nishida, R. (2007). Pharmacophagy of methyl eugenol by males enhances sexual selection of *Bactrocera carambolae*. *J. Chem. Ecol.* 33, 1272–1282. doi:10.1007/s10886-007-9295-0
- Yan, X. Z., Wang, Z. Y., Ma, L., Song, C. F., Zhao, J. Y., Wang, C. Z., et al. (2023). Electroantennogram and behavioural responses of *Plutella xylostella* to volatiles from the non-host plant *Mentha spicata*. *J. Appl. Entomol.* 147, 511–519. doi:10.1111/jen.13144
- Zhang, J. (1991). Trapping effect of attractants on fruit fly pests. *Plant Quar.* 5, 401–404.
- Zhang, J., Liu, W., Chang, H., Wang, Q., Yuan, J., Liu, L., et al. (2024). Methyl eugenol regulates mating behavior in oriental fruit flies by enhancing lek attractiveness. *Natl. Sci. Rev.* nwae294. doi:10.1093/nsr/nwae294
- Zhang, X., Wei, C., Miao, J., Zhang, X., Wei, B., Dong, W., et al. (2019). Chemical compounds from female and male rectal pheromone glands of the guava fruit fly, *Bactrocera correcta*. *Insects* 10, 78. doi:10.3390/insects10030078



OPEN ACCESS

EDITED BY

Norman Arthur Ratcliffe,
Swansea University, United Kingdom

REVIEWED BY

Hakan Bozdoğan,
Ahi Evran University, Türkiye
Guenter Artur Schaub,
Ruhr University Bochum, Germany

*CORRESPONDENCE

Fernando Ariel Genta,
✉ genta@ioc.fiocruz.br,
gentafernando@gmail.com

RECEIVED 22 December 2023

ACCEPTED 30 April 2024

PUBLISHED 15 October 2024

CITATION

Costa MC, Moreira CJC, Oliveira PL, Juberg J, Castro DP and Genta FA (2024), Sugar feeding in triatomines: a new perspective for controlling the transmission of Chagas disease. *Front. Physiol.* 15:1360255. doi: 10.3389/fphys.2024.1360255

COPYRIGHT

© 2024 Costa, Moreira, Oliveira, Juberg, Castro and Genta. This is an open-access article distributed under the terms of the [Creative Commons Attribution License \(CC BY\)](#). The use, distribution or reproduction in other forums is permitted, provided the original author(s) and the copyright owner(s) are credited and that the original publication in this journal is cited, in accordance with accepted academic practice. No use, distribution or reproduction is permitted which does not comply with these terms.

Sugar feeding in triatomines: a new perspective for controlling the transmission of Chagas disease

Mariana C. Costa¹, Carlos J. C. Moreira²,
Pedro Lagerblad de Oliveira^{3,4}, José Juberg⁵,
Daniele Pereira de Castro^{1,4} and Fernando Ariel Genta^{1,4*}

¹Laboratório de Bioquímica e Fisiologia de Insetos, Instituto Oswaldo Cruz, Fundação Oswaldo Cruz, Rio de Janeiro, Brazil, ²Laboratório de Doenças Parasitárias, Instituto Oswaldo Cruz, Fundação Oswaldo Cruz, Rio de Janeiro, Brazil, ³Laboratório de Bioquímica de Artrópodes Hematófagos, Centro de Ciências da Saúde, Universidade Federal do Rio de Janeiro, Rio de Janeiro, Brazil, ⁴Instituto Nacional de Ciência e Tecnologia em Entomologia Molecular, Rio de Janeiro, Brazil, ⁵Laboratório Nacional e Internacional de Referência em Taxonomia de Triatomíneos, Instituto Oswaldo Cruz, Fundação Oswaldo Cruz, Rio de Janeiro, Brazil

Introduction: Triatomines are vectors of *Trypanosoma cruzi*, the etiological agent of Chagas disease. Currently, there is no vaccine against this disease. Thus, control of the insect vector population is the main strategy available to reduce the number of cases. Triatomines are considered obligate hematophagous, but different alternative feeding behaviors were described, such as haemolymphagy or plant feeding.

Methods: To determine the preference for sugar feeding in nymphs and adults of *Rhodnius prolixus*, the insects were exposed a piece of cotton containing bromophenol blue plus sucrose. In addition, we offered several sugars for different species of triatomines, and tested sugar meals as a route of delivery of insecticides in first-instar nymphs of *R. prolixus*. The effect of sugar feeding on the physiology of these different species of triatomines was recorded.

Results: First instar nymphs ingested sucrose more strongly than other stages, and showed high mortality rates. In different species of triatomines, sucrose induced an ingestion, but engorgement varied according to the species. *R. prolixus* nymphs showed an indiscriminate intake of various sugars, with very different physiological effects. Furthermore, ingesting different combinations of insecticides + sugar significantly reduced insect survival.

Discussion: In summary, we described for the first-time sugar feeding as a widespread behavior in several species of triatomines, and the possibility of the use of toxic sugar baits for the control of these vectors. The knowledge of feeding behavior in these insects can be fundamental for the development of new strategies to control Chagas disease.

KEYWORDS

triatomine, sugar feeding, Chagas disease, attractive toxic sugar bait (ATSB), *Rhodnius prolixus*

1 Introduction

Triatomines (Triatominae, Hemiptera, Reduviidae), popularly known as kissing bugs, are insect vectors of the flagellated protozoan, *Trypanosoma cruzi* (Protozoa, Sarcomastigophora, Kinetoplastida, Trypanosomatidae) (Chagas, 1909), which causes Chagas disease or American Trypanosomiasis. It is a severe and fatal pathology, endemic in the American continent and until now there is no vaccine or definitive cure for this illness. The World Health Organization estimated that there are about 6–7 million infected people in the world, causing approximately 10,000 deaths per year (World Health Organization, 2022). There is a huge concern that with global warming and migration of human populations, new cases of the disease can occur in the US, Europe or even Asia, with the spreading of insect vectors and the establishment of new cycles for the parasite (World Health Organization, 2022).

Transmission can occur through contact with the feces and urine of infected triatomines, in the bite area, mucous membranes at the lips or in the eye regions, as well as blood transfusion, organ transplantation, congenitally (mother to child) or oral route (Blanchet et al., 2014; Coura, 2015). In recent years, oral transmission was recorded with greater frequency in some countries in South America, mainly in northern Brazil (Pará, Amapá and Amazonas), Colombia, Venezuela, Bolivia, and French Guiana (Alarcón de Noya et al., 2010; Santalla et al., 2011; Blanchet et al., 2014; Soto et al., 2014; Vargas et al., 2018). This type of transmission occurred through the ingestion of contaminated material with parts of the infected triatomines and/or their feces. The different recorded outbreaks were attributed to the ingestion of contaminated foods, such as açai berries, guava juice, sugarcane juice, açai juice, bacaba juice, and contaminated water (Dias et al., 2008; Nóbrega et al., 2009; Alarcón de Noya et al., 2010; Blanchet et al., 2014; Vargas et al., 2018; Santana et al., 2019).

Currently, there are more than 150 species of triatomines in nature (Oliveira and Alevi, 2017; de Oliveira et al., 2018; Dorn et al., 2018; Lima-Cordón et al., 2019) and the genera *Panstrongylus*, *Rhodnius* and *Triatoma* are considered the main vectors of medical importance. These insects colonize several habitats, peridomicile (chicken coops, pens and stables), intradomicile and wild environments (palm trees, rocks, trunks, tree tops, animal nests, and bromeliads) (Jurberg et al., 2014). Although these insects were characterized by the obligate hematophagous feeding habit (Lehane, 2005), triatomines had alternative feedings, such as hemolymphagia, “cleptohematophagy” (cannibalism), coprophagy and/or feeding from sugary sources (Ryckman, 1951; Lorosa et al., 2000; Sandoval et al., 2000; Ruas-Neto et al., 2001; Díaz-Albiter et al., 2016).

Recent studies observed for the first time that first instar nymphs of *Rhodnius prolixus* ingested *Solanum lycopersicum* (cherry tomato), which resulted in several physiological gains for the insect such as reduced weight loss caused by desiccation, increased life expectancy and increased intake of blood (Díaz-Albiter et al., 2016). Furthermore, all instars of *R. prolixus* ingested 10% sucrose under laboratory conditions (Díaz-Albiter et al., 2016). Additionally, *R. prolixus* and *Panstrongylus geniculatus* adults ingested a drop of water, and adults of both species and fifth instar nymphs of *R. prolixus* also guava juice (Páez-Rondón et al., 2018).

Carbohydrates are organic molecules that have different functions in organisms, the most important is the supply of

energy (Nelson and Cox, 2014). In nature, sap from plants, leaves, fruits and floral nectars are sources of sugar for various insects, and the composition and concentration vary between species (Nicolson and Thornburg, 2007). The nectar is basically composed of sucrose, glucose and fructose, but a wide variety of sugars have also been reported in different studies (Baker, 1982; Nicolson and Thornburg, 2007; Antón et al., 2017), including xylose, raffinose, maltose, mellibiose, among others (Wykes, 1952; Percival, 1961; Van Wyk and Nicolson, 1995; Nicolson and Van Wyk, 1998).

It is important to point out that most adult insects, in Diptera for example, both males and females, need carbohydrates that are acquired in a daily basis directly from plants (in nectar or sap), aphid secretions, and ripe fruits (Cameron et al., 1995). In general, these sources of sugars are important for mating, survival, oviposition, as a general source of energy, also affecting the development and infectivity of intestinal parasites (Williams, 1970; Lewis and Domoney, 1996; Brazil and Brazil, 2003; Bates, 2007).

Because there is no vaccine available for Chagas disease, the control of the vector insect populations is the main strategy available to reduce the number of cases. Across Latin America, the basic strategy is the chemical control through the use of residual action insecticides, especially pyrethroids. However, continuous use of these compounds can generate resistance in triatomine populations (Zerba, 1999; Vassena et al., 2000; Picollo et al., 2005; Echeverría et al., 2018), making it necessary to develop other control strategies. Within this context, several known methods are not directly applicable to the control of triatomines and, therefore, the discovery of a new methodology, effective, low cost and applicable in the field, such as the elaboration of sugar baits, for example, may be essential to reduce the impact of this disease.

Toxic sugar baits were widely studied and had been successfully tested on vector insects, mainly in Diptera, as an insecticide delivery strategy (Müller and Schlein, 2008; Müller et al., 2010; Qualls et al., 2015; Gu et al., 2020). This method was implemented in the field or in residential environments, being harmless to humans due to its low toxicity. Sugar acted as a phagostimulant, caused the insect to ingest the toxic solution, which ended up dying. Therefore, sugar baits pointed to new paths for the development of vector control, capable of altering the development of the insect and effectively reducing the transmission of various diseases. In a broader context, the association of this type of method can be a viable future alternative for the control of triatomines, which can be effectively applied in the field, for being a simple and economical strategy. Although many aspects related to the sugar feeding in kissing bugs are still unknown, these new vector control actions deserve more detailed investigations.

The purpose of this work was to investigate whether different species of triatomines were capable of ingesting sugar solutions in the laboratory, characterize the physiological effects in insects fed with different types of sugars, as well as, test sugar meals as a route for the delivery of insecticides in first-instar nymphs of *R. prolixus*. In summary, we described here the first report of ingestion of sugar solutions in several species of triatomines, which had been considered exclusive hematophagous, and we showed that 1st instar nymphs of *R. prolixus* ingested different combinations of insecticides with the sugar, that significantly reduced the insect survival. These facts lead to the conclusion that the description of new food sources opened new perspectives for the development of new control strategies against triatomines.

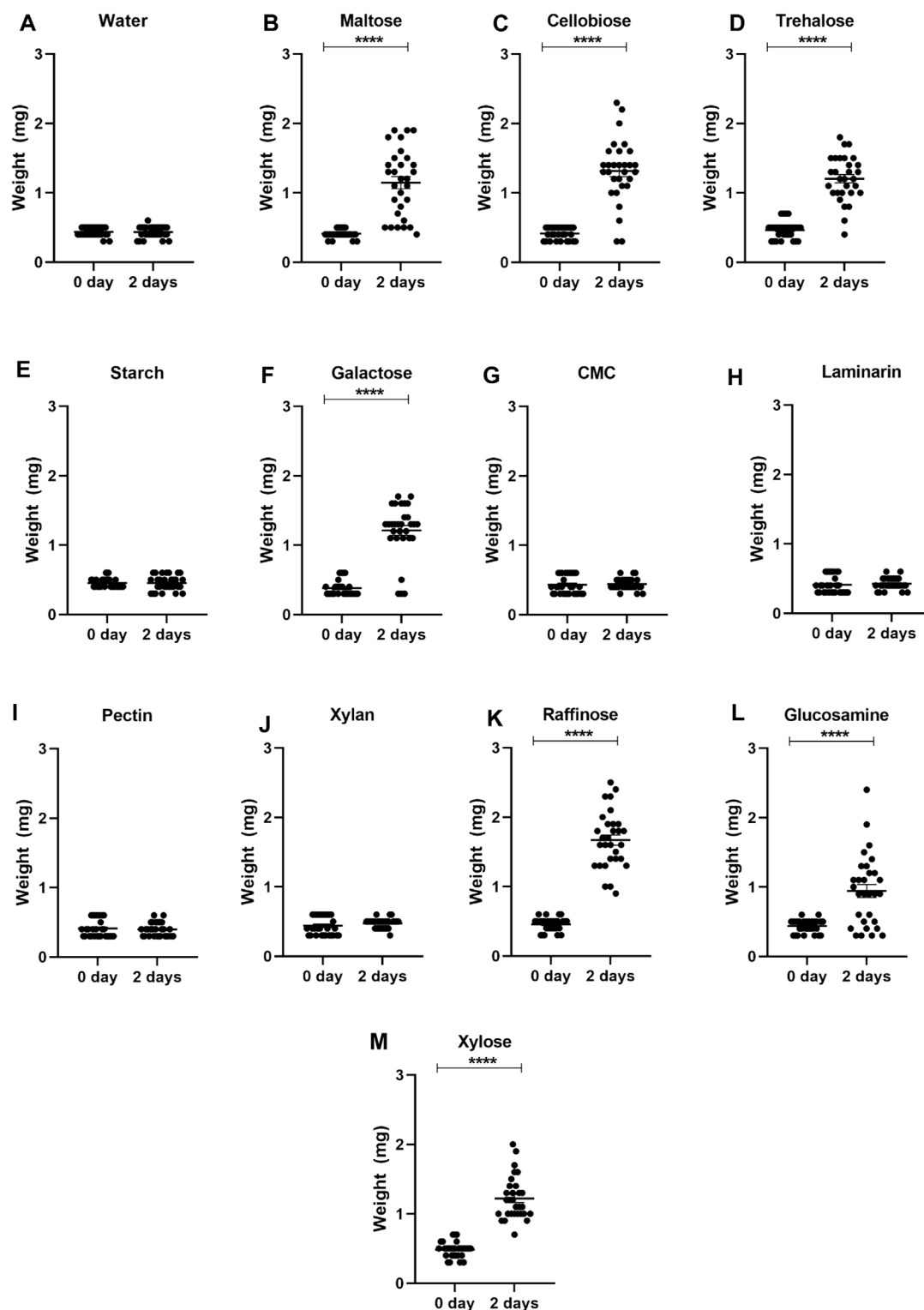
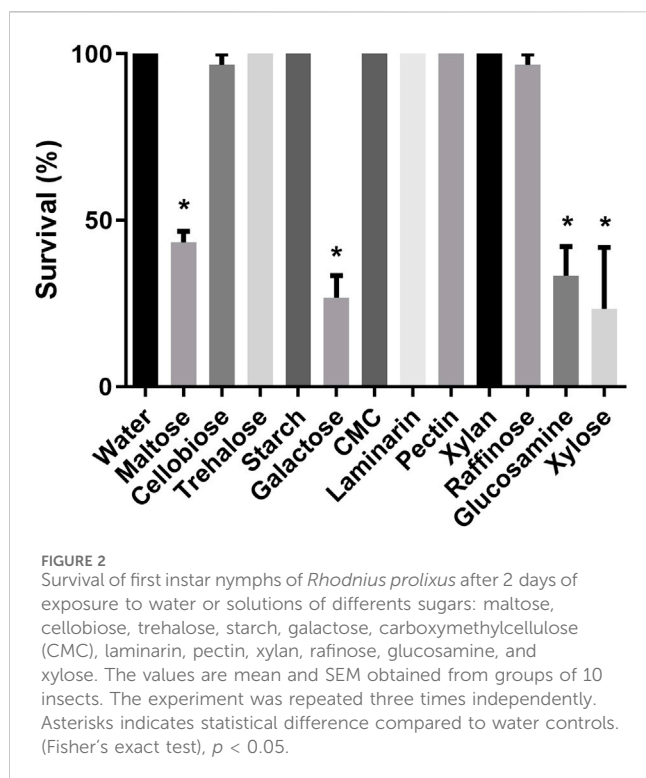


FIGURE 1

Weights of first instar nymphs of *Rhodnius prolixus* before (0 day) and after 2 days of exposure to water (A) or solutions of different sugars: maltose (B), cellobiose (C), trehalose (D), starch (E), galactose (F), carboxymethylcellulose (CMC) (G), laminarin (H), pectin (I), xylan (J), raffinose (K), glucosamine (L), and xylose (M). The values are mean and SEM obtained from groups of 10 insects. The experiment was repeated three times independently. Asterisks indicate significant differences compared to day 0 ($p < 0.0001$). Statistics: Unpaired t-test (water, maltose, trehalose, starafinosenose, glucosmine and xylose); Mann-Whitney test (cellobiose, galactose, CMC, laminarin, pectin and xylan).



2 Methods and scope of experiments

2.1 Insects maintenance

R. prolixus insects were obtained from an insectary at Laboratório de Bioquímica e Fisiologia de Insetos of Instituto Oswaldo Cruz at the Fundação Oswaldo Cruz. The triatomines fed defibrinated rabbit blood with the aid of an artificial apparatus (Azambuja and Garcia, 1997). The colony was bred at $28^{\circ} \pm 2^{\circ}\text{C}$ and $60\% \pm 5\%$ relative humidity.

Eggs from *Tritoma vitticeps*, *T. infestans*, *T. rubrovaria*, *T. dimidiata*, *Panstrongylus megistus*, and *Rhodnius neglectus* were obtained from Laboratório de Referência Nacional e Internacional em Taxonomia de Triatomíneos and Laboratório de Doenças Parasitárias at Instituto Oswaldo Cruz, Fiocruz. According to a previous investigation (Diaz-Albiter et al., 2016), first instar nymphs were used 14 days after hatching from the eggs and weighed (Electronic balance BEL model M214Ai, accuracy 0.1 mg, Piracicaba, Brazil). Only in the first series, that compared the ingestion of sucrose by nymphs and adults of *R. prolixus*, the period of starvation was unknown, and the insects were not weighed. Always ten insects were kept separately in a 100 mL glass vial containing 0.2 g cotton, wetted with 2 mL of the respective solution, closed by netting and placed in the insectary. Only in the toxic baits assays the conditions in the vials differed, they were kept inside an incubator at same temperature and humidity. The experiments were made in three biological replicates.

2.2 Offer of sugars to triatomines

To analyze the preference of sucrose intake in nymphs and adults of *R. prolixus* the piece of cotton was wetted with 10% (w/v) commercial

sucrose solution plus 0.5% (w/v) bromophenol blue. In the control groups the sucrose solution was replaced by ultrapure water. After 2 days of exposure, survival was recorded. Living insects were immobilized on ice and dissected (by separating the anterior and posterior midgut from the rest of the body) in 0.9% (w/v) physiological saline under the aid of a Luxeo 4Z stereomicroscope (Labomed, India). The intestines that turned visibly blue were counted.

To assess 1st instar *R. prolixus* nymphs feeding on the different sugar solutions, the following solutions were offered: maltose, cellobiose, trehalose, galactose, raffinose, and glucosamine at 10% (w/v); and xylose, starch, xylan, pectin, carboxymethylcellulose, and laminarin at 0.25% (w/v). Control group insects were exposed to a piece of cotton wetted with 2 mL of ultrapure water. After 2 days of exposure, the insects were weighed again and survival was recorded.

To determine whether different triatomine species ingest sucrose, five first-instar nymphs of *T. infestans*, *T. dimidiata*, *T. rubrovaria*, *T. vitticeps*, *P. megistus* and *R. neglectus* were offered sucrose and water (control) as in the comparison of nymphs and adults of *R. prolixus* (see above). After 2 days of exposure, the insects were weighed again, photographed (using a cell phone attached to a Luxeo 4Z stereomicroscope) and survival was recorded.

2.3 Effect of toxic sugar baits on *R. prolixus* survival

In this assay, we tested sugar baits as an insecticide delivery strategy for kissing bugs. Twenty first-instar nymphs of *R. prolixus* were exposed to a piece of cotton (0.3 mg) wetted in 300 μL of a 10% trehalose plus 3 μL of ethanol stock solution containing one of the following insecticides: Triflumuron 10 mM; Temephos 10 mM; Deltamethrin 5 mg/mL; Permethrin 20 mg/mL, and boric acid 1% (w/v). Separated groups of insects were exposed in the same conditions to insecticide solutions in water only. Control groups were exposed to 300 μL of ultrapure water, or 300 μL of 10% trehalose.

Therefore, a total of 12 groups were defined for the assays: (1) boric acid; (2) boric acid + trehalose; (3) temephos; (4) temephos + trehalose; (5) triflumuron; (6) triflumuron + trehalose; (7) deltamethrin; (8) deltamethrin + trehalose; (9) permethrin; (10) permethrin + trehalose; (11) water; (12) trehalose. Water and trehalose solution were used as negative and positive controls. All groups were weighed after 24 h of treatment with different compounds. The survival was evaluated daily for 4 days after exposure.

2.4 Statistical analysis

Statistical analyzes of all experiments were performed using the software GraphPad Prism version 9.0 for Windows, GraphPad Software, Boston, Massachusetts USA, www.graphpad.com. We evaluated the normality of data distribution using the D'Agostino & Pearson test. Data that had normal distributions were submitted to unpaired t -tests and data with non-normal distributions were analyzed with the non-parametric Mann-Whitney test. We used Fisher's exact test to analyze the survival experiments (Zar, 2010). The longevity curves were compared using the Log-rank (Mantel-Cox) test (Rai et al., 2021). The results represented the mean and the standard error of the mean (SEM). Significance was considered with $p < 0.05$.

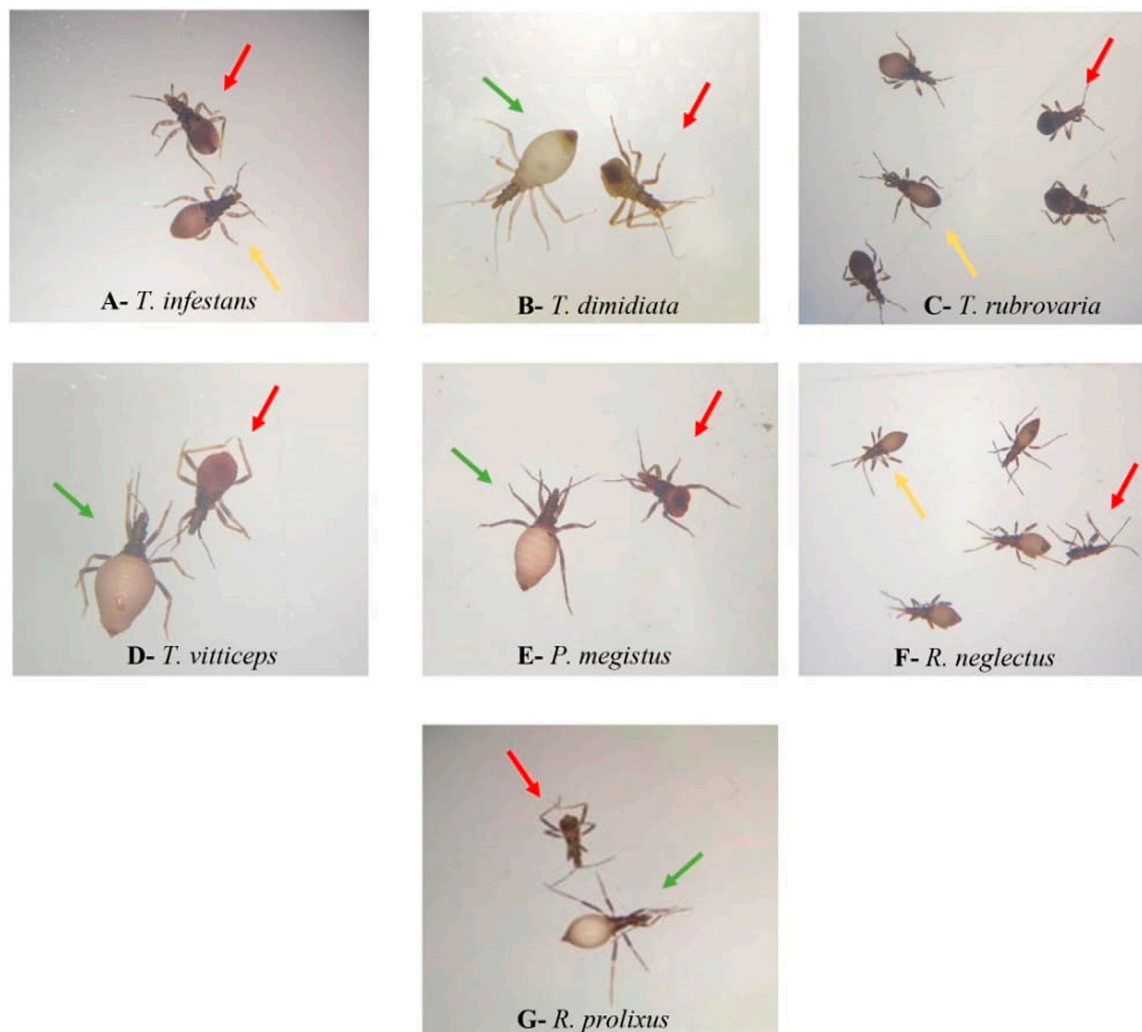


FIGURE 3
First instar nymphs of different triatomine species fully (green arrows) or partially (yellow arrows) engorged, next to visibly non-engorged insects (red arrows) after 2 days of exposure to sucrose 10%. *Triatoma infestans* (A), *Triatoma dimidiata* (B), *Triatoma rubrovaria* (C), *Triatoma vitticeps* (D), *Panstrongylus megistus* (E), *Rhodnius neglectus* (F), and *Rhodnius prolixus* (G).

3 Results

3.1 Ingestion of sugars by triatomines

Sucrose was offered to groups of different stages of *R. prolixus*, all containing 10 insects. None of the adults but $76\% \pm 12\%$ of first instar nymphs, $46\% \pm 3\%$ of second, $60\% \pm 15\%$ of third, $27\% \pm 27\%$ of fourth and $3\% \pm 3\%$ of fifth instar nymphs visibly engorged sucrose, indicated by the blue contents of the anterior midgut. The engorgement rates of fifth instar nymphs and adults differed significantly from those of first and third instar nymphs (Fisher's exact test, $p < 0.05$). None of the nymphs and adults ingested water. Considering the mortality rates, in the sucrose-offered groups, none of the fifth instar nymphs and adults died within the observation period of 2 days, but 60 ± 15 , 73 ± 3 , $76\% \pm 12\%$ and $90\% \pm 10\%$ of the groups of first, second, third and fourth instar nymphs died, respectively. No mortality in the water offered groups was observed. There was a positive Spearman correlation between the engorgement rates and mortalities [$r(16) = 0.920$, $p = 6.558 \cdot 10^{-8}$].

After observing the sucrose ingestion in nymphs and adults, we decided to assess if *R. prolixus* nymphs would ingest other types of sugars. Insects exposed to maltose, cellobiose, trehalose, galactose, raffinose, glucosamine, and xylose exhibited a significant increase in weight after 2 days of exposure (Figure 1), indicating an ingestion of the sugars. In contrast, insects exposed to starch, carboxymethylcellulose, laminarin, pectin, and xylan did not show weight gain. Again, control nymphs did not ingest water. Considering survival rates, all first instar nymphs that ingested trehalose survived and nearly all after ingestion of cellobiose and raffinose (Figure 2). Maltose, galactose, glucosamine and xylose killed more than 40%. Since starch, carboxymethylcellulose, laminarin, pectin and xylan had not been ingested, they did not affect the insects.

Sucrose solution was offered to first instar nymphs of *R. neglectus*, *R. prolixus*, *T. dimidiata*, *T. vitticeps*, *T. rubrovaria*, *T. infestans* and *P. megistus*. At least single nymphs were nearly fully or partially engorged (Figure 3; green and yellow arrows, respectively). None of the control

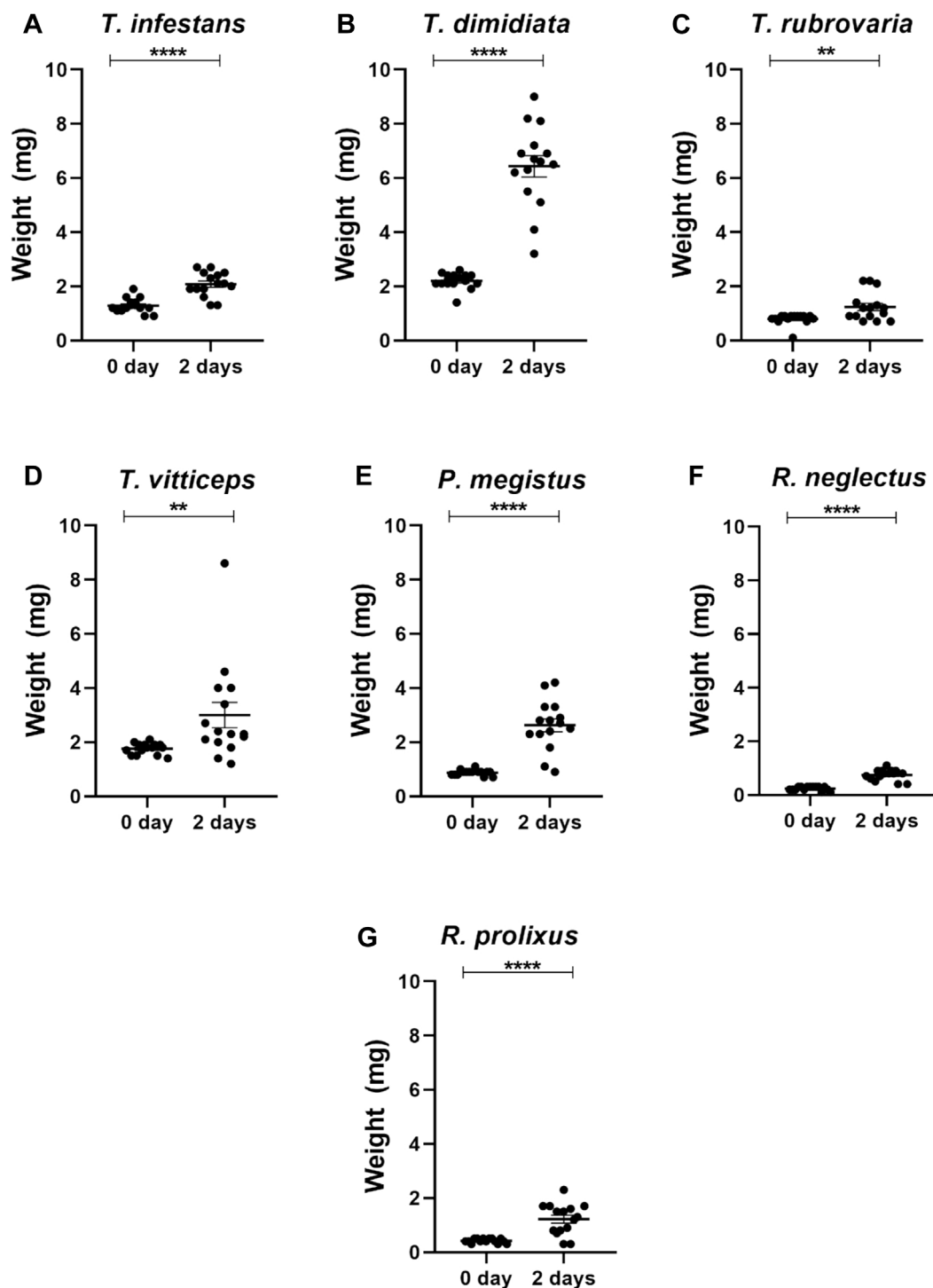
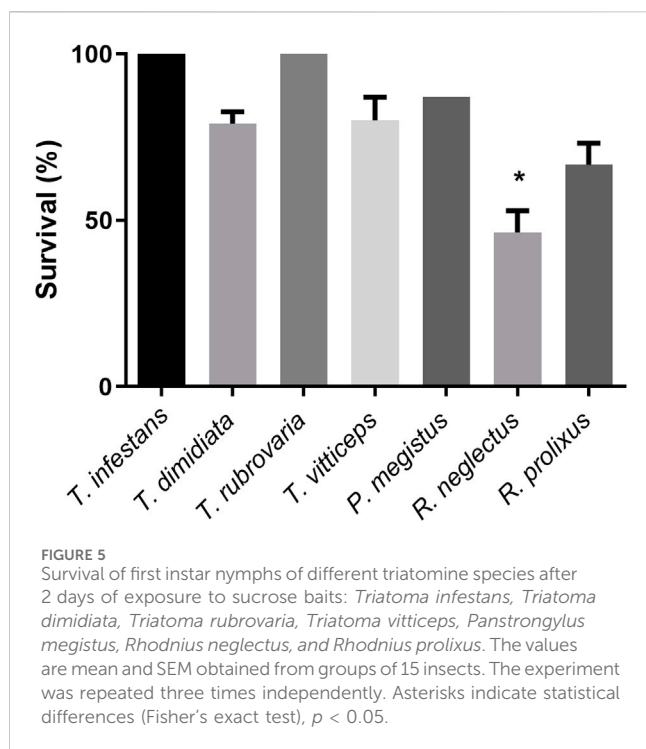


FIGURE 4

Weights of first instar nymphs of different triatomine species before (0 day) and after 2 days exposition to sucrose baits: *Triatoma infestans* (A), *Triatoma dimidiata* (B), *Triatoma rubrovaria* (C), *Triatoma vitticeps* (D), *Panstrongylus megistus* (E), *Rhodnius neglectus* (F), and *Rhodnius prolixus* (G). The values are mean and SEM obtained from groups of 15 insects. Asterisks indicate significant differences compared to day 0. Statistics: Unpaired t-test (*T. infestans*, *P. megistus*, *R. neglectus* and *R. prolixus*); Mann-Whitney test (*T. dimidiata*, *T. rubrovaria* and *T. vitticeps*). ** $p < 0.01$; **** $p < 0.0001$.

insects ingested water (red arrows). Whereas all *T. dimidiata* showed an increase in weight, the increases varied in the other species (Figure 4). After ingestion of low volumes, none of the first instars of *T. infestans*

and *T. rubrovaria* died within 2 days (Figure 5). The mortality rates of *R. prolixus*, *T. dimidiata*, *T. vitticeps* and *P. megistus* ranged between 10% and 30%, but 50% died in the group of *R. neglectus*.



3.2 Effect of toxic sugar baits on *R. prolixus*

Nymphs exposed to trehalose (control), boric acid + trehalose, triflumuron + trehalose, temephos + trehalose and deltamethrin + trehalose significantly increased their weight after 24 h of exposure to the different treatments, indicating that the insects ingested the insecticides in the presence of sugar (Figure 6). On the other hand, in nymphs exposed to water (control) and the insecticides without trehalose rarely the weight increased. This also occurred in the exposure to permethrin + trehalose. Since only two nymphs had ingested a small volume, the taste of pyrethroids might act against an ingestion. Analyzing the individual weights of live and dead insects after 24 h of exposure, in the insecticide + sugar combinations, the dead insects were those that were completely or partially engorged (Figure 7). Therefore, sugar had a phagostimulant effect on triatomines, and increased the effect of the toxic sugar baits in *R. prolixus* nymphs.

The presence of sugar with the boric acid insecticide resulted in a significant impact on insect survival, proved to be quite toxic for this species (Figure 8A; Supplementary Table S1A). Nymphs exposed to water had a survival rate of 85% after 4 days, trehalose 64.5%, boric acid 51.6% and boric acid + trehalose 30%.

Insects exposed to triflumuron had a survival after 4 days of 76.6% and triflumuron + trehalose 53.3% (Figure 8B; Supplementary Table S1B). These conditions were significantly different to each other (Supplementary Table S1B). Nymphs exposed to temephos after 4 days showed survival of 63.3% and temephos + trehalose 51.6% (Figure 8C), and both groups showed significant reduction in survival when compared to water (Supplementary Table S1C). Insects exposed to deltamethrin showed survival after 4 days of 78.3% and deltamethrin + trehalose of 50% (Figure 8D). The survival rate of the group treated with deltamethrin + trehalose was significantly lower when compared to deltamethrin or water

groups (Supplementary Table S1D). Nymphs exposed to permethrin after 4 days had a survival of 68.3% and permethrin + trehalose 60% (Figure 8E). The survival rates of both groups above were reduced significantly when compared to the control group with water (Supplementary Table S1E).

4 Discussion

The study of the feeding behavior in kissing bugs was crucial to better understand its basic biology and, thus, develop new control strategies to reduce the population of Chagas disease vectors (Oliveira and Genta, 2021). In this study, we tested several sugars, in different species of triatomines, to characterize the sugary solutions intake and physiological effects on these insects. Additionally, we tested sugar baits as an insecticide delivery strategy for triatomine bugs. All instars of *R. prolixus* (except adults) ingested sucrose in laboratory conditions. No water engorgement was observed in *R. prolixus* nymphs and adults, demonstrating that insects are not significantly attracted to water. Interestingly, sugar intake is more frequent in first instar nymphs. This probably happened because adult insects had greater energy reserves and were not in the same stage of fasting and malnutrition (Collier et al., 1981). The mortality in triatomines after exposure to sucrose was directly related to their specific age, as first instar nymphs had lower survival. Nymphs engorged more frequently when they were exposed to 10% sucrose and not to water. However, mortality was higher at this concentration. In other concentrations of sucrose, insects showed no avidity and, consequently, do not become engorged and do not die (data not shown). First instar nymphs of *R. prolixus* exposed to *S. lycopersicum* (cherry tomatoes) ingested plant tissues, and that improved the fitness of the insect (Díaz-Albiter et al., 2016). An increase in the amount of blood ingested and urine excreted was observed, such as decreased mortality, increased longevity, and reduced weight loss caused by desiccation. Taken together with our data, the physiological gain in insects exposed to tomato probably was not due to ingested sucrose, but perhaps to other sugars or other compounds of the secondary metabolism of the plant, which had beneficial effects for *R. prolixus*. It is clear that sugary feeding was not enough as an exclusive food source for triatomines, because these insects did not complete their biological cycle without a blood meal (García and Azambuja, 1985). It was not clear if sugary feeding has a nutritional role in the physiology of kissing bugs in nature. However, it might be possible that during a period of food restriction, these insects could alternatively feed on vegetables, and sugary food could somehow keep the insect alive for longer periods of fasting. In this respect, da Lage et al. (2024) recently reported the presence of plant DNA in field triatome samples, and the presence of amylase in *R. prolixus* genome.

As mentioned before, triatomines had different food sources in the laboratory. Nymphs ingested the hemolymph of cockroaches, and in the absence of vertebrates, haemolymphagy could be an alternative food source as a means of survival for the insect (Lorosa et al., 2000). This is coherent with the lack of toxicity observed for trehalose in our experiments. However, this behavior is restricted to some triatomine species (Durán et al., 2016).

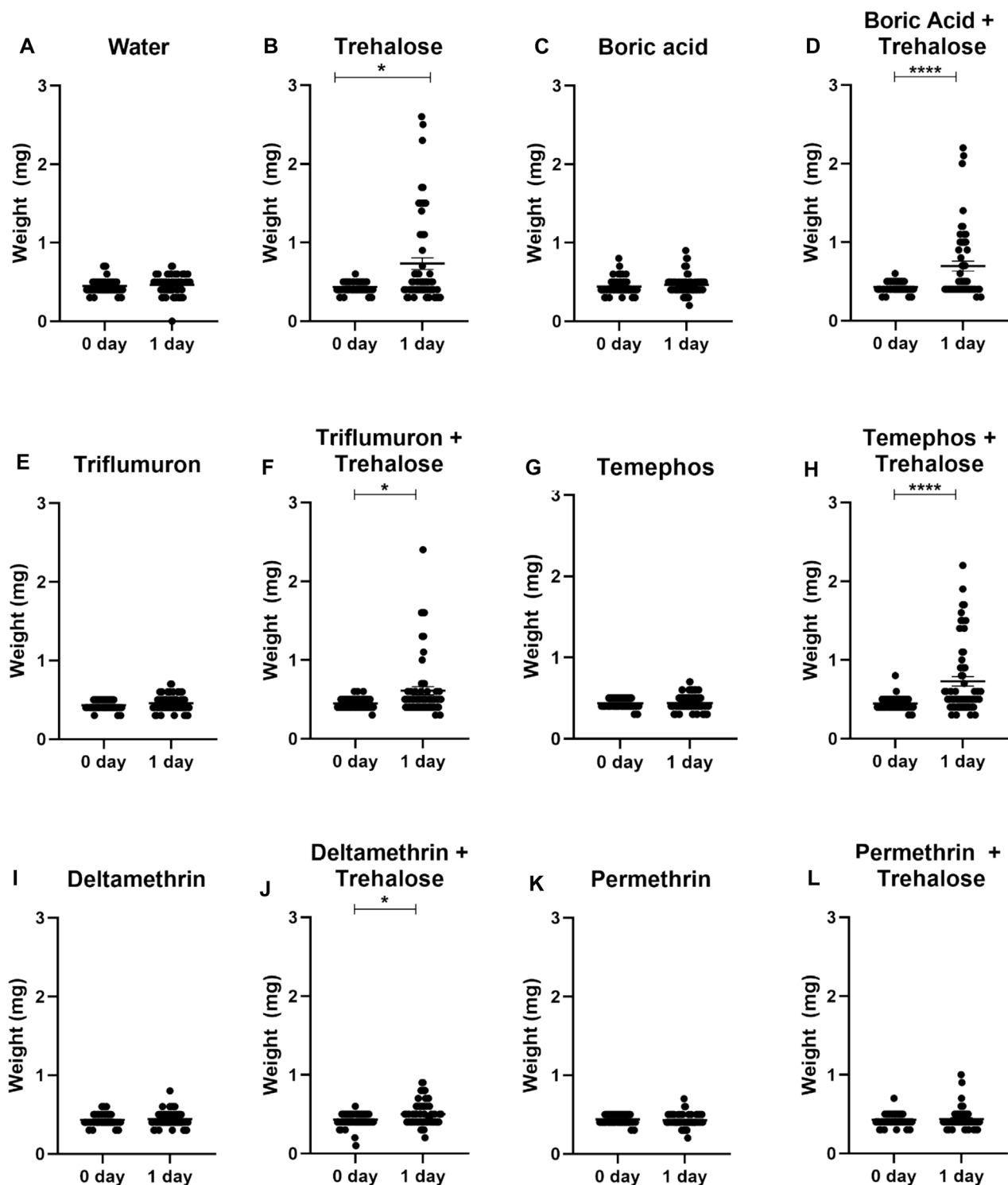


FIGURE 6
Weights of first instar nymphs of *Rhodnius prolixus* before (0 day) and after 1 day exposure to baits with water (A), trehalose (B), boric acid (C), boric acid + trehalose (D), triflumuron (E), triflumuron + trehalose (F), temephos (G), temephos + trehalose (H), deltamethrin (I), deltamethrin + trehalose (J), permethrin (K), permethrin + trehalose (L). The experiment was repeated three times independently, with 20 insects in each group. Asterisks indicate significant differences compared to day 0. Statistics: Unpaired t-test (triflumuron, temephos and permethrin); Mann-Whitney test (water, trehalose, acid boric, acid boric + trehalose, triflumuron + trehalose, temephos + trehalose, deltamethrin, deltamethrin + trehalose and permethrin + trehalose). * $p < 0.05$; **** $p < 0.0001$.

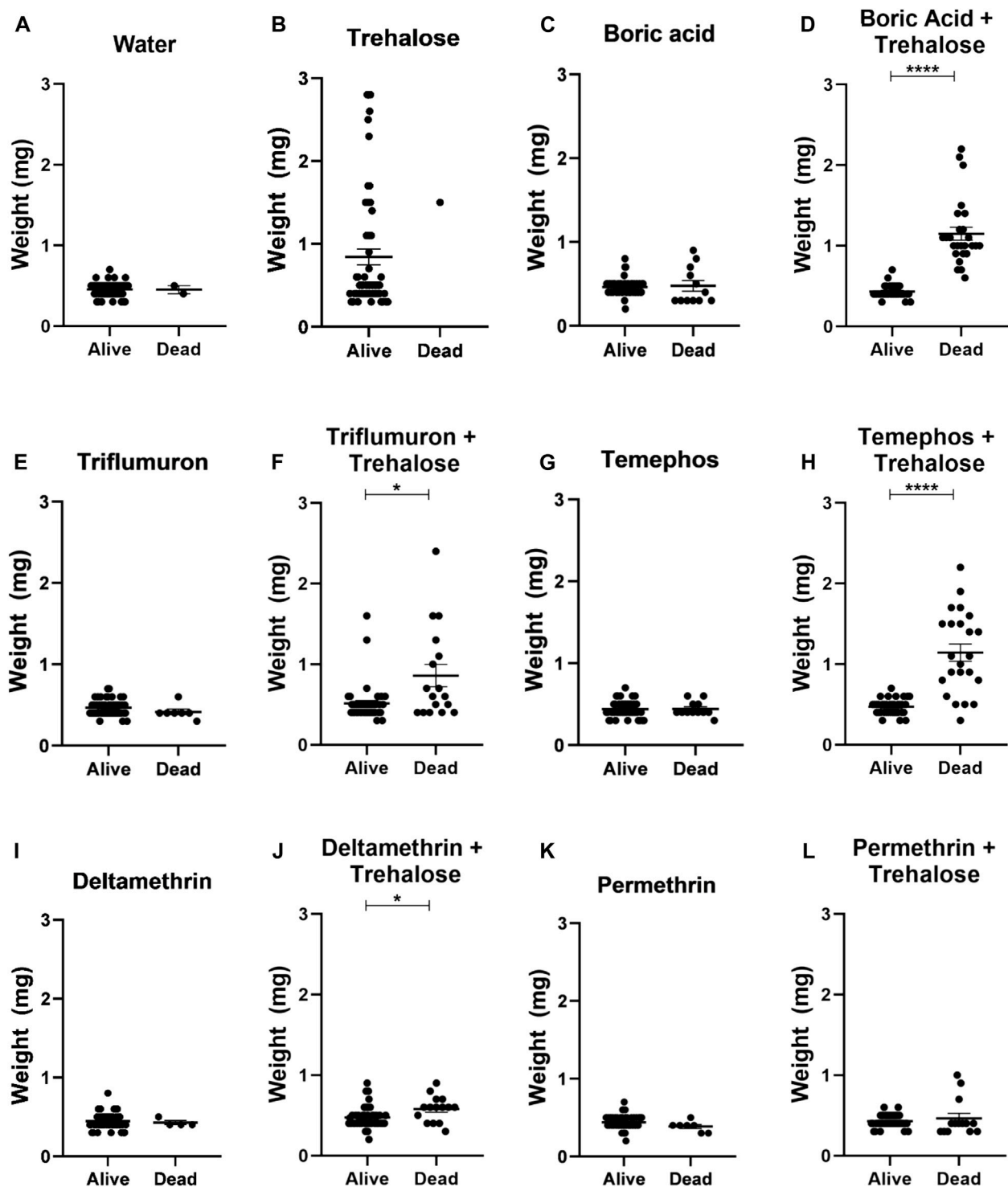


FIGURE 7

Weights of live and dead first instar *Rhodnius prolixus* nymphs after 1 day of exposure to baits with water (A), trehalose (B), boric acid (C), boric acid + trehalose (D), triflumuron (E), triflumuron + trehalose (F), temephos (G), temephos + trehalose (H), deltamethrin (I), deltamethrin + trehalose (J), permethrin (K), permethrin + trehalose (L). The experiment was repeated three times independently, with 20 samples in each group. Asterisks indicate significant differences compared to day 0. Statistics: Unpaired t-test (triflumuron, temephos and temephos + trehalose); Mann-Whitney test (water, trehalose, acid boric, acid boric + trehalose, triflumuron + trehalose, deltamethrin, deltamethrin + trehalose and permethrin + trehalose). * $p < 0.05$; **** $p < 0.0001$.

When we performed a screening with different sugars, there was an indiscriminate intake, but with different physiological outcomes. The toxicity of some sugars, especially polysaccharides, was not

conclusively assessed, due to the lack of ingestion. Triatomines that fed on trehalose showed a high engorgement rate and none died. Probably the effects of ingested trehalose were more associated with

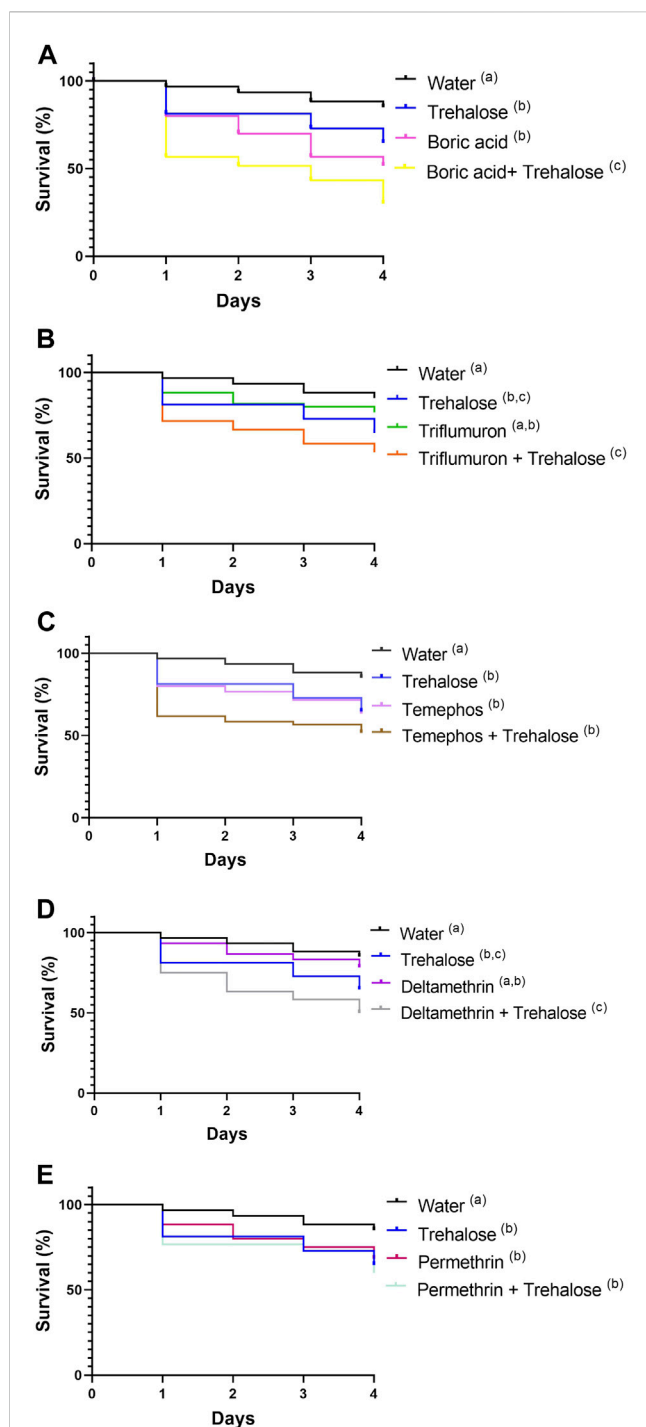


FIGURE 8
Survival of first instar nymphs of *Rhodnius prolixus* during exposure to baits containing: boric acid, boric acid + trehalose (A), triflumuron, triflumuron + trehalose (B), temephos, temephos + trehalose (C), deltamethrin, deltamethrin + trehalose (D), permethrin, permethrin + trehalose (E); water, trehalose (controls). All experiments were performed simultaneously with the same control groups. The experiment was repeated three times independently, with 20 insects in each group. Different letters denote curves that are significantly different by log-rank analysis (Mantel-Cox, $p < 0.05$).

haemolymphagy rather than phytophagy. Therefore, there was a possibility that the insects were adapted to ingest this sugar. In summary, the sugary feeding in triatomines was completely

nonspecific, with no discrimination between different sugars, and the detection of the sugar solution seemed to occur after initial contact. However, in our experiments there was no choice between sugars, so the insect had only the options between feeding or starving. Other experimental designs must be used to assess particular feeding preferences.

The polysaccharides that were not ingested as starch, carboxymethylcellulose, laminarin, pectin, and xylan were probably sugars with low sweet taste. Triatomines preferred sweeter sugars, such as sucrose. Another factor that possibly contributed to the low ingestion was the higher viscosity of the solutions, which may have decreased the palatability and, consequently, the attractivity to the nymphs.

All the seven tested triatomine species ingested sugar solutions and significantly increased their weight, and showed a phagostimulating effect, but engorgement varied according to the species. Of note, when these insects were exposed to water or saline solutions, we did not observe engorgement (data not shown). Engorgement was previously seen only when the insect feeds on blood, ATP, or 2,3-diphosphoglycerate. ATP was widely known in the literature as a chemical phagostimulant in *R. prolixus* (Friend and Smith, 1971; Friend and Smith, 1982), as well as 2,3-diphosphoglycerate (Macarini, 1983). Therefore, it was the first time that sugars were reported to be a phagostimulants for triatomines.

Accordingly, 1st instar nymphs of *R. prolixus* ingested different combinations of insecticides + sugar and the presence of sugar in the insecticide bait significantly reduced insect survival. Remarkably, among all the insecticides tested, boric acid was highly effective, since we observed a high rate of engorgement and a low survival rate when compared to the controls. The results were in accordance with several studies of toxic sugar baits where boric acid has been shown to be effective against various dipterans (Naranjo et al., 2013; Bhami and Das, 2015). Toxic sugar baits may be an interesting new tool for the control of triatomines. Sugar feeding resulted in ingestion of the insecticide by the triatomine, which meant a route of action that is completely different to the current insecticides available for triatomine control, that work by residual contact with treated surfaces. This might have implications for exploring new insecticide mechanisms, as well as making the surviving of refractory individuals more difficult.

An important consequence of this new delivery system for triatomines was the use of lower concentrations of insecticides, when we compared to other strategies. For example, a bait with hexachlorocyclohexane 1% (v/v) that explored the water drinking behavior of triatomines was proposed (Lima et al., 1992). For comparison, we observed similar results using 0.01% boric acid. For the pyrethroids tested, it was difficult to make a direct comparison, because the known toxicities for triatomines were reported in contact experiments, after the treatment of surfaces. However, a treated paper with 25 cm² contained 20 µg deltamethrin or 46 µg cypermethrin at 50% lethal concentration (Alzogaray and Zerba, 2001), an amount which was in the same range of the sugar baits presented here, with 15 µg deltamethrin or 60 µg permethrin. Nevertheless, it was clear that the environmental impact of a sugar bait was lower than a treated surface, because ingestion was a more targeted delivery mode than contact. From the insecticides tested, Triflumuron allowed the best comparison between different scenarios. *Rhodnius prolixus* was fed with blood containing 4.8 g/L Triflumuron, which is 133 times higher than the 0.036 g/L dose used in our experiments (Henriques et al., 2016). It

was not clear, however, if the high toxicity observed in some of our experiments was a result of a special sensitivity of the sugar-fed gut to the insecticides, or sublethal effects of the sugars ingested. Additionally, sugar baits could be explored to the delivery of anti-parasitic compounds or microorganisms with anti-*T.cruzi* activity, in a paratransgenesis approach that was explored before by other groups, where the delivery of the microorganisms was an important limiting factor (Hurwitz et al., 2011).

In conclusion, sugar feeding was a widespread behavior in triatomines, with different physiological outcomes. *Rhodnius prolixus* actively ingested different monosaccharides and disaccharides, but this behavior was observed only in nymphs. Some of the sugars had strong toxic effects on *R. prolixus*, especially sucrose, but this effect varied in other triatomine species. However, more research is needed to explain the effects of ingestion of sugary feeding in these insects and the mechanisms of sucrose toxicity, addressing both evolutionary and physiological points of view. Besides that, different insecticides, mainly boric acid, were used in toxic sugar baits against triatomines. More detailed knowledge of the role of sugar meals in triatomines may be important for the development of new control tools against these vector insects.

Data availability statement

The original contributions presented in the study are included in the article/**Supplementary Material**, further inquiries can be directed to the corresponding author.

Ethics statement

Experimental protocols for the maintenance of triatomines and blood feeding were approved by Ethics Committee in Animal Experimentation (CEUA/FIOCRUZ) under protocol number LW019/17.

Author contributions

MC: Conceptualization, Data curation, Formal Analysis, Investigation, Methodology, Visualization, Writing–original draft, Writing–review and editing. CM: Resources, Writing–review and editing. PL: Conceptualization, Funding acquisition, Project administration, Resources, Writing–review and editing. JJ: Resources, Writing–review and editing. DC: Conceptualization, Funding acquisition, Methodology, Project administration, Resources, Writing–review and editing. FG: Conceptualization,

Data curation, Formal Analysis, Funding acquisition, Investigation, Methodology, Project administration, Resources, Supervision, Writing–original draft, Writing–review and editing.

Funding

The author(s) declare that financial support was received for the research, authorship, and/or publication of this article. MC was a Ph.D. student in the Parasite Biology Post-graduation program at the Oswaldo Cruz Institute (CAPES). FG and PL are research fellows of the agencies CNPq (Produtividade em Pesquisa, grant no. 312305/2022-2) and Faperj (Cientistas do Nosso Estado, grant no. E-26/200.454/2023). This work was also funded by Fundação Oswaldo Cruz (grant. no. IOC-008-FIO-22-2-21).

Acknowledgments

We are grateful to José Carlos Nascimento Oliveira, Maria José da Silva de Souza, and Francisco Luiz Ancelmo for the technical maintenance of the triatomine colonies.

Conflict of interest

The authors declare that the research was conducted in the absence of any commercial or financial relationships that could be construed as a potential conflict of interest.

The author(s) declared that they were an editorial board member of Frontiers, at the time of submission. This had no impact on the peer review process and the final decision.

Publisher's note

All claims expressed in this article are solely those of the authors and do not necessarily represent those of their affiliated organizations, or those of the publisher, the editors and the reviewers. Any product that may be evaluated in this article, or claim that may be made by its manufacturer, is not guaranteed or endorsed by the publisher.

Supplementary material

The Supplementary Material for this article can be found online at: <https://www.frontiersin.org/articles/10.3389/fphys.2024.1360255/full#supplementary-material>

References

- Alarcón de Noya, B., Díaz-Bello, Z., Colmenares, C., Ruiz-Guevara, R., Mauriello, L., Zavala-Jaspe, R., et al. (2010). Large urban outbreak of orally acquired acute Chagas disease at a school in Caracas, Venezuela. *J. Infect. Dis.* 201, 1308–1315. doi:10.1086/651608
- Alzogaray, R. A., and Zerba, E. N. (2001). Third instar nymphs of *Rhodnius prolixus* exposed to α -cyanopyrethroids: from hyperactivity to death. *Arch. Insect Biochem. Physiol.* 46, 119–126. doi:10.1002/arch.1022
- Antoñ, S., Komoñ-Janczara, E., and Denisow, B. (2017). Floral nectary, nectar production dynamics and chemical composition in five nocturnal *Oenothera* species (Onagraceae) in relation to floral visitors. *Planta* 246, 1051–1067. doi:10.1007/s00425-017-2748-y
- Azambuja, P., and Garcia, E. S. (1997). "Care and maintenance of triatomine colonies," in *The molecular biology of insect disease vectors: a methods manual*. Editors J. M. Crampton, C. Ben Beard, and C. Louis (Dordrecht: Springer Netherlands), 56–64. doi:10.1007/978-94-009-1535-0

- Baker, E. A. (1982). "Chemistry and morphology of plant epicuticular waxes," in *The plant cuticle*. Editors F. D. Cuttler, K. L. Alvin, and C. E. Price (London: Academic Press), 139–166.
- Bates, P. A. (2007). Transmission of *Leishmania* metacyclic promastigotes by phlebotomine sand flies. *Int. J. Parasitol.* 37, 1097–1106. doi:10.1016/j.ijpara.2007.04.003
- Bhami, L. C., and Das, S. S. M. (2015). Boric acid ovicidal trap for the management of *Aedes* species. *J. Vector Borne Dis.* 52, 147–152. doi:10.4103/0972-9062.159500
- Blanchet, D., Brenière, S. F., Schijman, A. G., Bisio, M., Simon, S., Véron, V., et al. (2014). First report of a family outbreak of Chagas disease in French Guiana and posttreatment follow-up. *Infect. Genet. Evol.* 28, 245–250. doi:10.1016/j.meegid.2014.10.004
- Brazil, R. P., and Brazil, B. G. (2003). "Biologia de flebotomíneos neotropicais," in *Flebotomíneos do Brasil*. Editors E. F. Rangel and R. Lainson (Rio de Janeiro: Editora Fiocruz), 257–274.
- Cameron, M. M., Pessoa, F. A. C., Vasconcelos, A. W., and Ward, R. D. (1995). Sugar meal sources for the phlebotomine sandfly *Lutzomyia longipalpis* in Ceará State. *Braz. Med. Vet. Entomol.* 9, 263–272. doi:10.1111/j.1365-2915.1995.tb00132.x
- Chagas, C. (1909). Nova tripanozomíase humana: estudos sobre a morfologia e o ciclo evolutivo do *Schizotrypanum cruzi* n. gen., n. sp., agente etiológico de nova entidade morbida do homem. *Mem. Inst. Oswaldo Cruz* 1, 159–218. doi:10.1590/S0074-02761909000200008
- Collier, B. D., Rabinovich, J. E., Bosque, C., and Rodriguez, E. (1981). An energy budget for *Rhodnius prolixus* (Hemiptera: Reduviidae) under laboratory conditions. *J. Med. Entomol.* 18, 257–265. doi:10.1093/jmedent/18.4.257
- Coura, J. R. (2015). The main sceneries of Chagas disease transmission. The vectors, blood and oral transmissions - a comprehensive review. *Mem. Inst. Oswaldo Cruz* 110, 277–282. doi:10.1590/0074-0276140362
- Da Lage, J. L., Fontenelle, A., Filée, J., Merle, M., Béranger, J. M., Almeida, C. E., et al. (2024). Evidence that hematophagous triatomine bugs may eat plants in the wild. *Insect biochem. Mol. Biol.* 165, 104059. doi:10.1016/j.ibmb.2023.104059
- de Oliveira, J., Ayala, J. M., Justi, S. A., da Rosa, J. A., and Galvão, C. (2018). Description of a new species of *Nesotriatoma* using, 1944 from Cuba and revalidation of synonymy between *Nesotriatoma bruneri* (using, 1944) and *N. flavida* (neiva, 1911) (Hemiptera, Reduviidae, triatominae). *J. Vector Ecol.* 43, 148–157. doi:10.1111/jvec.12294
- Dias, J. P., Bastos, C., Araújo, E., Mascarenhas, A. V., Martins Netto, E., Grassi, F., et al. (2008). Acute Chagas disease outbreak associated with oral transmission. *Rev. Soc. Bras. Med. Trop.* 41, 296–300. doi:10.1590/S0037-86822008000300014
- Díaz-Albiter, H. M., Ferreira, T. N., Costa, S. G., Rivas, G. B., Gumiel, M., Cavalcante, D. R., et al. (2016). Everybody loves sugar: first report of plant feeding in triatomines. *Parasit. Vectors* 9, 114. doi:10.1186/s13071-016-1401-0
- Dorn, P. L., Justi, S. A., Dale, C., Stevens, L., Galvão, C., Lima-Cordón, R., et al. (2018). Description of *Triatoma mopan* sp. n. from a cave in Belize (Hemiptera, Reduviidae, triatominae). *Zookeys* 775, 69–95. doi:10.3897/zookeys.775.22553
- Durán, P., Siñani, E., and Depickère, S. (2016). On triatomines, cockroaches and haemolymphagy under laboratory conditions: new discoveries. *Mem. Inst. Oswaldo Cruz* 111, 605–613. doi:10.1590/0074-02760160027
- Echeverría, J. E., Bustamante Gomez, M. B., Pessoa, G. C. D. Á., Cortez, M. R., Rodriguez, A. N., and Diotaiuti, L. G. (2018). Resistance to deltamethrin by domestic and wild *Triatoma infestans* populations in the municipality of Toro Toro, Potosi, Bolivia. *Parasit. Vectors* 11, 92. doi:10.1186/s13071-018-2663-5
- Friend, W. G., and Smith, J. J. B. (1971). Feeding in *Rhodnius prolixus*: potencies of nucleoside phosphates in initiating gorging. *J. Insect Physiol.* 17, 1315–1320. doi:10.1016/0022-1910(71)90196-X
- Friend, W. G., and Smith, J. J. B. (1982). ATP analogues and other phosphate compounds as gorging stimulants for *Rhodnius prolixus*. *J. Insect Physiol.* 28, 371–376. doi:10.1016/0022-1910(82)90050-6
- Garcia, E. S., and Azambuja, P. (1985). A protein diet initiates oogenesis in *Rhodnius prolixus*. *Braz. J. Med. Biol. Res.* 18 (2), 195–199.
- Gu, Z. Y., He, J., Teng, X. D., Lan, C. J., Shen, R. X., Wang, Y. T., et al. (2020). Efficacy of orally toxic sugar baits against contact-insecticide resistant *Culex quinquefasciatus*. *Acta Trop.* 202, 105256. doi:10.1016/j.actatropica.2019.105256
- Henriques, B. S., Genta, F. A., Mello, C. B., Silva, L. R., Codogno, T. F., Oliveira, A. F. R., et al. (2016). Triflumuron effects on the physiology and reproduction of *Rhodnius prolixus* adult females. *Biomed. Res. Int.* 2016, 8603140. doi:10.1155/2016/8603140
- Hurwitz, I., Fieck, A., Read, A., Hillesland, H., Klein, N., Kang, A., et al. (2011). Paratransgenic control of vector borne diseases. *Int. J. Biol. Sci.* 7, 1334–1344. doi:10.7150/ijbs.7.1334
- Jurberg, J., Rodrigues, J. M. S., Moreira, F. F. F., Dale, C., Cordeiro, I. R. S., Lamas Jr, V. D., et al. (2014). *Atlas iconográfico dos triatomíneos do Brasil (vetores da doença de Chagas)*. Rio de Janeiro: Instituto Oswaldo Cruz.
- Lehane, M. (2005). *The biology of blood-sucking in insects*. Cambridge: Cambridge University Press. doi:10.1017/CBO9780511610493
- Lewis, D. J., and Domoney, C. R. (1966). Sugar meals in phlebotominae and Simuliidae (Diptera). *Proc. R. Entomol. Soc.* 41, 175–179. doi:10.1111/j.1365-3032.1966.tb00340.x
- Lima, M. M., Rey, L., and Mello, R. P. D. (1992). Lethal effect of a bait for *Rhodnius prolixus* (Hemiptera: Reduviidae), the vector of Chagas' disease, containing hexachlorocyclohexane (HCH), under laboratory conditions. *Rev. Inst. Med. Trop. Sao Paulo* 34, 295–301. doi:10.1590/S0036-46651992000400005
- Lima-Cordón, R. A., Monroy, M. C., Stevens, L., Rodas, A., Rodas, G. A., Dorn, P. L., et al. (2019). Description of *Triatoma huehuetenanguensis* sp. n., a potential Chagas disease vector (Hemiptera, Reduviidae, Triatominae). *Zookeys* 820, 51–70. doi:10.3897/zookeys.820.27258
- Lorosa, E., Jurberg, J., and Souza, A. (2000). Hemolinf de Dictyoptera na manutenção do ciclo biológico silvestre de *Triatoma rubrovaria* (Blanchard, 1843) e *Triatoma circummaculata*. *Entomol. Vectores* 7, 287–296.
- Macarini, J. D. (1983). Diphosphoglycerate rather than ATP as a physiological phagostimulant factor for *Rhodnius prolixus*. *Experientia* 39, 159–160. doi:10.1007/BF01958873
- Müller, G. C., Junnila, A., and Schlein, Y. (2010). Effective control of adult *Culex pipiens* by spraying an attractive toxic sugar bait solution in the vegetation near larval habitats. *J. Med. Entomol.* 47, 63–66. doi:10.1603/033.047.0108
- Müller, G. C., and Schlein, Y. (2008). Efficacy of toxic sugar baits against adult cistern-dwelling *Anopheles claviger*. *Trans. R. Soc. Trop. Med. Hyg.* 102, 480–484. doi:10.1016/j.trstmh.2008.01.008
- Naranjo, D. P., Qualls, W. A., Müller, G. C., Samson, D. M., Roque, D., Alimi, T., et al. (2013). Evaluation of boric acid sugar baits against *Aedes albopictus* (Diptera: Culicidae) in tropical environments. *Parasitol. Res.* 112, 1583–1587. doi:10.1007/s00436-013-3312-8
- Nelson, D. L., and Cox, M. M. (2014). *Princípios de Bioquímica de Lehninger*. Porto Alegre: Artmed.
- Nicolson, S. W., and Thornburg, R. W. (2007). "Nectar chemistry," in *Nectaries and nectar*. Editors S. W. Nicolson, M. Nepi, and E. Pacini (Dordrecht: Springer), 215–264. doi:10.1007/978-1-4020-5937-7_5
- Nicolson, S. W., and Van Wyk, B.-E. (1998). Nectar sugars in proteaceae: patterns and processes. *Aust. J. Bot.* 46, 489–504. doi:10.1071/BT97039
- Nóbrega, A. A., Garcia, M. H., Tatto, E., Obara, M. T., Costa, E., Sobel, J., et al. (2009). Oral transmission of Chagas disease by consumption of açai palm fruit, Brazil. *Braz. Emerg. Infect. Dis.* 15, 653–655. doi:10.3201/eid1504.081450
- Oliveira, J. de, and Alevi, K. C. C. (2017). Taxonomic status of *Panstrongylus herreri* Wygodzinsky, 1948 and the number of Chagas disease vectors. *Rev. Soc. Bras. Med. Trop.* 50, 434–435. doi:10.1590/0037-8682-0125-2017
- Oliveira, P. L., and Genta, F. A. (2021). "Blood digestion in triatomine insects," in *Triatominae - the biology of Chagas disease vectors*. Editors A. Guarneri and M. Lorenzo (Cham: Springer), 265–284. doi:10.1007/978-3-030-64548-9_12
- Páez-Rondón, O., Aldana, E., Dickens, J., and Otálora-Luna, F. (2018). Ethological description of a fixed action pattern in a kissing bug (Triatominae): vision, gustation, proboscis extension and drinking of water and guava. *J. Ethol.* 36, 107–116. doi:10.1007/s10164-018-0547-y
- Percival, M. S. (1961). Types of nectar in angiosperms. *New Phytol.* 60, 235–281. doi:10.1111/j.1469-8137.1961.tb06255.x
- Piccolo, M. I., Vassena, C., Orihuela, P. S., Barrios, S., Zaidemberg, M., and Zerba, E. (2005). High resistance to pyrethroid insecticides associated with ineffective field treatments in *Triatoma infestans* (Hemiptera: Reduviidae) from northern Argentina. *J. Med. Entomol.* 42, 637–642. doi:10.1093/jmedent/42.4.637
- Qualls, W. A., Müller, G. C., Khallayoune, K., Revay, E. E., Zhioua, E., Kravchenko, V. D., et al. (2015). Control of sand flies with attractive toxic sugar baits (ATSB) and potential impact on non-target organisms in Morocco. *Parasit. Vectors* 8, 87. doi:10.1186/s13071-015-0671-2
- Rai, S., Mishra, P., and Ghoshal, U. C. (2021). Survival analysis: a primer for the clinician scientists. *Indian J. Gastroenterol.* 40, 541–549. doi:10.1007/s12664-021-01232-1
- Ruas-Neto, A. L., Corseuil, E., and Cavalleri, A. (2001). Development of rupestrian triatomines (Hemiptera, Reduviidae, triatominae) following hemolymphagy on blaberids (blattodea: blaberidae) in Rio grande do sul state, Brazil. *Entomol. Vectores* 8, 205–216.
- Ryckman, R. E. (1951). Recent observations of cannibalism in *Triatoma* (Hemiptera: Reduviidae). *J. Parasitol.* 37, 433–434. doi:10.2307/3273249
- Sandoval, C. M., Joya, M. I., Gutierrez, R., and Angulo, V. M. (2000). Cleptohaematophagy of the triatomine bug *Belminus herreri*. *Med. Vet. Entomol.* 14, 100–101. doi:10.1046/j.1365-2915.2000.00210.x
- Santalla, J., Oporto, P., Espinoza, E., Rios, T., and Brutus, L. (2011). Primer brote reportado de la enfermedad de Chagas en la Amazonía Boliviana: reporte de 14 casos agudos por transmisión oral de *Trypanosoma cruzi* en Guayamerín, Beni-Bolivia. *Biofarbo* 19, 52–58.
- Santana, R. A. G., Guerra, M. G. V. B., Sousa, D. R., Couceiro, K., Ortiz, J. V., Oliveira, M., et al. (2019). Oral transmission of *Trypanosoma cruzi*, Brazilian amazon. *Emerg. Infect. Dis.* 25, 132–135. doi:10.3201/eid2501.180646

- Soto, H., Tibaduiza, T., Montilla, M., Triana, O., Suárez, D. C., Torres, M. T., et al. (2014). Investigation of vectors and reservoirs in an acute Chagas outbreak due to possible oral transmission in Aguachica, Cesar, Colombia. *Cad. Saude Publica* 30, 746–756. doi:10.1590/0102-311X00024013
- Van Wyk, B. E., and Nicolson, S. W. (1995). Xylose is a major nectar sugar in *Protea* and *Faurea*. *South Afr. J. Sci.* 91, 151–153.
- Vargas, A., Malta, J. M. A. S., Costa, V. M., Cláudio, L. D. G., Alves, R. V., Cordeiro, G. D. S., et al. (2018). Investigation of an outbreak of acute Chagas disease outside the amazon region, in Rio grande do norte state, Brazil, 2016. *Cad. Saude Publica* 34, e00006517. doi:10.1590/0102-311x00006517
- Vassena, C. V., Picollo, M. I., and Zerba, E. N. (2000). Insecticide resistance in Brazilian *Triatoma infestans* and Venezuelan *Rhodnius prolixus*. *Med. Vet. Entomol.* 14, 51–55. doi:10.1046/j.1365-2915.2000.00203.x
- Williams, P. (1970). Phlebotomine sandflies and leishmaniasis in British Honduras (Belize). *Trans. R. Soc. Trop. Med. Hyg.* 64, 317–368. doi:10.1016/0035-9203(70)90171-9
- World Health Organization (2022). Chagas disease (also known as American trypanosomiasis). Available at: [https://www.who.int/news-room/fact-sheets/detail/chagas-disease-\(american-trypanosomiasis\)](https://www.who.int/news-room/fact-sheets/detail/chagas-disease-(american-trypanosomiasis)) (Accessed September 16, 2022).
- Wykes, G. R. (1952). An investigation of the sugars present in the nectar of flowers of various species. *New Phytol.* 51, 210–215. doi:10.1111/j.1469-8137.1952.tb06127.x
- Zar, J. H. (2010). *Biostatistical analysis*. Hoboken: Prentice Hall.
- Zerba, E. N. (1999). Susceptibility and resistance to insecticides of Chagas disease vectors. *Medicina* 59, 41–46.



OPEN ACCESS

APPROVED BY

Frontiers Editorial Office, Frontiers Media SA,
Switzerland

*CORRESPONDENCE

Frontiers Production Office,
✉ production.office@frontiersin.org

RECEIVED 24 September 2024

ACCEPTED 24 September 2024

PUBLISHED 16 October 2024

CITATION

Frontiers Production Office (2024) Erratum:
Sugar feeding in triatomines: a new perspective
for controlling the transmission of
Chagas disease.

Front. Physiol. 15:1501103.

doi: 10.3389/fphys.2024.1501103

COPYRIGHT

© 2024 Frontiers Production Office. This is an
open-access article distributed under the terms
of the [Creative Commons Attribution License](#)
(CC BY). The use, distribution or reproduction in
other forums is permitted, provided the original
author(s) and the copyright owner(s) are
credited and that the original publication in this
journal is cited, in accordance with accepted
academic practice. No use, distribution or
reproduction is permitted which does not
comply with these terms.

Erratum: Sugar feeding in triatomines: a new perspective for controlling the transmission of Chagas disease

Frontiers Production Office*

Frontiers Media SA, Lausanne, Switzerland

KEYWORDS

triatomine, sugar feeding, chagas disease, attractive toxic sugar bait (ATSB),
Rhodnius prolixus

An Erratum on

Sugar feeding in triatomines: a new perspective for controlling the transmission of Chagas disease

by Costa MC, Moreira CJC, Oliveira PLd, Juberg J, Castro DPd and Genta FA (2024). *Front. Physiol.* 15:1360255. doi: [10.3389/fphys.2024.1360255](#)

Due to a production error, an incorrect **editor's** name was listed. The correct name of the editor is "Norman Arthur Ratcliffe."

The publisher apologizes for this mistake. The original version of this article has been updated.



OPEN ACCESS

EDITED BY

Gunter Artur Schaub,
Ruhr University Bochum, Germany

REVIEWED BY

Zhaojiang Guo,
Chinese Academy of Agricultural
Sciences, China
Carlos Peres Silva,
Federal University of Santa Catarina, Brazil

*CORRESPONDENCE

D. M. P. Oliveira,
✉ danioliveira@iq.ufrj.br

RECEIVED 21 August 2024

ACCEPTED 09 October 2024

PUBLISHED 29 October 2024

CITATION

Lanzaro MD, Padilha I, Ramos LFC,
Mendez APG, Menezes A, Silva YM,
Martins MR, Junqueira M, Nogueira FCS,
AnoBom CD, Dias GM, Gomes FM and
Oliveira DMP (2024) Cry1Ac toxin binding in
the velvetbean caterpillar *Anticarsia
gemmatalis*: study of midgut aminopeptidases
N.
Front. Physiol. 15:1484489.
doi: 10.3389/fphys.2024.1484489

COPYRIGHT

© 2024 Lanzaro, Padilha, Ramos, Mendez,
Menezes, Silva, Martins, Junqueira, Nogueira,
AnoBom, Dias, Gomes and Oliveira. This is an
open-access article distributed under the
terms of the [Creative Commons Attribution
License \(CC BY\)](#). The use, distribution or
reproduction in other forums is permitted,
provided the original author(s) and the
copyright owner(s) are credited and that the
original publication in this journal is cited, in
accordance with accepted academic practice.
No use, distribution or reproduction is
permitted which does not comply with
these terms.

Cry1Ac toxin binding in the velvetbean caterpillar *Anticarsia gemmatalis*: study of midgut aminopeptidases N

M. D. Lanzaro¹, I. Padilha¹, L. F. C. Ramos¹, A. P. G. Mendez²,
A. Menezes², Y. M. Silva¹, M. R. Martins¹, M. Junqueira¹,
F. C. S. Nogueira¹, C. D. AnoBom¹, G. M. Dias², F. M. Gomes^{2,3}
and D. M. P. Oliveira^{1*}

¹Departamento de Bioquímica, Instituto de Química, Universidade Federal do Rio de Janeiro, Rio de Janeiro, Brazil, ²Instituto de Biofísica Carlos Chagas Filho, Universidade Federal do Rio de Janeiro, Rio de Janeiro, Brazil, ³Instituto Nacional de Entomologia Molecular, Rio de Janeiro, Brazil

The velvetbean caterpillar *Anticarsia gemmatalis* is one of the main soybean defoliators in Brazil. Currently, the main biopesticide used to control insect pests worldwide is the bacteria *Bacillus thuringiensis* (Bt), which produces entomopathogenic Crystal toxins (Cry) that act in the midgut of susceptible insects, leading them to death. The mode of action of Cry toxins in the midgut involves binding to specific receptors present on the brush border of epithelial cells such as aminopeptidase N (APN), alkaline phosphatase (ALP), cadherin, and others. Mutations in these receptors, among other factors, may be involved in the development of resistance; identification of functional Cry receptors in the midgut of *A. gemmatalis* is crucial to develop effective strategies to overcome this possible scenario. This study's goal is to characterize APNs of *A. gemmatalis* and identify a receptor for Cry1Ac in the midgut. The interaction of Bt spores with the midgut epithelium was observed *in situ* by immunohistochemistry and total aminopeptidase activity was estimated in brush border membrane vesicle (BBMV) samples, presenting higher activity in challenged individuals than in control ones. Ten APN sequences were found in a *A. gemmatalis* transcriptome and subjected to different *in silico* analysis, such as phylogenetic tree, multiple sequence alignment and identification of signal peptide, activity domains and GPI-anchor signal. BBMV proteins from 5th instar larvae were submitted to a ligand blotting using activated Cry1Ac toxin and a commercial anti-Cry polyclonal antibody; corresponding bands of proteins that showed binding to Cry toxin were excised from the SDS-PAGE gel and subjected to mass spectrometry analysis, which resulted in the identification of seven of those APNs. Quantitative PCR was realized to compare expression levels between individuals subjected to sublethal infection with Bt spores and control ones, presenting up- and downregulations upon Bt infection. From these results, we can infer that aminopeptidases N in *A. gemmatalis* could be involved in the mode of action of Cry toxins in its larval stage.

KEYWORDS

aminopeptidase N, Cry toxin, receptor, *Bacillus thuringiensis*, *Anticarsia gemmatalis*

1 Introduction

Bacillus thuringiensis (Berliner, 1915; Bacillales: Bacillaceae) (Bt) is a gram-positive, spore-forming bacteria known for its entomopathogenic effect against susceptible insects (Bravo et al., 2007; Sanchis, 2011). During its sporulation phase of growth, it produces insecticidal proteins as crystal inclusions (Cry toxins) that are pathogenic to several insect models, including known insect pests from the orders Lepidoptera, Coleoptera, and Hymenoptera (Bravo et al., 2007). For this reason, these proteins have been used worldwide in insecticidal sprays and, in later years, incorporated in genetically engineered crops (Horikoshi et al., 2021b; Pozebon et al., 2020; Bernardi et al., 2012).

Soybean (*Glycine max* (L.) Merrill, 1917) is one of the major agricultural commodities worldwide, with great importance in the global market, with projections that indicate that the Brazilian share of global trade could increase to over 60% until 2033 (dos Reis et al., 2020; Valdes et al., 2023). Brazil is currently the main producer and exporter of soybean (CONAB, 2023; FAO, 2024), with 154.6 million tons of grains produced in the 2022/23 harvest (CONAB, 2023). The velvetbean caterpillar *Anticarsia gemmatilis* (Hübner, 1818; Lepidoptera: Erebidae) is one of the soybean's main defoliators in the Americas (Hoffman-Campo et al., 2000; Bernardi et al., 2012), causing great damage to the production of this grain. While chemical pesticides have typically been used in *A. gemmatilis* control, Bt-based biopesticides have been thoroughly used in the management of this species' populations in the field (Knaak and Fiuza, 2005; Fernandes et al., 2021). In recent years, genetically modified soybean cultivars expressing insecticidal Cry proteins from *B. thuringiensis* (Bt crops) are quickly becoming a key tool in the management of pests, after its commercial availability (Pozebon et al., 2020; Bernardi et al., 2012; Chattopadhyay and Banerjee, 2018). Bt soybean MON 87701 × MON 89788 (Intacta RR2 PRO[®]) provides protection against *A. gemmatilis* in a high-dose manner, presenting high levels of Cry1Ac expression throughout the planting season conferring complete neonate mortality and effectively managing their populations in the field (Tabashnik et al., 2023; Horikoshi et al., 2021a; Bernardi et al., 2012).

Once ingested, Bt crystals are solubilized in the insect midgut alkaline environment, originating Cry protoxins, which are further activated by midgut proteases. Upon activation, Cry toxins bind to specific receptors in the midgut brush border membranes of epithelial cells and undergo conformational changes that cause the formation of oligomers, which are then inserted into the cell membrane. Cry toxin oligomerization at the plasma membrane forms pores, which leads to osmotic imbalance and cell lysis, which ultimately leads to insect death (Bravo et al., 2005; Adang et al., 2014; Palma et al., 2014; Melo et al., 2014; Liu et al., 2021). Four classes of proteins seem to be the major gut receptors for Cry toxins: aminopeptidase N (APN), alkaline phosphatase (ALP), cadherin (CAD), and ATP binding cassette subfamily C member 2 (ABCC2) transporters (Endo, 2022; Soberón et al., 2018; Bravo et al., 2004; Bravo et al., 2007; Gómez et al., 2002; Gómez et al., 2006; Pacheco et al., 2009). After activation, Cry toxins bind to APNs, abundant in lipid rafts in the membrane, which promotes the localization and concentration of activated toxins in these regions (Xu et al., 2014; Liu et al., 2021). The abundance of APN and its lower affinity for Cry toxins compared to receptors

like CAD may allow it to act as a "toxin sink" that concentrates Cry proteins at the midgut membrane surface. APN can then pass the toxin to other receptors while also facilitating insertion of the oligomeric pore complex into the membrane. Accordingly, a decrease in total aminopeptidase activity was observed in strains resistant to Cry toxins (Yang et al., 2010). The APN (EC.3.4.11.2) consists of a class of metalloproteases that act in the midgut brush border of insect larvae cleaving N-terminal amino acids from peptides during digestion (Adang, 2004). Knight et al. (1994) first identified an APN as a Cry toxin-binding protein and putative receptor in *Manduca sexta* and since then several other works have identified these proteins as Cry receptors in different insect species (Adang, 2004; Pigott and Ellar, 2007; Liu et al., 2021). APNs present features such as aminopeptidase motif "GAMENWG," Zn⁺⁺-binding motif "HEXXHX18E," a signal peptide in the N-terminal end and GPI-anchor peptide in the C-terminal end, which facilitates their attachment to the brush border, along with several O- and N-glycosylation sites (Pigott and Ellar, 2007; Adang, 2004). Based on their amino acid sequence similarity, they are classified into 13 clusters in Lepidoptera, with several isoforms expressed in the midgut (Guo et al., 2020; Crava et al., 2010; Hughes, 2014; Lin et al., 2014). The identification of lepidopteran APNs has allowed studies of the role of these proteins in the mode of action of Cry toxins, demonstrating their involvement in the pathogenesis of Bt toxins, mainly as functional receptors for these toxins (Gill and Ellar, 2002; Rajagopal et al., 2003; Wang et al., 2005).

Despite the importance of the velvetbean caterpillar (*A. gemmatilis*) as a major soybean pest, limited research has been conducted on the functional receptors for Cry toxins in this species. Previous studies have demonstrated the binding of various Cry toxins to *A. gemmatilis*' midgut brush border membrane vesicles (BBMV) through competition-binding assays (Bel et al., 2017; Bel et al., 2019) and to the midgut epithelial tissue using biotinylated toxins (Fiuza et al., 2013). Additionally, a membrane-associated alkaline phosphatase (ALP) characterized in the midgut of *A. gemmatilis* showed interaction with Cry1Ac toxin *in vitro* through enzyme-linked immunosorbent assay (da Silva et al., 2019), suggesting its potential role as a Cry toxin ligand. Even though APNs are commonly described and studied as potential Cry receptors in other lepidopteran species, no works described these proteins in *A. gemmatilis*. In this study, we characterized *A. gemmatilis*' aminopeptidases (AgAPNs) and identified those that positively bound to Cry toxin *in vitro*; analyses of AgAPN gene expression after Bt spore feeding bioassays demonstrated that some of these proteins could be involved in Cry's mode of action, due to changes in expression in this condition. These findings will contribute to future works, aiding the understanding of potential APN role in Cry toxin mode of action in *A. gemmatilis*.

2 Materials and methods

2.1 Insects

A colony of *A. gemmatilis* was established in the lab using eggs obtained from EMBRAPA SOJA, Londrina, PR, Brazil. Larvae

were reared on an artificial diet previously described by Hoffmann-Campo et al. (1985) and maintained under 25°C ± 3°C, 70% ± 10% humidity, and 14:10 h (light/dark) photoperiod.

2.2 Immunohistochemistry

For the immunohistochemistry assay, 0.5 mg/mL of Bt spores was mixed in the artificial diet fed to 4th–5th instar larvae; the control group was fed in an artificial diet mixed with distilled water. Samples were obtained after 12 h of Bt exposure and controls without exposure to the spores were also monitored under the same conditions. Challenged and control larvae were dissected and the gut of each was washed in phosphate-buffered saline [PBS; 137 mM NaCl, 2.7 mM KCl, 10 mM phosphate (pH 7.4)] to remove any unbound material before sample fixation. Tissues were fixed in 4% formaldehyde, 0.1% glutaraldehyde in 0.1 M sodium cacodylate buffer (pH 7.2) (Gomes et al., 2013) and stored in 4°C until use, for no longer than a week. After fixation, tissues were washed in 0.1 M sodium cacodylate buffer and incubated in blocking buffer (2% bovine serum albumin, 0.3% Triton X-100, PBS) for 2 h, followed by incubation in 1:250 commercial polyclonal primary anti-*B. thuringiensis* Cry1Ab Toxin antibody (Abcam Inc.; catalog number #ab51586) for 2 h in blocking buffer. After being washed in the blocking buffer, the tissues were incubated in 1:500 anti-rabbit Alexa-488-conjugated secondary antibody for 2 h, washed and incubated in 0.1 µg/mL DAPI. Whole gut samples were observed in a Zeiss 910 LSM confocal microscope.

2.3 In silico analysis of APN sequences

Raw RNA-Seq data of *A. gemmatilis* was obtained from a previously published study by Pezenti et al. (2021) (SRA accession number: PRJNA387150). The transcriptome was reassembled following the pipeline described in the original publication. APN amino acid sequences were identified through eggNOG-mapper (Cantalapiedra et al., 2021) and aligned using the Clustal W server (<https://www.ebi.ac.uk/jdispatcher/msa/clustalo>). For the phylogenetic tree, recovered APN sequences from nine lepidopteran species (*M. sexta*, *Heliothis virescens*, *Spodoptera frugiperda*, *Spodoptera litura*, *Helicoverpa armigera*, *Trichoplusia ni*, *Bombyx mori*, *Plutella xylostella*, and *Ostrinia furnacalis*), along with five sequences of *Homo sapiens*' APNs to form an outgroup (Supplementary Table S1). Alignment was conducted with Clustal W on MEGA 11 (Tamura et al., 2021) and the phylogenetic analysis was performed in RAxML (Random Accelerated Maximum Likelihood) (Stamatakis, 2014) software using the maximum likelihood (ML) method with a bootstrapping procedure with 1,000 replicates. The tree was visualized by FigTree (<http://tree.bio.ed.ac.uk/software/figtree/>). The presence and location of signal peptide cleavage sites in the APN amino acid sequences were determined using the SignalP 5.0 Server (<https://services.healthtech.dtu.dk/services/SignalP-5.0/>). The presence of glycosylphosphatidylinositol (GPI) anchors was predicted using the PredGPI software (<https://busca.biocomp.unibo.it/predgpi/>). Potential N-linked and O-linked glycosylation sites were analyzed using the NetNGlyc1.0 (<https://services.healthtech.dtu.dk/services/NetNGlyc-1.0/>) and NetOGlyc4.0 (<https://services.healthtech.dtu.dk/services/NetOGlyc-4.0/>) programs, respectively. Schematic representations of the APN sequences, including the locations of signal peptide cleavage sites, GPI anchors, and glycosylation sites, were generated using the Illustrator for Biological Sequences (IBS, 2022) software (<https://ibs.renlab.org/#/home>).

2.4 Preparation of midgut brush border membrane vesicles (BBMVs)

Midguts from 5th instar larvae of *A. gemmatilis* were longitudinally dissected and washed in saline solution (NaCl 0.15 M). The samples were stored in ice-cold SET buffer (0.15 M sucrose, 17 mM tris[hydroxymethyl]aminomethane (Tris), 5 mM ethylene glycol-bis(β-aminoethyl ether)-N,N,N',N'-tetraacetic acid (EGTA); pH 7.5) and kept at −20°C until use, for no longer than a week. BBMVs were prepared following the MgCl₂ differential precipitation method described in Wolfersberger et al. (1987) with some modifications. Briefly, the dissected midgut-epithelium samples were homogenized in SET buffer with a glass potter, and an equal volume of 24 mM MgCl₂ was added to the homogenate. Samples were incubated on ice for 15 min and then centrifuged at 3,000 g for 15 min at 4°C. The pellet was discarded, and the supernatant was centrifuged at 36,603 g for 30 min at 4°C. The pellet was resuspended in SET buffer and the centrifugation cycle was repeated. The final pellet was resuspended in 4-(2-hydroxyethyl) piperazine-1-ethane-sulfonic acid (HEPES) buffer (50 mM; pH 7.2). This resuspended pellet (P3) containing the proteins from BBMVs was quantified for total protein content using Pierce™ 660 nm Protein Assay (Thermo Scientific); bovine serum albumin (BSA; Sigma Chemical Company) was used as standard. The BBMV protein profile was observed by (12%) sodium dodecyl sulfate polyacrylamide gel electrophoresis (SDS-PAGE) (Laemmli, 1970).

2.5 Total leucine aminopeptidase activity in midgut BBMV samples

For total leucine aminopeptidase activity assay, a sublethal concentration of Bt spores (0.1323 mg/mL) was mixed in the artificial diet fed to 4th–5th instar larvae; the control group was fed in the artificial diet mixed with distilled water. This sublethal concentration was estimated in a bioassay that determined lethal concentrations of Bt spores to *A. gemmatilis* colony kept in the lab (data not shown). After 48 h of exposure to Bt, midguts were dissected and pooled (4 midguts per sample), with three biological replicates performed for the assay. Samples were then subjected to the preparation of BBMVs protocol and used in the total aminopeptidase activity assay. Total protein concentration was determined using the Pierce™ 660 nm Protein Assay Kit (Thermo Scientific) according to the manufacturer's instructions, with bovine serum albumin (BSA) as the standard. Samples were diluted to a final concentration of 0.05 mg/mL in 0.1 M Tris-HCl buffer (pH 8.6) for the measurement of total aminopeptidase activity. Total aminopeptidase activity was assessed using the chromogenic substrate leucine-p-nitroanilide (LpNA) (Sigma, St. Louis, MO), as previously described by Valaitis et al. (1999) and Erlanger et al.

(1961). Briefly, 5 µg of each diluted sample was mixed with 0.5 mM LpNA in 0.1 M Tris-HCl buffer (pH 8.6) in a microplate well. The enzymatic reaction was monitored by measuring the increase in optical absorbance at 405 nm using a SpectraMax[®] M2e microplate reader (Molecular Devices). Absorbance readings were taken every 30 s for a total of 15 min.

The mean velocity (Mean V) was calculated as an increase of absorbance per min in the linear portion of initial velocity of the enzymatic reaction using the GraphPad Prism 8.0. One unit of the enzyme activity was defined as the amount of enzyme that hydrolyzed 1 µmol of substrate to chromogenic product per min. Specific aminopeptidase activity calculations were performed based on the extinction coefficient ($9.9 \text{ mM}^{-1} \text{ cm}^{-1}$) for p-nitroaniline (Hafkenschied, 1984). APN activity was estimated from 3 reactions (replicates) for each condition (control and challenged) and sample type. Specific APN activities were presented as means and standard errors of the mean (SEM). Two-way ANOVA was used to determine differences in APN activity between the two conditions (control and challenged) for each sample.

2.6 Cry toxin purification and activation

B. thuringiensis subesp. *kurstaki* LFB-FIOCRUZ 475 (Bt) was kindly provided by Leon Rabinovitch (CCGB/IOC/Fiocruz/MS). This strain was used to produce Cry toxins, following Coleção de Culturas do Gênero *Bacillus* e Gêneros Correlatos (CCGB, Fundação Oswaldo Cruz) instructions. Bt spores were grown during 48 h in Nutrient Broth medium (Himedia) at 200 rpm at 37°C. This pre-inoculum was transferred to a new volume of nutrient broth and was shaken in the same growth conditions for 5 days until complete sporulation, as recommended instruction. After that, the culture was centrifuged at 7,500 g for 30 min at 4°C and the pellet was collected as spores/crystals-enriched fraction. Crystalline inclusions were solubilized by incubating the pellet in a 50 mM sodium carbonate buffer (pH 9.6) containing 0.1% 2-mercaptoethanol (SC buffer) under agitation for 2 h at room temperature. The mixture was centrifuged at 16,000 g for 30 min at 4°C. The supernatant was labeled as whole Cry1Ac toxin (WCT; about 130 kDa) and was either stored or further activated. WCT activation was performed by overnight incubation at 4°C with bovine pancreas trypsin (2 mg/mL). Following incubation, activated WCT was concentrated in an Amicon 30,000 MWCO spin filter for the removal of remnant trypsin. The molecular weight and the toxin integrity were checked by 10% SDS-PAGE (data not shown). This sample was named Cry1Ac toxin and used in the toxin overlay assay described below.

2.7 Toxin overlay assay in midgut BBMVs proteins

The midgut BBMVs proteins (50 µg) were separated by 12% SDS-PAGE (Laemmli, 1970), transferred to a nitrocellulose membrane, and Ponceau S was used to confirm protein transfer (Towbin et al., 1979). Following, the membrane was incubated in Blocking Buffer [5% (w/v) skimmed milk powder in Tris buffered-saline (TBS, pH 7.4) containing 0.1% Tween-20] overnight. For ligand blotting

analysis (Toxin Overlay Assay - TOA), the membrane was incubated in 5 mL of TOA Blocking Buffer [3% (w/v) BSA in Tris buffered-saline (TBS, pH 7.4) containing 0.1% Tween-20] and containing WCT (Cry1Ac toxin) for 7 h at room temperature to interact with respective BBMVs proteins. BSA was used as a negative control. The unbound toxins were removed by washing the blots with 5 mL of TOA Blocking Buffer, three times. Following, this blot was individually incubated with a polyclonal anti-*B. thuringiensis* Cry1Ab Toxin antibody (Abcam Inc.) (1:5,000 dilution in TOA Blocking Buffer) overnight; the section containing the activated Cry1Ac toxin was cut off from the membrane and incubated only with blocking buffer as a negative control. The membrane was then incubated with an anti-rabbit alkaline phosphatase-conjugated antibody (Sigma Aldrich). Finally, the blot was developed using NBT/BCIP (0.5 mM nitro blue tetrazolium, 0.57 mM 5-bromo-4-chloro-3-indolyl-phosphate) substrate in alkaline phosphatase buffer (10 mM Tris [pH 9.6], 100 mM NaCl, 5 mM MgCl_2).

2.8 Sample preparation for LC-MS/MS analysis

Protein samples for mass spectrometry analysis were obtained from a 12% SDS-PAGE gel. Two bands corresponding to those that demonstrated binding to Cry1Ac in the ligand blot were excised from the gel. Coomassie R stain was removed from the excised bands. Reduction was performed by incubating the samples with 10 mM dithiothreitol (DTT) in 50 mM ammonium bicarbonate for 1 h at 30°C. Following reduction, alkylation was carried out by adding 40 mM iodoacetamide and incubating the samples for 30 min in the dark. After alkylation, the samples were washed with Milli-Q[®] water and dehydrated using 90% acetonitrile. The samples were then vacuum-dried to remove all traces of acetonitrile. Protein digestion was performed using commercial trypsin (Promega) at a 1:50 (w/w) enzyme-to-protein ratio. The samples were incubated with trypsin overnight at 37°C. Following digestion, 0.1% trifluoroacetic acid (TFA) was added to the samples, and they were incubated at room temperature for 1 h.

Tryptic peptides were purified using manual reversed-phase chromatography with Poros 50 R2 resin (PerSeptive Biosystems) and subsequently vacuum-dried. The peptides were then solubilized in 0.1% formic acid for injection into the mass spectrometer. Samples were analyzed using a nanoLC-MS/MS system consisting of an EASY II-nano LC (Proxeon Biosystem) coupled to a Q-Exactive Plus (Thermo Fisher Scientific) mass spectrometer. A total of 1 µg of peptides was loaded onto a manually packed pre-column (100 µm × 2 cm) containing C-18 ReproSil 5 µm resin (Dr. Maisch) and then separated on a 20 cm analytical column packed with ReproSil-pur C18-AQ 3 µm resin (Dr. Maisch). Chromatographic separation was performed using a linear gradient of solution B (95% ACN, 0.1% TFA) from 5% to 20 s, followed by an increase to 40% over 8 min, then to 95% over 4 min, and finally maintained at 95% for 8 min. The flow rate was set to 250 nL/min. Mass spectra % over 40 min were acquired in positive mode using a Top 10 data-dependent acquisition (DDA) method. MS1 scans were acquired in the Orbitrap analyzer with a mass range of 350–1,800 m/z, a resolution of 60,000 (at m/z 400), a minimum signal threshold of 10,000, and an isolation window of 2.0. The 10 most intense ions

were selected for fragmentation by collision-induced dissociation (CID) with a normalized collision energy of 30 and a dynamic exclusion time of 30 s.

2.9 LC-MS/MS data analysis for protein identification

The spectra obtained from the LC-MS/MS analyses were processed using Proteome Discoverer 2.1 Software (Thermo Scientific) with the Sequest HT search engine against an *A. gemmatalis* protein database. This database was generated through a *de novo* assembly of the *A. gemmatalis* transcriptome based on raw data from a published study by Pezenti et al. (2021) (SRA accession number: PRJNA387150). For the search, the following parameters were used: precursor tolerance of 10 ppm, fragment tolerance of 0.1 Da, tryptic cleavage specificity, two maximum missed cleavage sites allowed, fixed modification of carbamidomethyl (Cys) and oxidation (Met). Peptides with high confidence were selected, and only identifications with *q* values equal to or less than 0.01 FDR were considered.

2.10 Gene expression analysis

Samples for analysis of gene expression were obtained in a feeding bioassay, in which a sublethal concentration of Bt spores (0.1323 mg/mL) was mixed in the artificial diet fed to 4th–5th instar larvae; the control group was fed in the artificial diet mixed with distilled water. After 24, 48 and 72 h of exposure to Bt, midguts were dissected and pooled (4 midguts per sample), with five biological replicates performed for the assay. Specimens were dissected and midgut epithelia were cleaned and used for total RNA extraction with TRI Reagent® (Sigma-Aldrich). Total RNA was quantified using NanoDrop One/One^c Microvolume UV-Vis Spectrophotometer (ThermoFisher Scientific), following the manufacturer's recommendations. Total RNA (500 ng) was reverse transcribed using GoScript™ Reverse Transcriptase kit (Promega) following the manufacturer's recommendations. For cDNA amplification, primers were designed following the re-annotation of a previously published *A. gemmatalis* transcriptome (Pezenti et al., 2021) (Table 1).

Primers were validated by RT-PCR using GoTaq Hot Start Colorless Master Mix (Promega) and the Veriti® 96-Well Thermal Cycler (Applied Biosystems). The cycling conditions were as follows: 94°C for 2 min, followed by 40 cycles of 94°C for 30 s, 52°C for 30 s, 72°C for 1 min. This stage was followed by 72°C for 10 min. Resulting amplification was visualized in 2% agarose gels using GelRed® Nucleic Acid Gel Stain (Biotium) following manufacturer's recommendations.

Quantitative real-time PCR (qRT-PCR) was performed using qPCRBIO SyGreen Mix (PCR Biosystems) and the ViiA™ 7 Real-Time PCR System (Applied Biosystems). The qRT-PCR cycling conditions were as follows: 50°C for 2 min, 95°C for 10 min, followed by 40 cycles of 95°C for 30 s, 60°C for 30 s, and 72°C for 30 s. Relative expression levels were analyzed using the $2^{-\Delta\Delta CT}$ method, using the expression level of the housekeeping gene elongation factor 1- α (ELF-1 α) as a reference gene normalizer.

2.11 Statistical analysis

The results were submitted to one- and two-Way ANOVA (followed by Sidak's multiple comparisons test), using the GraphPad Prism 8 software. Differences were considered significant at $p < 0.05$.

3 Results

3.1 Cry1Ac binds to epithelial cells in the midgut of *Anticarsia gemmatalis*

To verify the immobilization of Cry toxins in the *A. gemmatalis* gut, we conducted an experiment where 5th instar *A. gemmatalis* larvae were fed with a sublethal Bt spore dose (0.5 mg/mL) for 12 h. After incubation with anti-*B. thuringiensis* Cry1Ab polyclonal antibody, Bt toxin was identified as a punctate pattern along the whole midgut epithelia (Figures 1B, C), suggesting a possible interaction with the apical portion of epithelial cells. Fluorescence was specific to the midgut and not observed in negative controls (Figure 1A). These findings suggest that Cry toxins interact with *A. gemmatalis*' brush border membrane proteins, where APNs are known to be localized.

3.2 *In silico* analysis of aminopeptidases N from *Anticarsia gemmatalis*

To identify putative APN expressed by *A. gemmatalis*, we analyzed a previously published *A. gemmatalis* whole-body RNA-Seq dataset (Pezenti et al., 2021). The analysis of the *de novo* assembly of the transcriptome data resulted in the identification of 10 APN contigs, which are listed in Table 1. Of those, eight were full length sequences, hence being used in all posterior analysis; aminopeptidase N13 and aminopeptidase N-like isoform X2 were left out of most analyses since the sequences were only partial, impairing the results.

Alignment of deduced translated amino acid sequences of AgAPNs through multiple sequence alignment and the search for the presence of characteristic gluzincin aminopeptidase activity motif "GAMENWG" and the consensus zinc-binding motif "HEXXHX18H" showed the presence of both motifs in nearly all sequences (Figure 2A).

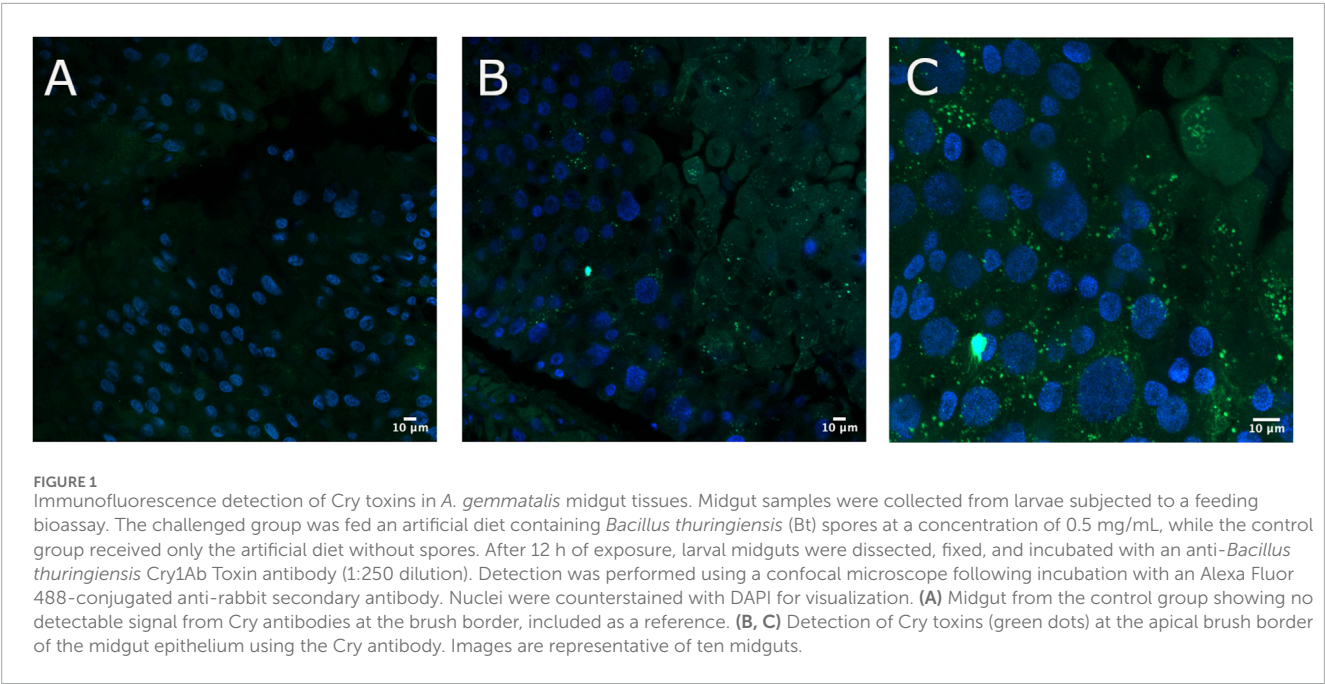
The predicted N-terminal signal peptide cleavage site location was present in most of the sequences, varying between them; no signal peptide was predicted for AgAPN11 (Figure 2B). Further, a putative C-terminal GPI-anchor signal was predicted for AgAPN3, AgAPN4, AgAPN8, AgAPN6 and AgAPN2. No GPI-anchor site was predicted for AgAPN5, AgAPN10 and AgAPN11. Several potential O-glycosylation sites and one N-glycosylation site were identified in all sequences.

For the phylogenetic tree, APN proteins from different Lepidoptera species, belonging to the thirteen APN classes (Guo et al., 2020), were downloaded from NCBI and UniProt databases (Supplementary Table S1) to construct the tree using

TABLE 1 Aminopeptidase N contigs from *A. gemmatalis* identified in the transcriptome (Pezenti et al., 2021).

Seq name ^a	Description ^b	Name ^c	Length ^d
TRINITY_DN21	ASU92546.1aminopeptidase N	AgAPN2	957
TRINITY_DN1045	QFP12817.1aminopeptidase N 1	AgAPN3	1,020
TRINITY_DN3057	AAL26894.1aminopeptidase N3	AgAPN4	954
TRINITY_DN2475	AWT22999.1aminopeptidase N5	AgAPN5	494
TRINITY_DN1607	ASU92547.1aminopeptidase N	AgAPN6	958
TRINITY_DN2592	AWT23001.1aminopeptidase N8	AgAPN8	938
TRINITY_DN465	XP_026737338.1aminopeptidase N	AgAPN10	939
TRINITY_DN4662	XP_047022343.1aminopeptidase N-like isoform X1	AgAPN11	1,092
TRINITY_DN37122	WAK99423.1aminopeptidase N 13		131
TRINITY_DN50751	XP_049705234.1aminopeptidase N isoform X2		174

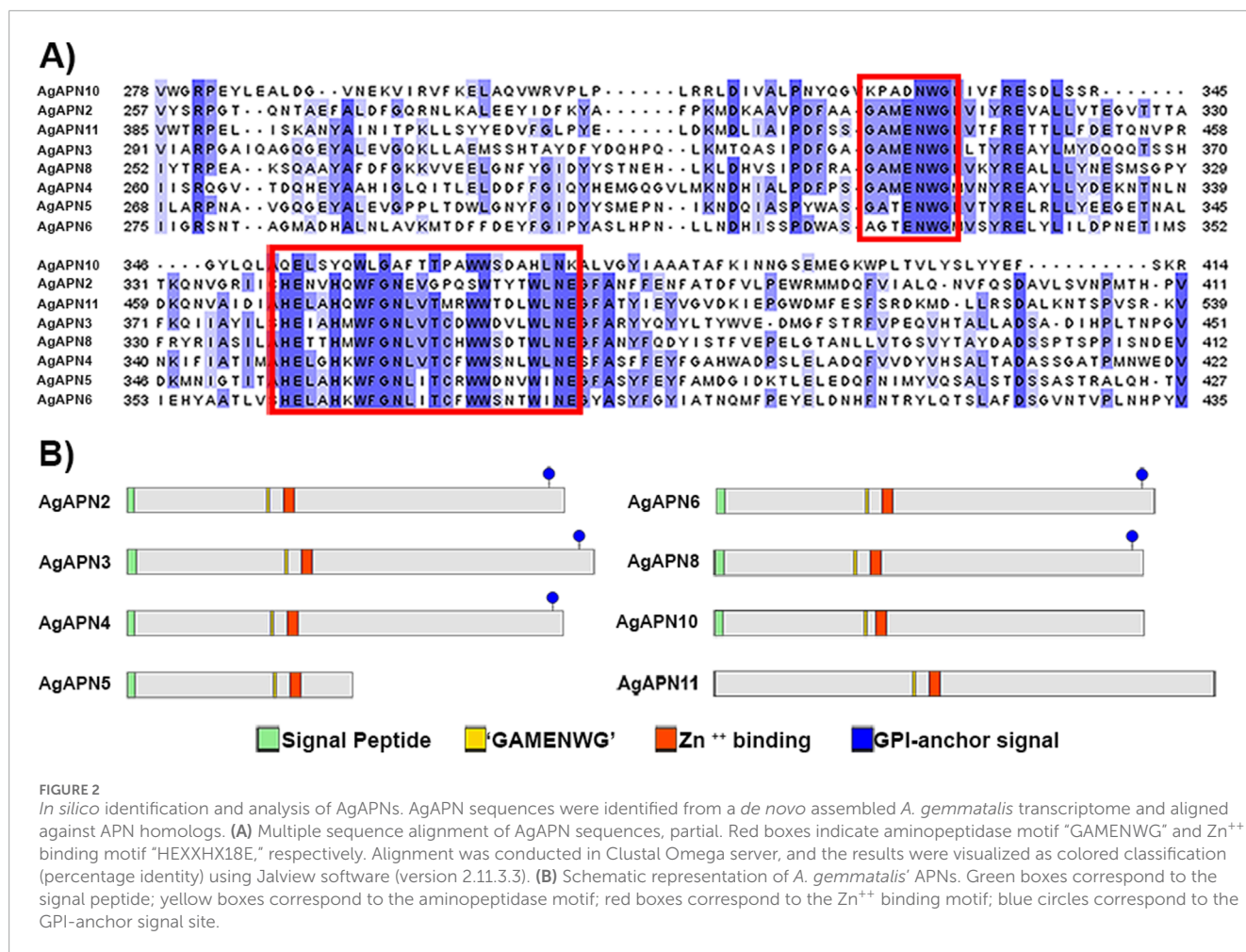
^aName of the contig in the transcriptome data;
^bDescription of the contig identification through egg NOG-mapper (Cantalapiedra et al., 2021) in the transcriptome data;
^cAll sequences were renamed after *in silico* analysis and those names are listed;
^dLength of the sequences in number of amino acids.



the maximum-likelihood method (Figure 3). This type of analysis has been broadly utilized to demonstrate the clustering of APN genes into different clusters, with high evolutionary conservation in each class (Guo et al., 2020; Wang et al., 2023). Following the genome-wide unified nomenclature and classification of APN genes in lepidopoteran insects (Guo et al., 2020), we designated APN genes in *A. gemmatalis* as AgAPN2, AgAPN3, AgAPN4, AgAPN5, AgAPN6, AgAPN8, AgAPN10 and AgAPN11.

3.3 Total aminopeptidase activity in the midgut

To evaluate aminopeptidase microvilli association and Bt modulation of aminopeptidase activity, we obtained fractionated samples from the midgut BBMVs of challenged and control individuals. Accordingly, we observed a Bt-upregulation of the aminopeptidase activity associated with the microvilli fraction (Figure 4).



3.4 Identification of Cry1Ac-binding proteins by LC-MS/MS

To identify Cry binding proteins in *A. gemmatilis*, we conducted a toxin overlay assay using Cry1Ac activated toxin on SDS-PAGE separated midgut BBMVs proteins. The results presented in Figure 4 clearly show that Cry1Ac toxin interacted with membrane proteins, specifically with two bands of approximately 110-kDa and 65-kDa (Figure 5).

A new electrophoresis was performed from the same BBMVs sample and bands in the same positions where there was binding to Cry1Ac in the TOA were excised and analyzed together by mass spectrometry. Results identified 1,152 proteins (Supplementary Table S1); the samples for this assay contained all proteins present in the two excised bands. Among them, seven AgAPNs were found (Table 2), suggesting that they could act as receptors for this toxin in *A. gemmatilis* midgut. The high number of unique peptides increases reliability in these results. It was possible to identify an alkaline phosphatase, which can also act as a receptor in the midgut, with a similar role in the progression of the infection.

3.5 APN expression analysis after exposure to Bt spores

To evaluate differences in expression of APNs between control individuals and challenged with Bt spores individuals, we performed RT-qPCR analysis of all AgAPNs described in this work upon 24, 48 and 72 h of exposure (Figure 6). Regarding the different conditions of exposure, AgAPN10, AgAPN4, AgAPN5, AgAPN6 and AgAPN11 did not present any significant difference in expression between the challenged and control groups in any of the time points. Genes of AgAPN2 and AgAPN3 of the challenged group presented an upregulation in 24 h of exposure in comparison with the control group, with a decrease in expression in the following time points and no significant difference from the control group. AgAPN8, on the other hand, presented downregulation of expression from 48 to 72 h in comparison with the control group. AgAPN5 and AgAPN6 did not present any significant difference of expression between treatments in each time point but did present a tendency downregulation in the challenged group from 48 to 72 h in relation to the initial period of exposure.

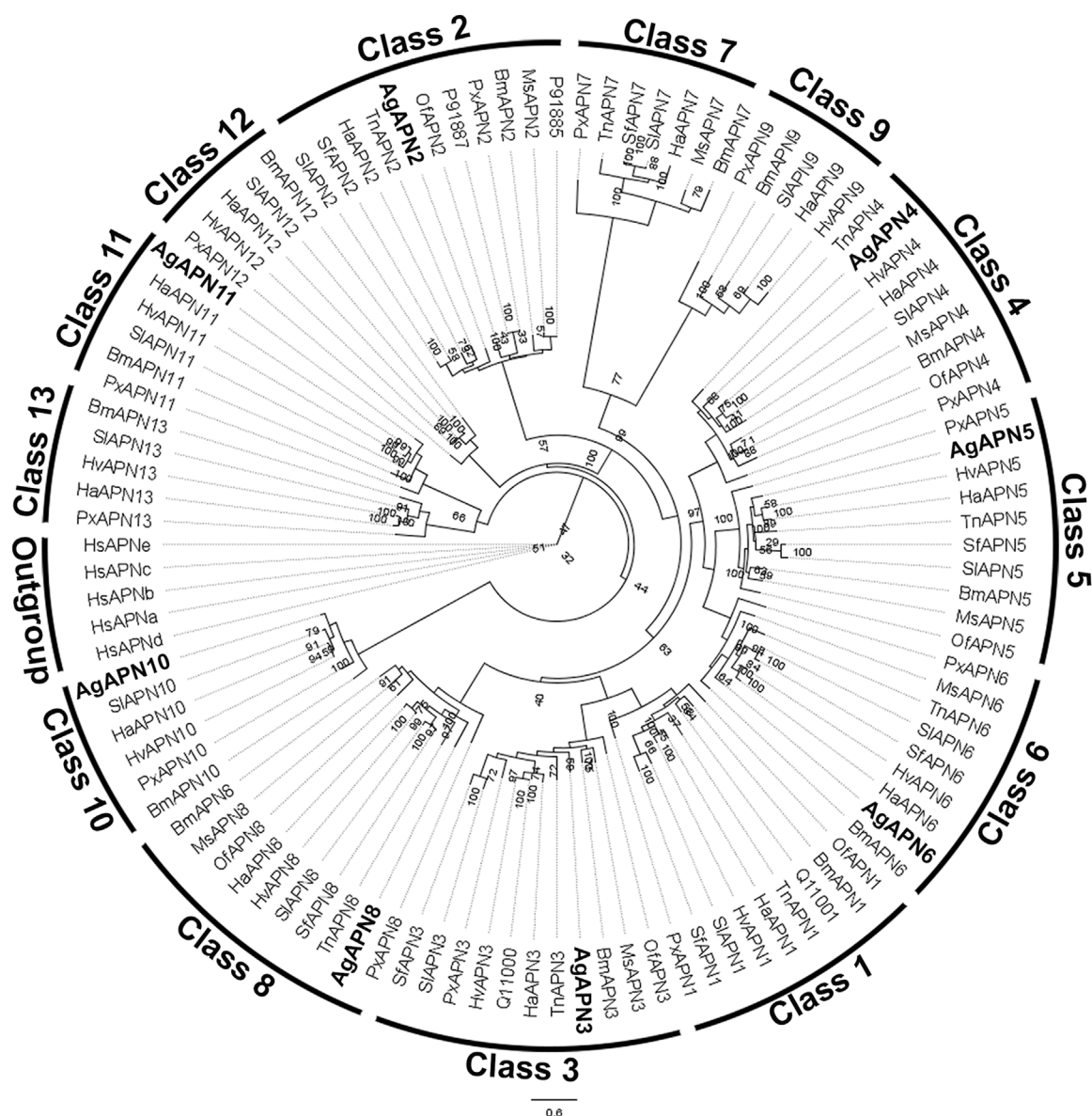


FIGURE 3

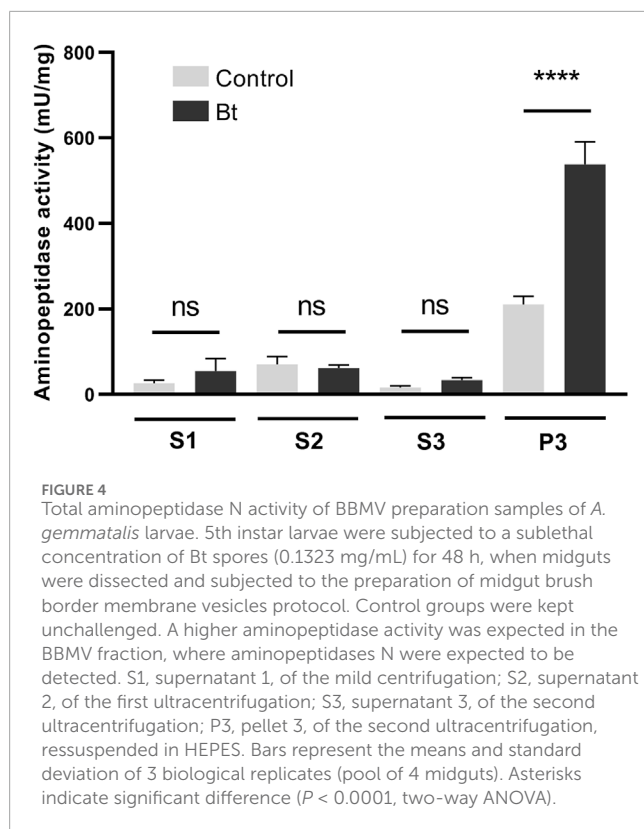
Phylogenetic tree of AgAPN sequences. Analysis conducted in RAxML software, using the maximum likelihood method with 1,000 bootstraps. Five *Homo sapiens* APNs were used as an outgroup and APNs from nine lepidopteran species (*Bombyx mori*, *Helicoverpa armigera*, *Heliothis virescens*, *Manduca sexta*, *Ostrinia furnacalis*, *Plutella xylostella*, *Spodoptera frugiperda*, *Spodoptera litura* and *Trichoplusia ni*) were used to conduct the analysis (Supplementary Table S1). Eight APNs of *A. gemmatilis* were indicated by bold.

4 Discussion

B. thuringiensis (Bt) is the most widely used bacteria for control of insect pests due to its production of parasporal entomopathogenic crystals during sporulation, known as Cry toxins (Liu et al., 2021). These are toxic by ingestion, acting in the midgut of susceptible insects where, after solubilization and activation, the Cry proteins oligomerize and form pores, which are then inserted in the epithelial membrane. This disrupts the cellular membrane, causing leakage of cellular contents and osmotic imbalance and allowing gut bacteria to invade the cells and the hemolymph, leading to septicemia; this ultimately triggers the

infected insect to stop eating, alongside with the infection events that culminates in insect death (Liu et al., 2021). This infection triggers host responses, modulating different pathways and molecules, to counteract these effects (Pinos et al., 2021).

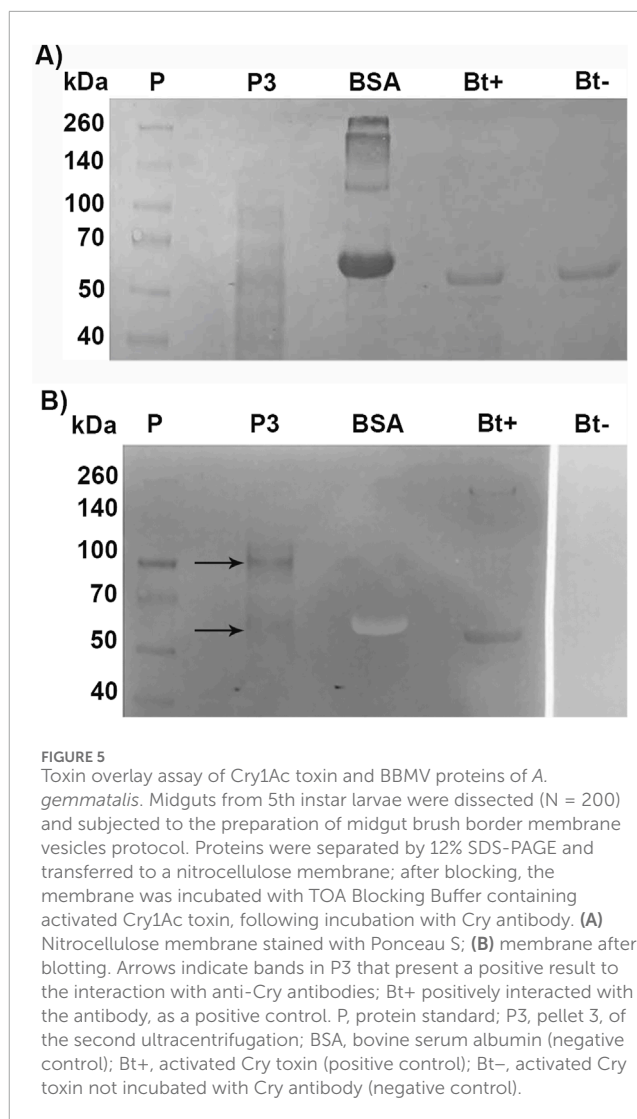
The binding of Cry1Ac toxin to brush border membrane vesicles (BBMV) from *A. gemmatilis* midguts was demonstrated by the fractionation of total aminopeptidase activity, revealing increased activity in BBMV fractions of larvae fed a diet containing Bt spores. This rise in aminopeptidase activity is consistent with previous reports that describe elevated APN activity following Cry toxin exposure (Ingle et al., 2001). These findings were further supported by immunohistochemistry, which confirmed the



interaction of Cry1Ac with the midgut epithelium, as previously shown in other lepidopterans (Chauhan et al., 2021; Valaitis, 2011; Chen et al., 2005; Aimanova, Zhuang, and Gill, 2006).

Despite its importance as a major soybean defoliator, few studies addressed the molecular basis of Cry toxins' mode of action on the midgut of *A. gemmatilis*. Bel et al. (2017), Bel et al. (2019) and Fiuza et al. (2013) identified Cry toxin binding to the midgut brush border tissue but did not identify a functional receptor for these toxins. Da Silva et al. (2019) characterized a membrane-associated alkaline phosphatase that binds to Cry1Ac toxin, but further studies would be required to describe it as a functional receptor. APNs have been extensively described as Cry toxin receptors in many insect pest species; these proteins consist in a group of glycoproteins attached to the midgut epithelial membrane through a GPI-anchor (Sato, 2002; Pardo-Lopez et al., 2013; Flores-Escobar et al., 2013; Herrero et al., 2016; Liu et al., 2021).

Ten APNs were identified from the transcriptome data of *A. gemmatilis* (Pezenti et al., 2021) with eight full-length sequences that were subsequently analyzed. A phylogenetic tree containing APNs from seven other lepidopteran species, belonging to the eight described classes of APNs in insects (Crava et al., 2010; Hughes, 2014; Lin et al., 2014), showed that the eight AgAPNs were distributed into different classes and named accordingly (AgAPN2, AgAPN3, AgAPN4, AgAPN5, AgAPN6, AgAPN8, AgAPN10 and AgAPN11), following the genome-wide unified nomenclature and classification of APN genes in lepidopteran insects (Guo et al., 2020). *In silico* analysis of the sequences revealed the presence of characteristic motifs "GAMENWG" and "HEXXHX18E" in most of the sequences; AgAPN10, AgAPN5 and AgAPN6 do not present the entire "GAMENWG" motif and AgAPN10 also does

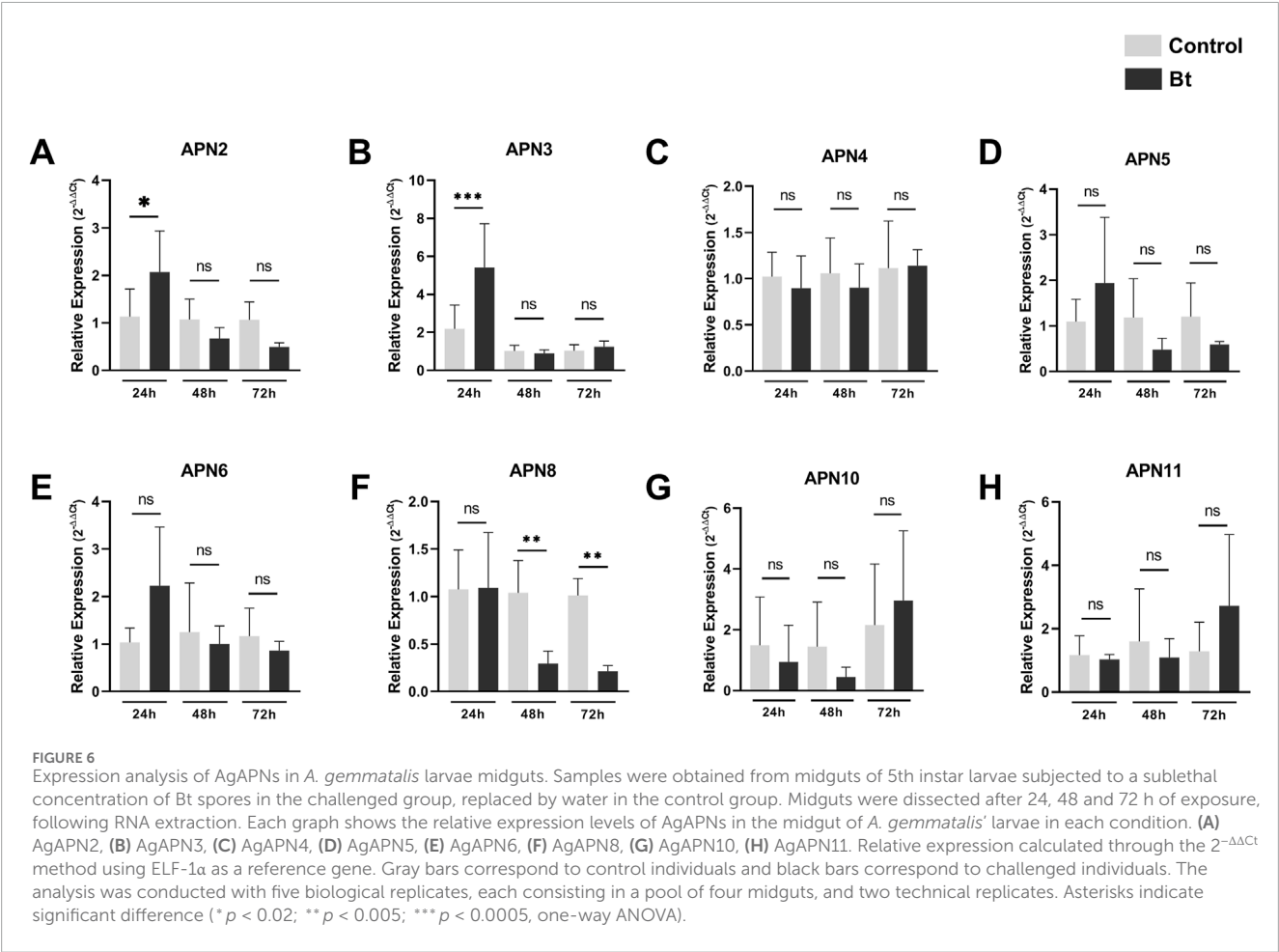


not present the entire "HEXXHX18E" motif. C-terminal GPI-anchor signal was identified for AgAPN2, AgAPN3, AgAPN4, AgAPN6 and AgAPN8 and N-terminal signal peptide cleavage site was identified in all sequences except for AgAPN11. It was interesting to note that AgAPN11 lacked both C-terminal GPI-anchor signal and N-terminal signal peptide cleavage site; a similar occurrence has been described for AjAPN9 in *Achaea janata* (Chauhan et al., 2021).

APN was initially shown as a Cry1Ac binding protein through TOA ligand blot analysis (Knight et al., 1994; Sangadala et al., 1994). Our present ligand-binding study revealed interaction of *A. gemmatilis* midgut epithelial cell membrane proteins with the activated Cry1Ac toxin obtained from *B. thuringiensis* sor. *kurstaki*, with a prominent interaction primarily seen with a ~100 kDa protein, as well as a minor interaction with a ~60 kDa protein. Corresponding bands from an SDS-PAGE were then excised and the identities of the proteins were confirmed by mass spectrometry analysis, in which several AgAPN sequences were identified; the same experiment was conducted for *M. sexta*, in which mass spectrometry of a band that positively bound to Cry2Ab toxin

TABLE 2 A. *gemmatalis*’ midgut proteins that demonstrated binding to Cry1Ac identified by mass spectrometry.

Description		Coverage (%)	PSMs	Peptides	Unique peptides	MW (kDa)
DN1045	Aminopeptidase N3	30.2	386	24	24	114.515
DN2592	Aminopeptidase N8	17.6	181	20	20	105.34
DN3057	Aminopeptidase N4	19.6	178	16	16	108.692
DN1607	Aminopeptidase N6	27.4	89	21	21	109.464
DN21	Aminopeptidase N2	21.4	81	16	16	108
DN2475	Aminopeptidase N5	18.2	49	9	7	55.881
DN4662	Aminopeptidase N-like isoform X1	2.28	3	2	2	123.359
DN56	Membrane-bound alkaline phosphatase-like	6	11	3	3	59.612



identified the protein as an APN (Onofre et al., 2017), and for *Athethis lepigone*, another lepidopteran species (Wang et al., 2017). Of the seven AgAPNs identified, four figured among the 100 highest PSMs (peptide spectrum match), which corresponds to a score of matches between experimental MS/MS spectra to the theoretical spectra predicted for the tryptic peptides, in which proteins with peptides best matched with the experimental spectrum are considered the most likely candidates (Wu et al., 2006). Therefore, supporting the presence of those proteins in the samples analyzed. An alkaline phosphatase (ALP), present in the transcriptome data, was also identified in the mass spectrometry analysis; this protein is frequently grouped with APNs, mainly because it is also anchored

to the membrane by an GPI-anchor, besides displaying a similar role during the toxin's mode of action (Ziga-Navarrete et al., 2021; Liu et al., 2021). As mentioned before, our group published a work characterizing an ALP from *A. gemmatalis* and describing an *in vitro* binding to Cry1Ac (da Silva et al., 2019); our data corroborate this finding.

In resistant strains, expression of genes encoding Cry receptors is commonly downregulated, whereas non-receptor paralogs are upregulated, believed to compensate for the absence of the down-regulated ones (Guo et al., 2022). The cabbage looper, *Trichoplusia ni*, presented down-regulation of TnAPN1 in Cry-resistant strains (Tiewisiri and Wang, 2011); tolerant strains of the castor semilooper larvae (*A. janata*) presented reduced expression of AjAPN2 while AjAPN4 was up-regulated (Chauhan et al., 2021); resistant strains of *Spodoptera exigua* reared in-lab lacked expression of a SeAPN1, whereas susceptible insects positively expressed this gene (Herrero et al., 2005). For *Chilo suppressalis*, knockdown of CsAPN6 and CsAPN8 reduced the larvae's sensitivity to transgenic rice expressing Cry1 toxins (Sun et al., 2020), and previous studies had demonstrated the involvement of APNs in the toxin's mode of action (Qiu et al., 2017; Wang et al., 2017). In our analysis we could identify an upregulation of AgAPN2 and AgAPN3 genes at 24 h of exposure to Bt spores, followed by a decrease in the following time points, as well as AgAPN5 and AgAPN6. Expression levels of AgAPN8 also demonstrated a downregulation, with great significance values. All these results could indicate a possible role of some AgAPNs in the mode of action of the Cry1Ac toxin in *A. gemmatalis*, but further studies are required for their characterization as putative receptors in the midgut, such as silencing through RNA interference and CRISPR/Cas9.

In conclusion, the identification of some AgAPNs as Cry-binding proteins in the ligand blot, as well as the expression analysis of all isoforms, could give us a direction in the sense of which of those proteins could be in fact involved in this process in *A. gemmatalis* midgut. Overall, this study gives a perspective of Cry1Ac possible receptors in *A. gemmatalis*, enhancing our understanding of this mode of action in this great agricultural pest.

Data availability statement

The mass spectrometry proteomics data have been deposited to the ProteomeXchange Consortium via the PRIDE (Perez-Riverol et al., 2022) partner repository with the dataset identifier PXD055041.

Ethics statement

Ethical approval was not required for the study involving animals in accordance with the local legislation and institutional requirements because this manuscript presents research on animals that do not require ethical approval for their study.

Author contributions

ML: Conceptualization, Investigation, Methodology, Supervision, Validation, Visualization, Writing–original draft, Writing–review and editing. IP: Investigation, Visualization, Writing–review and editing. LR: Investigation, Methodology, Writing–review and editing. AMd: Investigation, Writing–review and editing. AMe: Investigation, Writing–review and editing. YS: Investigation, Writing–review and editing. MM: Investigation, Writing–review and editing. MJ: Resources, Writing–review and editing. FN: Resources, Writing–review and editing. CA: Funding acquisition, Resources, Writing–review and editing. GD: Resources, Writing–review and editing. FG: Funding acquisition, Methodology, Resources, Visualization, Writing–review and editing. DO: Conceptualization, Funding acquisition, Methodology, Project administration, Resources, Supervision, Validation, Visualization, Writing–original draft, Writing–review and editing.

Funding

The author(s) declare that financial support was received for the research, authorship, and/or publication of this article. This work was supported by Carlos Chagas Filho Foundation for Supporting Research in the State of Rio de Janeiro (FAPERJ grants numbers E-26/210.173/2023 and E-26/210.996/2019); Coordination for the Improvement of Higher Education Personnel (CAPES - Finance Code 001).

Acknowledgments

We are grateful to Professor Rafael Dias Mesquita (Federal University of Rio de Janeiro) for the aid with the phylogenetic analysis, providing servers to run our experiment. We are also grateful to Professors Ana Claudia do Amaral Melo, Anderson de Sá Pinheiro, Bianca Cruz Neves, Marcia Regina Soares da Silva, Mônica Ferreira Moreira Carvalho Cardoso and Rodrigo Volcan Almeida (Federal University of Rio de Janeiro) for kindly providing laboratory supplies and facilities. To João Henrique de Oliveira Rangel, Igor Oliveira de Almeida and Danielle Aline da Silva Ribeiro for the help in maintaining the insect colony.

Conflict of interest

The authors declare that the research was conducted in the absence of any commercial or financial relationships that could be construed as a potential conflict of interest.

Publisher's note

All claims expressed in this article are solely those of the authors and do not necessarily represent those of

their affiliated organizations, or those of the publisher, the editors and the reviewers. Any product that may be evaluated in this article, or claim that may be made by its manufacturer, is not guaranteed or endorsed by the publisher.

References

- Adang, M. J. (2004). Insect aminopeptidase N. *Handb. Proteolytic Enzym.* 296–299. doi:10.1016/b978-0-12-079611-3.50079-3
- Adang, M. J., Crickmore, N., and Jurat-Fuentes, J. L. (2014). Diversity of *Bacillus thuringiensis* crystal toxins and mechanism of action. *Adv. Insect Physiology*, 39–87. doi:10.1016/b978-0-12-800197-4.00002-6
- Aimanova, K. G., Zhuang, M., and Gill, S. S. (2006). Expression of cryIac cadherin receptors in insect midgut and cell lines. *J. Invertebr. Pathology* 92 (3), 178–187. doi:10.1016/j.jip.2006.04.011
- Bel, Y., Sheets, J. J., Tan, S. Y., Narva, K. E., and Escriche, B. (2017). Toxicity and binding studies of *Bacillus thuringiensis* cryIac, cryIf, cryIc, and cry2a proteins in the soybean pests *Anticarsia gemmatilis* and *Chrysodeixis (Pseudoplusia) includens*. *Appl. Environ. Microbiol.* 83 (11), 003266–e417. doi:10.1128/aem.00326-17
- Bel, Y., Zack, M., Narva, K., and Escriche, B. (2019). Specific binding of *Bacillus thuringiensis* cryIea toxin, and cryIac and CryIa competition analyses in *Anticarsia gemmatilis* and *Chrysodeixis includens*. *Sci. Rep.* 9 (1), 18201. doi:10.1038/s41598-019-54850-3
- Bernardi, O., Malvestiti, G. S., Dourado, P. M., Oliveira, W. S., Martinelli, S., Berger, G. U., et al. (2012). Assessment of the high-dose concept and level of control provided by Mon 87701 × Mon 89788 soybean against *Anticarsia gemmatilis* and *Pseudoplusia includens* (Lepidoptera: noctuidae) in Brazil. *Pest Manag. Sci.* 68 (7), 1083–1091. doi:10.1002/ps.3271
- Bravo, A., Gill, S. S., and Soberón, M. (2007). Mode of action of *Bacillus thuringiensis* cry and cyt toxins and their potential for insect control. *Toxicon* 49 (4), 423–435. doi:10.1016/j.toxicon.2006.11.022
- Bravo, A., Gómez, I., Conde, J., Muñoz-Garay, C., Sánchez, J., Miranda, R., et al. (2004). Oligomerization triggers binding of a *Bacillus thuringiensis* CryIAb pore-forming toxin to aminopeptidase N receptor leading to insertion into membrane microdomains. *Biochimica Biophysica Acta (BBA) - Biomembr.* 1667 (1), 38–46. doi:10.1016/j.bbamem.2004.08.013
- Bravo, A., Soberón, M., and Gill, S. S. (2005). *Bacillus thuringiensis*: mechanisms and use. *Compr. Mol. Insect Sci.*, 175–205. doi:10.1016/b0-44-45192-6/00081-8
- Cantalapiedra, C. P., Hernández-Plaza, A., Letunic, I., Bork, P., and Huerta-Cepas, J. (2021). EggNOG-mapper v2: functional annotation, orthology assignments, and domain prediction at the metagenomic scale. *Mol. Biol. Evol.* 38 (12), 5825–5829. doi:10.1093/molbev/msab293
- Chattopadhyay, P., and Banerjee, G. (2018). Recent advancement on chemical arsenal of BT toxin and its application in pest management system in Agricultural Field. 3 *Biotech.* 8 (4), 201. doi:10.1007/s13205-018-1223-1
- Chauhan, V. K., Dhania, N. K., Lokya, V., Bhuvanachandra, B., Padmasree, K., and Dutta-Gupta, A. (2021). Midgut aminopeptidase N expression profile in castor semilooper (*Achaea janata*) during sublethal cry toxin exposure. *J. Biosci.* 46 (1), 29. doi:10.1007/s12038-021-00148-4
- Chen, G., Wang, Y., Liu, Y., Chen, F., and Han, L. (2020). Differences in midgut transcriptomes between resistant and susceptible strains of *Chilo suppressalis* to cryIc toxin. *BMC Genomics* 21 (1), 634. doi:10.1186/s12864-020-07051-6
- Chen, J., Brown, M. R., Hua, G., and Adang, M. J. (2005). Comparison of the localization of *Bacillus thuringiensis* CryIa δ -endotoxins and their binding proteins in larval midgut of tobacco hornworm, *Manduca sexta*. *Cell Tissue Res.* 321 (1), 123–129. doi:10.1007/s00441-005-1124-6
- CONAB (2023). Acompanhamento da Safra Brasileira de Grãos.
- Crava, C. M., Bel, Y., Lee, S. F., Manachini, B., Heckel, D. G., and Escriche, B. (2010). Study of the aminopeptidase N gene family in the Lepidopterans *Ostrinia nubilalis* (Hübner) and *Bombyx mori* (L.): sequences, mapping and expression. *Insect Biochem. Mol. Biol.* 40 (7), 506–515. doi:10.1016/j.ibmb.2010.04.010
- da Silva, G., Costa Ramos, L. F., Dos Santos Seckler, H., Mendonça Gomes, F., Reis Cortines, J., Ramos, I., et al. (2019). Biochemical characterization of digestive membrane-associated alkaline phosphatase from the velvet bean caterpillar *Anticarsia gemmatilis*, archives of insect biochemistry and physiology. *Arch. Insect Biochem. Physiol.* 102 (1), e21591. doi:10.1002/arch.21591
- dos Reis, L. C., Santos e Silva, C. M., Bezerra, B. G., and Spyrides, M. H. C. (2020). Caracterização da variabilidade da precipitação no MATOPIBA, região produtora de soja. *Rev. Bras. Geogr. Física* 13 (4), 1425–1441. doi:10.26848/rbgf.v13.4.p1425-1441
- Endo, H. (2022). Molecular and kinetic models for pore formation of *Bacillus thuringiensis* cry toxin. *Toxins* 14 (7), 433. doi:10.3390/toxins14070433
- Erlanger, B. F., Kokowsky, N., and Cohen, W. (1961). The preparation and properties of two new chromogenic substrates of Trypsin. *Archives Biochem. Biophysics* 95 (2), 271–278. doi:10.1016/0003-9861(61)90145-x
- FAO (2024). Faostat. Available at: <https://www.fao.org/faostat/> (Accessed August 09, 2024).
- Fernandes, F. O., de Souza, T. D., Sanches, A. C., Dias, N. P., Desiderio, J. A., and Polanczyk, R. A. (2021). Sub-lethal effects of a Bt-based bioinsecticide on the biological conditioning of *Anticarsia gemmatilis*. *Ecotoxicol. Lond. Engl.* 30 (10), 2071–2082. doi:10.1007/s10646-021-02476-5
- Fiuzza, L. M., Knaak, N., da Silva, R. F. P., and Henriques, J. A. P. (2013). Receptors and lethal effect of *Bacillus thuringiensis* insecticidal crystal proteins to the *Anticarsia gemmatilis* (Lepidoptera, Noctuidae). *ISRN Microbiol.* 2013, 940284–940287. doi:10.1155/2013/940284
- Flores-Escobar, B., Rodríguez-Magadan, H., Bravo, A., Soberón, M., and Gómez, I. (2013). Differential role of *Manduca sexta* aminopeptidase-N and alkaline phosphatase in the mode of action of cryIaa, CryIAb, and cryIac toxins from *Bacillus thuringiensis*. *Appl. Environ. Microbiol.* 79 (15), 4543–4550. doi:10.1128/aem.01062-13
- Gill, M., and Ellar, D. (2002). Transgenic drosophila reveals a functional *in vivo* receptor for the *Bacillus thuringiensis* toxin cryIac1. *Insect Mol. Biol.* 11 (6), 619–625. doi:10.1046/j.1365-2583.2002.00373.x
- Gomes, F. M., Carvalho, D. B., Machado, E. A., and Miranda, K. (2013). Ultrastructural and functional analysis of secretory goblet cells in the midgut of the Lepidopteran *Anticarsia gemmatilis*. *Cell Tissue Res.* 352 (2), 313–326. doi:10.1007/s00441-013-1563-4
- Gómez, I., Arenas, I., Benítez, I., Miranda-Ríos, J., Becerril, B., Grande, R., et al. (2006). Specific epitopes of domains II and III of *Bacillus thuringiensis* CryIAb toxin involved in the sequential interaction with cadherin and aminopeptidase-N receptors in *Manduca sexta*. *J. Biol. Chem.* 281 (45), 34032–34039. doi:10.1074/jbc.m604721200
- Gómez, I., Sánchez, J., Miranda, R., Bravo, A., and Soberón, M. (2002). Cadherin-like receptor binding facilitates proteolytic cleavage of helix α -1 in domain I and oligomer pre-pore formation of *Bacillus thuringiensis* cryIab toxin. *FEBS Lett.* 513 (2–3), 242–246. doi:10.1016/s0014-5793(02)02321-9
- Guo, Z., Guo, L., Qin, J., Ye, F., Sun, D., Wu, Q., et al. (2022). A single transcription factor facilitates an insect host combating *Bacillus thuringiensis* infection while maintaining fitness. *Nat. Commun.* 13 (1), 6024. doi:10.1038/s41467-022-33706-x
- Guo, Z., Kang, S., Sun, D., Gong, L., Zhou, J., Qin, J., et al. (2020). MAPK-dependent hormonal signaling plasticity contributes to overcoming *Bacillus thuringiensis* toxin action in an insect host. *Nat. Commun.* 11 (1), 3003. doi:10.1038/s41467-020-16608-8
- Hafkenschield, J. C. M. (1984). “Aminopeptidases and amino acid arylamidases in methods of enzymatic analysis,” in *Enzymes 3; peptidases, proteinases and their inhibitors*. Editor J. Bergmeyer (Weinheim: Verlag Chemie), 2–34.
- Herrero, S., Bel, Y., Hernández-Martínez, P., and Ferré, J. (2016). Susceptibility, mechanisms of response and resistance to *Bacillus thuringiensis* toxins in *Spodoptera* spp. *Curr. Opin. Insect Sci.* 15, 89–96. doi:10.1016/j.cois.2016.04.006
- Herrero, S., Gechev, T., Bakker, P. L., Moar, W. J., and de Maagd, R. A. (2005). *Bacillus thuringiensis* CryIca-resistant *Spodoptera exigua* lacks expression of one of four aminopeptidase N genes. *BMC Genomics* 6 (1), 96. doi:10.1186/1471-2164-6-96
- Hoffman-Campo, C. B., Moscardi, F., Correa-Ferreira, B. S., Oliveira, L. J., Sosa-Gomez, D. R., Panizzi, A. R., et al. (2000). *Pragas da soja no Brasil e seu manejo integrado*. Londrina: EMBRAPA-CNPSo, 70.
- Hoffmann-Campo, C. B., de Oliveira, E. B., and Moscardi, F. (1985). Criação massal da lagarta da soja (*Anticarsia gemmatilis*). Available at: <https://www.infoteca.cnptia.embrapa.br/infoteca/handle/doc/445420>.
- Horikoshi, R. J., Bernardi, O., Godoy, D. N., Semeão, A. A., Willse, A., Corazza, G. O., et al. (2021a). Resistance status of Lepidopteran soybean pests following large-scale use of Mon 87701 × Mon 89788 soybean in Brazil. *Sci. Rep.* 11 (1), 21323. doi:10.1038/s41598-021-00770-0
- Horikoshi, R. J., Dourado, P. M., Berger, G. U., de S Fernandes, D., Omoto, C., Willse, A., et al. (2021b). Large-scale assessment of Lepidopteran soybean pests and efficacy of cryIac soybean in Brazil. *Sci. Rep.* 11 (1), 15956. doi:10.1038/s41598-021-95483-9

Supplementary material

The Supplementary Material for this article can be found online at: <https://www.frontiersin.org/articles/10.3389/fphys.2024.1484489/full#supplementary-material>

- Hughes, A. L. (2014). Evolutionary diversification of aminopeptidase N in Lepidoptera by conserved clade-specific amino acid residues. *Mol. Phylogenetics Evol.* 76, 127–133. doi:10.1016/j.ympev.2014.03.014
- IBS (2022). 2.0: an upgraded illustrator for the visualization of biological sequences. *Nucleic Acids Res.* doi:10.1093/nar/gkac373
- Ingle, S. S., Trivedi, N., Prasad, R., Kuruvilla, J., Rao, K. K., and Chhatpar, H. S. (2001). Aminopeptidase-N from the *Helicoverpa armigera* (Hubner) brush border membrane vesicles as a receptor of *Bacillus thuringiensis* cryIac δ -endotoxin. *Curr. Microbiol.* 43 (4), 255–259. doi:10.1007/s002840010297
- Knaak, N., and Fiuza, L. M. (2005). Histopathology of *Anticarsia gemmatilis* Hübner (Lepidoptera; Noctuidae) treated with Nucleopolyhedrovirus and *Bacillus thuringiensis* serovar kurstaki. *Braz. J. Microbiol.* 36 (2), 196–200. doi:10.1590/s1517-83822005000200017
- Knight, P. J., Crickmore, N., and Ellar, D. J. (1994). The receptor for *Bacillus thuringiensis* cryIa(c) delta-endotoxin in the brush border membrane of the Lepidopteran *Manduca sexta* is aminopeptidase N. *Mol. Microbiol.* 11 (3), 429–436. doi:10.1111/j.1365-2958.1994.tb00324.x
- Laemmli, U. K. (1970). Cleavage of structural proteins during the assembly of the head of bacteriophage T4. *Nature* 227 (5259), 680–685. doi:10.1038/227680a0
- Lei, Y., Zhu, X., Xie, W., Wu, Q., Wang, S., Guo, Z., et al. (2014). Midgut transcriptome response to a Cry toxin in the diamondback moth, *Plutella xylostella* (Lepidoptera: plutellidae). *Gene* 533 (1), 180–187. doi:10.1016/j.gene.2013.09.091
- Lin, P., Cheng, T., Jin, S., Jiang, L., Wang, C., and Xia, Q. (2014). Structural, evolutionary and functional analysis of APN genes in the lepidoptera *Bombyx mori*. *Gene* 535 (2), 303–311. doi:10.1016/j.gene.2013.11.002
- Liu, L., Li, Z., Luo, X., Zhang, X., Chou, S. H., Wang, J., et al. (2021). Which is stronger? A continuing battle between cry toxins and insects. *Front. Microbiol.* 12, 665101. doi:10.3389/fmicb.2021.665101
- Melo, A. L., Soccol, V. T., and Soccol, C. R. (2014). *Bacillus thuringiensis*: mechanism of action, resistance, and new applications: a Review. *Crit. Rev. Biotechnol.* 36 (2), 317–326. doi:10.3109/07388551.2014.960793
- Onofre, J., Gaytán, M. O., Peña-Cardena, A., García-Gomez, B. I., Pacheco, S., Gómez, I., et al. (2017). Identification of aminopeptidase-N2 as a Cry2Ab binding protein in *Manduca sexta*. *Peptides* 98, 93–98. doi:10.1016/j.peptides.2017.01.006
- Pacheco, S., Gómez, I., Gill, S. S., Bravo, A., and Soberón, M. (2009). Enhancement of insecticidal activity of *Bacillus thuringiensis* cryIa toxins by fragments of a toxin-binding cadherin correlates with oligomer formation. *Peptides* 30 (3), 583–588. doi:10.1016/j.peptides.2008.08.006
- Palma, L., Muñoz, D., Berry, C., Murillo, J., and Caballero, P. (2014). *Bacillus thuringiensis* toxins: an overview of their biocidal activity. *Toxins* 6 (12), 3296–3325. doi:10.3390/toxins6123296
- Pardo-López, L., Soberón, M., and Bravo, A. (2013). *Bacillus thuringiensis* insecticidal three-domain cry toxins: mode of action, insect resistance and consequences for crop protection. *FEMS Microbiol. Rev.* 37 (1), 3–22. doi:10.1111/j.1574-6976.2012.00341.x
- Perez-Riverol, Y., Bai, J., Bandla, C., García-Seisdedos, D., Hewapathirana, S., Kamatchinathan, S., et al. (2022). The PRIDE database resources in 2022: a Hub for mass spectrometry-based proteomics evidences. *Nucleic Acids Res.* 50 (D1), D543–D552. doi:10.1093/nar/gkab1038
- Pezenti, L. F., Sosa-Gómez, D. R., de Souza, R. F., Vilas-Boas, L. A., Gonçalves, K. B., da Silva, C. R. M., et al. (2021). Transcriptional profiling analysis of susceptible and resistant strains of *Anticarsia gemmatilis* and their response to *Bacillus thuringiensis*. *Genomics* 113 (4), 2264–2275. doi:10.1016/j.ygeno.2021.05.012
- Pigott, C. R., and Ellar, D. J. (2007). Role of receptors in *Bacillus thuringiensis* crystal toxin activity. *Microbiol. Mol. Biol. Rev.* 71 (2), 255–281. doi:10.1128/mmbr.00034-06
- Pinos, D., Andrés-Garrido, A., Ferré, J., and Hernández-Martínez, P. (2021). Response mechanisms of invertebrates to *Bacillus thuringiensis* and its pesticidal proteins. *Microbiol. Mol. Biol. Rev.* 85 (1), e00007–e00020. doi:10.1128/mmbr.00007-20
- Pozebon, H., Marques, R. P., Padilha, G., O Neal, M., Valmorinda, I., Bevilacqua, J. G., et al. (2020). Arthropod invasions versus soybean production in Brazil: a Review. *J. Econ. Entomology* 113 (4), 1591–1608. doi:10.1093/jeet/toaa108
- Qiu, L., Cui, S., Liu, L., Zhang, B., Ma, W., Wang, X., et al. (2017). Aminopeptidase N1 is involved in *Bacillus thuringiensis* cryIac toxicity in the beet armyworm, *Spodoptera exigua*. *Sci. Rep.* 7 (1), 45007. doi:10.1038/srep45007
- Rajagopal, R., Agrawal, N., Selvapandiyani, A., Sivakumar, S., Ahmad, S., and Bhatnagar, R. K. (2003). Recombinantly expressed isoenzymic aminopeptidases from *Helicoverpa armigera* (American cotton bollworm) midgut display differential interaction with closely related *Bacillus thuringiensis* insecticidal proteins. *Biochem. J.* 370 (3), 971–978. doi:10.1042/bj20021741
- Sanchis, V. (2011). From microbial sprays to insect-resistant transgenic plants: history of the biopesticide *Bacillus thuringiensis*. A Review. *Agron. Sustain. Dev.* 31 (1), 217–231. doi:10.1051/agro/2010027
- Sangadala, S., Walters, F. S., English, L. H., and Adang, M. J. (1994). A mixture of *Manduca sexta* aminopeptidase and phosphatase enhances *Bacillus thuringiensis* insecticidal cryIa(c) toxin binding and 86RB(+)-K+ efflux in vitro. *J. Biol. Chem.* 269 (13), 10088–10092. doi:10.1016/s0021-9258(17)36993-4
- Sato, R. (2002). Aminopeptidase N as a receptor for *Bacillus thuringiensis* cry toxins. *Adv. Microb. Control Insect Pests*, 1–13. doi:10.1007/978-1-4757-4437-8_1
- Soberón, M., Monnerat, R., and Bravo, A. (2018). Mode of action of cry toxins from *Bacillus thuringiensis* and resistance mechanisms. *Toxinology*, 15–27. doi:10.1007/978-94-007-6449-1_28
- Stamatakis, A. (2014). RAXML version 8: a tool for phylogenetic analysis and post-analysis of large phylogenies. *Bioinforma. Oxf. Engl.* 30 (9), 1312–1313. doi:10.1093/bioinformatics/btu033
- Sun, Y., Yang, P., Jin, H., Liu, H., Zhou, H., Qiu, L., et al. (2020). Knockdown of the aminopeptidase N genes decreases susceptibility of *Chilo suppressalis* larvae to cryIab/cryIac and cryIca. *Pesticide Biochem. Physiology* 162, 36–42. doi:10.1016/j.pestbp.2019.08.003
- Tabashnik, B. E., Fabrick, J. A., and Carrière, Y. (2023). Global patterns of insect resistance to transgenic BT crops: the first 25 years. *J. Econ. Entomology* 116 (2), 297–309. doi:10.1093/jeet/toac183
- Tamura, K., Stecher, G., and Kumar, S. (2021). MEGA11: molecular evolutionary genetics analysis version 11. *Mol. Biol. Evol.* 38 (7), 3022–3027. doi:10.1093/molbev/msab120
- Tiewsi, K., and Wang, P. (2011). Differential alteration of two aminopeptidases n associated with resistance to *Bacillus thuringiensis* toxin cryIac in cabbage looper. *Proc. Natl. Acad. Sci.* 108 (34), 14037–14042. doi:10.1073/pnas.1102555108
- Towbin, H., Staehelin, T., and Gordon, J. (1979). Electrophoretic transfer of proteins from polyacrylamide gels to nitrocellulose sheets: procedure and some applications. *Proc. Natl. Acad. Sci. Sep* 76 (9), 4350–4354. doi:10.1073/pnas.76.9.4350
- Valaitis, A. P. (2011). Localization of *Bacillus thuringiensis* cryIa toxin-binding molecules in gypsy moth larval gut sections using fluorescence microscopy. *J. Invertebr. Pathology* 108, 69–75. doi:10.1016/j.jip.2011.07.001
- Valaitis, A. P., Augustin, S., and Clancy, K. M. (1999). Purification and characterization of the western spruce budworm larval midgut proteinases and comparison of gut activities of laboratory-reared and field-collected insects. *Insect Biochem. Mol. Biol.* 29 (5), 405–415. doi:10.1016/s0965-1748(99)00017-x
- Valdes, C., Gillespie, J., and Dohlman, E. (2023). *Soybean production, marketing costs, and export competitiveness in Brazil and the United States*. Economic Information Bulletin: United States Department of Agriculture, Economic Research Service
- Visweshwar, R., Sharma, H. C., Akbar, S. M. D., and Sreeramulu, K. (2015). Elimination of gut microbes with antibiotics confers resistance to *Bacillus thuringiensis* toxin proteins in *Helicoverpa armigera* (Hubner). *Appl. Biochem. Biotechnol.* 177 (8), 1621–1637. doi:10.1007/s12010-015-1841-6
- Wang, C., Deng, Z., Yuan, J., Xu, K., Sha, L., Guan, X., et al. (2023). Removal of an aminopeptidase N from midgut brush border does not affect susceptibility of *Spodoptera litura* (Lepidoptera: Noctuidae) larvae to four insecticidal proteins of *Bacillus thuringiensis* (Bacillales: Bacillaceae). *J. Econ. Entomol.* 116 (1), 223–232. doi:10.1093/jeet/toac184
- Wang, L., Gu, S. H., Nangong, Z. Y., Song, P., and Wang, Q. Y. (2017). Aminopeptidase N5 (APN5) as a putative functional receptor of cryIac toxin in the larvae of *Aethis lepigone*. *Curr. Microbiol.* 74 (4), 455–459. doi:10.1007/s00284-017-1215-0
- Wang, P., Zhang, X., and Zhang, J. (2005). Molecular characterization of four midgut aminopeptidase N isozymes from the Cabbage Looper, *Trichoplusia ni*. *Insect Biochem. Mol. Biol.* 35 (6), 611–620. doi:10.1016/j.ibmb.2005.02.002
- Wang, X. Y., Du, L. X., Liu, C. X., Gong, L., Han, L. Z., and Peng, Y. F. (2017). RNAi in the Striped Stem Borer, *Chilo suppressalis*, establishes a functional role for aminopeptidase N in cryIab intoxication. *J. Invertebr. Pathology* 143, 1–10. doi:10.1016/j.jip.2016.11.004
- Wolfersberger, M., Luethy, P., Maurer, A., Parenti, P., Sacchi, F., Giordana, B., et al. (1987). Preparation and partial characterization of amino acid transporting brush border membrane vesicles from the larval midgut of the cabbage butterfly (Pieris brassicae). *A. Comp. Physiol.* 86 (2), 301–308. doi:10.1016/0300-9629(87)90334-3
- Wu, F.-X., Gagné, P., Droit, A., and Poirier, G. G. (2006). RT-PSM, a real-time program for peptide-spectrum matching with statistical significance. *Rapid Commun. mass Spectrom.* RCM 20 (8), 1199–1208. doi:10.1002/rcm.2435
- Xu, C., Wang, B. C., Yu, Z., and Sun, M. (2014). Structural insights into *Bacillus thuringiensis* Cry, Cyt and parasporin toxins. *Toxins* 6 (9), 2732–2770. doi:10.3390/toxins6092732
- Yang, Y., Zhu, Y. C., Ottea, J., Husseneder, C., Leonard, B. R., Abel, C., et al. (2010). Molecular characterization and RNA interference of three midgut aminopeptidase N isozymes from *Bacillus thuringiensis*-susceptible and -resistant strains of sugarcane borer, *Diatraea saccharalis*. *Insect Biochem. Mol. Biol.* 40 (8), 592–603. doi:10.1016/j.ibmb.2010.05.006
- Ziga-Navarrete, F., Bravo, A., Sobern, M., and Gmez, I. (2021). Role of GPI-anchored membrane receptors in the mode of action of *Bacillus thuringiensis* cry toxins. *Integr. Pest Manag. Pest Control - Curr. Future Tactics*. doi:10.5772/30718



OPEN ACCESS

EDITED BY

Ana Claudia A. Melo,
Federal University of Rio de Janeiro, Brazil

REVIEWED BY

Alma Altúzar-Molina,
Instituto de Ecología (INECOL), Mexico
Fang (Rose) Zhu,
The Pennsylvania State University (PSU),
United States

*CORRESPONDENCE

Zhi-Rong Sun,
✉ Szr13885907638@163.com
Man-Qun Wang,
✉ mqwang@mail.hzau.edu.cn

RECEIVED 29 September 2024

ACCEPTED 15 November 2024

PUBLISHED 04 December 2024

CITATION

Yi S-C, Yu J-L, Abdelkhalek ST, Sun Z-R and
Wang M-Q (2024) Identification and odor
exposure regulation of odorant-binding
proteins in *Picromerus lewisi*.
Front. Physiol. 15:1503440.
doi: 10.3389/fphys.2024.1503440

COPYRIGHT

© 2024 Yi, Yu, Abdelkhalek, Sun and Wang.
This is an open-access article distributed
under the terms of the [Creative Commons
Attribution License \(CC BY\)](#). The use,
distribution or reproduction in other forums is
permitted, provided the original author(s) and
the copyright owner(s) are credited and that
the original publication in this journal is cited,
in accordance with accepted academic
practice. No use, distribution or reproduction
is permitted which does not comply with
these terms.

Identification and odor exposure regulation of odorant-binding proteins in *Picromerus lewisi*

Shan-Cheng Yi¹, Jia-Ling Yu¹, Sara Taha Abdelkhalek^{1,2},
Zhi-Rong Sun^{3*} and Man-Qun Wang^{1*}

¹Hubei Insect Resources Utilization and Sustainable Pest Management Key Laboratory, College of Plant Science and Technology, Huazhong Agricultural University, Wuhan, China, ²Department of Entomology, Faculty of Science, Ain Shams University, Cairo, Egypt, ³Southwest Guizhou Autonomous Prefecture Tobacco Company, Xingren, China

The highly developed sensitive olfactory system is essential for *Picromerus lewisi* Scott (Hemiptera: Pentatomidae) adults, an widely distributed natural predatory enemy, to locate host plants. During this process, odorant-binding proteins (OBPs) are thought to have significant involvement in the olfactory recognition. However, the roles of OBPs in the olfactory perception of *P. lewisi* are not frequently reported. Here, we conducted odor exposure and transcriptome sequencing experiments using healthy and *Spodoptera litura*-infested tobacco plants as odor sources. The transcriptomic data revealed that the alteration in the expression of mRNA levels upon exposure to odor was sex-dependent. As the expression profiles differed significantly between male and female adults of *P. lewisi*. A total of 15 *P. lewisi* OBPs (PlewOBPs) were identified from the *P. lewisi* transcriptome. Sequence and phylogenetic analysis indicated that PlewOBPs can be classified into two subfamilies (classic OBP and plus-C OBP). The qRT-PCR results showed that the transcript abundance of 8 *PlewOBPs* substantially altered following exposure to *S. litura*-infested tobacco plants, compared to the blank control or healthy plants. This implies that these *PlewOBPs* may have an olfactory function in detecting *S. litura*-infested tobacco plants. This study establishes the foundation for further understanding of the olfactory recognition mechanism of *P. lewisi* and helps discover novel targets for functional characterization in future research.

KEYWORDS

Picromerus lewisi, *Spodoptera litura*, odor exposure, transcriptome, odorantbinding proteins

1 Introduction

Insects utilize a diverse array of molecular sensors to detect and respond to their external environment (Gadenne et al., 2016; Hare, 2011; Howe and Jander, 2008). In this process, various chemosensory-related proteins are involved in the transduction of signals within antennae, such as odorant-binding proteins (OBPs), chemosensory proteins (CSPs), odorant receptors (ORs), odorant degrading enzymes (ODEs), and sensory neuron membrane proteins (SNMPs) (Leal, 2013; Paoli and Galizia, 2021; Tunstall et al., 2012). The OBPs are a family of compact soluble proteins (12–30 kDa) that selectively bind and transport hydrophobic molecules across the hydrophilic

sensillum lymph surrounding sensory neurons (Tunstall et al., 2012; Rihani et al., 2021; Pelosi et al., 2018; Sun et al., 2018). This ultimately leads to the activation of odorant receptors (ORs).

Insect OBPs are characterized by the presence of three interlocking disulfide bonds, which are formed by highly conserved cysteine (Cys) residues. OBPs can be categorized into four subfamilies based on the number of preserved Cys residues: classic OBPs (have six conserved Cys residues), minus-C OBPs (have four conserved Cys residues), plus-C OBPs (have eight conserved Cys and proline residues), and atypical OBPs (have 9–10 Cys residues and a long C-terminus) (Manoharan et al., 2013; Vieira and Rozas, 2011; Zhou et al., 2010; Vieira et al., 2007). Multiple investigations have confirmed that OBPs can selectively recognize and evaluate specific chemical signals (Yang et al., 2024; Xiang et al., 2023; Sims et al., 2023; Li E.-T. et al., 2023; Huang et al., 2023). Thus, their function goes beyond just passive transportation. The knockdown of *BdorOBP83a-2* in *Bactrocera dorsalis* (Diptera: Tryptetidae) resulted in a significant reduction of 60%–70% in the electroantennogram (EAG) response to methyl eugenol (Wu et al., 2016). It also caused a 30%–50% increase in flight time to reach the odor source. This study demonstrates that *BdorOBP83a-2* plays a crucial role in mediating the responses of the oriental fruit fly to semiochemicals (Wu et al., 2016). The OBP3 identified in *Acyrtosiphon pisum* (Hemiptera: Aphididae) has an important function in the discrimination of the alarm pheromone (*E*)- β -farnesene compared to its homologous proteins OBP1 and OBP8 (De Biasio et al., 2015). *Drosophila melanogaster* flies with *OBP57e* and *OBP57d* knock-out displayed altered behavioral responses to hexanoic and octanoic acids (Yasukawa et al., 2010; Matsuo et al., 2007; Harada et al., 2008). Furthermore, when *OBP57d* and *OBP57e* from *D. simulans* and *D. sechellia* were introduced, the preference for the oviposition site in *D. melanogaster* *OBP57d/e^{KO}* flies shifted to match that of the original species. These studies indicated that OBPs were essential for mediating olfactory behavioral responses.

The transcriptional expression of the majority of OBPs is mainly restricted to the antennae, maxillary palp, and proboscis of the insect's head (Yi et al., 2023; Wang et al., 2020; Dong et al., 2023). Studies showed that exposing the olfactory system to external odorant cues alters the transcriptional levels of chemosensory-related proteins involved in detecting of the tested odorant (He et al., 2023; Anton and Rössler, 2021; Guerrieri et al., 2012). Discovery of this phenomenon originated from investigations on the deorphanization of ORs in *Mus musculus* (Rodentia: Muridae), employing a mechanism appropriately known as deorphanization of receptors based on expression alteration of mRNA levels (DREAM) (von der Weid et al., 2015). To date, this strategy has been effectively applied in several studies of insect OBPs. In *Diaphorina citri* (Hemiptera: Chermidae), *DcitOBP7* showed significant changes in expression levels, either upregulation or downregulation induced by methyl salicylate, linalool, and R-(+)-limonene. Moreover, the suppression of messenger RNA (mRNA) expression of *DcitOBP7* using the RNA interference (RNAi) resulted in a significant reduction in EAG activity and adult behavioral responses of *D. citri* to tested volatiles and the preferred host, *Murraya paniculata* (Sapindales: Rutaceae) (Liu et al., 2021). In *Holotrichia oblita* (Coleoptera: Melolonthidae), *HoblOBP13* and *HoblOBP9* were upregulated upon exposure to one of the female

attractants (*E*)-2-hexenol and phenethyl alcohol. The female beetles that performed post-RNAi treatments targeting *HoblOBP13* and *HoblOBP9* exhibited an apparent reduction in attraction towards (*E*)-2-hexenol and phenethyl alcohol compared to water-injected beetles and those treated with GFP-dsRNA (Yin et al., 2019). Although the DREAM strategy sometimes showed a high amount of false positive predictions, it could still provide insights of the chemical communication between insects and their external environment (Koerte et al., 2018).

Picromerus lewisi (Hemiptera: Pentatomidae) is an important natural enemy insect with strong predation on the larvae of various lepidopteran pests, including *Spodoptera litura*, *Spodoptera frugiperda*, *Mythimna separate*, and *Leucania separata*. A previous study has identified the expression profiles of cytochrome P450 monooxygenases, carboxylesterase, and glutathione S-transferase genes across various tissues and developmental stages (Li et al., 2022; Li W. et al., 2023). Our previous investigations using a Y-tube olfactometer showed that *P. lewisi* adults had a significant preference for *S. litura*-infested tobacco plants compared to the healthy ones (unpublished data). However, the specific olfactory mechanisms underlying this behavioral preference remain unclear. In this study, we conducted transcriptome sequencing on the head of *P. lewisi* following exposure to healthy and *S. litura*-infested tobacco plants. A total of 18 *P. lewisi* libraries were constructed and sent for *de novo* assembly. Subsequently, we performed identification and phylogenetic analysis of *PlewOBPs*. Finally, we analyzed the differential expression profiles of different treatments on male and female *P. lewisi*, and validated the transcription abundance of all identified *PlewOBPs* using qRT-PCR. The provided results establish the foundation for further comprehension of the olfactory recognition mechanism of *P. lewisi*.

2 Materials and methods

2.1 Materials

The adult *P. lewisi* samples were reared in a controlled environment chamber with a temperature of 25°C \pm 3°C, relative humidity (RH) of 65% \pm 5%, and a light-dark cycle of 14:10 (L:D). The first-hatched *P. lewisi* larvae were fed with 10% honey water. After the 2nd larval instar, *P. lewisi* larvae were provided with *L. separata* larvae of the corresponding instar. At the same time, *S. litura* larvae were fed on fresh tobacco leaves in an artificially controlled environment maintained at 25°C \pm 3°C, 40% \pm 5% RH, and natural light only.

The Yunnan Tobacco 87 plants were cultivated in a controlled environment with a temperature of 25°C \pm 3°C, RH of 65% \pm 5%, and a light-dark cycle of 14 L:10 D. The seeds were planted in seedling trays (a hole depth of 5 cm, an upper aperture of 4 cm, and a lower aperture of 2 cm) for 30 days. Subsequently, the seedlings were transferred to two-color pots (upper aperture of 14 cm, lower aperture of 12 cm, and height of 13 cm), and then the plants continued to grow for 30 days. Tobacco plants exhibiting robust and healthy growth and devoid of any pests and diseases were selected for the experiments.

2.2 Odor exposure and tissue collection

Following 6 h of starvation, six 4th instar larvae of *S. litura* were affixed to the 3rd and 4th leaves of tobacco plants in a top-to-bottom manner. To prevent the escape of *S. litura* larvae, the plants were enclosed in cages with 120 mesh screens. The *S. litura* larvae were removed after consuming 20% of the leaves. In exposure experiments, tobacco plants were used 18–30 h after the *S. litura* commenced feeding. The root and soil portion of the plants were wrapped in tin foil and placed in a hermetically sealed glass container. The airflow from the air pump passed consecutively through two closed containers, one filled with activated carbon and the other with pure water. The purified and humidified air was directed into the glass containers housing tobacco plants and then out through the air outlet, with the flow rate being regulated by an airflow meter. Once the device was connected, the flow rate of the flow meter was adjusted to 400 mL/min, and the test proceeded once the flow rate had reached an equilibrium level. The gas maintained a consistent flow rate throughout the treatment and was directly directed into the preservation box housing the *P. lewisi* adults.

A total of three distinct odor sources for conducting the odor exposure experiments. The first group served as a control, devoid of any odorants (CK group). The healthy and *S. litura*-infested tobacco plants were used as the source of odor in the HT and IT group, respectively. Each odor exposure experiments group comprises 15 mature *P. lewisi* individuals (male or female), with three biological replicates. After 1 h of odor exposure treatment, the entire head of the *P. lewisi* adult samples was collected and promptly placed in RNase-free tubes and stored in liquid nitrogen.

2.3 RNA extraction and cDNA synthesis

Total RNA was extracted from preserved tissues using TRIzol reagent (Invitrogen, Carlsbad, CA, United States) following the manufacturer's instructions. The integrity and quantity of RNA samples were assessed by using 1% agarose gel electrophoresis and a spectrophotometer (Eppendorf Bio Photometer Plus, Hamburg, Germany), respectively. A complementary DNA (cDNA) was synthesized from 1 µg of total RNA via reverse transcription, using a Prime-Script II 1st Strand cDNA Synthesis Kit (TaKaRa Bio, Otsu, Japan) according to the pamphlet instructions. This kit uses DNase in the initial step to eliminate the effect of DNA on qRT-PCR.

2.4 Transcriptome analysis

All samples were conveyed to Personalbio Technology Co. Ltd. (Shanghai, China) for Illumina sequencing using a 100 bp paired-end sequencing strategy. The sequencing data was filtered to obtain high-quality, clean reads for subsequent analysis. For unreferenced transcriptome sequencing, the clean reads were transcribed using Trinity software for further analysis. The unigenes were functionally annotated using the NR, GO, KEGG, eggNOG, Swiss-Prot, and Pfam databases. The number of reads for each sample was compared to each gene to calculate the FPKM value. Differentially expressed genes were identified by the DESeq software package, with

thresholds of \log_2 (fold change) ≥ 1 , and P -value ≤ 0.05 set significant differences.

2.5 Identification and phylogenetic analysis of odorant-binding proteins

The transcriptome annotation results were used to select the unigenes that included the annotated content of “odorant-binding protein”, “odorant binding protein”, and “OBPs”. The identification of potential open reading frames (ORFs) and their corresponding amino acid sequences was determined using the ORF FINDER (<https://www.ncbi.nlm.nih.gov/orffinder/>). Hemipteran-based phylogenetic analysis of PlewOBPs was performed using the MEGA-X program. The N-terminal signal peptide sequences of PlewOBPs were predicted using the SignalP-5.0 server (<http://www.cbs.dtu.dk/services/SignalP/>). The mature amino acid sequences were aligned using the MAFFT multiple sequence alignment (<https://mafft.cbrc.jp/alignment/server/>). A neighbor-joining tree was constructed using the p-distance model and pairwise deletion of gaps. The bootstrapping process was performed by resampling the amino acid positions of 1,000 replicas, and branches with bootstrap cutoff of <50% were collapsed. The tree was ultimately examined and modified using the Evolview-v2 (<https://evolgenius.info/evolview-v2/>) and Adobe Illustrator CC 2019 program.

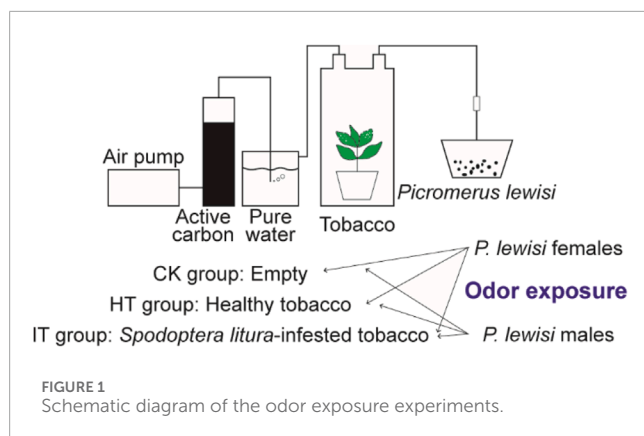
2.6 qRT-PCR

The relative mRNA expression levels of 15 full-length *PlewOBPs* genes were determined using qRT-PCR under various treatments. A qRT-PCR reaction was performed on a LightCycler[®] 96 System using the Hieff[®] qPCR SYBR Green Master Mix (No Rox) (Yeasen, Shanghai, China). Each reaction was systematically run in triplicates with three independent biological replicates. Gene-specific primers of *PlewOBPs* were designed using the Primer-BLAST service (https://www.ncbi.nlm.nih.gov/tools/primer-blast/index.cgi?LINK_LOC=BlastHome). The comparative $2^{-\Delta\Delta CT}$ method was used to calculate the relative transcript levels in each sample. The data was assessed using a one-way analysis of variance (ANOVA) and Tukey's honestly significant difference (HSD) *post hoc* test.

3 Results and discussion

3.1 Head transcriptome of *Picromerus lewisi*

A grand number of 765,095,950 Illumina paired-end reads were generated from 18 *P. lewisi* libraries. Each library was sequenced using samples obtained from the heads of 15 adult individuals (female or male) (Figure 1). After the trimming of adaptors and the filtration of low-quality reads, a total of 754,299,698 high-quality reads were obtained with 96.79% Q30 bases. Subsequently, we used the entire set of reads to create a *de novo* transcriptome assembly using Trinity (see methods). The assembly process resulted in the formation of 156,008 transcripts, which collectively had 276 million



base pairs (bp). These transcripts encoded a total of 75,039 unigenes, with an N50 value of 1728 bp (Supplementary Table S1).

The annotation process involved using BLAST and HMMER software to perform local alignments against various databases, including NR, GO, KEGG, Pfam, eggNOG, and Swissprot. This resulted in annotation for 19,762 (26.34%), 10,287 (13.71%), 7,766 (10.35%), 8,898 (11.86%), 15,770 (21.02%), and 10,639 (14.18%) unigenes, respectively (Figure 2A). Out of the total data set, 55,277 unigenes (75.37%) did not receive a BlastX hit, possibly due to misassembly or insufficient representation in the NR database. The assembled transcriptome of *P. lewisi* showed a significant resemblance to *Halyomorpha halys* (Hemiptera: Pentatomidae), with 12,221 (61.84%) of the annotated unigenes showing the closest similarity to that particular species (Figure 2B). It was expected as *H. halys* has the most thoroughly annotated genome among of stink bugs in the pentatomidae family (Sparks et al., 2020; Paula et al., 2016).

Further functional classification of gene ontology (GO) was performed. The GO database consists of three major categories: biological processes (BP), cellular components (CC) and molecular function (MF). In total, 24 biological processes, 20 cellular components and 14 molecular functions were identified (Figure 2C). The categories more directly related to insect olfaction in the list of BP were a response to stimulus and localization. The unigenes exhibited enrichment in cellular processes, biological regulation and metabolic processes in the BP. Most of the unigenes in the CC list were associated with cells, cell components, and organelles. Finally, in the list of MF, these were annotated to the functional classes of binding, catalytic activity, and transcription regulator activity. These predominant GO annotations in BP, CC, and MF were comparable to those observed in the antennal transcriptomes of the *H. halys*, *Adelphocoris lineolatus* (Hemiptera: Miridae), and *Apolygus lucorum* (Hemiptera: Miridae) (Paula et al., 2016; Xiao et al., 2017; Chen et al., 2017; Ji et al., 2013). This similarity is noteworthy, considering that the transcriptomes were obtained from the head of *P. lewisi*. However, the annotations differed from the predominant BP and MF detected in the antennal transcriptomes of *Chinavia ubica* (Hemiptera: Pentatomidae), *Dichelops melacanthus* (Hemiptera: Pentatomidae), or *Euschistus heros* (Hemiptera: Pentatomidae) (Farias et al., 2015). The GO enrichment variations could be attributed to their distinct dietary preferences.

3.2 Identification of odorant-binding proteins

OBPs are compact, globular, water-soluble proteins with a signal peptide at the N-terminal region and six Cys residues in conserved positions (Zhou et al., 2008). The Cys motif is a highly conserved tertiary protein structure consisting of six α -helices coordinated by three disulfide bridges (Zhou et al., 2004; Xu et al., 2003; Wang et al., 2014). It is commonly employed as a signature for the identification of OBP. Based on the sequence similarity to insect OBPs, a total of 15 PlewOBPs were identified in the transcriptome. The number of PlewOBPs is much lower compared to *H. halys* (30 HhalOBPs), *A. lineolatus* (31 AlineOBPs), and *A. lucorum* (38 AlucOBPs) (Paula et al., 2016; Yuan et al., 2015; Xiao et al., 2018; Gu et al., 2011). A plausible explanation is that their total RNA is more comprehensive than ours due to the extraction of RNA from various all developmental stages or tissues or because they possess whole genome sequences. *Picromerus lewisi* had a similar number of OBPs to other stink bugs, specifically 19 in *Tropidothorax elegans* (Hemiptera: Lygaeidae), 18 in *Cyrtorhinus lividipennis* (Hemiptera: Miridae), and 17 in *Rhodnius prolixus* (Hemiptera: Reduviidae) (Song et al., 2018; Wang et al., 2018; Wang et al., 2017; Oliveira et al., 2017).

All 15 PlewOBPs have intact ORFs with lengths ranging from 396 to 663 bp. The authenticity of the nucleotide sequences of all PlewOBPs was confirmed by cloning and sequencing. Out of the 15 PlewOBPs, 11 of them have a signal peptide at their N-terminal. Like other hemipterans OBPs, PlewOBPs sequences were categorized into two types based on the presence of the characteristic OBP Cys signature: “classic” OBP and “plus-C” OBP. Based on the hemipteran “classic” OBP Cys motif (C1-X₂₂₋₃₂-C2-X₃-C3-X₃₆₋₄₆-C4-X₈₋₁₄-C5-X₈-C6), we have classified 12 PlewOBPs (PlewOBP 1–8, 10–12, and 15) sequences as “classic” OBPs (Supplementary Figure S1). The remaining three PlewOBP proteins (PlewOBP 9, 13, and 14) belong to the “plus-C” OBP family (Supplementary Figure S1), and fit to the Cys spacing pattern (C1-X₈₋₄₁-C2-X₃-C3-X₃₉₋₄₇-C4-X₁₇₋₂₉-C4a-X₉-C5-X₈-C₆-P-X₉₋₁₁-C6a).

A neighbour-joining tree consisting of 119 mature OBPs was constructed from six Hemipteran species to confirm the intraspecific divergence of their OBPs. The Hemipteran OBP protein family generates an expansive tree, with distinct clades for both “classic” and “plus-C” OBP sequences (Figure 3). In the phylogenetic tree, OBPs of the same subfamily exhibit local clustering, while OBPs of the same subfamily are distributed evenly throughout the entire tree, forming separate central clusters. These results provide evidence of significant duplication and specialization of OBPs within Heteroptera. However, this finding diverges from aphids, which have the most orthologous sequences in different species (Xue et al., 2016; Wang et al., 2019; Song et al., 2021). In this work, we found no intraspecific orthologous genes within the same species of stink bugs. Nevertheless, there is a slightly higher rate of orthologues between related species. 10 of 15 PlewOBPs have homologous sequences to the OBPs found in other Hemiptera insects with a high bootstrap value, indicating a high probability that these sequences come from a common ancestor and are preserved for shared functions in plant bug species. PlewOBPs also have paralogs, such as PlewOBP5 and PlewOBP6, which may have undergone horizontal duplication duplicated from the same ancestor through natural selection to acquire an additional function.

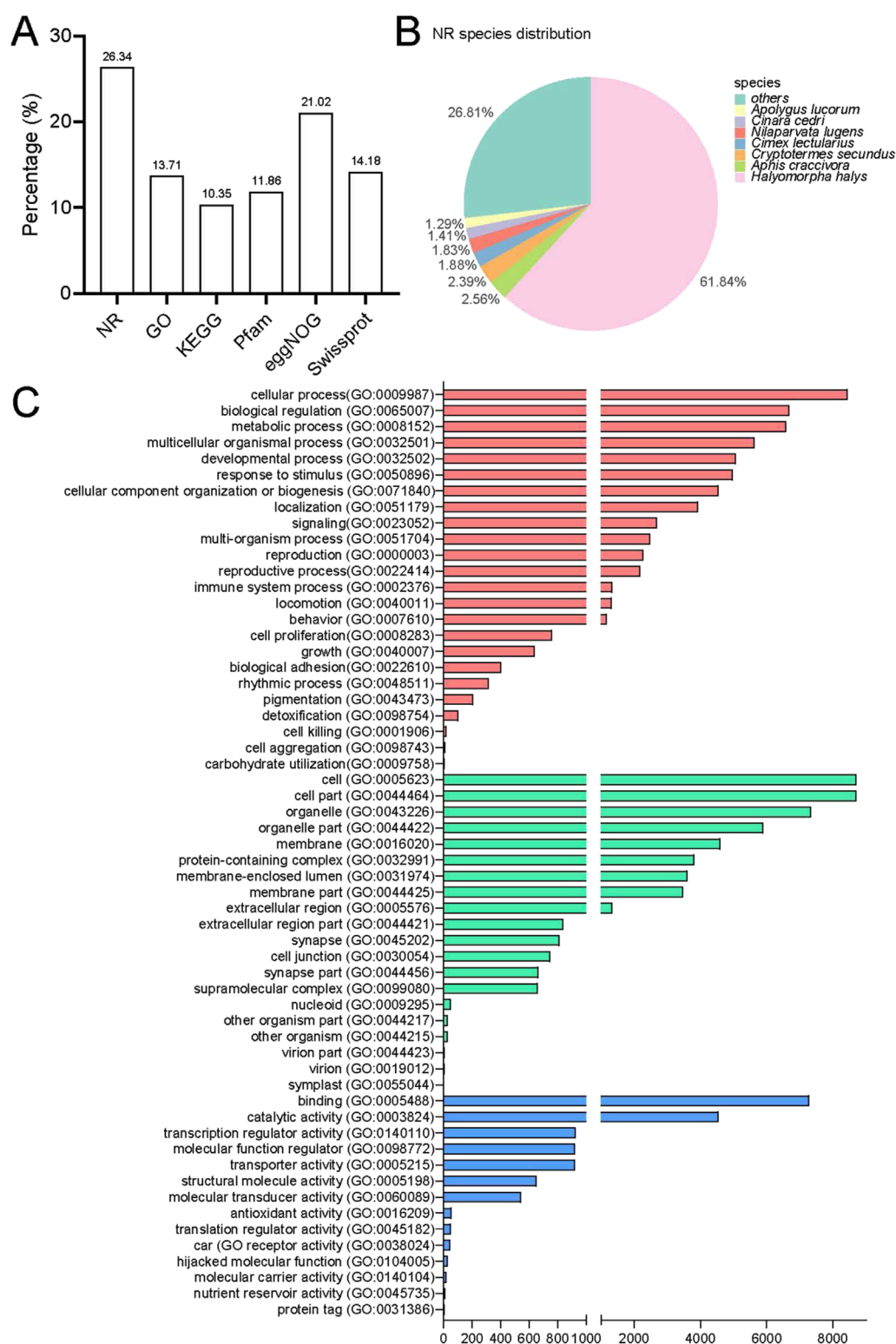
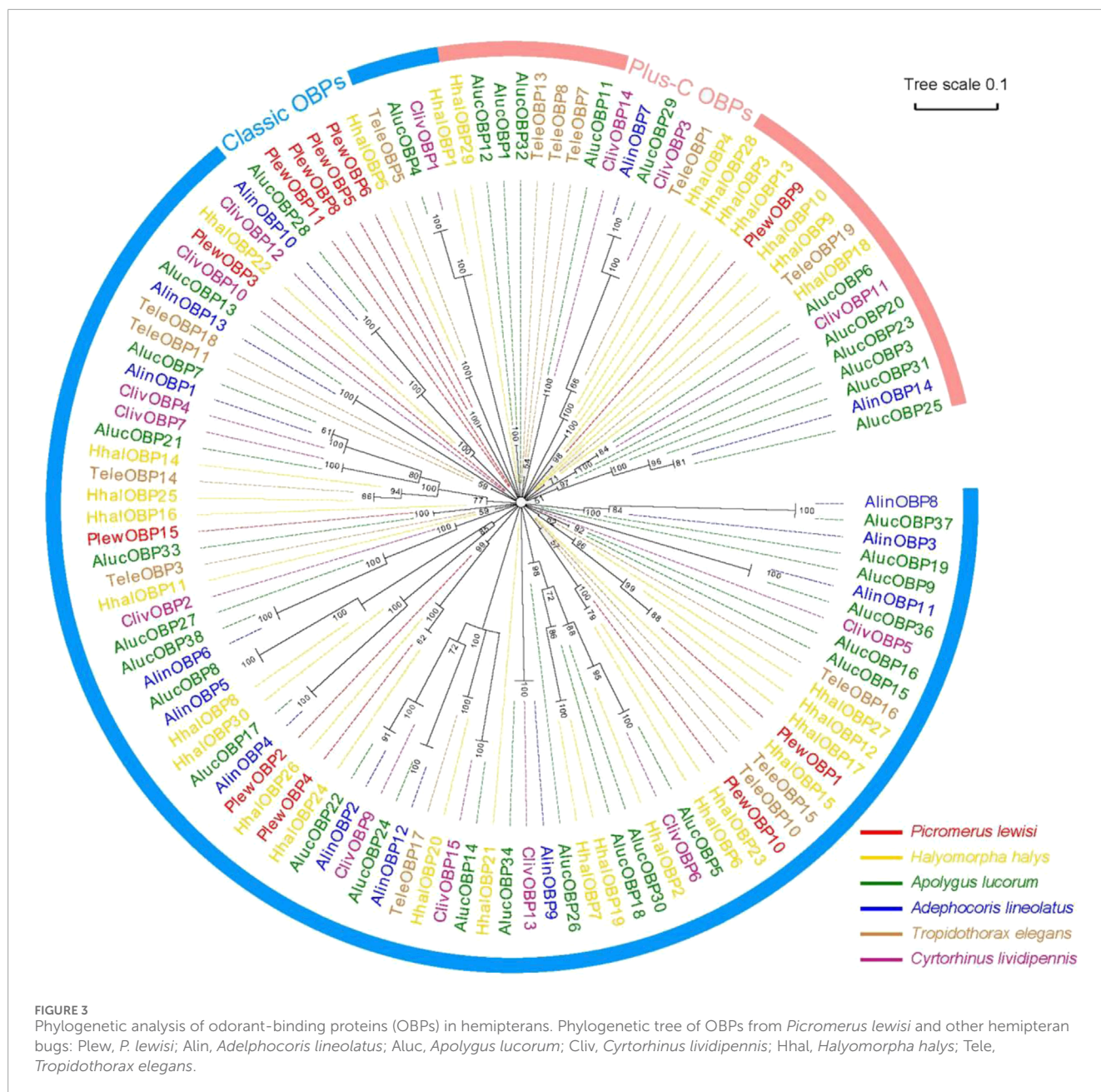


FIGURE 2

Annotation information for the head transcriptome of *Picromerus lewisi*. (A) Summary of annotations in different databases. (B) Species distribution in the NR database. (C) Functional classification of GO annotations.



3.3 Overall differential expression profiles

The identification of differentially expressed genes (DEGs) was carried out by the DESeq software package, with an absolute log2 (fold change) value of ≥ 1 and a P -value ≤ 0.05 were considered as the threshold for significant differences. Within this framework, the transcript abundance of 325 genes was significantly altered when females were exposed to volatiles emitted by healthy tobacco plants for 1 h. 112 genes demonstrated lower abundance, while 213 showed more abundance when compared to blank control (Figure 4A). Similarly, in males, a total of 93 genes showed decreased abundance out of the 331 genes that were differentially detected. Conversely, 238 genes revealed increased abundance in the HT

group compared to the control group (Figure 4B). The *S. litura*-infested tobacco plants exhibited a higher propensity for genes to change in transcript abundance than healthy plants. Exposure of adult females to infested tobacco resulted in the upregulation of 254 genes and the downregulation of 184 ones (Figure 4C). Additionally, 223 genes were upregulated, and 200 were downregulated in adult males (Figure 4D).

We conducted GO analysis to better understand the genes responsible for the variation between sexes and various treatments. Upon assessing the transcripts in male and female bugs, we observed distinct differences in the GO enrichment patterns of differentially expressed genes induced by healthy or infested tobacco plants (Supplementary Figures S2–S5). There was minimal overlap of GO

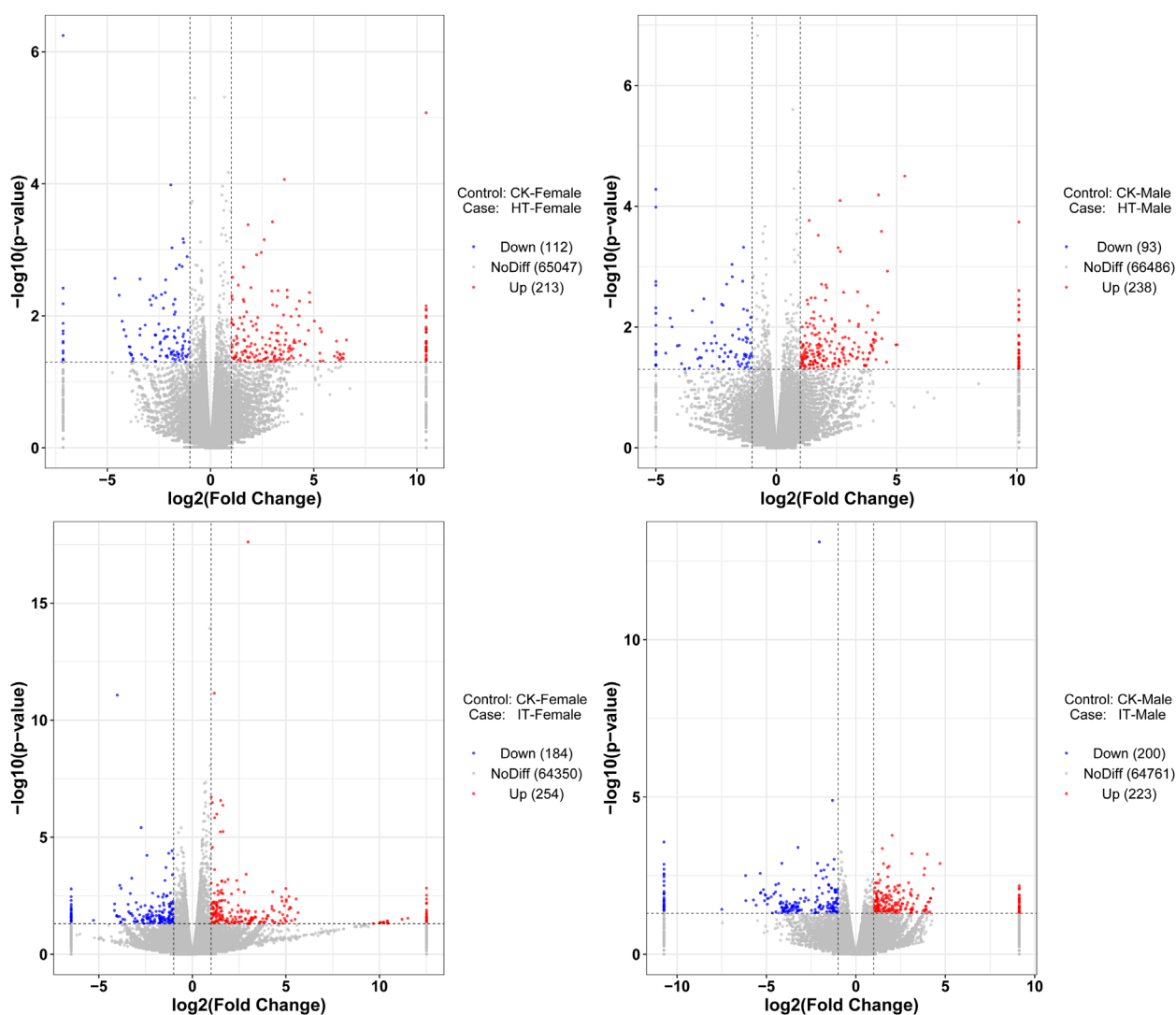


FIGURE 4

Volcano plot of RNA sequencing from different treatments. The vertical dashed lines represent the 2-fold expression difference thresholds; the horizontal dashed line represents the p -value = 0.05 threshold. Red dots indicate genes with significant upregulation, blue dots indicate genes with significant downregulation, and gray dots indicate genes with non-significant differential expression.

enrichment terms between males and females within the same treatment and across different treatments within the same sex. The Wayne diagram analysis corroborated these findings, revealing that only a few genes were simultaneously up- or downregulated between different treatments or sexes (Figure 5). Among which, the venom serine protease-like gene was the only annotated gene, potentially serving common roles in digestion and detoxification (He et al., 2024). It was unsurprising that genes can respond to environmental factors, leading to alterations in transcript abundance *in vivo*. The transcript abundance of a large variety of genes in *Anopheles gambiae* (Diptera: Culicidae) mosquitoes can be influenced by varied light conditions (Rund et al., 2013). Whereas transcriptomic data in *Aedes aegypti* (Diptera: Culicidae) revealed that prolonged exposure to 1-octen-3-ol modulated ORs and OBPs genes, as well as cytochrome P450 enzymes, insect cuticle proteins, and

glucuronosyltransferases families (Mappin et al., 2023). Abiotic environmental factors and biological factors such as courtship, mating, sex, and age can influence antennal chemosensory-related genes (Tallon et al., 2019; Alonso et al., 2019; Andersson et al., 2014; Siju et al., 2010). However, the transcriptome data in the present study revealed none differentially expressed *PlewOBPs*. One potential explanation is that this change in transcript levels correlates with the concentration and duration of odor exposure. The duration and concentration of our odor exposure experiments were insufficient (Duan et al., 2023). Conversely, minimal fold differences in gene expression may evade detection using transcriptome sequencing, as our screening criteria were based on thresholds of \log_2 (fold change) ≥ 1 . To gain a more comprehensive understanding of the pattern of changes in the *OBP* gene family, we performed qRT-PCR experiments with all *PlewOBPs*.

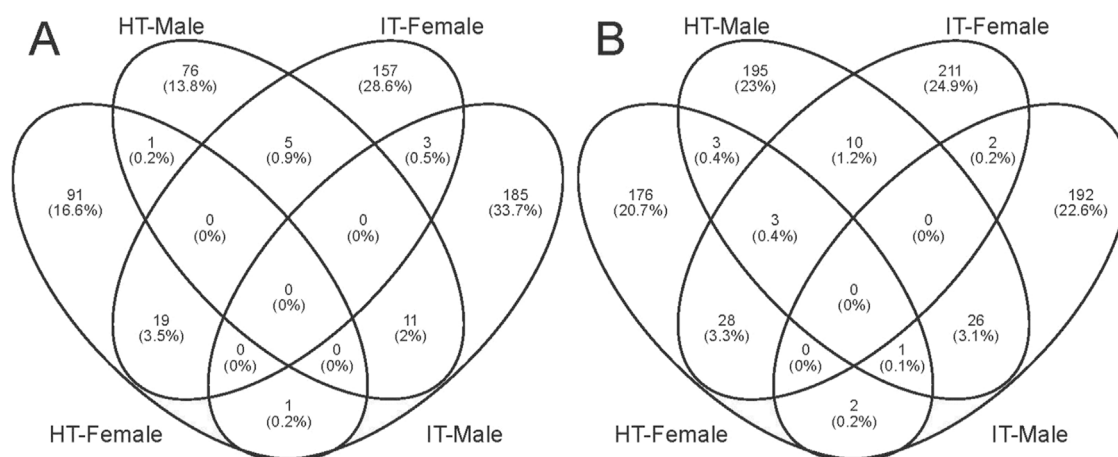


FIGURE 5 Wayne diagrams of differentially expressed genes. (A, B) Wayne diagrams of genes with significant downregulation and upregulation, respectively.

3.4 Expression profile of PlewOBPs after exposure to tobacco

To investigate the expression profile of *PlewOBPs* after exposure to different tobacco volatiles, we carried out qRT-PCR experiments. The results showed that exposure to tobacco volatiles significantly altered the transcript abundance of several *PlewOBPs* (Figure 6). The transcript abundance of three *PlewOBPs* (*PlewOBP2*, 4, and 12) was considerably changed in male adults exposed to *S. litura*-infested tobacco. *PlewOBP2* was the only upregulated gene in this group compared to the blank control. Four *PlewOBPs* (*PlewOBP2*, 6, 11, and 13) displayed significantly higher transcript abundance levels than the healthy tobacco exposure treatment. *PlewOBP4* had reduced transcript abundance in the IT group compared to the HT group. The transcript abundance of 5 *PlewOBPs* (*PlewOBP2*, 4, 7, 8, and 12) was significantly downregulated in female adults exposed to *S. litura*-infested tobacco compared to the blank control.

Compared to the HT group, *PlewOBP2*, 6, 7, and 8 exhibited significantly lower levels of transcript abundance, while *PlewOBP3* showed substantially higher levels of transcript abundance in the IT group. These numerous expressed *PlewOBPs* might be involved in regulating the behavioral activity of *P. lewisi* adults towards tobacco plants. The DREAM technique is the prevalent method for screening OBPs by examining substantial changes in mRNA expression levels upon exposure to odors and various biotic or abiotic factors (Chen et al., 2021). An study has shown that cucurbit chlorotic yellows virus (CCYV) infested *Bemisia tabaci* (Hemiptera: Aleyrodidae) exhibited increased orientation towards the host cucumber plant (He et al., 2023). Transcriptome analysis revealed 429 DEGs (407 upregulated and 22 downregulated) between CCYV-carrying and CCYV-free whitefly adults. Odorant-binding protein 5 (OBP5) was upregulated in CCYV-carrying whiteflies compared to CCYV-free ones and was proved to be involved in odor recognition and host localization. This transcriptional response is likely directly associated with the olfactory capabilities of OBPs, which may also aid insects in host location. In our

study, differentially expressed OBPs between the IT and HT groups may be involved in the recognition progress of herbivore-induced plant volatiles released by *S. litura*-infested tobacco. However, this method is always associated with false positives or false negatives (Koerte et al., 2018). Additional tests, such as RNAi, are supposed to validate the results of this experiment in the future.

Transcription sequencing consistently reveals insights into the molecular mechanisms that regulate several physiological states in insects. For instance, Rinker et al. (2013) showed that the transcript abundance of *A. gambiae* odorant receptors (AgORs) and their excitatory odorant response profiles corresponded with the shift from host-seeking to oviposition behaviors in blood-fed female mosquitoes (Rinker et al., 2013). In contrast, AgOBPs exhibited a more complex pattern of variation, reflecting the multifaceted roles of OBPs, devoid of any apparent regularity. Besides olfactory-related genes, many genes from various signaling pathways also showed significant changes in transcript abundance, such as cytochrome P450 (Mappin et al., 2023). The molecular mechanisms behind the changes in transcript abundance induced by these genes remain unclear. These substances may possess additional physiological relevance for insects, or OBP may exhibit a diminished interaction with other signaling pathways. Nonetheless, our study demonstrates that the alterations in gene transcript abundance resulting from odor exposure are preserved in insects.

In conclusion, both male and female *P. lewisi* demonstrated changes in their transcription profiles when exposed to healthy or *S. litura*-infested tobacco plant odor. The mRNA levels in *P. lewisi* showed a sex-dependent modification after exposure to odor. The mRNA expression profiles differed significantly between male and female adults. Transcription sequencing identified the presence of 15 *PlewOBPs*, and 8 showed significant changes in transcript abundance when exposed to *S. litura*-infested tobacco, compared to the blank control or healthy tobacco. These genes provide novel targets for functional characterization, which may, in turn, lead to the development of tools and strategies for insect behavior regulation.

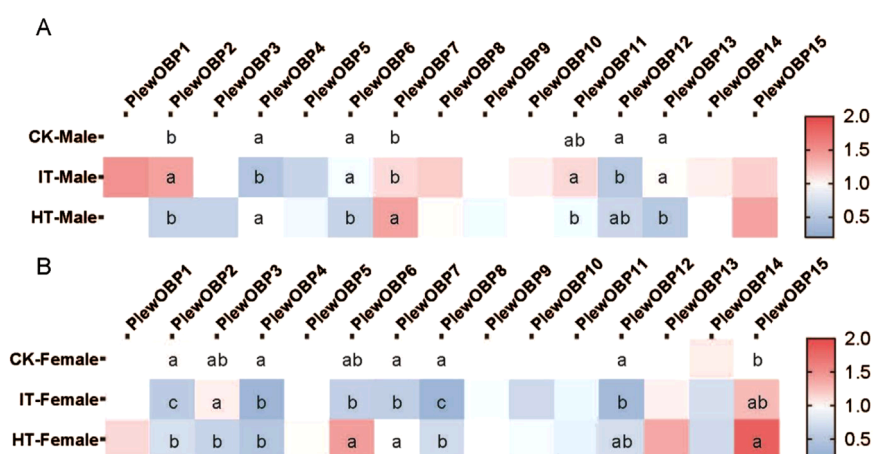


FIGURE 6

Heat map of expression profiles of PlewOBPs after odor exposure treatment. (A, B) The expression levels of PlewOBPs from male and female *Picromerus lewisi*, respectively. The results were analyzed using one-way ANOVA with Tukey's HSD *post hoc* test. The absence of lowercase letter indicates no significant difference.

Data availability statement

The data presented in the study are deposited in the NCBI repository (<https://www.ncbi.nlm.nih.gov/>), accession number SRR31441214.

Ethics statement

The manuscript presents research on animals that do not require ethical approval for their study.

Author contributions

S-CY: Formal Analysis, Investigation, Methodology, Writing—original draft. J-LY: Data curation, Investigation, Writing—original draft. SA: Writing—review and editing. Z-RS: Funding acquisition, Writing—review and editing. M-QW: Conceptualization, Funding acquisition, Project administration, Supervision, Writing—review and editing.

Funding

The author(s) declare that financial support was received for the research, authorship, and/or publication of this article. This work was supported and funded by Southwest Guizhou Autonomous Prefecture Tobacco Company (GJS.01.21-2020).

Conflict of interest

Author Z-RS was employed by Southwest Guizhou Autonomous Prefecture Tobacco Company.

The remaining authors declare that the research was conducted in the absence of any commercial or financial relationships that could be construed as a potential conflict of interest.

Generative AI statement

The author(s) declare that no Generative AI was used in the creation of this manuscript.

Publisher's note

All claims expressed in this article are solely those of the authors and do not necessarily represent those of their affiliated organizations, or those of the publisher, the editors and the reviewers. Any product that may be evaluated in this article, or claim that may be made by its manufacturer, is not guaranteed or endorsed by the publisher.

Author disclaimer

The expression levels of PlewOBPs from male and female *Picromerus lewisi*, respectively. The results were analyzed using one-way ANOVA with Tukey's HSD *post hoc* test. The absence of lowercase letter indicates no significant difference.

Supplementary material

The Supplementary Material for this article can be found online at: <https://www.frontiersin.org/articles/10.3389/fphys.2024.1503440/full#supplementary-material>

References

- Alonso, D. P., Campos, M., Troca, H., Kunii, R., Tripet, F., and Ribolla, P. E. M. (2019). Gene expression profile of *Aedes aegypti* females in courtship and mating. *Sci. Rep.* 9 (1), 15492. doi:10.1038/s41598-019-52268-5
- Andersson, M. N., Videvall, E., Walden, K. K. O., Harris, M. O., Robertson, H. M., and Löfstedt, C. (2014). Sex- and tissue-specific profiles of chemosensory gene expression in a herbivorous gall-inducing fly (Diptera: cecidomyiidae). *BMC Genomics* 15 (1), 501. doi:10.1186/1471-2164-15-501
- Anton, S., and Rössler, W. (2021). Plasticity and modulation of olfactory circuits in insects. *Cell Tissue Res.* 383 (1), 149–164. doi:10.1007/s00441-020-03329-z
- Chen, D., Chen, F., Chen, C., Chen, X., and Mao, Y. (2017). Transcriptome analysis of three cotton pests reveals features of gene expressions in the mesophyll feeder *Apolygus lucorum*. *Sci. China Life Sci.* 60 (8), 826–838. doi:10.1007/s11427-017-9065-3
- Chen, X., Lei, Y., Li, H., Xu, L., Yang, H., Wang, J., et al. (2021). CRISPR/Cas9 mutagenesis abolishes odorant-binding protein BdorOBP56f-2 and impairs the perception of methyl eugenol in *Bactrocera dorsalis* (Hendel). *Insect Biochem. Mol. Biol.* 139, 103656. doi:10.1016/j.ibmb.2021.103656
- De Biasio, F., Riviello, L., Bruno, D., Grimaldi, A., Congiu, T., Sun, Y. F., et al. (2015). Expression pattern analysis of odorant-binding proteins in the pea aphid *Acyrtosiphon pisum*. *Insect Sci.* 22 (2), 220–234. doi:10.1111/1744-7917.12118
- Dong, C., Huang, C., Ning, X., Liu, B., Qiao, X., Qian, W., et al. (2023). Transcriptome analysis used to identify and characterize odorant binding proteins in *Agasicles hygrophila* (Coleoptera: chrysomelidae). *J. Insect Sci.* 23 (5), 16. doi:10.1093/jisesa/iead081
- Duan, S.-G., Liu, A., Wang, C., Zhang, R. L., Lu, J., and Wang, M. Q. (2023). Homeotic protein distal-less regulates NlObp8 and NlCsp10 to impact the recognition of linalool in the Brown planthopper *Nilaparvata lugens*. *J. Agric. Food Chem.* 71 (27), 10291–10303. doi:10.1021/acs.jafc.3c02293
- Farias, L. R., Schimmelpfeng, P. H. C., Togawa, R. C., Costa, M. M. C., Grynberg, P., Martins, N. F., et al. (2015). Transcriptome-based identification of highly similar odorant-binding proteins among neotropical stink bugs and their egg parasitoid. *PLOS ONE* 10 (7), e0132286. doi:10.1371/journal.pone.0132286
- Gadenne, C., Barrozo, R. B., and Anton, S. (2016). Plasticity in insect olfaction: to smell or not to smell? *Annu. Rev. Entomology* 61 (1), 317–333. doi:10.1146/annurev-ento-010715-023523
- Gu, S.-H., Wang, S. P., Zhang, X. Y., Wu, K. M., Guo, Y. Y., Zhou, J. J., et al. (2011). Identification and tissue distribution of odorant binding protein genes in the lucerne plant bug *Adelphocoris lineolatus* (Goeze). *Insect Biochem. Mol. Biol.* 41 (4), 254–263. doi:10.1016/j.ibmb.2011.01.002
- Guerrieri, F., Gemenio, C., Monsempes, C., Anton, S., Jacquin-Joly, E., Lucas, P., et al. (2012). Experience-dependent modulation of antennal sensitivity and input to antennal lobes in male moths (*Spodoptera littoralis*) pre-exposed to sex pheromone. *J. Exp. Biol.* 215 (13), 2334–2341. doi:10.1242/jeb.060988
- Harada, E., Haba, D., Aigaki, T., and Matsuo, T. (2008). Behavioral analyses of mutants for two odorant-binding protein genes, Obp57d and Obp57e, in *Drosophila melanogaster*. *Genes and Genet. Syst.* 83 (3), 257–264. doi:10.1266/ggs.83.257
- Hare, J. D. (2011). Ecological role of volatiles produced by plants in response to damage by herbivorous insects. *Annu. Rev. Entomology* 56 (1), 161–180. doi:10.1146/annurev-ento-120709-144753
- He, F., Gao, Y. W., Ye, Z. X., Huang, H. J., Tian, C. H., Zhang, C. X., et al. (2024). Comparative transcriptomic analysis of salivary glands between the zoophytophagous *Cyrtorhinus lividipennis* and the phytozoophagous *Apolygus lucorum*. *BMC Genomics* 25 (1), 53. doi:10.1186/s12864-023-09956-4
- He, H., Li, J., Zhang, Z., Yan, M., Zhang, B., Zhu, C., et al. (2023). A plant virus enhances odorant-binding protein 5 (OBP5) in the vector whitefly for more actively olfactory orientation to the host plant. *Pest Manag. Sci.* 79 (4), 1410–1419. doi:10.1002/ps.7313
- Howe, G. A., and Jander, G. (2008). Plant immunity to insect herbivores. *Annu. Rev. Plant Biol.* 59 (1), 41–66. doi:10.1146/annurev-arplant.59.032607.092825
- Huang, Y., Hu, W., and Hou, Y.-M. (2023). Host plant recognition by two odorant-binding proteins in *Rhynchophorus ferrugineus* (Coleoptera: Curculionidae). *Pest Manag. Sci.* 79 (11), 4521–4534. doi:10.1002/ps.7654
- Ji, P., Liu, J. T., Zhu, X. Q., Guo, Y. Y., Zhou, J. J., et al. (2013). Identification and expression profile analysis of odorant-binding protein genes in *Apolygus lucorum* (Hemiptera: Miridae). *Appl. Entomology Zoology* 48 (3), 301–311. doi:10.1007/s13355-013-0188-0
- Koerte, S., Keese, I. W., Khallaf, M. A., Cortés Llorca, L., Grosse-Wilde, E., Hansson, B. S., et al. (2018). Evaluation of the DREAM technique for a high-throughput deorphanization of chemosensory receptors in *Drosophila*. *Front. Mol. Neurosci.* 11, 366. doi:10.3389/fnmol.2018.00366
- Leal, W. S. (2013). Odorant reception in insects: roles of receptors, binding proteins, and degrading enzymes. *Annu. Rev. Entomol.* 58 (1), 373–391. doi:10.1146/annurev-ento-120811-153635
- Li, E.-T., Wu, H. J., Qin, J. H., Luo, J., Li, K. B., Cao, Y. Z., et al. (2023a). Involvement of Holotrichia parallel odorant-binding protein 3 in the localization of oviposition sites. *Int. J. Biol. Macromol.* 242, 124744. doi:10.1016/j.ijbiomac.2023.124744
- Li, W., Wang, X., Jiang, P., Yang, M., Li, Z., Huang, C., et al. (2022). A full-length transcriptome and gene expression analysis of three detoxification gene families in a predatory stink bug, *Picromerus lewisii*. *Front. Physiology* 13. doi:10.3389/fphys.2022.1016582
- Li, W., Zou, J., Yang, X., Yang, M., Jiang, P., Wang, X., et al. (2023b). Identification of metabolizing enzyme genes associated with xenobiotics and odorants in the predatory stink bug *Arma custos* based on transcriptome analysis. *Heliyon* 9 (8), e18657. doi:10.1016/j.heliyon.2023.e18657
- Liu, X.-Q., Jiang, H. B., Fan, J. Y., Liu, T. Y., Meng, L. W., Liu, Y., et al. (2021). An odorant-binding protein of Asian citrus psyllid, *Diaphorina citri*, participates in the response of host plant volatiles. *Pest Manag. Sci.* 77 (7), 3068–3079. doi:10.1002/ps.6352
- Manoharan, M., Ng Fuk Chong, M., Vaitinadapoulé, A., Frumence, E., Sowdhamini, R., and Offmann, B. (2013). Comparative genomics of odorant binding proteins in *Anopheles gambiae*, *Aedes aegypti*, and *Culex quinquefasciatus*. *Genome Biol. Evol.* 5 (1), 163–180. doi:10.1093/gbe/evs131
- Mappin, F., Bellantuono, A. J., Ebrahimi, B., and DeGennaro, M. (2023). Odor-evoked transcriptomics of *Aedes aegypti* mosquitoes. *PLOS ONE* 18 (10), e0293018. doi:10.1371/journal.pone.0293018
- Matsuo, T., Sugaya, S., Yasukawa, J., Aigaki, T., and Fuyama, Y. (2007). Odorant-Binding Proteins Obp57d and Obp57e Affect Taste Perception and Host-Plant Preference in *Drosophila sechellia*. *PLOS Biol.* 5 (5), e118. doi:10.1371/journal.pbio.0050118
- Oliveira, D. S., Brito, N. F., Nogueira, F. C. S., Moreira, M. F., Leal, W. S., Soares, M. R., et al. (2017). Proteomic analysis of the kissing bug *Rhodnius prolixus* antenna. *J. Insect Physiology* 100, 108–118. doi:10.1016/j.jinsphys.2017.06.004
- Paoli, M., and Galizia, G. C. (2021). Olfactory coding in honeybees. *Cell Tissue Res.* 383 (1), 35–58. doi:10.1007/s00441-020-03385-5
- Paula, D. P., Togawa, R. C., Costa, M. M. C., Grynberg, P., Martins, N. F., and Andow, D. A. (2016). Identification and expression profile of odorant-binding proteins in *Halyomorpha halys* (Hemiptera: pentatomidae). *Insect Mol. Biol.* 25 (5), 580–594. doi:10.1111/imb.12243
- Pelosi, P., Iovinella, I., Zhu, J., Wang, G., and Dani, F. R. (2018). Beyond chemoreception: diverse tasks of soluble olfactory proteins in insects. *Biol. Rev.* 93 (1), 184–200. doi:10.1111/brv.12339
- Rihani, K., Ferveur, J.-F., and Briand, L. (2021). The 40-year mystery of insect odorant-binding proteins. *Biomolecules* 11 (4), 509. doi:10.3390/biom11040509
- Rinker, D. C., Pitts, R. J., Zhou, X., Suh, E., Rokas, A., and Zwiebel, L. J. (2013). Blood meal-induced changes to antennal transcriptome profiles reveal shifts in odor sensitivities in *Anopheles gambiae*. *Proc. Natl. Acad. Sci.* 110 (20), 8260–8265. doi:10.1073/pnas.1302562110
- Rund, S. S. C., Gentile, J. E., and Duffield, G. E. (2013). Extensive circadian and light regulation of the transcriptome in the malaria mosquito *Anopheles gambiae*. *BMC Genomics* 14 (1), 218. doi:10.1186/1471-2164-14-218
- Siju, K. P., Hill, S. R., Hansson, B. S., and Ignell, R. (2010). Influence of blood meal on the responsiveness of olfactory receptor neurons in antennal sensilla trichodea of the yellow fever mosquito, *Aedes aegypti*. *J. Insect Physiology* 56 (6), 659–665. doi:10.1016/j.jinsphys.2010.02.002
- Sims, C., Birkett, M. A., Oldham, N. J., Stockman, R. A., and Withall, D. M. (2023). Pea aphid odorant-binding protein ApisOBP6 discriminates between aphid sex pheromone components, aphid alarm pheromone and a host plant volatile. *Insect biochem. Mol. Biol.* 162, 104026. doi:10.1016/j.ibmb.2023.104026
- Song, Y.-Q., Song, Z. Y., Dong, J. F., Lv, Q. H., Chen, Q. X., and Sun, H. Z. (2021). Identification and comparative expression analysis of odorant-binding proteins in the reproductive system and antennae of *Aethis dissimilis*. *Sci. Rep.* 11 (1), 13941. doi:10.1038/s41598-021-93423-1
- Song, Y.-Q., Sun, H.-Z., and Du, J. (2018). Identification and tissue distribution of chemosensory protein and odorant binding protein genes in *Tropidothorax elegans* Distant (Hemiptera: Lygaeidae). *Sci. Rep.* 8 (1), 7803. doi:10.1038/s41598-018-26137-6
- Sparks, M. E., Bansal, R., Benoit, J. B., Blackburn, M. B., Chao, H., Chen, M., et al. (2020). Brown marmorated stink bug, *Halyomorpha halys* (Stål), genome: putative underpinnings of polyphagy, insecticide resistance potential and biology of a top worldwide pest. *BMC Genomics* 21 (1), 227. doi:10.1186/s12864-020-6510-7
- Sun, J. S., Xiao, S., and Carlson, J. R. (2018). The diverse small proteins called odorant-binding proteins. *Open Biol.* 8 (12), 180208. doi:10.1098/rsob.180208
- Tallon, A. K., Hill, S. R., and Ignell, R. (2019). Sex and age modulate antennal chemosensory-related genes linked to the onset of host seeking in the yellow-fever mosquito, *Aedes aegypti*. *Sci. Rep.* 9 (1), 43. doi:10.1038/s41598-018-36550-6
- Tunstall, N. E., and Warr, C. G. (2012). “Chemical communication in insects: the peripheral odour coding system of *Drosophila melanogaster*,” in *Sensing in nature*. Editor C. López-Larrea (New York, NY: Springer US), 59–77.

- Vieira, F. G., and Rozas, J. (2011). Comparative genomics of the odorant-binding and chemosensory protein gene families across the arthropoda: origin and evolutionary history of the chemosensory system. *Genome Biol. Evol.* 3, 476–490. doi:10.1093/gbe/evr033
- Vieira, F. G., Sánchez-Gracia, A., and Rozas, J. (2007). Comparative genomic analysis of the odorant-binding protein family in 12 *Drosophila* genomes: purifying selection and birth-and-death evolution. *Genome Biol.* 8 (11), R235. doi:10.1186/gb-2007-8-11-r235
- von der Weid, B., Rossier, D., Lindup, M., Tuberosa, J., Widmer, A., Col, J. D., et al. (2015). Large-scale transcriptional profiling of chemosensory neurons identifies receptor-ligand pairs *in vivo*. *Nat. Neurosci.* 18 (10), 1455–1463. doi:10.1038/nn.4100
- Wang, G.-Y., Zhu, J. L., Zhou, W. W., Liu, S., Khairul, Q. M., Ansari, N. A., et al. (2018). Identification and expression analysis of putative chemoreception genes from *Cyrtorhinus lividipennis* (Hemiptera: Miridae), a key predator of the rice planthoppers in asia. *Environ. Entomol.* 46 (3), 654–662. doi:10.1093/ee/nvx075
- Wang, G.-Y., Zhu, M. F., Jiang, Y. D., Zhou, W. W., Liu, S., Heong, K. L., et al. (2017). Identification of candidate odorant-binding protein and chemosensory protein genes in *Cyrtorhinus lividipennis* (Hemiptera: Miridae), a key predator of the rice planthoppers in asia. *Environ. Entomol.* 46 (3), 654–662. doi:10.1093/ee/nvx075
- Wang, J., Li, D. Z., Min, S. F., Zhou, S. S., and Wang, M. Q. (2014). Analysis of chemosensory gene families in the beetle *Monochamus alternatus* and its parasitoid *Dastarcus helophoroides*. *Comp. Biochem. Physiology Part D Genomics Proteomics* 11, 1–8. doi:10.1016/j.cbd.2014.05.001
- Wang, Q., Zhou, J. J., Liu, J. T., Huang, G. Z., Xu, W. Y., Zhang, Q., et al. (2019). Integrative transcriptomic and genomic analysis of odorant binding proteins and chemosensory proteins in aphids. *Insect Mol. Biol.* 28 (1), 1–22. doi:10.1111/imb.12513
- Wang, S.-N., Shan, S., Yu, G. Y., Wang, H., Dhillon, K. H., Khashaveh, A., et al. (2020). Identification of odorant-binding proteins and functional analysis of antenna-specific AplaOBP1 in the emerald ash borer, *Agrilus planipennis*. *J. Pest Sci.* 93 (2), 853–865. doi:10.1007/s10340-019-01188-4
- Wu, Z., Lin, J., Zhang, H., and Zeng, X. (2016). BdorOBP83a-2 mediates responses of the oriental fruit fly to semiochemicals. *Front. Physiology* 7, 452. doi:10.3389/fphys.2016.00452
- Xiang, D., Abdelnabby, H., and Wang, M.-Q. (2023). Predicted structure of odorant-binding protein 12 from *Monochamus alternatus* (Hope) suggests a mechanism of flexible odorant-binding. *Int. J. Biol. Macromol.* 243, 125152. doi:10.1016/j.ijbiomac.2023.125152
- Xiao, Y., Sun, L., Ma, X. Y., Dong, K., Liu, H. W., Wang, Q., et al. (2017). Identification and characterization of the distinct expression profiles of candidate chemosensory membrane proteins in the antennal transcriptome of *Adelphocoris lineolatus* (Goeze). *Insect Mol. Biol.* 26 (1), 74–91. doi:10.1111/imb.12272
- Xiao, Y., Sun, L., Wang, Q., Zhang, Q., Gu, S. H., Khashaveh, A., et al. (2018). Molecular characterization and expression analysis of putative odorant carrier proteins in *Adelphocoris lineolatus*. *J. Asia-Pacific Entomology* 21 (3), 958–970. doi:10.1016/j.aspen.2018.07.016
- Xu, P. X., Zwiebel, L. J., and Smith, D. P. (2003). Identification of a distinct family of genes encoding atypical odorant-binding proteins in the malaria vector mosquito, *Anopheles gambiae*. *Insect Mol. Biol.* 12 (6), 549–560. doi:10.1046/j.1365-2583.2003.00440.x
- Xue, W., Fan, J., Zhang, Y., Xu, Q., Han, Z., Sun, J., et al. (2016). Identification and expression analysis of candidate odorant-binding protein and chemosensory protein genes by antennal transcriptome of *Sitobion avenae*. *PLOS ONE* 11 (8), e0161839. doi:10.1371/journal.pone.0161839
- Yang, R., Li, D., Yi, S., Wei, Y., and Wang, M. (2024). Odorant-binding protein 19 in *Monochamus alternatus* involved in the recognition of a volatile strongly emitted from ovipositing host pines. *Insect Sci.* 31 (1), 134–146. doi:10.1111/1744-7917.13238
- Yasukawa, J., Tomioka, S., Aigaki, T., and Matsuo, T. (2010). Evolution of expression patterns of two odorant-binding protein genes, Obp57d and Obp57e, in *Drosophila*. *Gene* 467 (1), 25–34. doi:10.1016/j.gene.2010.07.006
- Yi, S.-C., Wu, Y. H., Yang, R. N., Li, D. Z., Abdelnabby, H., and Wang, M. Q. (2023). A highly expressed antennae odorant-binding protein involved in recognition of herbivore-induced plant volatiles in *Dastarcus helophoroides*. *Int. J. Mol. Sci.* 24, 3464. doi:10.3390/ijms24043464
- Yin, J., Wang, C., Fang, C., Zhang, S., Cao, Y., Li, K., et al. (2019). Functional characterization of odorant-binding proteins from the scarab beetle *Holotrichia obliata* based on semiochemical-induced expression alteration and gene silencing. *Insect Biochem. Mol. Biol.* 104, 11–19. doi:10.1016/j.ibmb.2018.11.002
- Yuan, H.-B., Ding, Y. X., Sun, L., Zhu, X. Q., Liu, H. W., et al. (2015). Molecular characterization and expression profiling of odorant-binding proteins in *Apolygus lucorum*. *PLOS ONE* 10 (10), e0140562. doi:10.1371/journal.pone.0140562
- Zhou, J. J., He, X. L., Pickett, J. A., and Field, L. M. (2008). Identification of odorant-binding proteins of the yellow fever mosquito *Aedes aegypti*: genome annotation and comparative analyses. *Insect Mol. Biol.* 17 (2), 147–163. doi:10.1111/j.1365-2583.2007.00789.x
- Zhou, J.-J., Huang, W., Zhang, G. A., Pickett, J. A., and Field, L. M. (2004). “Plus-C” odorant-binding protein genes in two *Drosophila* species and the malaria mosquito *Anopheles gambiae*. *Gene* 327 (1), 117–129. doi:10.1016/j.gene.2003.11.007
- Zhou, J. J., Vieira, F. G., He, X. L., Smadja, C., Liu, R., Rozas, J., et al. (2010). Genome annotation and comparative analyses of the odorant-binding proteins and chemosensory proteins in the pea aphid *Acyrtosiphon pisum*. *Insect Mol. Biol.* 19 (s2), 113–122. doi:10.1111/j.1365-2583.2009.00919.x



OPEN ACCESS

EDITED BY

Marcelo Salabert Gonzalez,
Fluminense Federal University, Brazil

REVIEWED BY

Phillip Obed Yobe Nkunika,
University of Zambia, Zambia
Fernando Ariel Genta,
Oswaldo Cruz Foundation (Fiocruz), Brazil

*CORRESPONDENCE

Sarita Kumar,
✉ saritakumar@andc.du.ac.in

RECEIVED 05 August 2024

ACCEPTED 12 November 2024

PUBLISHED 16 December 2024

CITATION

Sankar M, Yadav D and Kumar S (2024)
Evaluation of diflubenzuron–verapamil
combination strategy for eco-safe
management of *Aedes aegypti*.
Front. Physiol. 15:1476259.
doi: 10.3389/fphys.2024.1476259

COPYRIGHT

© 2024 Sankar, Yadav and Kumar. This is an open-access article distributed under the terms of the [Creative Commons Attribution License \(CC BY\)](#). The use, distribution or reproduction in other forums is permitted, provided the original author(s) and the copyright owner(s) are credited and that the original publication in this journal is cited, in accordance with accepted academic practice. No use, distribution or reproduction is permitted which does not comply with these terms.

Evaluation of diflubenzuron–verapamil combination strategy for eco-safe management of *Aedes aegypti*

Manu Sankar, Divya Yadav and Sarita Kumar*

Department of Zoology, Acharya Narendra Dev College, University of Delhi, New Delhi, India

Introduction: *Aedes aegypti*, the vector of multiple arboviral diseases, is a prime health concern worldwide. The surge in *Aedes*-borne diseases emphasizes the urgent need for efficient vector control measures. Synthetic pesticides used traditionally, however, present environmental concerns and issues like resistance development, causing the use of higher chemical doses. Hence, alternate interventions like the use of insect growth regulators (diflubenzuron; DFB) show promise because of their unique mechanism of action and environmental safety. Nevertheless, mosquitoes have the potential to develop resistance to any chemical. Thus, the present study investigates the use of DFB in combination with verapamil (DFB-V; 1:10) as a possible mosquito intervention measure.

Methods: The effects of both DFB and DFB-V were assessed on the larval development, adult emergence and expression of detoxification enzymes, non-specific esterases, glutathione S-transferase (GST), acetylcholinesterase (AChE), and monooxygenases in laboratory-reared (AND-*Ae. aegypti*) and wild-caught (GVD-*Ae. aegypti*) strains of *Ae. aegypti*. The effects on the survival of non-target organisms were also investigated.

Results: The investigations showed that DFB-V treatment of the *Ae. aegypti* fourth instars caused a 1.16–1.37 fold higher adult emergence suppression than DFB alone, reducing the IE_{50} values. The DFB treatment increased β -esterases, AChE, and monooxygenases but reduced the GST and α -esterase levels. The effects enhanced with the use of DFB-V, causing a significant decrease in α -esterase (7.7-fold) and an increase in monooxygenases (7.8-fold) ($p < 0.05$) in AND-*Ae. aegypti* compared to the wild-caught strain. The variation in enzyme levels in the two strains may be due to the stress caused by insecticides of different chemical natures used in the fields. No negative effects were observed on the non-target organisms—*Gambusia affinis*, *Mesocyclops thermocyclopoides*, and *Paramecium tetraurelia*.

Conclusion: The studies showed the growth regulatory efficacy of DFB and probable role of GST and α -esterases in increasing the effects of DFB when synergized with verapamil. Further, the DFB-V combination did not result in any significant negative effects on the non-target organisms ascertaining its safe use. This is the first report unraveling the effects of the DFB–verapamil combination on the defense mechanism

of *Ae. aegypti*. Further studies may assist in developing focused and eco-safe plans for managing *Ae. aegypti* populations effectively.

KEYWORDS

diflubenzuron, enzyme expression, mosquito management, non-targets, synergism, verapamil

1 Introduction

Aedes aegypti is a cosmopolitan vector transmitting various human arboviral diseases such as dengue, Zika, chikungunya, and yellow fever. Though prevalent worldwide, it is predominant in tropical and subtropical regions, situated between 35°N and 35°S latitudes, because of the favorable climatic conditions of temperature and humidity. Over recent decades, *Aedes*-borne diseases have increased, accounting for severe health hazards and loss of human lives. Among these, dengue fever is the most rapidly spreading illness, spanning a geographic range of Southeast Asia to the United States and Western Pacific nations. As per reports, roughly 70% of the dengue cases have been reported from Asia, presumably because of the favorable climatic conditions (WHO, 2024). The lack of operative vaccines and effective medications against *Aedes*-borne illnesses, except for yellow fever, has made the situation grave. Hence, the only tactic to alleviate these illnesses is managing the *Ae. aegypti* population below the threshold limits by employing various intervention measures in and around human settlements.

The mosquito population has been habitually tackled by eliminating breeding sites, avoiding human-mosquito contact by use of mosquito repellents, and killing various stages of their life cycle via employment of synthetic chemicals in the form of spray, dust, mosquito coils, etc. (Bharati and Saha, 2018). However, the extensive and intermittent usage of these chemicals and the favorable selection of more resilient individuals in natural field populations have resulted in the development of resistance in mosquitoes, aggravating the associated issues (Kumar et al., 2002; 2004; Borase et al., 2013). Apart from these, the harmful effects of these chemicals on the environment and human health have diverted the attention of health workers and vector control programmers towards alternative and relatively safer insecticides. Among these insecticides, insect growth regulators (IGRs), the fourth-generation insecticides, are considered a viable and sustainable option to be used against mosquitoes. They impede the growth and development of insects and reduce reproductive fitness by either inhibiting the synthesis of cuticular or peritrophic matrix chitin or interfering with the endocrine functions in the insects (Doucet and Retnakaran, 2012). Furthermore, these compounds are deemed safe for the environment due to their specificity to the target organisms, posing minimal risks to non-target and beneficial biota (Zibadee et al., 2011).

Diflubenzuron (DFB), also known as dimilin, is a benzoylphenyl urea chitin synthesis inhibitor that obstructs the growth and development of insects. It is a commonly used mosquito larvicide that has been approved by the World Health Organisation due to its efficacy and environmental safety (Sankar and Kumar, 2023). The permitted use of DFB in drinking water at the recommended dosage of ≤ 0.25 mg/L has resulted in its frequent use in mosquito

management programs. Various studies have demonstrated the control potential of diflubenzuron against different species of mosquitoes. These studies have shown that DFB caused effective inhibition of ecdysis in *Aedes* sp. larvae with residual activity (Chen et al., 2008), suppression of the *Culex pipiens* population (Pešić et al., 2022), and successful prevention of the *Anopheles* and *Culex* larval emergence leading to $\sim 80\%$ reduction in larval density (Eltahir et al., 2018).

Nonetheless, mosquitoes possess the capability to develop resistance to different xenobiotics through various mechanisms, such as reduced cuticular penetration of insecticide, increased levels of detoxifying enzymes, and target-site insensitivity (Yao et al., 2017; Karunaratne et al., 2018). The development of DFB resistance has been recognized in *Cx. pipiens* through a variety of mechanisms, evidenced by changes in cuticle thickness, chitin content, and chitin-synthase 1 gene overexpression in the resistant strains (Belinato and Valle, 2015; Porretta et al., 2019; Guz et al., 2020; Lucchesi et al., 2022). In Italy, *Cx. pipiens* strain developed 32.5-fold DFB resistance after 2 years of intensive application, which increased dramatically to 128-fold after another year of application (Grigoraki et al., 2017). The studies revealed the occurrence of I1043M and I1043L mutations in the chitin synthase gene of the resistant population. In addition, the biochemical detoxification of toxins is one of the most significant and rapidly developed mechanisms to provide immunity in insects (Enayati et al., 2005). A few studies have also indicated the possible role of ATP-binding cassette (ABC) transporters in imparting diflubenzuron resistance (Porretta et al., 2008). It has been shown that efflux transporter, P-glycoproteins (P-gps), actively transport toxic molecules out of the cells, reducing the concentrations that reach the target and thus leading to resistance (Epis et al., 2014). One of the inhibitors of P-gp transporters, verapamil, is regarded as a DFB synergist with the potential to reduce the development of DFB resistance in insects (Kang et al., 2016).

Our preliminary studies have shown the considerable efficacy of the diflubenzuron-verapamil combination (DFB-V; 1:10) in enhancing the effects of DFB. The present study aimed to evaluate the effect of diflubenzuron and a diflubenzuron-verapamil combination (1:10) on the adult emergence, total proteins, and levels of detoxification enzymes of early fourth instar larvae of two strains of *Ae. aegypti*; laboratory-reared insecticide-susceptible (AND-*Ae. aegypti*) and wild-caught (GVD-*Ae. aegypti*). The inhibition of adult emergence and titers of different enzymes, glutathione-S transferase, acetylcholinesterase (AChE), non-specific esterases (α and β), and CYP450 monooxygenases, were determined in both the strains after treatments. Along with these, the effects of DFB and DFB-V were also assessed on the non-target organisms: *Gambusia affinis*, *Mesocyclops thermocyclopoides*, and *Paramecium tetraurelia*. These studies ascertain the possible use of verapamil with DFB as a

synergist and could help devise an environmentally friendly strategy in vector control programs.

2 Materials and methods

2.1 Rearing of mosquitoes

The culture of *Ae. aegypti* had been maintained in a well-established rearing laboratory at Acharya Narendra Dev College, New Delhi, India. The mosquitoes were reared under controlled conditions of $28^{\circ}\text{C} \pm 1^{\circ}\text{C}$, $80\% \pm 5\%$ relative humidity, and a 14:10 L:D photo-regime. The larvae were hatched in dechlorinated water taken in enamel trays (15 in \times 15 in) and fed upon a 3:1 (w/w) mixture of dog biscuit and dry yeast powder (Warikoo and Kumar, 2013) for optimal development. Adults were allowed to emerge in the cloth cages containing water-soaked raisins in a Petri dish for feeding (Warikoo and Kumar, 2013). Female adults were provided periodic blood meals from albino rats sourced from the rearing house of the Department of Zoology set up for the purpose. The eggs were gathered on wet Whatman paper strips and hatched in dechlorinated water.

2.2 Chemicals required

The technical-grade diflubenzuron (DFB) with a purity level of 98.0% (CAS No. 35367-38-5) and verapamil with $\geq 99.0\%$ purity (CAS No. 152-11-4) were obtained from Sigma-Aldrich, India.

2.3 Strains of *Ae. aegypti* used for investigations

- Laboratory-reared insecticide-susceptible strain (AND-*Ae. aegypti*): The strain was obtained in 2009 from the International Centre for Genetic Engineering and Biotechnology, New Delhi, India, and maintained in the laboratory without the selection pressure of any insecticide.
- Govindpuri strain of *Ae. aegypti* (GVD-*Ae. aegypti*): Larvae were collected from the fields of the Govindpuri locality of Southeast Delhi, India (28.534°N , 77.265°E) and brought to the laboratory for investigations.

2.4 Adult emergence inhibition studies with diflubenzuron and diflubenzuron-verapamil combination (DFB-V)

The adult emergence inhibition potential of DFB and DFB-V was estimated in accordance with the WHO protocol (WHO, 2005). The combination of DFB-verapamil was prepared in a 1:10 ratio selected after preliminary investigations. The early fourth instar larvae of *Ae. aegypti* were treated with a series of DFB/DFB-V concentrations ranging from $0.0625 \mu\text{g/L}$ to $16 \mu\text{g/L}$ for 24 h in three replicates. In each replicate, a total of 20 larvae were treated with a homogenous mixture of 1 mL of a specific concentration of

DFB/DFB-V and 199 mL of distilled water. The surviving larvae were reared to record the adult emergence. Control sets were run simultaneously. The percent inhibition of adult emergence (IE%) was calculated as follows (Equation 1):

$$\text{IE\%} = 100 - \left\{ \frac{\text{TX}100}{\text{C}} \right\} \quad (1)$$

where T represents the percentage of adult emergence in treated sets, and C represents the percentage of adult emergence in the control set. The data were subjected to probit mortality-regression analysis by the SPSS 19.0 program, and IE_{50} dosages of diflubenzuron were computed along with other statistical parameters.

The synergistic potential of verapamil was calculated as per the formula (Equation 2) given below:

$$\text{Synergistic factor (SF)} = \frac{\text{IE}_{50} \text{ dosage of DFB alone}}{\text{IE}_{50} \text{ dosage of DFB-Verapamil}} \quad (2)$$

2.5 Biochemical characterization of detoxification enzymes

A total of fifty (50) early fourth instars of both the strains of *Ae. aegypti* were treated with the diflubenzuron alone and synergized DFB (DFB-V) at respective IE_{50} dosages. Twenty surviving larvae were randomly selected after 24 h of treatment and biochemically characterized for proteins and detoxifying enzymes using the standard WHO methodology (WHO, 1998), with a few modifications (Kona et al., 2018). Concurrent control assays were carried out.

2.5.1 Preparation of larval homogenate

Individually treated larva of each strain was homogenized in 200 μL of ice-cold autoclaved water, using a mini-homogenizer. Each larval homogenate was centrifuged at 4°C for 30 s at $17,000 \times g$. The supernatant was used to estimate proteins, glutathione S-transferase (GST), CYP450 monooxygenases, and non-specific esterases (α -esterases and β -esterases). The quantification of acetylcholinesterase was performed using the crude homogenate. The assays were conducted in three replicates. Each replicate consisted of 20 larvae, and each replicate was assayed twice.

2.5.2 Total proteins

Protein estimation in larvae of both the strains of *Ae. aegypti* treated with DFB or DFB-V was carried out using Bradford's (1976) methodology. The supernatant from each treatment (10 μL) was pipetted into a microtiter plate to which 300 μL of the Bio-Rad protein reagent was added. The homogenate was replaced in blank and standard with water and bovine serum albumin (BSA), respectively. After incubation for 5 min, the plate was read at 570 nm using an ELISA plate reader. The protein standard curve was plotted, and the total proteins in the larva were determined in mg/mL.

2.5.3 GST activity

A mixture of 50 μL of 2 mM GSH (reduced glutathione) and 50 μL of 1 mM CDNB (1-chloro-2,4-dinitrobenzene) was taken in a microtiter plate and supplemented with the 20 μL of the

larval homogenate supernatant. The absorbance was measured at 340 nm every minute for continuous 5 minutes (Brogden and Barber, 1990). The enzyme kinetics were computed, and GST activity was calculated as mol/min/mg of protein.

2.5.4 Non-specific esterase titers

10 μ L of the homogenate supernatant of *Ae. aegypti* larvae after each treatment was taken in a microtiter plate and mixed with 200 μ L of 3 mM solution of either α -naphthyl acetate or β -naphthyl acetate for respective α -esterase and β -esterase quantification. Subsequent to incubation for 15 min, a volume of 50 μ L of freshly made 6.3 mM fast blue stain solution was added to each, which resulted in the color change. The absorbance was recorded at 570 nm (Brogden and Dickinson, 1983), and the esterase activity was calculated as nmol of naphthol/min/mg of protein. The standards for calculating α -esterase and β -esterase activity were run with corresponding α -naphthol or β -naphthol.

2.5.5 CYP450 monooxygenase levels

A 20 μ L aliquot of the larval homogenate supernatant was taken in a microtiter plate and mixed with 80 μ L of 0.625 M potassium phosphate buffer (pH 7.2). It was then added to 200 μ L of a solution that contained one part of 0.25 M sodium acetate buffer (pH 5.0) and three parts of 8 mM methanolic solution of tetramethyl benzidine (TMBZ). Subsequently, 25 μ L of 0.88 M hydrogen peroxide was added to it, and absorbance was measured at 650 nm after incubation for 10–15 min at ambient temperature. The monooxygenase activity was expressed as mmol/mg of protein.

2.5.6 Inhibition in AChE activity

Two replicates of 25 μ L of the crude larval homogenate, placed in the microtiter plate, were supplemented with 145 μ L of 0.017 M Triton X-100 and 10 μ L of 0.01 M dithiobis 2-nitrobenzoic acid (DTNB). One replicate was mixed with 25 μ L of 0.01 M acetylthiocholine iodide (ASCHI), while the other was supplemented with 25 μ L of 0.01 M ASCHI + 0.1 M propoxur (500:1). The absorbance was measured at 405 nm after an incubation period of 1 h (Brogden and Barber, 1987).

The endpoint of the reaction was computed by dividing the AChE+propoxur activity by the AChE alone activity. The percent inhibition of acetylcholinesterase was calculated by the formula $[100 - (100\% \times \text{Endpoint})]$.

2.5.7 Statistical analysis

The Kolmogorov–Smirnov tests using SPSS 19 software were performed to check the normality of enzyme activities. The data obtained with different treatments were statistically analyzed by ANOVA (single-way variance analysis). Tukey's all-pairwise multiple comparison test was used to compare the means to determine the statistical significance of data at $p < 0.05$.

2.6 Effect on non-target organisms

Three non-target organisms, *G. affinis*, *M. thermocyclopoides*, and *P. tetraurelia*, were collected from pond water in the South Delhi region of India. Care was taken to collect the active organisms in good health and of similar size. Each organism was treated with

respective IE_{50} dosages of DFB and DFB-V for 24 h computed against *Ae. aegypti* fourth instar larvae. The organisms were added to a mixture of 249 mL of water and 1 mL of treatment dosage. *G. affinis* were treated in groups of 5, while *M. thermocyclopoides* and *P. tetraurelia* were treated in groups of 20 each. The effect of treatment was observed on the survival and morphological alteration of each organism. Each assay was carried out in three replicates. The control sets were run in parallel.

3 Results

3.1 Adult emergence inhibition studies

The adult emergence inhibition studies with DFB and DFB-V (1:10) against *Ae. aegypti* larvae showed dose-dependent efficacy; enhanced effects were obtained with DFB-V (Table 1; Figures 1, 2). Treatment of the *Ae. aegypti* fourth instars with DFB suppressed the adult emergence by 9.1%–100% with complete suppression at 16.0 μ g/L, while DFB-V could inhibit the emergence completely at 8.0 μ g/L. The DFB-V caused 1.16 and 1.37-fold higher suppression in laboratory-reared and wild-caught strains, respectively, than only DFB.

3.2 Total protein reserves

The larvae of AND-*Ae. aegypti* had 2.44-fold ($p < 0.05$) higher protein content compared to the larvae of GVD-*Ae. aegypti* strain. The larval treatment with IE_{50} dosages of DFB caused insignificant changes in the protein content by 1.02-fold ($p > 0.05$) and 1.06-fold ($p > 0.05$), respectively. However, treatment with an IE_{50} dose of DFB-V significantly reduced the total protein content in both laboratory-reared and wild-caught strains by 2.25-fold ($p < 0.05$) compared to the control. The respective reductions were, however, 2.29-fold and 2.16-fold ($p < 0.05$) when compared to the DFB-treated larvae (Table 2). Note that the wild-caught strains had significantly lower levels of proteins than the laboratory strain, irrespective of the treatment.

3.3 GST activity

The total and specific GST activity was found to be significantly reduced in wild-caught larvae compared to the laboratory-reared larvae, whether untreated or treated (Tables 3–6). Treatment of AND-*Ae. aegypti* larvae with DFB and DFB-V showed significant 1.52-fold and 2.64-fold ($p < 0.05$) decreases in GST activity compared to the control group (Tables 3, 4; Figure 3A), while higher reductions of 3.98-fold and 6.94-fold ($p < 0.05$) were observed in the GVD-*Ae. aegypti* (Tables 5, 6; Figure 3A).

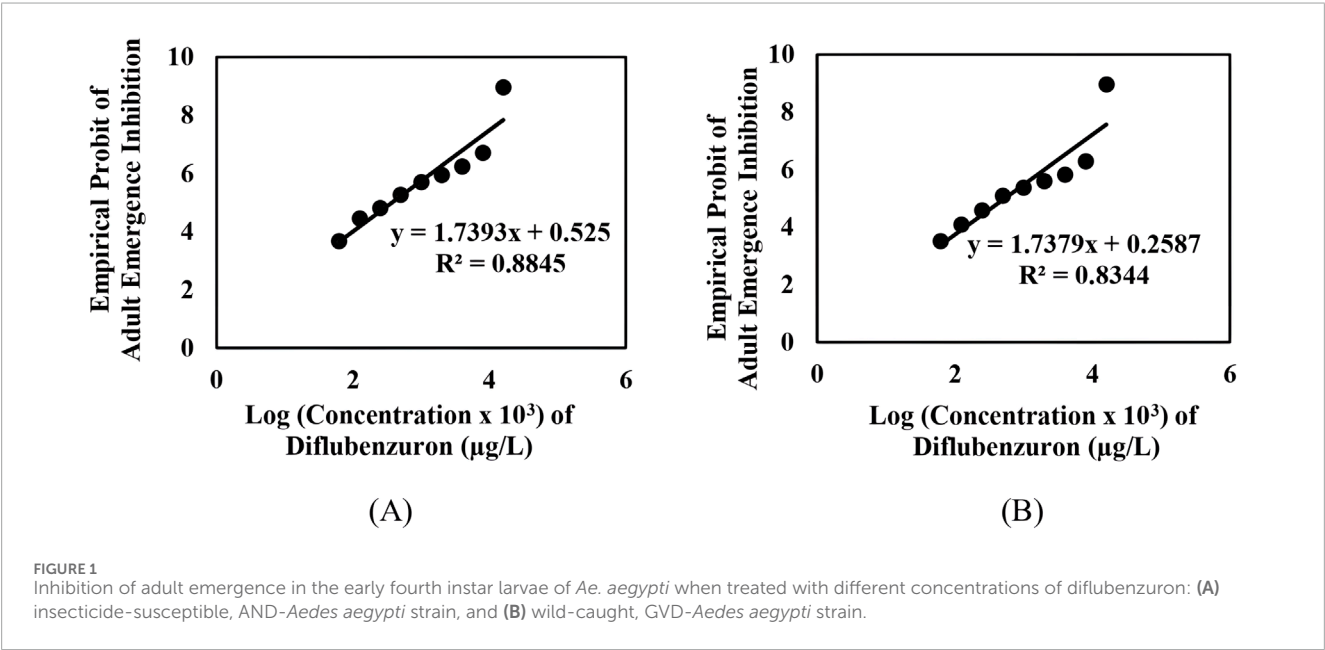
3.4 α -esterase activity

The laboratory-reared susceptible strain (AND-*Ae. aegypti*) larvae showed a significant ($p < 0.05$) drop of 2.16-fold in α -esterase activity when exposed to diflubenzuron (Tables 3, 4). The activity

TABLE 1 Inhibition of adult emergence from the early fourth instar larvae of *Aedes aegypti* treated with diflubenzuron and diflubenzuron-verapamil (1:10).

Treatment	IE ₅₀ concentration (µg/L) ± SEM	Slope ± SEM	χ ² (df)	p value	Synergistic factor (SF)
AND- <i>Ae. aegypti</i>					
Diflubenzuron alone	0.37 ± 0.0017 (0.31–0.45)	1.739 ± 0.865	5.576 (6)	0.472	1.156
Diflubenzuron - verapamil (1:10)	0.32 ± 0.0288 (0.27–0.38)	2.131 ± 0.103	3.739 (5)	0.558	
GVD- <i>Ae. aegypti</i>					
Diflubenzuron alone	0.63 ± 0.0230 (0.52–0.75)	1.737 ± 0.807	7.728 (6)	0.296	1.369
Diflubenzuron - verapamil (1:10)	0.46 ± 0.0230 (0.38–0.54)	2.192 ± 0.994	4.858 (5)	0.433	

IE values computed by probit mortality-regression analysis using SPSS v. 19 software. SEM: Standard error of the mean. IE₅₀ = the concentrations that inhibit 50% of adult emergence. χ² = chi-square. df = degree of freedom.



further reduced to a pronounced 7.70-fold ($p < 0.05$) on treatment with the DFB-V compared to the control group (Figure 3B). On the other hand, the wild-caught strain, which had 4.08-fold higher α -esterase activities than the laboratory strain, showed a comparatively smaller reduction of 1.2-fold ($p < 0.05$) on treatment with DFB alone and a decrease of 1.49-fold ($p < 0.05$) on treatment with DFB-V (Tables 5, 6).

3.5 β -esterase activity

Notably, a contrasting augmented effect was observed on the activity of β -esterase in both the tested strains of *Ae. aegypti*. The AND-*Ae. aegypti* larvae showed almost similar activity of 1.04-fold ($p > 0.05$), while an increase of 1.62-fold ($p < 0.05$) in β -esterase activity was found when they were treated with DFB and DFB-V, respectively (Tables 3, 4; Figure 3C). However, the GVD-*Ae. aegypti*

strain exhibited almost similar β -esterase activity of 1.03-fold ($p > 0.05$) on DFB treatment but a significant rise of 1.67-fold ($p < 0.05$) on DFB-V treatment. Like α -esterase and β -esterase levels were higher in the wild-caught strain than in the susceptible strain.

3.6 Percentage acetylcholinesterase inhibition

The control population of the wild-caught strain of *Ae. aegypti* showed a much higher percentage AChE inhibition than the susceptible strain. The inhibition of AChE activity however, decreased in both strains on larval treatment with DFB and DFB-V (Figure 3D). The AND-*Ae. aegypti* larvae showed a 1.11% and 1.54% ($p > 0.05$) decreased AChE inhibition with DFB and DFB-V treatment (Tables 3, 4). The percentage reductions recorded in

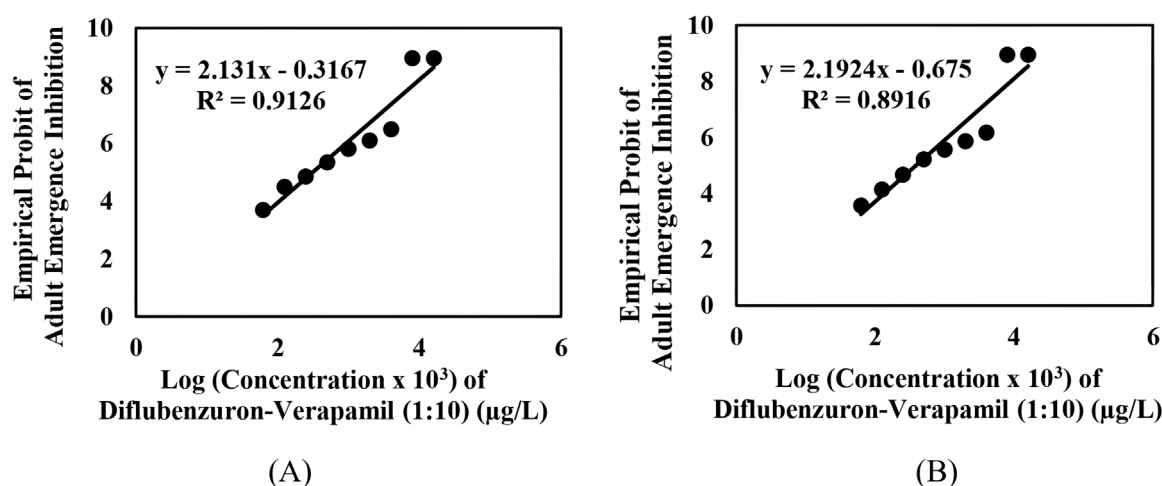


FIGURE 2

Inhibition of adult emergence in the early fourth instars of *Aedes aegypti* treated with different concentrations of diflubenzuron-verapamil (1:10): (A) insecticide-susceptible, AND-*Ae. aegypti* strain, and (B) wild-caught, GVD-*Ae. aegypti* strain.

TABLE 2 Protein content in early fourth instar larvae of *Aedes aegypti* treated with IE_{50} dose of diflubenzuron (DFB) and diflubenzuron + verapamil (DFB-V) (1:10) for 24 h.

Strains of <i>Ae. aegypti</i>	Protein content in early fourth instar larvae of <i>Ae. aegypti</i> \pm SEM (mg/mL)		
	Control	Treatment with DFB at IE_{50} dosage (0.37 μ g/L)	Treatment with DFB-V (1:10) at IE_{50} dosage (0.32 μ g/L)
Insecticide-susceptible strain (AND- <i>Ae. aegypti</i>)	5.265 \pm 0.050 ^a	5.361 \pm 0.141 ^a (+1.02)	2.337 \pm 0.123 ^b (−2.25)
Wild-caught strain (GVD- <i>Ae. aegypti</i>)	2.162 \pm 0.083 ^{a#}	2.294 \pm 0.079 ^{a#} (+1.06)	0.962 \pm 0.060 ^{b#} (−2.25)

IE_{50} refers to the concentration that inhibits 50% of adult emergence. Values with different letters in each row and different symbols in each column are significantly different ($p < 0.05$), one-way ANOVA, followed by Tukey's all-pairwise multiple comparison tests. Values in brackets refer to fold change from respective control. SEM: standard error of the mean.

GVD-*Ae. aegypti* larvae were 1.06% and 1.26% on treatment with DFB and DFB-V ($p < 0.05$), respectively.

not impart any negative effects on their survival, morphology, and behavior.

3.7 CYP450 monooxygenases

Like esterases, the CYP450 levels were higher in GVD-*Ae. aegypti* larvae than the insecticide-susceptible larvae. The respective treatment of AND-*Ae. aegypti* larvae with DFB and DFB-V registered 1.33-fold reduced but 7.8-fold ($p < 0.05$) enhanced CYP450 monooxygenase activity (Tables 3, 4; Figure 3E). On the other hand, the GVD-*Ae. aegypti* strain exhibited a 1.08-fold ($p > 0.05$) and 8.00-fold ($p < 0.05$) increase in CYP450 activity by respective DFB and DFB-V treatment (Tables 5, 6).

3.8 Effect on non-target organisms

The treatment of non-target organisms, *G. affinis*, *M. thermocyclopoides*, and *P. tetraurelia*, with the respective IE_{50} values of DFB or DFB-V obtained for *Ae. aegypti* early fourth instar did

4 Discussion

The present study was an attempt to examine the possible use of verapamil along with DFB to increase its efficiency against *Ae. aegypti*. The potential of DFB alone as well as in combination with verapamil (1:10) was assessed on the adult emergence and detoxification enzymes of *Ae. aegypti* larvae. The effect was assessed against two strains of dengue vector: a wild-caught GVD-*Ae. aegypti* strain and an insecticide-susceptible AND-*Aedes aegypti* strain maintained in the laboratory to understand their defense system. The compounds were also evaluated on common non-target species.

The larval treatment with DFB significantly inhibited adult emergence in both strains of *Ae. aegypti*. Enhanced inhibition in the adult emergence was obtained with the use of DFB-verapamil (1:10), which indicates the synergistic effect of verapamil on DFB and the plausible use of the mixture to control a mosquito population.

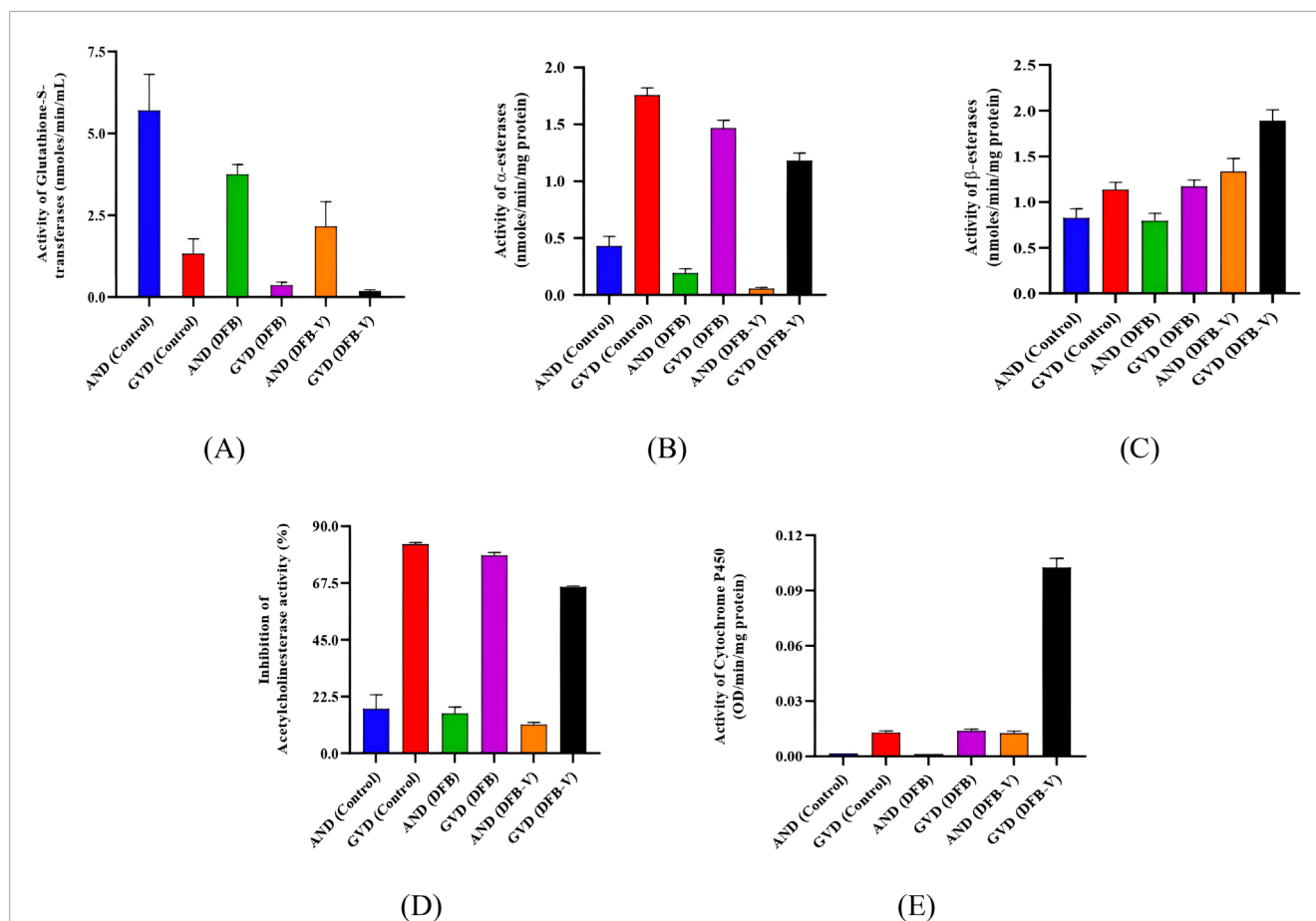


FIGURE 3

Specific activity of various detoxifying enzymes in the early fourth instars of AND-Ae. aegypti and GVD-Ae. aegypti strain of Ae. aegypti on exposure to IE₅₀ of diflubenzuron and diflubenzuron-verapamil (1:10). (A) Glutathione S-transferase activity, (B) α-esterase activity, (C) β-esterase activity, (D) percentage acetylcholinesterase inhibition, and (E) CYP450 activity. AND = AND-Ae. aegypti strain, GVD = GVD-Ae. aegypti strain, DFB = Treatment with diflubenzuron, DFB-V = Treatment with diflubenzuron and verapamil (1:10).

The results also showed higher inhibitory effects of DFB and DFB-V against the laboratory-reared susceptible strain compared to the wild-caught strain. This effect may possibly be due to the frequent and indiscriminate use of DFB and other toxicants in the fields, leading to the probable development of some extent of resistance. Furthermore, the higher effects of DFB-V against wild-caught larvae indicated higher synergism and the potential to reduce larval resistance. This could be helpful in managing DFB resistance in the field strains of Ae. aegypti and increasing DFB toxicity. The efficacy of DFB against Ae. aegypti has been demonstrated by Fansiri et al. (2022), who obtained an IE₅₀ value of 2.41 µg/L, which is much higher than that obtained in the present study. Toxicity estimation of DFB against Anopheles quadrimaculatus revealed 86.7% larval mortality at 12.5 µg/L (Zhu et al., 2007). The literature, however, reports limited studies that signify the use of verapamil as a synergist of DFB. Porretta et al. (2008) reported efficient synergism of DFB with verapamil against Ae. caspius, causing a reduction in the LD₅₀ value of diflubenzuron by 16.4-fold. Higher synergism obtained in the study may be ascribed to the variation in species, geographical location, and DFB resistance level of the strain.

The aberrant growth and development caused by exposure to a xenobiotic has been attributed to the altered levels and metabolism of various biochemical constituents present in an organism (Rodríguez-Ortega et al., 2003). The titer of major nutrients, such as proteins, carbohydrates, and fats, essential for an organism's growth, development, and physiological functions is a good indicator of the metabolic state of organisms (Zhu et al., 2012). The present study estimated the protein levels in the larvae of Ae. aegypti treated with DFB/DFB-V to correlate them with the detoxifying enzyme levels.

The results revealed an insignificant increase in total protein in Ae. aegypti larvae on treatment with IE₅₀ of diflubenzuron, which reduced significantly on DFB-V treatment. This suggests the potential of the verapamil-DFB combination to cause metabolic disruption that likely hindered the larvae's growth and development. Furthermore, lower protein content in the larvae of the wild-caught strain than the laboratory strain may be due to continual exposure stress of chemicals in the fields. It has been suggested that DFB treatment can cause a decrease in total proteins due to increased biodegradation rates of proteins (Muthusamy et al., 2011), decreased

TABLE 3 Total activity of detoxifying enzymes in the early fourth instar larvae of the insecticide-susceptible strain of *Aedes aegypti* (AND-*Ae. aegypti*) treated with IE_{50} dosage of diflubenzuron (DFB) and diflubenzuron + verapamil (DFB-V) (1:10) for 24 h.

Treatment	Total activity of detoxifying enzymes			
	Glutathione S-transferase (nmol \pm SEM)	α -esterase (mmol \pm SEM)	β -esterase (mmol \pm SEM)	Acetylcholinesterase (OD \pm SEM)
Control	0.950 \pm 0.189 ^a	0.023 \pm 0.005 ^a	0.044 \pm 0.006 ^a	0.824 \pm 0.056 ^a
DFB alone	0.625 \pm 0.047 ^b	0.010 \pm 0.002 ^b	0.043 \pm 0.005 ^a	0.841 \pm 0.024 ^a
DFB-V	0.360 \pm 0.097 ^c	0.001 \pm 0.001 ^c	0.031 \pm 0.002 ^b	0.885 \pm 0.008 ^a

Data represent the mean activity in 60 larvae (three replicates of 20 larvae each); SEM: standard error of the mean; IE_{50} refers to the concentration that inhibits 50% of adult emergence. Values with different letters in each column are significantly different ($p < 0.05$), one-way ANOVA, followed by Tukey's all-pairwise multiple comparison tests.

TABLE 4 Specific activity of detoxifying enzymes in the early fourth instar larvae of the insecticide-susceptible strain of *Aedes aegypti* (AND-*Ae. aegypti*) treated with IE_{50} dosage of diflubenzuron (DFB) and diflubenzuron + verapamil (DFB-V) (1:10) for 24 h.

Treatment	Specific activity of detoxifying enzymes			
	Glutathione S-transferase (nmol/min/mL \pm SEM)	α -esterase (nmol/min/mg protein \pm SEM)	β -esterase (nmol/min/mg protein \pm SEM)	Acetylcholinesterase (% inhibition \pm SEM)
Control	5.703 \pm 1.103 ^a	0.431 \pm 0.088 ^a	0.826 \pm 0.099 ^a	17.629 \pm 5.260 ^a
DFB alone	3.750 \pm 0.297 ^b	0.200 \pm 0.033 ^b	0.794 \pm 0.083 ^a	15.878 \pm 2.478 ^a
DFB-V	2.161 \pm 0.754 ^c	1.469 \pm 0.066 ^b	1.334 \pm 0.143 ^b	11.456 \pm 0.769 ^a

Data represent the mean activity in 60 larvae (three replicates of 20 larvae each); SEM: standard error of the mean; IE_{50} refers to the concentration that inhibits 50% of adult emergence. Values with different letters in each column are significantly different ($p < 0.05$), one-way ANOVA, followed by Tukey's all-pairwise multiple comparison tests.

TABLE 5 Total activity of detoxifying enzymes in the early fourth instar larvae of the wild-caught strain of *Aedes aegypti* (GVD-*Ae. aegypti*) treated with IE_{50} dosage of diflubenzuron (DFB) and diflubenzuron + verapamil (DFB-V) (1:10) for 24 h.

Treatment	Total activity of detoxifying enzymes				
	Glutathione S-transferase (nmol \pm SEM)	α -esterase (mmol \pm SEM)	β -esterase (mmol \pm SEM)	Acetylcholinesterase (OD \pm SEM)	Cytochrome P450 (mmol \pm SEM)
Control	0.221 \pm 0.055 ^a	0.038 \pm 0.002 ^a	0.013 \pm 0.002 ^a	0.171 \pm 0.007 ^a	0.311 \pm 0.039 ^a
DFB alone	0.062 \pm 0.014 ^b	0.034 \pm 0.002 ^b	0.040 \pm 0.003 ^a	0.215 \pm 0.011 ^b	0.348 \pm 0.030 ^a
DFB-V	0.032 \pm 0.005 ^c	0.011 \pm 0.001 ^c	0.018 \pm 0.001 ^b	0.341 \pm 0.004 ^c	1.076 \pm 0.07 ^b

Data represent mean activity in 60 larvae (three replicates of 20 larvae each); SEM: standard error of the mean; IE_{50} refers to the concentration that inhibits 50% of adult emergence. Values with different letters in each column are significantly different ($p < 0.05$), one-way ANOVA, followed by Tukey's all-pairwise multiple comparison tests.

TABLE 6 Specific activity of detoxifying enzymes in the early fourth instar larvae of the wild-caught strain of *Aedes aegypti* (GVD-*Aedes aegypti*) treated with IE_{50} dosage of diflubenzuron (DFB) and diflubenzuron + verapamil (DFB-V) (1:10) for 24 h.

Treatment	Specific activity of detoxifying enzymes				
	Glutathione S-transferase (nmol/min/mL \pm SEM)	α -esterase (nmol/min/mg protein \pm SEM)	β -esterase (nmol/min/mg protein \pm SEM)	Acetylcholinesterase (% inhibition \pm SEM)	Cytochrome P450 (OD/min/mg protein \pm SEM)
Control	1.325 \pm 0.458 ^a	1.758 \pm 0.063 ^a	1.135 \pm 0.081 ^a	82.898 \pm 0.677 ^a	0.013 \pm 0.001 ^a
DFB alone	0.369 \pm 0.087 ^b	1.469 \pm 0.066 ^b	1.171 \pm 0.070 ^a	78.465 \pm 1.113 ^b	0.014 \pm 0.001 ^a
DFB-V	0.191 \pm 0.033 ^c	1.182 \pm 0.066 ^c	1.891 \pm 0.117 ^b	65.951 \pm 0.402 ^c	0.102 \pm 0.005 ^b

Data represent mean activity in 60 larvae (three replicates of 20 larvae each); SEM: standard error of the mean; IE_{50} refers to the concentration that inhibits 50% of adult emergence. Values with different letters in each column are significantly different ($p < 0.05$), one-way ANOVA, followed by Tukey's all-pairwise multiple comparison tests.

enzyme activity, inhibited DNA synthesis (Hamouda, 2002), or DNA damage that shuts down essential genes responsible for protein production (El-Bermawy and Abulyazid, 1998).

Studies exploring the effects of DFB and DFB-V on the protein reserves of mosquitoes are not available in the literature. However, other IGRs have been tested against different insects, resulting in altered protein levels. Sublethal concentrations of lufenuron have reduced protein levels in *Ae. aegypti* (Panmei et al., 2021), *Pectinophora gossypiella* (Ahmed et al., 2012), and *Glyphodes pyloalis* (Piri Aliabadi et al., 2016). Likewise, inhibition of the protein content was recorded in the hemolymph of the fifth instar nymphs of *Schistocerca gregaria* when treated with three IGRs: pyriproxyfen, tebufenozide, and lufenuron (Ghoneim et al., 2012). In contrast, Linvy et al. (2018) found that application of methoxyfenozide (0.005–1 µg/5 µL acetone) significantly increased the total proteins in the hemolymph of *Spodoptera mauritia* larvae. The contrasting results could be due to variations in the IGR potency, sensitivity of species, immune system, or the treated developmental stage (Ghoneim et al., 2003).

Because all organisms have a defense mechanism to combat external stress by altering the expression of detoxification enzymes, the estimation of the activity of these enzymes becomes crucial to assess the capability of mosquitoes to bear this stress and perform normal physiological functions (Li and Liu, 2007). Hence, DFB- and DFB-verapamil-treated *Ae. aegypti* larvae were evaluated for the detoxification enzymes' activities. The investigations showed variably increased activities of a few enzymes (β-esterases, CYP450), higher activity of AChE due to decreased inhibition, but a decrease in α-esterase and GST activities in *Ae. aegypti* larvae post-treatment. A higher impact on enzyme activity was observed with DFB-V than DFB alone and on the wild-caught larvae compared to the susceptible strain. It is suggested that higher tolerance to DFB and higher alterations in the enzyme levels of wild-caught strains may be caused by the changes in the activity of detoxifying enzymes already induced by the stress caused by other chemicals applied in the fields.

The present investigations showed the probable involvement of β-esterases, AChE, and CYP450 in detoxifying DFB. These observations are aligned with the reports of Anwar and Abd El-Mageed (2005), who found that diflubenzuron increased β-esterase activity in cotton leafworms, *Spodoptera littoralis*, while decreasing α-esterase activity. In contrast, Hamdy and Azab (2002) found that chlorfluazuron and hexaflumuron increased α-esterase enzyme activity in *S. littoralis* while decreasing β-esterase enzyme levels. However, increased levels of both non-specific esterases have been reported in *Ae. aegypti* after lufenuron treatment (Panmei et al., 2021) and in *Spodoptera litura* after methoxyfenozide treatment (Wang et al., 2009). Suppressed esterase levels have been observed in *S. litura* on exposure to the sublethal doses of lufenuron, tebufenozide, and flufenoxuron (Bakr et al., 2013; Ismail, 2020).

The significant decrease in the GST activity in both the AND-*Ae. aegypti* and GVD-*Ae. aegypti* strains on treatment with diflubenzuron and its synergized form indicates its non-involvement in detoxification of DFB. These results are in accordance with the studies performed in *S. littoralis* larvae exposed to lufenuron and chlorfluazuron (Abou-Taleb et al., 2015). They reported 38.6% and 45.6% suppressed GST activity in the larvae on

respective treatment with 0.28 ppm and 0.62 ppm lufenuron. On the other hand, Panmei et al. (2021) showed a noticeable rise in GST activity in *Ae. aegypti* treated with lufenuron, indicating its possible role in lufenuron detoxification.

Unlike GST activity, 24 h of treatment with diflubenzuron increased CYP450 activity in the *Ae. aegypti* larvae of both the investigated strains, suggesting an effective and instant activation of the detoxification mechanism. In addition, decreased percentage inhibition of AChE in the treated larvae with respect to the control indicates the probable role of AChE in DFB detoxification. Similar observations have been recorded by Panmei et al. (2021) on lufenuron treatment of *Ae. aegypti* larvae, revealing a decreased percentage AChE inhibition and a rise in CYP450 levels. A similar rise in monooxygenases has been shown in *Lucilia cuprina*, the blowfly, on DFB exposure (Kotze et al., 1997). In contrast, lufenuron treatment (at LC₂₅ level) increased the percentage AChE inhibition in *S. littoralis* larvae (Ismail, 2020). It is apparent that the lufenuron toxicity in *Ae. aegypti* larvae plausibly blocked the action potential in the neurons, leading to AChE inhibition.

The present results have shown that DFB alone or in combination with verapamil at IE₅₀ values did not affect the survival of non-target organisms, *G. affinis*, *M. thermocyclopoides*, and *P. tetraurelia*. Numerous reports have suggested the safe use of DFB in the environment being non-toxic to non-target organisms, though a few studies have reported their toxic effects on fishes and invertebrates during acute and chronic exposures (Farlow et al., 1978; Abe et al., 2019; Moe et al., 2019). The impact assessment of DFB against aquatic insects—*Corixa punctata* and *Notonecta glauca*—and crustaceans—*Anisops sardea*, *Plea minutissima*, and *Daphnia magna*—revealed significant toxic effects on *C. punctata* and medium toxic effects on the rest (Seeradj et al., 2022). The toxic effects of DFB, however, depend upon the exposure duration, dosage used, and sensitivity of organisms.

The present study demonstrated the efficacy of DFB against laboratory and field strains of *Ae. aegypti* at very low dosages (0.37 µg/L; 0.63 µg/L), which were further reduced by the use of verapamil (0.32 µg/L; 0.46 µg/L). These doses are significantly low compared to the dosages recommended by WHO (0.25 mg/L) in potable water, which thus signifies DFB's safe use in the environment.

5 Conclusion

The present study showed the effective use of the diflubenzuron-verapamil combination against *Ae. aegypti* larvae, which caused higher adult emergence inhibition than diflubenzuron alone. The higher effects of the DFB-V combination obtained against the wild strain indicate its efficient use for mosquito management. In addition, the differential activities of detoxifying enzymes in DFB- and DFB-V-treated *Ae. aegypti* larvae and the higher impacts obtained with DFB-V and on the wild-caught larvae propose the plausible use of verapamil along with diflubenzuron for imparting higher efficacy. Moreover, the non-toxicity of DFB and DFB-V against non-target organisms indicates their safe use in the environment.

Data availability statement

The original contributions presented in the study are included in the article/supplementary material; further inquiries can be directed to the corresponding author.

Ethics statement

The manuscript presents research on animals that do not require ethical approval for their study.

Author contributions

MS: conceptualization, data curation, investigation, and writing—original draft. DY: data curation and writing—original draft. SK: supervision and writing—review and editing.

Funding

The author(s) declare that financial support was received for the research, authorship, and/or publication of this article. The research was funded by a grant (ID: 559/CSIRUGC NET DEC. 2018) received from the University Grants Commission (UGC), New Delhi.

References

- Abe, F. R., Machado, A. A., Coleone, A. C., da Cruze, C., and Machado-Neto, J. G. (2019). Toxicity of diflubenzuron and temephos on freshwater fishes: ecotoxicological assays with *Oreochromis niloticus* and *Hyphessobrycon eques*. *Water Air Soil Pollut.* 230, 77. doi:10.1007/s11270-019-4128-7
- Abou-Taleb, H. K., Zahran, H. M., and Gad, A. A. (2015). Biochemical and physiological effects of lufenuron and chlorfluazuron on *Spodoptera littoralis* (Boisd.) (Lepidoptera: Noctuidae). *J. Entomol.* 12 (2), 77–86. doi:10.3923/je.2015.77.86
- Ahmed, A. F., Moustafa, H. Z., and kandi, M. (2012). Toxicological and biochemical studies of lufenuron, chlorfluazuron and chromafenozide against *Pectinophora gossypiella* (Saunders). *Acad. J. Biol. Sci. C Physiol. Mol. Biol.* 4 (1), 37–47. doi:10.21608/eajbsf.2012.17281
- Anwar, E. M., and Abd El-mageed, A. E. M. (2005). Toxicity impacts of certain insect growth regulators on some biochemical activities of the cotton leafworm. *J. Agric. Res.* 83 (3), 915–935. doi:10.17221/3/2F2011-PPS
- Bakr, R. F., Abd Elaziz, M. F., El-Barky, N. M., Awad, M. H., El-Halim, A., and Hisham, M. E. (2013). The activity of some detoxification enzymes in *Spodoptera littoralis* (Boisd.) larvae (Lepidoptera–Noctuidae) treated with two different insect growth regulators. *Acad. J. Biol. Sci. C Physiol. Mol. Biol.* 5 (2), 19–27. doi:10.21608/EAJBSC.2013.16092
- Belinato, T. A., and Valle, D. (2015). The impact of selection with diflubenzuron, a chitin synthesis inhibitor, on the fitness of two Brazilian *Aedes aegypti* field populations. *PLoS One* 10 (6), e0130719. doi:10.1371/journal.pone.0130719
- Bharati, M., and Saha, D. (2018). Multiple insecticide resistance mechanisms in primary dengue vector, *Aedes aegypti* (Linn.) from dengue endemic districts of sub-Himalayan West Bengal, India. *PLoS One* 13 (9), e0203207. doi:10.1371/journal.pone.0203207
- Borase, H. P., Patil, C. D., Salunkhe, R. B., Narkhede, C. P., Salunke, B. K., and Patil, S. V. (2013). Photosynthesized silver nanoparticle: a potent mosquito biolarvicidal agent. *J. Nanomed. Biotherapeutic Discov.* 3, 1–7. doi:10.4172/2155-983X.1000111
- Bradford, M. M. (1976). A rapid and sensitive method for the quantitation of microgram quantities of protein utilizing the principle of protein-dye binding. *Anal. Biochem.* 72 (1–2), 248–254. doi:10.1006/abio.1976.9999
- Brogden, W. G., and Barber, A. M. (1987). Microplate assay of acetylcholinesterase inhibition kinetics in single mosquito homogenates. *Pestic. Biochem. Physiol.* 29 (3), 252–259. doi:10.1016/0048-3575(87)90155-6
- Brogden, W. G., and Barber, A. M. (1990). Microplate assay of glutathione-S-transferase activity for resistance detection in single mosquito triturates. *Comp. Biochem. Physiol. B* 96 (2), 339–342. doi:10.1016/0305-0491(90)90385-7
- Brogden, W. G., and Dickinson, C. M. (1983). A microassay system for measuring esterase activity and protein concentration in small samples and in high-pressure liquid chromatography eluate fractions. *Anal. Biochem.* 131 (2), 499–503. doi:10.1016/0003-2697(83)90204-x
- Chen, C. D., Seleena, B., Chiang, Y. F., and Lee, H. L. (2008). Field evaluation of the bioefficacy of diflubenzuron (Dimilin) against container-breeding *Aedes* sp. mosquitoes. *Trop. Biomed.* 25 (1), 80–86.
- Doucet, D., and Retnakaran, A. (2012). Insect chitin: metabolism, genomics and pest management. *Adv. Insect Physiol.* 43, 437–511. doi:10.1016/B978-0-12-391500-9.00006-1
- El-Bermawy, S. M., and Abulyazid, I. (1998). Genomic DNA polymorphism and biochemical assay in the pupal stage of Med-fly *Ceratitis capitata* (Wied). *Proc. Intern. Conf. Mol. Gent.* 1, 165–180.
- Eltahir, W. A., Elamin, M. O., Mahgoub, I., and Faraj, E. A. (2018). Efficacy of temephos and diflubenzuron use in malaria vector larvae control. *World J. Adv. hlthcare. Res.* 2 (5), 36–39. doi:10.1234/OJSDJ.V111.6
- Enayati, A. A., Ranson, H., and Hemingway, J. (2005). Insect glutathione transferases and insecticide resistance. *Insect Mol. Biol.* 14 (1), 3–8. doi:10.1111/j.1365-2583.2004.00529.x
- Epis, S., Porretta, D., Mastrantonio, V., Comandatore, F., Sasser, D., Rossi, P., et al. (2022). The impact of insect growth regulators on adult emergence inhibition and the fitness of *Aedes aegypti* field populations in Thailand. *Acta Trop.* 236, 106695. doi:10.1016/j.actatropica.2022.106695
- Fansiri, T., Pongsiri, A., Khongtak, P., Nitatsukprasert, C., Chittham, W., Jaichapor, B., et al. (2014). ABC transporters are involved in defense against permethrin insecticide in the malaria vector *Anopheles stephensi*. *Parasit. Vectors* 7, 349–357. doi:10.1186/1756-3305-7-349
- Farlow, J. E., Breaud, T. P., Steelman, C. D., and Schilling, P. E. (1978). Effects of the insect growth regulator difluhenuron on non-target aquatic populations in a Louisiana intermediate marsh. *Environ. Entomol.* 7 (2), 199–204. doi:10.1093/ee/7.2.199
- Ghoneim, K. S., Al-Dali, A. G., and Abdel-Ghaffar, A. A. (2003). Effectiveness of lufenuron (CGA-184699) and diofenolan (CGA-59205) on the general body

Acknowledgments

The authors thank the Principal of Acharya Narendra Dev College, University of Delhi, India, for providing research infrastructure and facilities. The authors are grateful to the University Grants Commission (UGC) for funding this research.

Conflict of interest

The authors declare that the research was conducted in the absence of any commercial or financial relationships that could be construed as a potential conflict of interest.

Publisher's note

All claims expressed in this article are solely those of the authors and do not necessarily represent those of their affiliated organizations, or those of the publisher, the editors, and the reviewers. Any product that may be evaluated in this article, or claim that may be made by its manufacturer, is not guaranteed or endorsed by the publisher.

- metabolism of the red palm weevil, *Rhynchophorus ferrugineus* (Curculionidae: Coleoptera). *Pak. J. Biol. Sci.* 6 (13), 1125–1129. doi:10.3923/pjbs.2003.1125.1129
- Ghoneim, K. S., Hamadah, K. S., and Tanani, M. A. (2012). Protein disturbance in the haemolymph and fat body of the desert locust *Schistocerca gregaria* as a response to certain insect growth regulators. *Bull. Environ. Pharmacol. Life Sci.* 1 (7), 73–83.
- Grigoraki, L., Puggioli, A., Mavridis, K., Douris, V., Montanari, M., Bellini, R., et al. (2017). Striking diflubenzuron resistance in *Culex pipiens*, the prime vector of West Nile Virus. *Sci. Rep.* 7 (1), 11699. doi:10.1038/s41598-017-12103-1
- Guz, N., Cagatay, N. S., Fotakis, E. A., Durmusoglu, E., and Vontas, J. (2020). Detection of diflubenzuron and pyrethroid resistance mutations in *Culex pipiens* from Mugla, Turkey. *Acta Trop.* 203, 105294. doi:10.1016/j.actatropica.2019.105294
- Hamdy, A. M., and Azab, A. M. (2002). "Effect of insect growth regulators and binary mixtures on enzymes activity of Egyptian cotton leafworm, *Spodoptera littoralis*, (Boisd.) larvae," in 2nd International conference of Plant Protection, Research Institute, Cairo, Egypt, 617–623.
- Hamouda, L. S. (2002). Toxicological and biochemical studies on the effect of admiral (IGR) and nuclear polyhedrosis virus (SNPV) on *Spodoptera littoralis* (Boisd.) larvae. *J. Egypt. Acad. Soc. Environ. Dev.* 2 (1), 15–29. doi:10.21608/eajbsa.2013.13361
- Ismail, S. M. (2020). Effect of sublethal doses of some insecticides and their role on detoxification enzymes and protein-content of *Spodoptera littoralis* (Boisd.) (Lepidoptera: Noctuidae). *Bull. Natl. Res. Cent.* 44 (1), 1–6. doi:10.1186/s42269-020-00294-z
- Kang, X. L., Zhang, M., Wang, K., Qiao, X. F., and Chen, M. H. (2016). Molecular cloning, expression pattern of multidrug resistance associated protein 1 (MRP1, ABCC1) gene, and the synergistic effects of verapamil on toxicity of two insecticides in the bird cherry-oat aphid. *Arch. Insect Biochem. Physiol.* 92 (1), 65–84. doi:10.1002/arch.21334
- Karunaratne, S. H. P. P., De Silva, W. A. P. P., Weeraratne, T. C., and Surendran, S. N. (2018). Insecticide resistance in mosquitoes: development, mechanisms and monitoring. *Ceylon J. Sci.* 47 (4), 299–309. doi:10.4038/cjs.v47i4.7547
- Kona, M. P., Kamaraju, R., Donnelly, M. J., Bhatt, R. M., Nanda, N., Chourasia, M. K., et al. (2018). Characterization and monitoring of deltamethrin-resistance in *Anopheles culicifacies* in the presence of a long-lasting insecticide-treated net intervention. *Malar. J.* 17 (1), 414. doi:10.1186/s12936-018-2557-1
- Kotze, A. C., Sales, N., and Barchia, I. M. (1997). Diflubenzuron tolerance associated with monooxygenase activity in field strain larvae of the Australian sheep blowfly (Diptera: Calliphoridae). *J. Econ. Entomol.* 90 (1), 15–20. doi:10.1093/jee/90.1.15
- Kumar, S., Thomas, A., Sahgal, A., Verma, A., Samuel, T., and Pillai, M. K. K. (2002). Effect of synergist, Piperonyl Butoxide, on the development of deltamethrin resistance in yellow fever mosquito, *Aedes aegypti* L. (Diptera: Culicidae). *Arch. Insect Biochem. Physiol.* 50, 1–8. doi:10.1002/arch.10021
- Kumar, S., Thomas, A., Sahgal, A., Verma, A., Samuel, T., and Pillai, M. K. K. (2004). Variations in the insecticides resistance spectrum of *Anopheles stephensi* Liston on selections with deltamethrin and deltamethrin/PBO combination. *Ann. Trop. Med. Parasitol.* 98, 861–871. doi:10.1179/000349804X3180
- Li, X. Z., and Liu, Y. H. (2007). Diet influences the detoxification enzyme activity of *Bactrocera tau* (Walker) (Diptera: Tephritidae). *Acta Entomol. Sin.* 50 (10), 989–995. doi:10.16380/J.KCXB.2007.10.009
- Linvy, V., Sridhu, P., Reshma, R. M., Resmitha, C., and Kannan, V. M. (2018). Storage protein in the hemolymph of 6th instar larvae of *Spodoptera mauritia* Boisd. (Lepidoptera: Noctuidae) is increased by the ecdysone mimic, methoxyfenozide. *Int. J. Entomol. Res.* 3 (2), 1–4.
- Lucchesi, V., Grimaldi, L., Mastrantonio, V., Porretta, D., Di Bella, L., Ruspandini, T., et al. (2022). Cuticle modifications and over-expression of the chitin-synthase gene in diflubenzuron-resistant phenotype. *Insects* 13 (12), 1109. doi:10.3390/insects13121109
- Moe, S. J., Hjermann, D., Ravagnan, E., and Bechmann, R. K. (2019). Effects of an aquaculture pesticide (diflubenzuron) on non-target shrimp populations: extrapolation from laboratory experiments to the risk of population decline. *Ecol. Model.* 413, 108833. doi:10.1016/j.ecolmodel.2019.108833
- Muthusamy, M., Shivakumar, S., Karthi, K., and Ramkumar, R. (2011). Pesticide detoxifying mechanism in field population of *Spodoptera litura* (Lepidoptera: Noctuidae) from South India. *Egypt. Acad. J. Biol. Sci. C Physiol. Mol. Biol.* 3 (1), 51–57. doi:10.21608/eajbsf.2011.17437
- Panmei, K., Samal, R. R., Lanbili, P., and Kumar, S. (2021). Influence of lufenuron on the nutrient content and detoxification enzyme expression in *Aedes aegypti* L. (Diptera: Culicidae). *Int. J. Trop. Insect Sci.* 41 (4), 2965–2973. doi:10.1007/s42690-021-00481-z
- Pešić, B., Kulišić, Z., Teodorović, R., Trailović, S. M., Djokić, V., and Djordjevic, M. (2022). Comparison of mosquito larvicidal formulations of diflubenzuron on *Culex pipiens* mosquitoes in belgrade, Serbia. *Acta Vet.* 72 (1), 87–99. doi:10.2478/acve-2022-0007
- Piri Aliabadi, F., Sahragard, A., and Ghadamyari, M. (2016). Lethal and sublethal effects of a chitin synthesis inhibitor, lufenuron, against *Glyphodes pyloalis* Walker (Lepidoptera: Pyralidae). *J. Crop Prot.* 5 (2), 203–214. doi:10.18869/MDARES.JCP.5.2.203
- Porretta, D., Fotakis, E. A., Mastrantonio, V., Chaskopoulou, A., Michaelakis, A., Kioulos, I., et al. (2019). Focal distribution of diflubenzuron resistance mutations in *Culex pipiens* mosquitoes from Northern Italy. *Acta Trop.* 193, 106–112. doi:10.1016/j.actatropica.2019.02.024
- Porretta, D., Gargani, M., Bellini, R., Medici, A., Punelli, F., and Urbanelli, S. (2008). Defence mechanisms against insecticides temephos and diflubenzuron in the mosquito *Aedes caspius*: the P-glycoprotein efflux pumps. *Med. Vet. Entomol.* 22 (1), 48–54. doi:10.1111/j.1365-2915.2008.00712.x
- Rodríguez-Ortega, M. J., Grøvisk, B. E., Rodríguez-Ariza, A., Goksøyr, A., and López-Barea, J. (2003). Changes in protein expression benefits in bivalve molluscs (*Chamaelea gallina*) exposed to four model environmental pollutants. *Proteomics* 3 (8), 1535–1543. doi:10.1002/pmic.200300491
- Sankar, M., and Kumar, S. (2023). A systematic review on the eco-safe management of mosquitoes with diflubenzuron: an effective growth regulatory agent. *Acta Ecol. Sin.* 43, 11–19. doi:10.1016/j.chnaes.2021.09.019
- Seeradj, N., Bendali-Saoudi, F., and Soltani, N. (2022). The effect of diflubenzuron (Dimilin® 25 WP) on some non-target aquatic insect and crustacean species. *Pol. J. Entomol.* 91 (4), 174–183. doi:10.5604/01.3001.0016.1930
- Wang, J., Tian, D., and Zhuang, J. (2009). Selection and risk assessment of *Spodoptera litura* (Fabricius) resistance to methoxyfenozide. *J. Agric. Sci.* 25 (1), 79–83.
- Warikoo, R., and Kumar, S. (2013). Impact of *Argemone mexicana* extracts on the cidal, morphological, and behavioural response of dengue vector, *Aedes aegypti* L. (Diptera: Culicidae). *Parasitol. Res.* 112 (10), 3477–3484. doi:10.1007/s00436-013-3528-7
- World Health Organization (1998). *Techniques to detect insecticide resistance mechanisms (field and laboratory manual)*. Geneva: WHO. Available at: <https://apps.who.int/iris/handle/10665/83780>.
- World Health Organization (2005). *Guidelines for laboratory and field testing of mosquito larvicides*. Geneva: WHO. Available at: <https://apps.who.int/iris/handle/10665/69101>.
- World Health Organisation (2024). *Fact sheets. Dengue and severe dengue*. Geneva: WHO. Available at: <https://www.who.int/news-room/fact-sheets/detail/dengue-and-severe-dengue> (Accessed January, 2024).
- Yao, R., Zhao, D.-D., Zhang, S., Zhou, L.-Q., Wang, X., Gao, C.-F., et al. (2017). Monitoring and mechanisms of insecticide resistance in *Chilo suppressalis* (Lepidoptera: crambidae), with special reference to diamides. *Pest Manag. Sci.* 73 (6), 1169–1178. doi:10.1002/ps.4439
- Zhu, K. Y., Heise, S., Zhang, J., Anderson, T. D., and Starkey, S. R. (2007). Comparative studies on effects of three chitin synthesis inhibitors on common malaria mosquito (Diptera: Culicidae). *J. Med. Entomol.* 44 (6), 1047–1053. doi:10.1603/0022-2585(2007)44[1047:csocot]2.0.co;2
- Zhu, Q., He, Y., Yao, J., Liu, Y., Tao, L., and Huang, Q. (2012). Effects of sublethal concentrations of the chitin synthesis inhibitor, hexaflumuron, on the development and hemolymph physiology of the cutworm, *Spodoptera litura*. *J. Insect Sci.* 12 (1), 27. doi:10.1673/031.012.2701
- Zibadee, A., Zibadee, I., and Sendi, J. J. (2011). A juvenile hormone analog, pyriproxyfen, affects some biochemical components in the hemolymph and fat bodies of *Eurygaster integriceps* Puton (Hemipter: scutelleridae). *Pestic. Biochem. Physiol.* 100, 289–298. doi:10.1016/j.pestbp.2011.05.002



OPEN ACCESS

EDITED BY

Ana Claudia A. Melo,
Federal University of Rio de Janeiro, Brazil

REVIEWED BY

Xue-Qing Yang,
Shenyang Agricultural University, China
Nathália F. Brito,
National Cancer Institute (INCA), Brazil

*CORRESPONDENCE

Tao Zhang,
✉ cauzht@163.com
Zhanlin Gao,
✉ zbs308@163.com

RECEIVED 04 August 2024

ACCEPTED 09 December 2024

PUBLISHED 06 January 2025

CITATION

Guo J, Liu P, Zhang X, An J, Li Y, Zhang T and
Gao Z (2025) Characterization of the ligand-
binding properties of odorant-binding protein
38 from *Riptortus pedestris* when interacting
with soybean volatiles.
Front. Physiol. 15:1475489.
doi: 10.3389/fphys.2024.1475489

COPYRIGHT

© 2025 Guo, Liu, Zhang, An, Li, Zhang and Gao.
This is an open-access article distributed under
the terms of the [Creative Commons Attribution
License \(CC BY\)](https://creativecommons.org/licenses/by/4.0/). The use, distribution or
reproduction in other forums is permitted,
provided the original author(s) and the
copyright owner(s) are credited and that the
original publication in this journal is cited, in
accordance with accepted academic practice.
No use, distribution or reproduction is
permitted which does not comply with these
terms.

Characterization of the ligand-binding properties of odorant-binding protein 38 from *Riptortus pedestris* when interacting with soybean volatiles

Jianglong Guo, Panjing Liu, Xiaofang Zhang, Jingjie An, Yaofa Li,
Tao Zhang* and Zhanlin Gao*

Plant Protection Institute, Hebei Academy of Agriculture and Forestry Sciences, Key Laboratory of
Integrated Pest Management on Crops in Northern Region of North China, Ministry of Agriculture and
Rural Affairs, IPM Innovation Center of Hebei Province, International Science and Technology Joint
Research Center on IPM of Hebei Province, Baoding, China

Background: *Riptortus pedestris* (Fabricius) (Hemiptera: Alydidae) is a major soybean pest throughout East Asia that relies on its advanced olfactory system for the perception of plant-derived volatile compounds and aggregation pheromones for conspecific and host plant localization. Odorant binding proteins (OBPs) facilitate the transport of odorant compounds across the sensillum lymph within the insect olfactory system, enabling their interaction with odorant receptors (ORs).

Methods: Real-time quantitative PCR (qRT-PCR) analyses, fluorescence-based competitive binding assays, and molecular docking analyses were applied to assess the expression and ligand-binding properties of OBP38 from *R. pedestris*.

Results: The qRT-PCR analyses revealed high levels of *RpedOBP38* expression in the antennae without any apparent sex bias, and it was also highly expressed in the adult stage. Recombinant *RpedOBP38* was prepared by expressing it in *E. coli* BL21 (DE3) followed by its purification with a Ni-chelating affinity column. *RpedOBP38* was found to bind most strongly to trans-2-decenal ($K_i = 7.440$) and trans-2-nonenal ($K_i = 10.973$), followed by β -pinene, (+) -4-terpineol, carvacrol, methyl salicylate, and (-)-carvone. The 3D structure of *RpedOBP38* contains six α -helices and three interlocked disulfide bridges comprising a stable hydrophobic binding pocket. In a final series of molecular docking analyses, several polar (e.g., His 94, Glu97) and nonpolar (e.g., Leu29, Ile59) residues were found to be involved in *RpedOBP38*-ligand binding.

Conclusion: These data support a role for *RpedOBP38* in the perception of volatiles derived from host plants, providing important insight into the mechanisms that govern olfactory recognition in *R. pedestris*, thereby informing the development of ecologically friendly approaches to managing *R. pedestris* infestations.

KEYWORDS

Riptortus pedestris, OBPs, soybean volatiles, fluorescence competitive binding, molecular docking

1 Introduction

The ability of insects to perceive pheromones, host-derived odorants, and the wide array of other peripheral chemical signals present in their surrounding environment is dependent on a complex olfactory system that ultimately shapes key physiological processes such as foraging, mating, and oviposition (Martin et al., 2011; Leal, 2013). The ability to accurately recognize and decipher these signals is thus vital for the ability of insects to survive and reproduce. Hydrophobic chemicals need to successfully penetrate the olfactory sensilla and the hydrophilic sensillum lymph in order to access the odorant receptors (ORs) present on sensory neuron surfaces, thereby triggering downstream signal transduction (Li et al., 2015; Zhou et al., 2022). To facilitate this process, specialized supporting cells produce odorant-binding proteins (OBPs), which are secreted into the olfactory sensillum lymph and play a vital role in the process of insect odorant reception (Leal, 2013; Paula et al., 2018). OBPs can selectively bind, solubilize, and transport odorant molecules as they diffuse into the sensillum lymph, thereby enabling the activation of ORs and associated downstream signaling pathways (Leal, 2013; Liu et al., 2023). Given the importance of OBPs during this initial stage of odorant reception, they hold great promise as molecular targets for pest control efforts and the development of superior integrated pest management (IPM) strategies (Zhou et al., 2010; Venthur and Zhou, 2018).

The OBPs produced by insects are low-molecular-weight (12–20 kDa) proteins approximately 100–200 amino acids in length that are water soluble and typically feature a ~20 amino acid N-terminal signal peptide sequence (Ahmed et al., 2017; Li J. B. et al., 2022; Zeng et al., 2019). The 3D structures of classical OBPs are stabilized by three disulfide bridges formed by six conserved cysteine residues (Leal et al., 1999; Scaloni et al., 1999; Pelosi et al., 2014). The patterns of conserved cysteines have also been used to define four other classes of OBPs, including “Dimer” OBPs with two typical cysteines, “Minus-C” OBPs that lack 1–2 cysteines, “Plus-C” OBPs with 2–3 extra cysteines, and “Atypical” OBPs with a long, atypical C-terminal domain (Zhou et al., 2010; Spinelli et al., 2012; Manoharan et al., 2013; Venthur et al., 2014; Zeng et al., 2019). Identified in 1981, the first characterized OBP in insects was found to be exclusively expressed in *Antberaea polyphemus* antennae, enabling male moths to detect a particular sex pheromone (*trans*-6, *cis*-11-hexadecadienyl acetate) such that they were able to locate conspecific females to engage in mating (Vogt and Riddiford, 1981). Advances in molecular biology and transcriptomic technologies have fueled the identification of a growing number of genes encoding OBPs in many orders of insects, including Coleoptera (e.g., 39 OBPs in *Phyllotreta striolata*, Xiao et al., 2023), Hemiptera (e.g., 49 OBPs in *Riptortus pedestris*, Li L. L. et al. (2022)), Diptera (e.g., 28 OBPs in *Liriomyza trifolii*, Zhang et al. (2022)), Lepidoptera (e.g., 31 OBPs in *Chilo sacchariphagus*, Liu et al. (2021a)), Hymenoptera (e.g., 21 OBPs in *Apis mellifera*, Forêt and Maleszka (2006)), Orthoptera (e.g., 22 OBPs in *Locusta migratoria*, Pelosi et al. (2018)). Experimental efforts have revealed that OBPs which are primarily expressed in the antennae of certain insects are capable of interacting with specific chemical ligands including host volatiles and pheromones (Zhang et al., 2020a; Rihani et al., 2021). AlepOBP6,

for instance, is predominantly expressed in the antennae of male *Athetis lepigone* individuals and can recognize both maize-derived volatile compounds and sex hormones produced by conspecific females (Li J. B. et al., 2022). In *Hippodamia variegata*, both males and females exhibit high levels of HvarOBP5 expression in their antennae, thus enabling the perception of plant and prey-derived volatiles (Tang et al., 2023). The behavioral responses of *Eupeodes corolla* to the aphid alarm pheromone (E)- β -farnesene have been shown to be regulated by EcorOBP15 (Wang et al., 2022). Several OBPs have also been demonstrated to be expressed in other organs with or without primary chemosensory functions, including mouthpart palps (Pregitzer et al., 2018), labella (Sparks et al., 2014), legs (Hull et al., 2014), thorax (Zhang et al., 2018), and reproductive organs (Sun et al., 2012). These OBPs can facilitate a range of physiological functions including the recognition of taste compounds, the solubilization of nutrients, and the augmentation of resistance against insecticides (Pelosi et al., 2018).

Riptortus pedestris (Fabricius) (Hemiptera: Alydidae), known as the bean bug, is a serious agricultural pest species that is widely distributed throughout China, Japan, Korea, and other nations in East Asia (Jung and Lee, 2018; Jin et al., 2022). *R. pedestris* is a polyphagous pest species, feeding on over 30 different plants across 13 families (including Gramineae, Cruciferae, and other crop families), although they exhibit a particular preference for soybeans and other leguminous plants (Mainali et al., 2014; Ahn et al., 2020). Large numbers of these bean bugs typically infest soybean fields in the late flowering or early pod-growing stages and persistently feed on and damage these plants until harvest time (Endo et al., 2011). Soybean leaves, stems, pods, and flowers can be damaged by both *R. pedestris* adults and nymphs through their piercing and sucking behaviors, resulting in leaf rolling, stunted growth, and seed pods that are shriveled or empty, culminating in serious reductions in soybean quality and yield (Ahn et al., 2020). *R. pedestris*-associated soybean damage has recently emerged as a particularly serious problem in the Huang-Huai-Hai region of China (Li L. L. et al., 2022). Soybean plants in this region often suffer from the staygreen phenomenon that can be caused by *R. pedestris* feeding, which results in leaves that remain green, shriveled pods, and maturity stage seed abortion in soybean plants (Li et al., 2019; Dong et al., 2022). The control of *R. pedestris* has traditionally been achieved through the application of pyrethroids or other broad-spectrum insecticides (Gao et al., 2019; Guo et al., 2023). Such insecticide-based management practices, however, entail many potentially serious issues including environmental pollution, elevated levels of insecticide resistance, and inadequate efficacy owing to the highly mobile nature of these insects and their behavioral avoidance of insecticides (Bae et al., 2019; Zhu et al., 2022). There is thus a pressing need to develop new, ecologically friendly olfaction-based strategies for the control of *R. pedestris* infestations.

R. pedestris rely on their highly-developed antennae harboring abundant sensilla to detect both adult male-derived aggregation pheromone and host plant-derived volatiles, thus facilitating conspecific and host location efforts (Leal et al., 1995; Kim et al., 2016; Roh et al., 2021; Song et al., 2022). Li J. B. et al. (2022) previously analyzed the *R. pedestris* genome and identified 49 candidate RpedOBPs, including RpedOBP38, which exhibited high levels of expression in the antennae. The specific involvement

of RpedOBP38 in the detection of host volatiles or other chemical signals, however, has yet to be documented. Accordingly, this study was devised to clarify the olfactory functions of RpedOBP38. To that end, the sequence of the *RpedOBP38* gene was initially analyzed, after which *RpedOBP38* expression was analyzed across a variety of tissues and developmental stages via real-time quantitative PCR (qRT-PCR). The binding affinity of RpedOBP38 for 36 volatiles (including 11 green leaf volatiles, 11 soybean volatiles, 10 volatiles associated with repellent activity, and 4 aggregation pheromone compounds) was characterized through a fluorescence binding assay. Lastly, homology modeling and molecular docking approaches were used to characterize the binding sites and key amino acids related to the ligand binding activity of RpedOBP38. Together, the results of these analyses provide a robust evidence base for the further molecular characterization of the mechanisms governing olfactory recognition in *R. pedestris*, thus supporting efforts to improve the integrated management of this economically significant pest species.

2 Materials and methods

2.1 Insect rearing and tissue collection

R. pedestris specimens were captured in July–August 2019 from soybean fields in Shijiazhuang, Hebei province, China. Adults and nymphs were reared as in prior reports (Guo et al., 2023). Briefly, these insects were housed at $26^{\circ}\text{C} \pm 1^{\circ}\text{C}$ under $60\% \pm 5\%$ relative humidity (RH) with a 16 h: 8 h (L:D) photoperiod in cages, and were fed dried seeds (variety Jidou 12) and soybean seedlings that were replaced every 5–7 days. Based on the study of Li L. L. et al. (2022), 3-day-old virgin male and female adults were processed to collect antennae (40 pairs), heads without antennae (from 10 individuals), thoraxes (from 4 individuals), abdomens (from 3 individuals), wings (from 40 individuals), and legs (from 20 individuals). In addition, antennae were collected from 2nd (200 pairs), 3rd (120 pairs), 4th (60 pairs), and 5th (60 pairs) instar nymphs, after which they were snap-frozen with liquid nitrogen and stored at -80°C .

2.2 Total RNA extraction and preparation

TRIzol (TransGen, China) was used to extract RNA according to the manufacturer's instructions, the quality of which was analyzed via 1.0% agarose gel electrophoresis and spectrophotometry with a NanoDrop™ 2000 instrument (Thermo Fisher Scientific, United States). Next, 1 μg of the extracted RNA was processed with All-in-One First-Strand cDNA Synthesis SuperMix (TransGen), and the resultant cDNA was stored at -20°C .

2.3 Sequence alignment and phylogenetic analyses

The SignalP 6.0 server (<https://services.healthtech.dtu.dk/services/SignalP-6.0/>) was used for signal peptide prediction, while ClustalX 2.0 was used for multiple alignment of the RpedOBP38 protein sequence and those of other Hemiptera

OBPs, with GeneDoc (<http://nrbsc.org/gfx/genedoc>) being used for result visualization. The amino acid sequences of other hemipteran species were downloaded by accessing the NCBI website. MEGA7 was used to construct a phylogenetic tree with the neighbor-joining method and bootstrap testing (1,000 replicates). The Poisson correction method was employed when calculating evolutionary distance.

2.4 RpedOBP38 expression profiles

RpedOBP38 expression was validated via qRT-PCR with an ABI QuantStudio6 Q6 Real-Time PCR System (Applied Biosystems, CA, United States) using primers designed with Premier 6 and prepared by Sangon Biotech Co., Ltd (Beijing, China) (Supplementary Table S1). Individual 20 μL reactions comprised 1 μL of cDNA, 0.6 μL each of F/R primers (10 μM), 10 μL of $2 \times$ FastFire qPCR PreMix (TianGen Biotech, Beijing, China), and 7.8 μL of ddH₂O. Reaction settings were: 94°C for 30 s; 40 cycles of 94°C for 5 s, 55°C for 15 s, and 72°C for 10 s. Relative *RpedOBP38* expression was assessed with the $2^{-\Delta\Delta\text{Ct}}$ method, using *EF1* and *Actin* as reference genes (Wang et al., 2023). Three independent biological replicates were analyzed per sample.

2.5 Recombinant plasmid construction

The *RpedOBP38* open reading frame (ORF) lacking a signal peptide sequence was PCR amplified with TransStart® FastPfu PCR SuperMix (TransGen Biotech). Primers used to construct an RpedOBP38 expression vector were as follows: Forward: 5'-GAT GAGGCGAAACAGATG-3', Reverse: 5'-TCACTGTAGATCTTC AGTTCC-3'. Amplification settings were as follows: 95°C for 1 min; 35 cycles of 95°C for 20 s, 55°C for 20 s, and 72°C for 1 min; 72°C for 5 min. The products of PCR amplification were ligated into the pEASY-Blunt E1 vector (TransGen Biotech) and transformed into *E. coli* Trans-T1. Sangon Biotech then sequenced and confirmed the amplified gene products, and positive recombinant pEASY-Blunt E1-RpedOBP38 plasmids were obtained for further use.

2.6 Recombinant RpedOBP38 purification

After transforming *E. coli* BL21 (DE3) with recombinant RpedOBP38 expression vectors, positive clones were isolated and used to initiate cultures in LB broth containing 50 $\mu\text{g}/\text{mL}$ ampicillin that were incubated at 37°C and 220 rpm. When the OD₆₀₀ reached 0.6, 1 mM of isopropyl β -D-thiogalactoside (IPTG) was added and bacteria were incubated under the same conditions for a further 6 h. Cells were then centrifuged (8,000 $\times g$, 4°C) and resuspended in 20 mL of PBS (pH 7.0). Cells were then ultrasonically disrupted, and homogenates were centrifuged (14,000 rpm, 20 min, 4°C). The supernatants were then assessed via 12% SDS-PAGE separation. Target proteins from the supernatant fractions were applied to a Ni-chelating affinity column (GE, United States), which was subsequently equilibrated with 100 mM NaCl, 20 mM Tris-HCl, pH 7.9, and eluted using an ascending imidazole concentration

series (50, 100, 150 and 200 mM). Dialysis was used to desalt the eluent, and target protein size and purity were assessed via SDS-PAGE. Recombinant protein concentrations were measured via Bradford assay.

2.7 Fluorescence competitive binding assay

Recombinant RpedOBP38 binding to putative chemical ligands was characterized with a microplate reader (BioTek Synergy H1, United States). Fluorescence intensity values at the excitation wavelength of 337 nm and a maximum fluorescence emission wavelength of 450 nm were plotted against the free concentration of ligand for the measurement of dissociation constants, selecting candidate ligands from among 36 volatile compounds that included 11 green leaf volatiles (Chen et al., 2018; Guo and Wang, 2019; Cheng et al., 2020; Hong et al., 2022; Tang et al., 2023; Zhu et al., 2023), 11 soybean volatiles (Wang et al., 2019a; Zhu et al., 2022), 10 repellent activity volatiles (Zhang et al., 2013; Zhang et al., 2014), and 4 aggregation pheromone compounds (Leal et al., 1995; Yasuda et al., 2007). HPLC-grade methanol was used for the dissolution of the probe N-phenyl-1-naphthylamine (1-NPN) and all ligands. The ability of RpedOBP38 to bind 1-NPN was assessed by using 10 mM PBS (pH 7.4) to prepare a 2 μ M purified protein solution, titrating with 1 mM 1-NPN in methanol to prepare final concentrations from 2–20 μ M. RpedOBP38 binding to each ligand was evaluated in a solution consisting of 2 μ M purified protein and 1-NPN, followed by titration through the addition of ligands until no further decrease in the fluorescence intensity was observed. Ligands were independently replicated three times, and dissociation constants for each ligand were measured as follows: $K_i = [IC_{50}]/(1 + [1-NPN]/K_{1-NPN})$, where IC_{50} denotes the ligand concentration when the fluorescence intensity is half of the initial value [1-NPN] is the free 1-NPN concentration, and K_{1-NPN} is the dissociation constant for the RpedOBP38/1-NPN complex (Campanacci et al., 2001). Based on the study of Cui et al. (2018), the strength of binding affinity could be indicated by K_i value, including very strong ($K_i < 6 \mu$ M), strong (6μ M $\leq K_i < 22 \mu$ M), moderate (22μ M $\leq K_i < 40 \mu$ M) and weak ($K_i > 40 \mu$ M).

2.8 Homology modelling and molecular docking analyses

RpedOBP38 tertiary structure modeling was performed with the I-TASSER server (Zheng et al., 2021), due to the <30% homology with the protein sequences in the Swiss-model server. The RpedOBP38 amino acid sequence was utilized as an input, utilizing the 10 template proteins exhibiting the highest sequence identity for the purposes of modeling (Supplementary Table S2). C-score values were used to choose the best model from among the top 5 (Supplementary Table S3), with C-scores generally falling in the [-5, 2] range, and higher scores being indicative of greater model confidence. For the chosen ligands, the PubChem database (<https://pubchem.ncbi.nlm.nih.gov/>) was accessed to download 3D structures that were subsequently converted into the mol2 format with Open Babel GUI v.3.1.1 (O'Boyle et al., 2011). Molecular docking analyses of the interactions between RpedOBP38 and

seven ligands were performed with AutoDock Vina (v.1.1.2) (Trott and Olson, 2010) using default parameters. PyMOL v.2.0 (Schrödinger, LLC) was used for the visualization of the molecular docking results, and interaction forces were examined with PLIP (<https://plip-tool.biotec.tu-dresden.de/plipweb/plip/index>).

2.9 Statistical analyses

RpedOBP38 expression was analyzed across various *R. pedestris* tissues and developmental stages using one-way ANOVA with Tukey's multiple comparison test. $p < 0.05$ was selected as the cut-off for significance, and SPSS 20.0 (IBM 2011) was used for all statistical analyses, while GraphPad Prism 8.0 was used for figure generation.

3 Results

3.1 RpedOBP38 sequence analyses

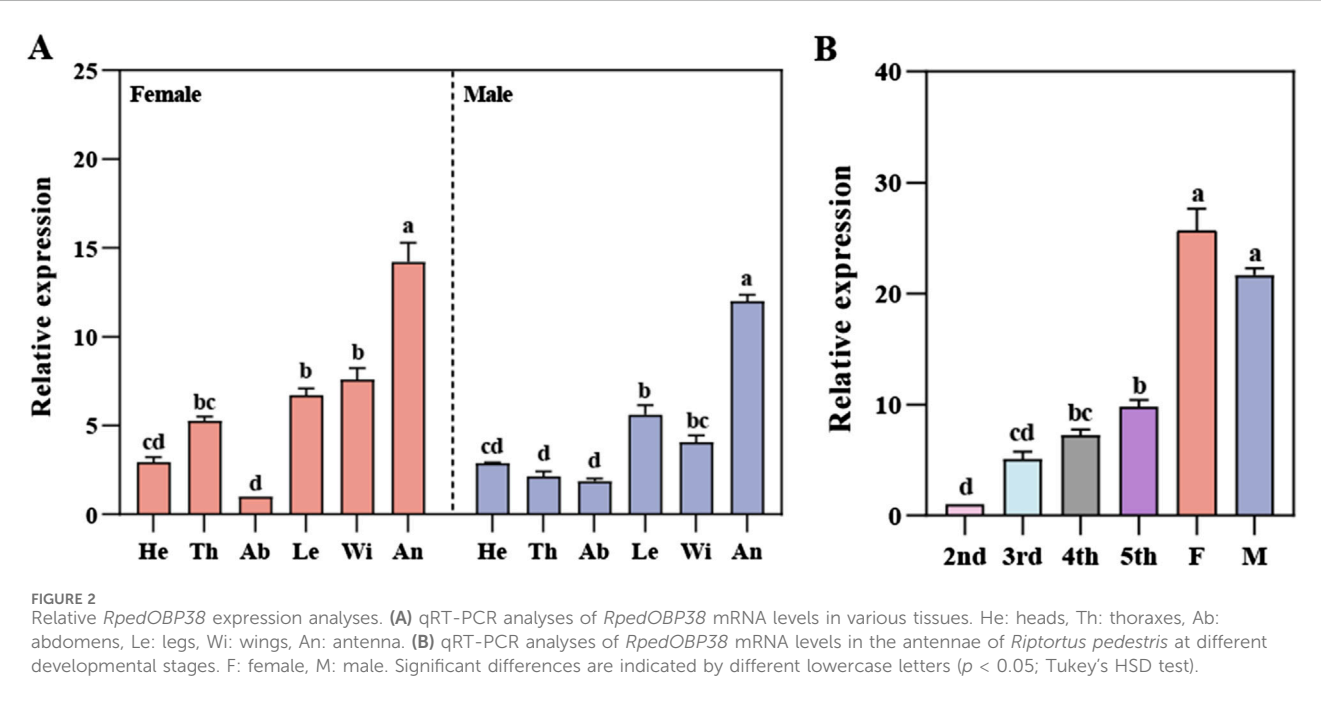
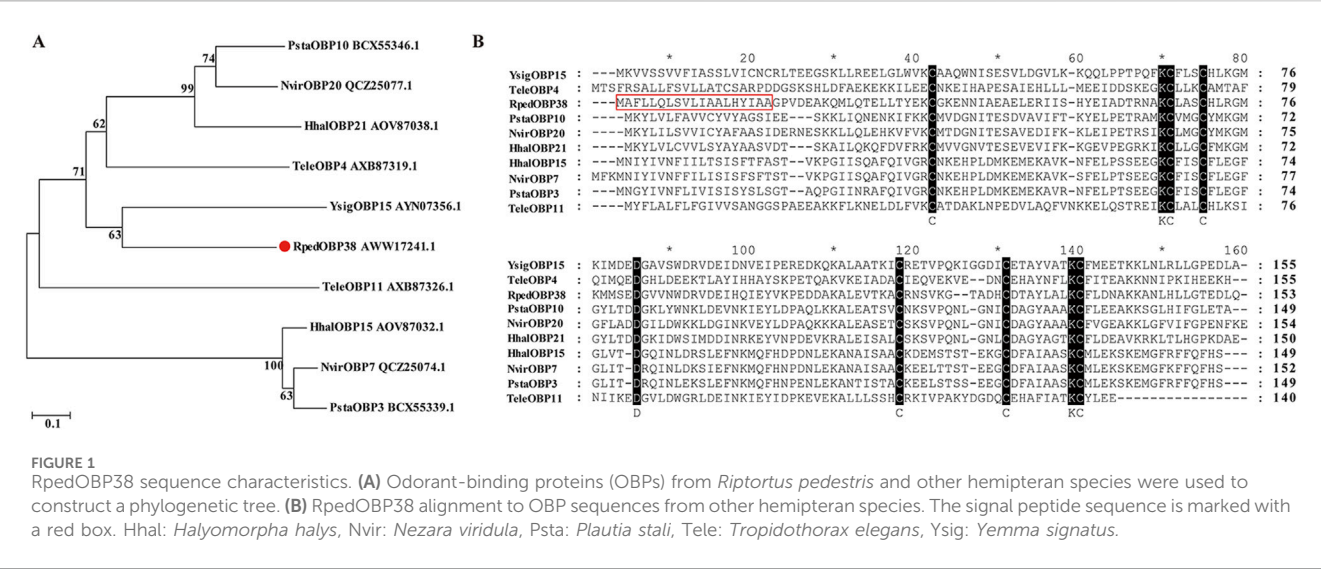
RpedOBP38 cDNA sequences were downloaded from the *R. pedestris* genome (Li J. B. et al., 2022). The RpedOBP38 ORF was found to consist of 462 bp encoding a 153-amino-acid (aa) protein, with a 19-aa N-terminal signal peptide. This protein had a predicted molecular mass of 15.08 kDa and a predicted isoelectric point of 5.20. BLASTp similarity analyses revealed some level of sequence identity with OBPs from other Hemiptera species, including YsigOBP15 from *Yemma signatus* (43.42%), PstaOBP3 from *Plautia stali* (38.78%), HhalOBP15 from *Halyomorpha halys* (37.50%), TeleOBP5 from *Tropidothorax elegans* (36.23%), and NvirOBP20 from *Nezara viridula* (35.71%). Phylogenetic tree analyses revealed the clustering of RpedOBP38 and YsigOBP15 from *Y. signatus* (Figure 1A). Sequence alignment also revealed the presence of six conserved cysteine residues within RpedOBP38 (Figure 1B), consistent with its classification within the classical OBP family.

3.2 Evaluation of RpedOBP38 expression patterns

RpedOBP38 expression across tissues and developmental stages was next characterized by qPCR, revealing significant differences in RpedOBP38 among tissues in both female ($F_{5, 12} = 65.68$, $P < 0.001$) and male ($F_{5, 12} = 129.09$, $P < 0.001$) adults, with the highest expression levels in the antennae of adult females and males, respectively (Figure 2A). Antennae RpedOBP38 expression levels rose with increasing developmental stages, with significant differences among stages ($F_{5, 12} = 106.62$, $P < 0.001$), and expression levels being highest in adult antennae. However, there was no significant sex difference for RpedOBP38 expression levels (Figure 2B).

3.3 Characterization of RpedOBP38 binding to 1-NPN and candidate ligands

After expressing recombinant RpedOBP38 in *E. coli* BL21 (DE3), it was purified, yielding a final recombinant



RpedOBP38 concentration of 0.603 mg/mL. SDS-PAGE analyses confirmed a similar target protein size to the predicted size (Figure 3A). The ability of RpedOBP38 to bind 1-NPN was then assessed, revealing strong binding between RpedOBP38 and 1-NPN (dissociation constant [K_d]): 4.059 $\mu\text{mol/L}$). Binding curve analyses and Scatchard plots revealed the presence of a single binding site, indicating that 1-NPN was a highly suitable probe for subsequent binding analyses (Figure 3B).

In total, 36 volatile compounds including 11 green leaf volatiles, 11 soybean volatiles, 10 volatiles associated with repellent activity, and 4 aggregation pheromone compounds were chosen for the evaluation of RpedOBP38 ligand binding. The resultant analyses demonstrated the ability of RpedOBP38 to strongly bind to the soybean volatiles *trans*-2-decenal ($K_i = 7.440 \mu\text{M}$), *trans*-2-nonenal

($K_i = 10.973 \mu\text{M}$) and methyl salicylate ($K_i = 21.065 \mu\text{M}$) (Figure 3C; Table 1). It also exhibited strong or moderate binding to three volatiles associated with repellent activity ((+) -4-terpineol, $K_i = 14.017 \mu\text{M}$; carvacrol, $K_i = 19.446 \mu\text{M}$; (-)-carvone, $K_i = 27.215 \mu\text{M}$) (Figure 3D; Table 1). In contrast, it exhibited weak binding activity for the tested aggregation pheromone compounds ($K_i > 40 \mu\text{M}$) (Table 1).

3.4 Homology modeling and molecular docking analyses

When the I-TASSER server was used to construct 3D models of the structure of RpedOBP38, the first model among the top five

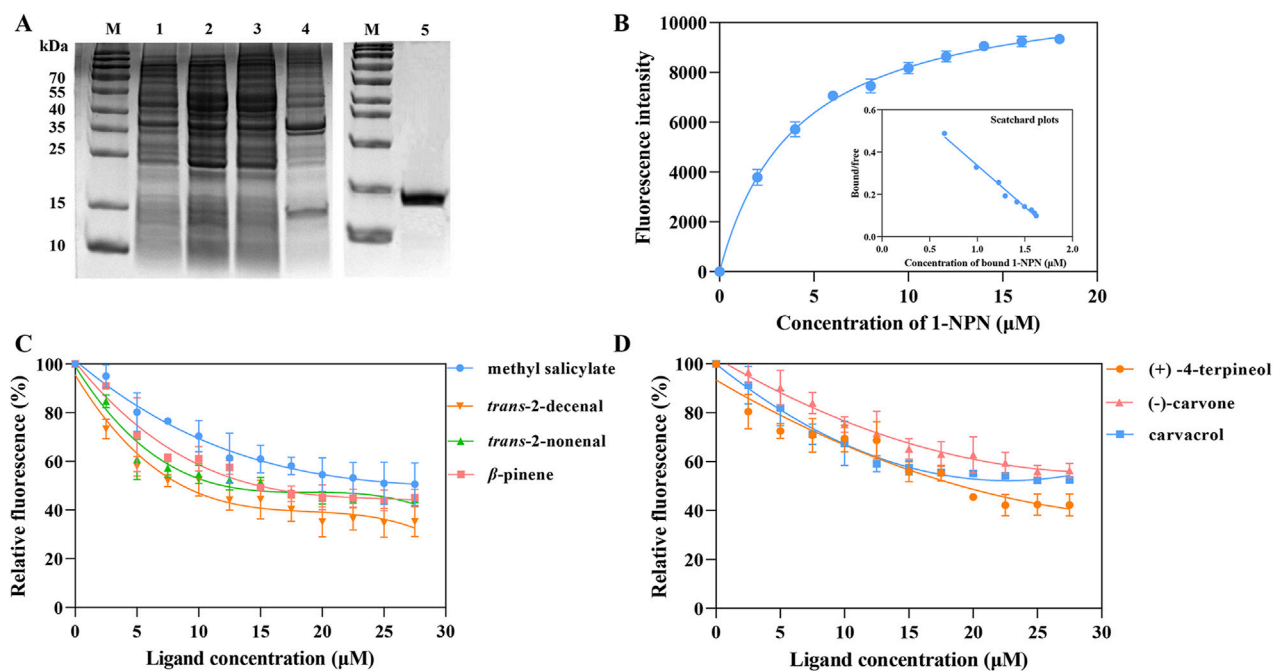


FIGURE 3

Characterization of RpedOBP38 ligand binding properties. (A) SDS-PAGE analyses pertaining to recombinant RpedOBP38 expression and purification. Lane 1: non-induced pEasy-Blunt E1-RpedOBP38; Lane 2: induced pEasy-Blunt E1-RpedOBP38; Lane 3: Supernatant of induced pEasy-Blunt E1-RpedOBP38; Lane 4: precipitation of induced pEasy-Blunt E1-RpedOBP38; Lane 5: purified RpedOBP38. (B) Binding curves and scatchard plots correspond to the interaction between the fluorescent probe 1-NPN and RpedOBP38. (C, D) Binding curves corresponding to interactions between RpedOBP38 and green leaf volatiles, soybean volatiles. (C) or repellent volatiles (D).

generated models exhibited the highest C-score of -1.13 (Supplementary Table S3). This predicted RpedOBP38 model contained six α -helices designated $\alpha 1$ (Pro21-Glu42), $\alpha 2$ (Glu47-Ser55), $\alpha 3$ (Cys67-Gly75), $\alpha 4$ (Trp87-Glu97), $\alpha 5$ (Pro101-Ala113), and $\alpha 6$ (His124-Ala142) that were folded around a hydrophobic cavity. It also harbored three interlocking disulfide bridges formed by links between Cys39 in $\alpha 1$ and Cys71 in $\alpha 3$, Cys67 in $\alpha 3$ and Cys125 in $\alpha 6$, and Cys114 in $\alpha 5$ and Cys134 in $\alpha 6$, providing further stability to the hydrophobic structure of this protein (Figure 4A).

Based on the fluorescence competitive binding assays performed above, β -pinene, methyl salicylate, trans-2-nonenal, trans-2-decenal (+) -4-terpineol (-)-carvone, and carvacrol were chosen as target ligands for molecular docking analyses. All seven of these ligands exhibited negative binding energy values when interacting with RpedOBP3 ranging from -5.71 to -4.20 (Table 2). Hydrogen bonds, hydrophobic interactions, and π -stacking were all found to contribute to these RpedOBP38-ligand binding interactions (Figures 4B–H). Both polar (e.g., Lys133, Glu97, His 94, Thr31) and nonpolar (e.g., Ile59, Leu136, Val85, Phe135) residues within the hydrophobic RpedOBP38 cavity were found to contribute to intermolecular binding interactions. Some of these amino acid residues were found to bind to multiple ligands, including 10 (Glu32, Ile59, Val85, Ile96, Thr111, Tyr129, Ala131, Lys133, Phe135, and Leu136) that were able to bind to three ligands, and 5 (Leu29, Thr31, Ile93, His94, and Glu97) that were able to bind to three ligands (Table 2).

4 Discussion

OBPs have been identified across many insect species to date and have been confirmed to be integral to the recognition of exogenous chemical signals and the regulation of physiological activities (Venthur and Zhou, 2018). OBPs have been established as promising molecular targets when screening for odorous compounds with attractant or repellent properties, informing the development of push-pull pest control strategies (Zhang et al., 2021; Song et al., 2022; Zhu et al., 2022; Zhu et al., 2023). For instance, CquiOBP1 of *Culex quinquefasciatus* was used as a target to guide the successful synthesis of a blend of trimethylamine and nonanal through the combination of conventional and reverse chemical ecology methodological approaches (Leal et al., 2008). The ability of certain OBPs to bind to aphid alarm pheromone has also enabled the design and synthesis of novel (*E*)- β -farnesene analogs with repellent and insecticidal activity for *Acythosiphon pisum* (Sun et al., 2011). In light of the importance of OBPs and the rising demand for environmentally friendly approaches to managing pest species, OBPs have emerged as a research hotspot in the insect chemical ecology space.

Initial sequencing analyses performed in this study revealed that RpedOBP38 had 153 amino acids in length with a 19-aa N-terminal signal peptide and six conserved cysteine residues, consistent with its classification as a member of the classic OBP family (Pelosi et al., 2006; Brito et al., 2016). Phylogenetic analyses can be used to infer evolutionary relationships for particular genes across species,

TABLE 1 Binding affinities of all tested ligands to RpedOBP38.

Ligands	CAS number	IC50 (μmol/L)	Ki (μmol/L)
Green leaf volatiles			
<i>trans</i> -2-hexenal	6,728-26-3	>40	>40
octanal	124-13-0	>40	>40
nonanal	124-19-6	>40	>40
β-myrcene	123-35-3	>40	>40
<i>trans</i> -caryophyllene	87-44-5	>40	>40
α-pinene	13,877-91-3	>40	>40
geraniol	106-24-1	>40	>40
camphene	565-00-4	>40	>40
β-pinene	127-91-3	16.393 ± 0.261	12.315 ± 0.196
(+)-α-pinene	7,785-70-8	>40	>40
(-)-α-pinene	7,785-26-4	>40	>40
Soybean volatiles			
hexanal	66-25-1	>40	>40
1-hexanol	111-27-3	>40	>40
1-octen-3-ol	3,391-86-4	>40	>40
3-octanone	106-68-3	>40	>40
<i>cis</i> -3-hexen-1-ol	928-96-1	>40	>40
<i>cis</i> -3-hexenyl acetate	3,681-71-8	>40	>40
methyl salicylate	119-36-8	28.039 ± 5.938	21.065 ± 4.461
<i>trans</i> -2-hexenyl acetate	2,497-18-9	>40	>40
<i>trans</i> -2-octenal	2,548-87-0	>40	>40
<i>trans</i> -2-nonenal	18,829-56-6	14.606 ± 0.821	10.973 ± 0.617
<i>trans</i> -2-decenal	3,913-81-3	9.904 ± 0.970	7.440 ± 0.729
Volatiles with repellent activity			
eugenol	97-53-0	>40	>40
isoeugenol	97-54-1	>40	>40
(-) -4-terpineol	20,126-76-5	>40	>40
(+) -4-terpineol	2,438-10-0	18.658 ± 0.428	14.017 ± 0.321
γ-terpinene	99-85-4	>40	>40
cineole	470-82-6	>40	>40
α-terpinene	99-86-5	>40	>40
(-) -carvone	6,485-40-1	36.226 ± 5.169	27.215 ± 3.883
(+) -carvone	2,244-16-8	>40	>40
carvacrol	499-75-2	25.898 ± 0.443	19.456 ± 0.333
Pheromone compounds			
<i>trans</i> -2-hexenyl hexanoate	53,398-86-0	>40	>40
(E)-2-hexenyl (Z)-3-hexenoate (E2-6:Z3Hex)	53,398-87-1	>40	>40

(Continued on following page)

TABLE 1 (Continued) Binding affinities of all tested ligands to RpedOBP38.

Ligands	CAS number	IC50 (μmol/L)	Ki (μmol/L)
(E)-2-hexenyl (Z)-2-hexenoate (E2-6:E2Hex)	54,845-28-2	>40	>40
myristyl isobutyrate	167,871-30-9	>40	>40

'Ki > 40 μM' means that the binding ability of RpedOBP38 recombinant protein to this ligand was considered weak.

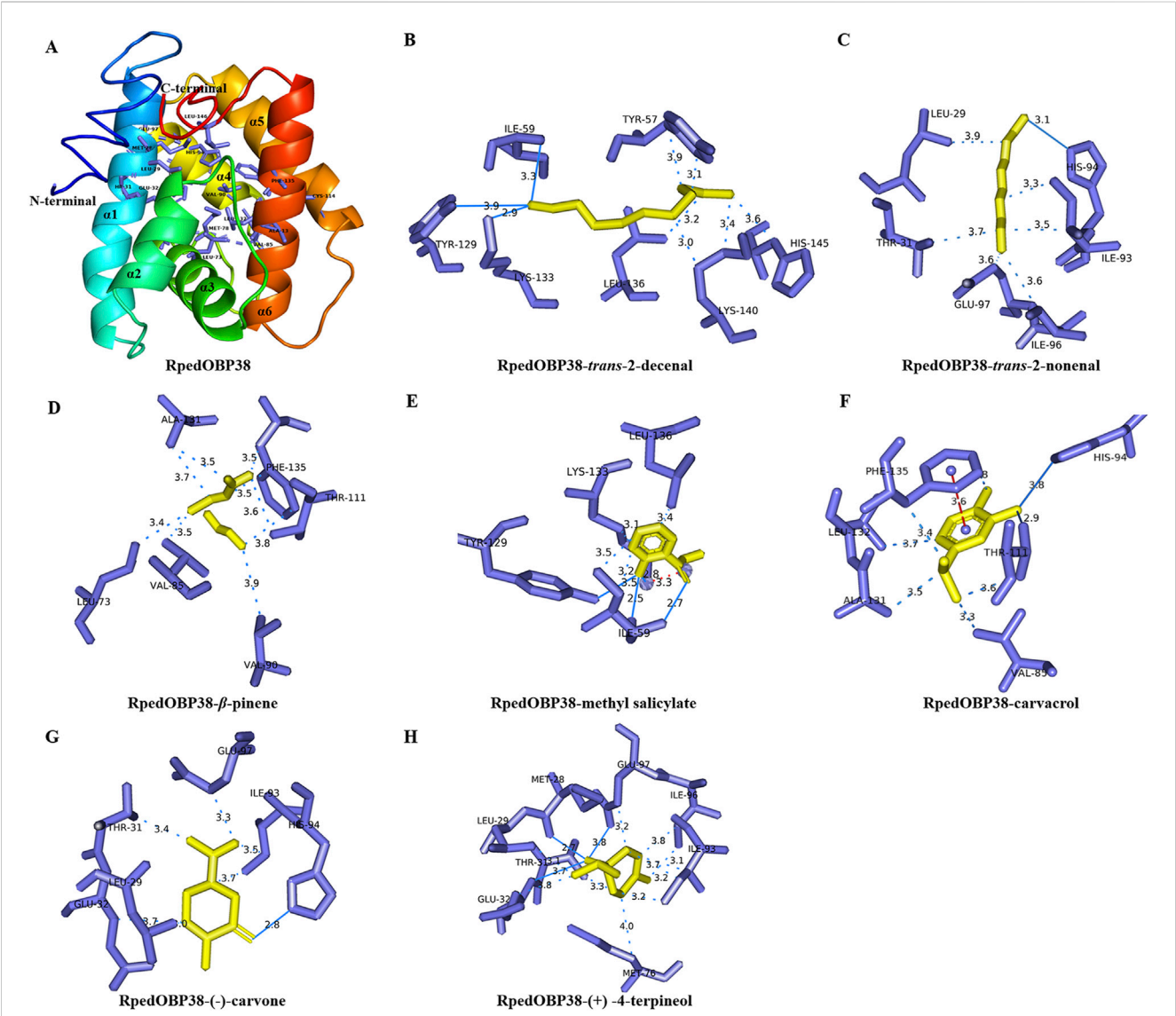


FIGURE 4 Molecular docking of ligands within the putative RpedOBP38 ligand binding pocket. (A) A structural model of RpedOBP38. The indicated amino acid residues correspond to key residues within the predicted RpedOBP38 pocket. (B–H) Molecular docking analyses for interactions between RpedOBP38 and *trans*-2-decenal (B), *trans*-2-nonenal (C), β -pinene (D), methyl salicylate (E), carvacrol (F) (–)-carvone (G), and (+) -4-terpineol (H). Hydrogen bonds are indicated with blue lines, while hydrophobic interactions are denoted using blue dashed lines, and π -stacking is represented using red dashed lines.

thereby informing functional analyses such that they have been widely used for characterizing insect OBPs (Chen et al., 2018; Zhang et al., 2022; Tang et al., 2023; Zhu et al., 2023). In this study, RpedOBP38 and YsigOBP15 from *Y. signatus* clustered together, suggesting their evolution from a shared ancestor and their potential for similar physiological functions. Analyzing the patterns of insect OBP expression across developmental stages and tissues is vital for the clarification of the physiological functions of these factors (Ju et al., 2014; Wang et al., 2019b; Li et al., 2020). In general, OBPs are likely to play a role in the recognition of chemical signals if they are expressed at high levels in antennae and other olfactory organs (Chen et al., 2018; Li et al., 2020; Hong et al., 2022; Zhang et al., 2022;

TABLE 2 Prediction of key amino acid residues involved in the docking of RpedOBP38 to different ligands.

Ligands	Binding energy (kcal/mol)	Closer contact interacting residues
β -pinene	−5.07	LEU73, VAL85, VAL90, THR111, ALA131, PHE135
methyl salicylate	−5.42	ILE59 , TYR129 , LYS133 , <i>LYS133</i> , LEU136
<i>trans</i> -2-nonenal	−4.20	LEU29, THR31, ILE93, HIS94 , ILE96, GLU97
<i>trans</i> -2-decenal	−5.17	TRY57, ILE59 , TYR129 , LYS133 , LEU136, LYS140, HIS145
(+)-4-terpineol	−5.30	MET28 , LEU29, THR31, GLU32 , MET76, ILE93, ILE96, GLU97
(−)-carvone	−5.71	LEU29, THR31, GLU32, ILE93, HIS94 , GLU97
carvacrol	−5.52	VAL85, HIS94 , THR111 , ALA131, LEU132, <i>PHE135</i>

Amino acids in bold font represent hydrogen bond, amino acids in italic represent π -stacking, and other amino acids represent hydrophobic interaction.

Tang et al., 2023). Higher levels of *RpedOBP38* expression were noted in the antennae relative to other tissues in this study, with no significant difference between females and males. This result was in line with a prior report by Li L. L. et al (2022), indicating that *RpedOBP38* may play an important role in the recognition of host volatiles and/or aggregation pheromones by *R. pedestris*. Other groups have also reported similar outcomes. For instance, Huang et al. (2018) reported the specific expression of *AipsOBP2* in *Agrotis ipsilon* antennae and found that it was capable of binding both host volatiles and sex pheromones. Cheng et al. (2020) additionally noted the strong binding of *SmosOBP12*, which was expressed at high levels in the antennae of female *Sitodiplosis mosellana*, to host volatiles derived from wheat including hexyl acetate and 3-hexanol. *R. pedestris* reportedly harbor many different olfactory sensors on their antennae (Kim et al., 2016), and are attracted to soybean-derived volatile compounds and aggregation pheromones released by conspecific males (Leal et al., 1995; Song et al., 2022). High levels of *RpedOBP38* expression were also noted in the adult stage, suggesting its potential involvement as a mediator of soybean volatile and aggregation pheromone recognition in *R. pedestris*.

Given the role that OBPs play as carriers in the context of chemical communication in insects, there is a need to clarify the affinity of these compounds for exogenous organic factors including pheromones and host-derived odorants, thereby potentially offering insight into the structural features of cognate ligands to guide reverse chemical ecology studies (D’Onofrio et al., 2020). Fluorescence competitive binding have been established as a reliable means of assessing *in vitro* binding between OBPs and their ligands (He et al., 2019; D’Onofrio et al., 2020). This approach has been successfully implemented across various species of insects including *Diaphorina citri* (Liu et al., 2021b), *Liomyza trifolii* (Zhang et al., 2022), *R. pedestris* (Zhu et al., 2022), *Bradysia odoriphaga* (Zhu et al., 2023), and *Hippodamia variegata* (Tang et al., 2023). In this study, the ability of *RpedOBP38* to bind to 11 green leaf volatiles, 11 soybean volatiles, 10 volatiles with repellent activity, and 4 aggregation pheromone compounds was assessed. In total, it was found to bind to three soybean volatiles (*trans*-2-decenal, *trans*-2-nonenal, methyl salicylate) and one green leaf volatile (β -pinene). Host plant volatiles have been shown to promote feeding, avoidance, oviposition, and a range of other behavioral responses (Anderson et al., 1993; Leal et al., 1994; Zhu et al., 2022). *RpedOBP38* may thus play a role in the detection of soybean volatiles, although behavioral and RNA interference assays will be necessary to confirm this

hypothesis. Zhu et al. (2022) previously demonstrated the ability of *RpedOBP4* to bind other soybean volatiles including 1-hexanol and *trans*-2-hexenyl acetate, supporting the potential involvement of multiple OBPs in the process of host plant recognition in line with what has been reported by Li et al. (2017). *RpedOBP38* was also able to bind less strongly to plant essential oil-derived volatiles with repellent activity ((+) -4-terpineol (−)-carvone, carvacrol) that exhibit high levels of repellency for various insect species (Quintana et al., 2009; Zhang et al., 2014). However, the binding affinity of *RpedOBP38* for tested aggregation pheromones was low ($K_i > 40 \mu\text{M}$), suggesting that binding to these compounds may be primarily mediated by other chemosensory proteins including *RpedCSP12* (Yin et al., 2023). Notably, *RpedOBP38* exhibited distinct binding affinity levels for certain isomers as in the case of (+) -4-terpineol ($K_i = 14.02 \mu\text{M}$) and (−) -4-terpineol ($K_i > 40 \mu\text{M}$), or (−)-carvone ($K_i = 27.22 \mu\text{M}$) and (+)-carvone ($K_i > 40 \mu\text{M}$). Factors including carbon chain length, conformational changes, and structural features can thus likely shape *RpedOBP38* binding affinity (Chen et al., 2018; Hong et al., 2022).

The physiological functions of a given protein are determined by its 3D structure, and insect OBPs generally harbor a hydrophobic cavity formed from multiple α -helices, with some of the amino acids therein facilitating interactions between these OBPs and their ligands (He et al., 2019; Zhang et al., 2020b; Yang et al., 2021; Zhu et al., 2023). Molecular modeling analyses performed herein revealed the presence of a hydrophobic binding pocket within *RpedOBP38* that was stabilized by six α -helices and three interlocking disulfide bridges. This is consistent with similar reports for *DcitOBP7* in *Diaphorina citri* (Liu et al., 2021a), and *PyasOBP2* in *Pachyrhinus yasumatsui* (Hong et al., 2022), suggesting that they may engage in similar ligand-binding mechanisms. Molecular docking analyses revealed negative binding energy values for interactions between *RpedOBP38* and seven analyzed ligands, implying strong protein-ligand interactions, consistent with the fluorescence competitive binding assay results. OBP-ligand binding is generally mediated by types of intermolecular forces including hydrogen bonds, van der Waals interactions, and hydrophobic interactions (Zhuang et al., 2014; Li et al., 2021; Hong et al., 2022). In this study, hydrogen bonds, hydrophobic interactions, and π -stacking were all found to shape *RpedOBP38*-ligand interactions, with molecular docking analyses also revealing the distribution of several polar (e.g., Lys133, Glu97, His 94, Thr31) and nonpolar (e.g., Ile59, Leu136, Val85, Phe135) residues within

the RpedOBP38 hydrophobic pocket jointly contributing to such intermolecular binding. This aligns well with other reports for insect OBPs, including the Val114, Thr9, and Val111 residues in *Grapholita Molesta* OBP2 (Li et al., 2016), Tyr77, Ile41, Ala116, and Lys38 in *Apibid Sitobion* OBP9 (Ullah et al., 2020), Leu33, Phe8, Met76, Ile30, Tyr47, Asp29, and Lys120 in *R. pedestris* OBP4 (Zhu et al., 2022), and Lys43, His64, and Leu42 in *H. variegata* OBP5 (Tang et al., 2023). Some of these amino acids were found to be capable of binding to more than one ligand, including Leu29, Thr31, His94, Glu97, Ile59, and Lys133, in line with what has previously been described in both *Athetis lepigone* (Li L. L. et al., 2022) and *R. pedestris* (Zhu et al., 2022). These residues may thus be particularly important mediators of RpedOBP38-ligand binding, highlighting an opportunity for site-directed mutagenesis to validate this hypothesis in the future (Zhu et al., 2020).

In summary, these experiments revealed that RpedOBP38, which was highly expressed in the antennae of adult *R. pedestris*, is a classical OBP family member that clusters most closely with YsigOBP15 from *Y. signatus*. Fluorescence competitive binding analyses demonstrated the ability of RpedOBP38 to bind strongly to two soybean volatiles (*trans*-2-decenal, $K_i = 7.440 \mu\text{M}$; *trans*-2-nonenal, $K_i = 10.973 \mu\text{M}$; methyl salicylate, $K_i = 21.065 \mu\text{M}$) and to bind strongly or moderately to volatiles associated with repellent activity ((+) -4-terpineol, $K_i = 14.017 \mu\text{M}$; carvacrol, $K_i = 19.456 \mu\text{M}$; (-)-carvone, $K_i = 27.215 \mu\text{M}$). Through 3D modeling and molecular docking analyses, RpedOBP38 was found to harbor six α -helices that form a stable hydrophobic binding pocket, with the Leu29, Thr31, His94, Glu97, Ile59, and Lys133 amino acid residues all playing key roles in the ability of this OBP to bind its ligands. Together, these results offer further insight into the mechanisms that govern olfactory recognition in *R. pedestris*. In order to more deeply elucidate the function of RpedOBP38, future studies are planned to analyse the exact role of RpedOBP38 in the recognition of more green leaf volatiles and soybean volatiles using a combination of behavioural experiments, electrophysiological experiments, and RNA inference (Zhu et al., 2022). Furthermore, we attempt to use RpedOBP38 as a control target, devise ecologically friendly behavioural inhibitors to disrupt the feeding behavior of *R. pedestris* and thus improve the management of *R. pedestris* (Zhu et al., 2022).

Data availability statement

The datasets presented in this study can be found in online repositories. The names of the repository/repositories and accession number(s) can be found in the article/Supplementary Material.

Ethics statement

The manuscript presents research on animals that do not require ethical approval for their study.

Author contributions

JG: Data curation, Formal Analysis, Funding acquisition, Visualization, Writing–original draft. PL: Methodology, Software, Validation, Visualization, Writing–original draft. XZ: Data curation, Formal Analysis, Software, Writing–original draft. JA: Data curation, Formal Analysis, Resources, Validation, Writing–review and editing. YL: Data curation, Validation, Writing–review and editing. TZ: Conceptualization, Investigation, Project administration, Writing–review and editing. ZG: Conceptualization, Funding acquisition, Investigation, Supervision, Writing–review and editing.

Funding

The author(s) declare that financial support was received for the research, authorship, and/or publication of this article. This work was supported by National Natural Science Foundation of China (32302358), HAAFS Agriculture Science and Technology Innovation Project (2022KJCXX-ZBS-4), Natural Science Foundation of Hebei Province (C2022301052), and Key research and Development Program of Hebei Province (22326513D).

Acknowledgments

We would like to thank all the reviewers who participated in the review during the preparation of this manuscript. We are also grateful to Hui-Fang Zhou from the Plant Protection Institute, Hebei Academy of Agricultural and Forestry Sciences, for her contribution in insect collection.

Conflict of interest

The authors declare that the research was conducted in the absence of any commercial or financial relationships that could be construed as a potential conflict of interest.

Publisher's note

All claims expressed in this article are solely those of the authors and do not necessarily represent those of their affiliated organizations, or those of the publisher, the editors and the reviewers. Any product that may be evaluated in this article, or claim that may be made by its manufacturer, is not guaranteed or endorsed by the publisher.

Supplementary material

The Supplementary Material for this article can be found online at: <https://www.frontiersin.org/articles/10.3389/fphys.2024.1475489/full#supplementary-material>

References

- Ahmed, T., Zhang, T., Wang, Z., He, K., and Bai, S. (2017). Molecular cloning, expression profile, odorant affinity, and stability of two odorant-binding proteins in *Macrocentrus cingulum* Brischke (Hymenoptera: braconidae). *Arch. Insect Biochem.* 94 (2), e21374. doi:10.1002/arch.21374
- Ahn, J. J., Choi, K. S., and Koh, S. (2020). Population parameters and growth of *Riptortus pedestris* (Fabricius) (Hemiptera: Alydidae) under elevated CO₂ concentrations. *Entomol. Res.* 51 (1), 12–23. doi:10.1111/1748-5967.12479
- Anderson, P., Hilker, M., Hansson, B. S., Bombosch, S., Klein, B., and Schildknecht, H. (1993). Oviposition deterring components in larval frass of *Spodoptera littoralis* (Boisd.) (Lepidoptera: noctuidae): a behavioural and electrophysiological evaluation. *J. Insect Physiol.* 39 (2), 129–137. doi:10.1016/0022-1910(93)90104-Y
- Bae, S., Yi, H., Yoon, Y., Jang, Y., Kim, Y., and Maharijan, R. (2019). Attraction of stink bugs to rocket traps with different combinations of wing and landing board color. *J. Asia-Pac. Entomol.* 22 (1), 243–249. doi:10.1016/j.aspen.2019.01.007
- Brito, N. F., Moreira, M., and Melo, A. C. A. (2016). A look inside odorant-binding proteins in insect chemoreception. *J. Insect Physiol.* 95 (6), 51–65. doi:10.1016/j.jinsphys.2016.09.008
- Campanacci, V., Krieger, J., Bette, S., Sturgis, J. N., Lartigue, A., Cambillau, C., et al. (2001). Revisiting the specificity of *Mamestra brassicae* and *Antheraea polyphemus* pheromone-binding proteins with a fluorescence binding assay. *J. Biol. Chem.* 276 (23), 20078–20084. doi:10.1074/jbc.M100713200
- Chen, X. L., Li, G. W., Xu, X. L., and Wu, J. X. (2018). Molecular and functional characterization of odorant binding protein 7 from the oriental fruit moth *Grapholita molesta* (Busck) (Lepidoptera: tortricidae). *Front. Physiol.* 9, 1762. doi:10.3389/fphys.2018.01762
- Cheng, W. N., Zhang, Y. D., Yu, J. L., Liu, W., and Zhu-Salzman, K. (2020). Functional analysis of odorant-binding proteins 12 and 17 from wheat blossom midge *Sitodiplosis mosellana* Géhin (Diptera: cecidomyiidae). *Insects* 11 (12), 891–906. doi:10.3390/insects11120891
- Cui, X. N., Liu, D. G., Sun, K. K., He, Y., and Shi, X. Q. (2018). Expression profiles and functional characterization of two odorant-binding proteins from the apple budpest beetle *Agrilus mali* (Coleoptera: buprestidae). *J. Econ. Entomol.* 11 (3), 1420–1432. doi:10.1093/jee/toy066
- Dong, Y. M., Huang, X. G., Yang, Y. X., Li, J. F., Zhang, M. Q., Shen, H., et al. (2022). Characterization of salivary secreted proteins that induce cell death from *Riptortus pedestris* (Fabricius) and their roles in insect-plant interactions. *Front. Plant Sci.* 13, 912603. doi:10.3389/fpls.2022.912603
- D'Onofrio, C., Zaremska, V., Zhu, J., Knoll, W., and Pelosi, P. (2020). Ligand-binding assays with OBPs and CSPs. *Method. Enzymol.* 642, 229–258. doi:10.1016/b.s.mie.2020.05.006
- Endo, N., Wada, T., and Sasaki, R. (2011). Seasonal synchrony between pheromone trap catches of the bean bug, *Riptortus pedestris* (Heteroptera: Alydidae) and the timing of invasion of soybean fields. *Appl. Entomol. Zool.* 46 (4), 477–482. doi:10.1007/s13355-011-0065-7
- Forêt, S., and Maleszka, R. (2006). Function and evolution of a gene family encoding odorant binding-like proteins in a social insect, the honey bee (*Apis mellifera*). *Genome Res.* 16 (11), 1404–1413. doi:10.1101/gr.5075706
- Gao, Y., Chen, J. H., and Shi, S. S. (2019). Research progress on soybean stink bug (*Riptortus pedestris*). *Chin. J. Oil Crop Sci.* 41 (5), 804–815. doi:10.19802/j.issn.1007-9084.2019033
- Guo, H., and Wang, C. Z. (2019). The ethological significance and olfactory detection of herbivore-induced plant volatiles in interactions of plants, herbivorous insects, and parasitoids. *Arthropod-Plant Inte* 13 (2), 161–179. doi:10.1007/s11829-019-09672-5
- Guo, J. L., An, J. J., Chang, H., Li, Y. F., Dang, Z. H., Wu, C., et al. (2023). The lethal and sublethal effects of lambda-cyhalothrin and emamectin benzoate on the soybean pest *Riptortus pedestris* (Fabricius). *Toxics* 11 (2), 971–989. doi:10.3390/toxics11120971
- He, P., Chen, G. L., Li, S., Wang, J., Ma, Y. F., Pan, Y. F., et al. (2019). Evolution and functional analysis of odorant binding proteins in three rice planthoppers: *Nilaparvata lugens*, *Sogatella furcifera*, and *Laodelphax striatellus*. *Pest Manag. Sci.* 75 (6), 1606–1620. doi:10.1002/ps.5277
- Hong, B., Chang, Q., Zhai, Y. Y., Ren, B. W., and Zhang, F. (2022). Functional characterization of odorant binding protein PysOBP2 from the jujube bud weevil, *Pachyrhinus ysumatsui* (Coleoptera: Curculionidae). *Front. Physiol.* 13, 900752. doi:10.3389/fphys.2022.900752
- Huang, G. Z., Liu, J. T., Zhou, J. J., Wang, Q., Dong, J. Z., Zhang, Y. J., et al. (2018). Expression and functional comparisons of two general odorant binding proteins in *Agrotis ipsilon*. *Insect biochem. molec.* 98, 34–47. doi:10.1016/j.ibmb.2018.05.003
- Hull, J. J., Perera, O. P., and Snodgrass, G. L. (2014). Cloning and expression profiling of odorant-binding proteins in the tarnished plant bug, *Lygus lineolaris*. *Insect Mol. Biol.* 23 (1), 78–97. doi:10.1111/imb.12064
- Jin, Y., Zhang, W. D., Dong, Y. M., and Xia, A. (2022). Feeding behavior of *Riptortus pedestris* (Fabricius) on soybean: electrical penetration graph analysis and histological investigations. *Insects* 13 (6), 511–523. doi:10.3390/insects13060511
- Ju, Q., Li, X., Jiang, X. J., Qu, M. J., Guo, X. Q., Han, Z. J., et al. (2014). Transcriptome and tissue-specific expression analysis of obp and csp genes in the Dark Black Chafer. *Arch. Insect Biochem.* 87 (4), 177–200. doi:10.1002/arch.21188
- Jung, M., and Lee, D. H. (2018). Characterization of overwintering behaviors and sites of bean bug, *Riptortus pedestris* (Hemiptera: Alydidae), under laboratory and field conditions. *Environ. Entomol.* 47 (5), 1280–1286. doi:10.1093/ee/nyy123
- Kim, J., Park, K. C., Roh, H. S., Kim, J., Oh, H. W., Kim, J. A., et al. (2016). Morphology and distribution of antennal sensilla of the bean bug *Riptortus pedestris* (Hemiptera: Alydidae): antennal sensilla of *R. pedestris*. *Microsc. Res. Tech.* 79 (6), 501–511. doi:10.1002/jemt.22658
- Leal, W. S. (2013). Odorant Reception in insects: roles of receptors, binding proteins, and degrading enzymes. *Annu. Rev. Entomol.* 58, 373–391. doi:10.1146/annurev-ento-120811-153635
- Leal, W. S., Barbosa, R. M. R., Xu, W., Ishida, Y., Syed, Z., Latte, N., et al. (2008). Reverse and conventional chemical ecology approaches for the development of oviposition attractants for *Culex mosquitoes*. *PLoS ONE* 3 (8), e3045. doi:10.1371/journal.pone.0003045
- Leal, W. S., Higuchi, H., Mizutani, N., Nakamori, H., Kadosawa, T., and Ono, M. (1995). Multifunctional communication in *Riptortus clavatus* (Heteroptera: Alydidae): conspecific nymphs and egg parasitoid *Ooencyrtus nezarae* use the same adult attractant pheromone as chemical cue. *J. Chem. Ecol.* 21 (7), 973–985. doi:10.1007/BF02033802
- Leal, W. S., Nikonova, L., and Peng, G. (1999). Disulfide structure of the pheromone binding protein from the silkworm moth, *Bombyx mori*. *FEBS Lett.* 464 (1–2), 85–90. doi:10.1016/S0014-5793(99)01683-X
- Leal, W. S., Ono, M., Hasegawa, M., and Sawada, M. (1994). Kairomone from dandelion, *Taraxacum officinale*, attractant for scarab beetle *Anomala octiescostata*. *J. Chem. Ecol.* 20 (7), 1697–1704. doi:10.1007/BF02059891
- Li, D. X., Li, C. B., and Liu, D. G. (2021). Analyses of structural dynamics revealed flexible binding mechanism for the *Agrilus mali* odorant binding protein 8 towards plant volatiles. *Pest Manag. Sci.* 77 (4), 1642–1653. doi:10.1002/ps.6184
- Li, G. W., Chen, X. L., Li, B. L., Zhang, G. H., Li, Y. P., and Wu, J. X. (2016). Binding properties of general odorant binding proteins from the oriental fruit moth, *Grapholita molesta* (Busck) (Lepidoptera: tortricidae). *PLoS ONE* 11 (5), e0155096. doi:10.1371/journal.pone.0155096
- Li, G. W., Du, J., Li, Y. P., and Wu, J. X. (2015). Identification of putative olfactory genes from the oriental fruit moth *Grapholita molesta* via an antennal transcriptome analysis. *PLoS ONE* 10 (11), e0142193. doi:10.1371/journal.pone.0142193
- Li, J. B., Yin, M. Z., Yao, W. C., Ma, S., Dewar, Y., Liu, X. Z., et al. (2022a). Genome-wide analysis of odorant-binding proteins and chemosensory proteins in the bean bug *Riptortus pedestris*. *Front. Physiol.* 13, 949607. doi:10.3389/fphys.2022.949607
- Li, K., Zhang, X. X., Guo, J. Q., Penn, H., Wu, T. T., Li, L., et al. (2019). Feeding of *Riptortus pedestris* on soybean plants, the primary cause of soybean staygreen syndrome in the Huang-Huai-Hai river basin. *Crop J.* 7 (3), 360–367. doi:10.1016/j.cj.2018.07.008
- Li, L. L., Huang, J. R., Xu, J. W., Yao, W. C., Yang, H. H., Shao, L., et al. (2022b). Ligand-binding properties of odorant binding protein 6 in *Aethis lepigone* to sex pheromones and maize volatiles. *Pest Manag. Sci.* 78 (1), 52–62. doi:10.1002/ps.6606
- Li, M. Y., Jiang, X. Y., Qi, Y. Z., Huang, Y. J., Li, S. G., and Liu, S. G. (2020). Identification and expression profiles of 14 odorant-binding protein genes from *Pieris rapae* (Lepidoptera: pieridae). *J. Insect Sci.* 20 (5), 2–10. doi:10.1093/jisesa/ieaa087
- Li, Z. Q., Zhang, S., Cai, X. M., Luo, J. Y., Dong, S. L., Cui, J. J., et al. (2017). Three odorant binding proteins may regulate the behavioural response of *Chrysopa pallens* to plant volatiles and the aphid alarm pheromone (E)- β -farnesene. *Insect Mol. Biol.* 26 (3), 255–265. doi:10.1111/imb.12295
- Liu, J. B., Liu, J., Yi, J. Q., Mao, Y. K., Li, J. H., Sun, D. L., et al. (2021). Transcriptome characterization and expression analysis of chemosensory genes in *Chilo sacchariphagus* (Lepidoptera Crambidae), a key pest of sugarcane. *Front. Physiol.* 12, 636353. doi:10.3389/fphys.2021.636353
- Liu, Q., Yin, M. Z., Ma, S., Gu, N., Qian, L. F., Zhang, Y. N., et al. (2023). Ligand-binding properties of chemosensory protein 1 in *Callosobruchus chinensis* to mung bean volatiles. *Pestic. Biochem. Phys.* 192, 105394. doi:10.1016/j.pestbp.2023.105394
- Liu, X. Q., Jiang, H. B., Fan, J. Y., Liu, T. X., Meng, L. W., Liu, Y., et al. (2021). An odorant-binding protein of Asian citrus psyllid, *Diaphorina citri*, participates in the response of host plant volatiles. *Pest Manag. Sci.* 77 (7), 3068–3079. doi:10.1002/ps.6352
- Mainali, B. P., Kim, H. J., Yoon, Y. N., Oh, I. S., and Bae, S. D. (2014). Evaluation of different leguminous seeds as food sources for the bean bug *Riptortus pedestris*. *J. Asia-Pacific Entomol.* 17 (2), 115–117. doi:10.1016/j.aspen.2013.11.007
- Manoharan, M., Chong, M. N. F., Vaitinadapoulou, A. G., Etienne, F., Sowdhamini, R., and Bernard, O. (2013). Comparative genomics of odorant binding proteins in *Anopheles gambiae*, *Aedes aegypti*, and *Culex quinquefasciatus*. *Genome Biol. Evol.* 5 (1), 163–180. doi:10.1093/gbe/evs131

- Martin, J. P., Beyerlein, A., Dacks, A. M., Reisenman, C. E., Riffell, J. A., Lei, H., et al. (2011). The neurobiology of insect olfaction: sensory processing in a comparative context. *Prog. Neurobiol.* 95 (3), 427–447. doi:10.1016/j.pneurobio.2011.09.007
- O'Boyle, N. M., Bank, M., James, C. A., Morley, C., Vandermeersch, T., and Hutchison, G. R. (2011). Open babel: an open chemical toolbox. *J. cheminformatics* 3 (1), 33. doi:10.1186/1758-2946-3-33
- Paula, D. P., Togawa, R., Costa, M., Grynberg, P., Martins, N. F., and Andow, D. (2018). Systemic and sex-biased regulation of OBP expression under semiochemical stimuli. *Sci. Rep.* 8 (1), 6035. doi:10.1038/s41598-018-24297-z
- Pelosi, P., Iovinella, I., Zhu, J., Wang, G., and Dani, F. (2018). Beyond chemoreception: diverse tasks of soluble olfactory proteins in insects. *Biol. Rev.* 93 (1), 184–200. doi:10.1111/brv.12339
- Pelosi, P., Mastrogiamoco, R., Iovinella, I., Tuccori, E., and Persaud, K. C. (2014). Structure and biotechnological applications of odorant-binding proteins. *Appl. Microbiol. Biot.* 98 (1), 61–70. doi:10.1007/s00253-013-5383-y
- Pelosi, P., Zhou, J., Ban, L., and Calvello, M. (2006). Soluble proteins in insect chemical communication. *Cell. Mol. Life Sci.* 63 (14), 1658–1676. doi:10.1007/s00018-005-5607-0
- Pregitzer, P., Zielonka, M., Eichhorn, A. S., Jiang, X., Krieger, J., and Breer, H. (2018). Expression of odorant-binding proteins in mouthpart palps of the desert locust *Schistocerca gregaria*. *Insect Mol. Biol.* 28 (2), 264–276. doi:10.1111/imb.12548
- Quintana, L. S. N., Olivero-Verbel, J., and Stashenko, E. (2009). Repellent activity of essential oils: a review. *Bioresour. Technol.* 101 (1), 372–378. doi:10.1016/j.biortech.2009.07.048
- Rihani, K., Ferreux, J. F., and Briand, L. (2021). The 40-year mystery of insect odorant-binding proteins. *Biomolecules* 11 (4), 509–536. doi:10.3390/biom11040509
- Roh, G. H., Cha, D. H., and Park, C. G. (2021). Olfactory attraction to aggregation pheromone is mediated by distal flagellum of antennal segments in *Riptortus pedestris*. *J. Asia-Pacific Entomol.* 24 (1), 415–420. doi:10.1016/j.aspen.2021.01.005
- Scaloni, A., Monti, M., Angeli, S., and Pelosi, P. (1999). Structural analysis and disulfide-bridge pairing of two odorant-binding proteins from *Bombyx mori*. *Biochem. Biophys. Res. Commun.* 266 (2), 386–391. doi:10.1006/bbrc.1999.1791
- Song, J. Y., Lee, G., Jung, J., Moon, J. K., and Kim, S. G. (2022). Effect of soybean volatiles on the behavior of the bean bug, *Riptortus pedestris*. *J. Chem. Ecol.* 48 (2), 207–218. doi:10.1007/s10886-021-01343-1
- Sparks, J. T., Bohbot, J. D., and Dickens, J. C. (2014). The genetics of chemoreception in the labella and tarsi of *Aedes aegypti*. *Insect biochem. molec.* 48 (1), 8–16. doi:10.1016/j.ibmb.2014.02.004
- Spinelli, S., Lagarde, A., Iovinella, I., Legrand, P., Tegoni, M., Pelosi, P., et al. (2012). Crystal structure of *Apis mellifera* OBP14, a C-minus odorant-binding protein, and its complexes with odorant molecules. *Insect biochem. molec.* 42 (1), 41–50. doi:10.1016/j.ibmb.2011.10.005
- Sun, Y. F., Qiao, H. L., Ling, Y., Yang, S. X., Rui, C. H., Pelosi, P., et al. (2011). New analogues of (E)- β -farnesene with insecticidal activity and binding affinity to aphid odorant-binding proteins. *J. Agric. Food Chem.* 59 (6), 2456–2461. doi:10.1021/jf104712c
- Sun, Y. L., Huang, L. Q., Pelosi, P., and Wang, C. Z. (2012). Expression in antennae and reproductive organs suggests a dual role of an odorant-binding protein in two sibling *Helicoverpa* species. *PLoS ONE* 7 (1), e30040. doi:10.1371/journal.pone.0030040
- Tang, H. Y., Xie, J. X., Liu, J. T., Khashaveh, A., Liu, X. X., Yi, C. Q., et al. (2023). Odorant-binding protein HvarOBP5 in ladybird *Hippodamia variegata* regulates the perception of semiochemicals from preys and habitat plants. *J. Agric. Food Chem.* 71 (2), 1067–1076. doi:10.1021/acs.jafc.2c07355
- Trott, O., and Olson, A. J. (2010). AutoDock Vina: improving the speed and accuracy of docking with a new scoring function, efficient optimization, and multithreading. *J. Comput. Chem.* 31 (2), 455–461. doi:10.1002/jcc.21334
- Ullah, R. M. K., Quershi, S. R., Adeel, M. M., Abdelnabby, H., Waris, M. I., Duan, S. G., et al. (2020). An odorant binding protein (SaveOBP9) involved in chemoreception of the wheat aphid *Sitobion avenae*. *Int. J. Mol. Sci.* 21 (21), 8331. doi:10.3390/ijms21218331
- Venthur, H., Mutis, A., Zhou, J., and Quiroz, A. (2014). Ligand binding and homology modelling of insect odorant-binding proteins. *Physiol. Entomol.* 39 (3), 183–198. doi:10.1111/phen.12066
- Venthur, H., and Zhou, J. (2018). Odorant receptors and odorant-binding proteins as insect pest control targets: a comparative analysis. *Front. Physiol.* 9, 1163. doi:10.3389/fphys.2018.01163
- Vogt, R. G., and Riddiford, L. M. (1981). Pheromone binding and inactivation by moth antennae. *Nature* 293 (5828), 161–163. doi:10.1038/293161a0
- Wang, B., Dong, W. Y., Li, H. M., D'Onofrio, C., Bai, P. H., Chen, R. P., et al. (2022). Molecular basis of (E)- β -farnesene-mediated aphid location in the predator *Eupeodes corollae*. *Curr. Biol.* 32 (5), 951–962.e7. doi:10.1016/j.cub.2021.12.054
- Wang, J. Z., Peng, G., Luo, Y. Q., and Tao, J. (2019). Characterization and expression profiling of odorant-binding proteins in *Anoplophora glabripennis* Motsch. *Gene* 693 (1), 25–36. doi:10.1016/j.gene.2018.12.075
- Wang, L., Bi, Y. D., Liu, M., Li, W., Liu, M., Di, S. F., et al. (2019). Identification and expression profiles analysis of odorant-binding proteins in soybean aphid, *Aphis glycines* (Hemiptera: aphididae). *Insect Sci.* 27 (5), 1019–1030. doi:10.1111/1744-7917.12709
- Wang, L. Y., Liu, Q. Y., Guo, P., Gao, Z. L., Chen, D., Zhang, T., et al. (2023). Evaluation of reference genes for quantitative real-time PCR analysis in the bean bug, *Riptortus pedestris* (Hemiptera: Alydidae). *Insects* 14 (12), 960–973. doi:10.3390/insects14120960
- Xiao, Y., Sun, L., Wu, Y. H., Wang, Q., Zhang, Y. J., Jing, X. F., et al. (2023). The larvae of *Phyllotreta striolata* share the same olfactory cues for locating Brassicaceae plant with conspecific adults. *J. Pest Sci.* 97 (2), 979–992. doi:10.1007/s10340-023-01690-w
- Yang, Y. T., Luo, L., Tian, L. X., Zhao, C. W., Niu, H. L., Hu, Y. F., et al. (2021). Function and characterization analysis of BodoOBP8 from *Bradysia odoriphaga* (Diptera: sciaridae) in the recognition of plant volatiles and sex pheromones. *Insects* 12 (10), 879–891. doi:10.3390/insects12100879
- Yasuda, T., Mizutani, N., Honda, Y., Endo, N., Yamaguchi, T., Moriya, S., et al. (2007). A supplemental component of aggregation attractant pheromone in the bean bug *Riptortus clavatus* (Thunberg) (Heteroptera: Alydidae), related to food exploitation. *Appl. Entomol. Zool.* 42 (1), 161–166. doi:10.1303/aez.2007.161
- Yin, M. Z., Li, J. Q., Liu, Q., Ma, S., Hu, Z. Z., Liu, X. Z., et al. (2023). Binding properties of chemosensory protein 12 in *Riptortus pedestris* to aggregation pheromone (E)-2-hexenyl (Z)-3-hexenoate. *Pestic. Biochem. Phys.* 194, 105513. doi:10.1016/j.pestbp.2023.105513
- Zeng, Y., Yang, Y. T., Wu, Q. J., Wang, S. L., Xie, W., and Zhang, Y. J. (2019). Genome-wide analysis of odorant-binding proteins and chemosensory proteins in the sweet potato whitefly, *Bemisia tabaci*. *Insect Sci.* 26 (4), 620–634. doi:10.1111/1744-7917.12576
- Zhang, F. M., Merchant, A., Zhao, Z. B., Zhang, Y. H., Zhang, J., Zhang, Q. W., et al. (2020). Characterization of MaltOBP1, a minus-c odorant-binding protein, from the Japanese pine sawyer beetle, *Monochamus alternatus* Hope (Coleoptera: cerambycidae). *Front. Physiol.* 11, 212. doi:10.3389/fphys.2020.00212
- Zhang, J., Luo, D., Wu, P., Li, H. Z., Zhang, H. Y., and Zheng, W. W. (2018). Identification and expression profiles of novel odorant binding proteins and functional analysis of OBP99a in *Bactrocera dorsalis*. *Arch. Insect Biochem.* 98 (1), e21452. doi:10.1002/arch.21452
- Zhang, Q. H., Schneidmiller, R., and Hoover, D. (2013). Essential oils and their compositions as spatial repellents for pestiferous social wasps. *Pest Manag. Sci.* 69 (4), 542–552. doi:10.1002/ps.3411
- Zhang, Q. H., Schneidmiller, R. G., Hoover, D. R., Zhou, G. J., Margaryan, A., and Bryant, P. (2014). Essential oils as spatial repellents for the brown marmorated stink bug, *Halyomorpha halys* (Stål) (Hemiptera: pentatomidae). *J. Appl. Entomol.* 138 (7), 490–499. doi:10.1111/jen.12101
- Zhang, Q. K., Li, Z. B., Chen, D. K., Wu, S. Y., Wang, H. H., Li, Y. L., et al. (2022). The molecular identification, odor binding characterization, and immunolocalization of odorant-binding proteins in *Liriomyza trifolii*. *Pestic. Biochem. Phys.* 181 (6), 105016. doi:10.1016/j.pestbp.2021.105016
- Zhang, X., Huang, C., Wu, Q., Yang, N. W., Qian, W. Q., and Wan, F. H. (2021). Advances in the study of general odorant binding proteins in insects. *J. Biosaf.* 30 (1), 11–19. doi:10.3969/j.issn.2095-1787.2021.01.003
- Zhang, X. Q., Yan, Q., Li, L. L., Xu, J. W., Mang, D. Z., Wang, X. L., et al. (2020). Different binding properties of two general-odorant binding proteins in *Aethis lepigone* with sex pheromones, host plant volatiles and insecticides. *Pestic. Biochem. Phys.* 164, 173–182. doi:10.1016/j.pestbp.2020.01.012
- Zheng, W., Zhang, C. X., Li, Y., Pearce, R., Bell, E. W., and Zhang, Y. (2021). Folding non-homologous proteins by coupling deep-learning contact maps with I-TASSER assembly simulations. *Cell Rep. Methods* 1, 100014. doi:10.1016/j.crmeth.2021.100014
- Zhou, J. J., Field, L., and He, X. L. (2010). Insect odorant-binding proteins: do they offer an alternative pest control strategy? *Outlooks Pest Manag.* 21 (1), 31–34. doi:10.1564/21feb08
- Zhou, X., Wang, Z., Cui, G. C., Du, Z. M., Qian, Y. L., Yang, S. M., et al. (2022). Binding properties of odorant-binding protein 4 of *Tirathaba rufivena* to areca catechu volatiles. *Plants* 11 (2), 167–178. doi:10.3390/plants11020167
- Zhu, J., Zaremska, V., D'Onofrio, C., Knoll, W., and Pelosi, P. (2020). Site-directed mutagenesis of odorant-binding proteins. *Method. Enzymol.* 642, 301–324. doi:10.1016/b.s.mie.2020.05.014
- Zhu, J. Q., Wang, F., Zhang, Y. J., Yang, Y. T., and Hua, D. K. (2023). Odorant-binding protein 10 from *Bradysia odoriphaga* (Diptera: sciaridae) binds volatile host plant compounds. *J. Insect Sci.* 23 (1), 7–8. doi:10.1093/jisesa/iead004
- Zhu, X. Y., Li, J. B., Liu, L., Dewar, Y., Zhang, H., Zhang, H. R., et al. (2022). Binding properties of odorant-binding protein 4 from bean bug *Riptortus pedestris* to soybean volatiles. *Insect Mol. Biol.* 31 (6), 760–771. doi:10.1111/imb.12802
- Zhuang, X., Wang, Q., Wang, B., Zhong, T., Cao, Y., Li, K. B., et al. (2014). Prediction of the key binding site of odorant-binding protein of *Holotrichia obliqua* Faldermann (Coleoptera: scarabaeidae). *Insect Mol. Biol.* 23 (3), 381–390. doi:10.1111/imb.12088



OPEN ACCESS

EDITED BY

Marcelo Salabert Gonzalez,
Fluminense Federal University, Brazil

REVIEWED BY

Phillip Obed Yobe Nkunka,
University of Zambia, Zambia
Haq Abdul Shaik,
Academy of Sciences of the Czech Republic
(ASCR), Czechia

*CORRESPONDENCE

Hamzeh Izadi,
✉ izadi@vru.ac.ir

RECEIVED 12 December 2024

ACCEPTED 24 February 2025

PUBLISHED 14 March 2025

CITATION

Izadi H (2025) Endocrine and enzymatic shifts during insect diapause: a review of regulatory mechanisms.

Front. Physiol. 16:1544198.

doi: 10.3389/fphys.2025.1544198

COPYRIGHT

© 2025 Izadi. This is an open-access article distributed under the terms of the [Creative Commons Attribution License \(CC BY\)](#). The use, distribution or reproduction in other forums is permitted, provided the original author(s) and the copyright owner(s) are credited and that the original publication in this journal is cited, in accordance with accepted academic practice. No use, distribution or reproduction is permitted which does not comply with these terms.

Endocrine and enzymatic shifts during insect diapause: a review of regulatory mechanisms

Hamzeh Izadi*

Department of Plant Protection, Faculty of Agriculture, Vali-e-Asr University of Rafsanjan, Rafsanjan, Iran

Insect diapause is a vital survival strategy that enables insects to enter a state of suspended development, allowing them to withstand unfavorable environmental conditions. During diapause, insects significantly lower their metabolic rate and build up energy reserves, which they gradually utilize throughout this period. The regulation of diapause involves a complex interaction of hormones and enzymes. Juvenile hormones (JHs) affect adults and larvae differently; in adults, the absence of JH typically triggers diapause, while in larvae, the presence of JH encourages this state. Ecdysteroids, which regulate molting and metamorphosis, are carefully controlled to prevent premature development. Reduced signaling of insulin-like peptides enhances stress resistance and promotes energy storage. Several enzymes play crucial roles in the metabolic adjustments necessary for diapause. These adjustments include the degradation of JH, the ecdysteroidogenic pathway, and the metabolism of fatty acids, glycogen, cryoprotectants, and stress responses. Understanding diapause's molecular and biochemical mechanisms is essential for fundamental entomological research and practical applications. Despite recent advances, many aspects of diapause regulation, especially the interactions among hormonal pathways and the role of enzymes, remain poorly understood. This review analyzes approximately 250 papers to consolidate current knowledge on the enzymatic and hormonal regulation of diapause. It offers a comprehensive overview of key processes based on recent studies and suggests future research directions to fill gaps in our understanding of this significant biological phenomenon. The review also lays the groundwork for enhancing pest control strategies and ecological conservation by deepening our understanding of diapause mechanisms.

KEYWORDS

diapause, enzymes, hormones, cold tolerance, cryophysiology, dormancy

Introduction

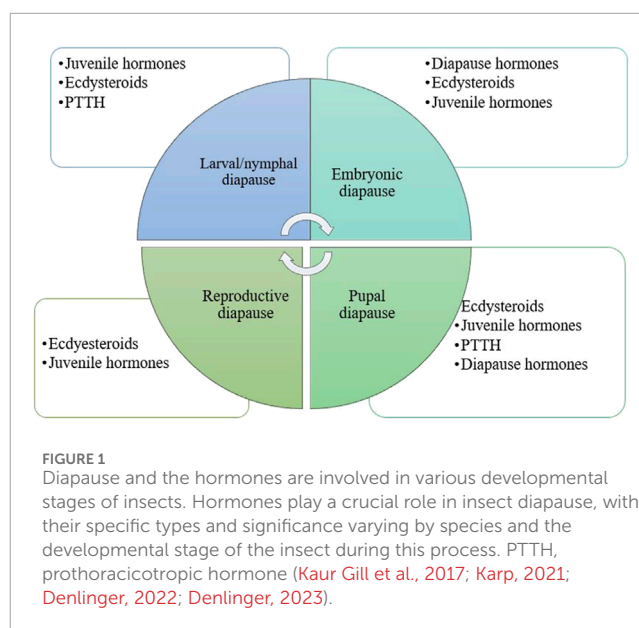
Diapause

Insects have developed various survival strategies to cope with unfavorable environmental conditions, with diapause being one of the most remarkable (Denlinger, 2023). Diapause is a developmental arrest involving significant metabolic suppression. This adaptive trait is ecologically important as it synchronizes the insect's life cycles with optimal environmental conditions, playing a crucial role in species distribution and

evolution (Hand et al., 2016; Kaur Gill et al., 2017; Tougeron, 2019). A complex interaction of genetic, hormonal, and enzymatic mechanisms controls the regulation of diapause. Environmental signals, such as photoperiod and temperature, act as primary cues for initiating diapause. These signals are translated into physiological responses through hormonal systems, including juvenile hormones (JHs), ecdysteroids, and insulin-like peptides (ILPs). Enzymatic pathways and hormonal signals are intricately interconnected during insect diapause, collaboratively regulating metabolic suppression, enhancing stress resistance, and arresting development. Hormones serve as master regulators, with enzymatic pathways acting as effectors to precisely initiate, maintain, and terminate diapause. Additionally, dynamic feedback loops and crosstalk between hormonal signals and enzymatic activities tightly coordinate this process. The delicate balance between hormonal modulation and enzymatic regulation is critical for diapause survival and successful post-diapause reactivation (Kaur Gill et al., 2017; Roncalli et al., 2021; Lebenzon et al., 2022; Denlinger, 2023). Key enzymatic pathways involved in diapause include lipid metabolism, glycogen storage, and the synthesis of cryoprotectants such as trehalose, glycerol, and sorbitol. These molecules prevent cellular damage during prolonged periods of environmental stress, such as freezing or desiccation. Additionally, antioxidant enzymes play a vital role in neutralizing reactive oxygen species (ROS) generated during metabolic suppression, safeguarding cellular integrity (Weber et al., 1967; Shinoda and Itoyama, 2003; Tollarova, 2008; Niwa and Niwa, 2014; Denlinger, 2023). Despite decades of research, many aspects of the molecular and biochemical regulation of diapause remain poorly understood. Existing studies often focus on specific species or limited aspects of diapause regulation, leaving gaps in our understanding of how hormonal and enzymatic pathways interact to maintain diapause and respond to environmental changes. This knowledge is not only theoretically important but also has practical implications. Insights into the mechanisms of diapause can enhance pest management strategies by predicting periods of insect vulnerability and improving the overwintering success of beneficial insects used in biological control. This review brings together current knowledge on hormonal and enzymatic regulation of diapause, focusing on their roles in metabolic adjustment, stress tolerance, and developmental arrest. By integrating recent findings, the manuscript aims to identify key gaps in understanding and propose future directions for research in this rapidly evolving field.

Diapause and insect's developmental stage

Diapause can occur at any developmental stage of insects (Figure 1). Embryonic diapause is a phase of halted development in embryogenesis that many insect species use to synchronize egg hatching with the most favorable conditions. A dramatic reduction or complete cessation of mitotic activity characterizes the process. Embryonic diapause can happen during any stage of embryonic development (Karp, 2021). Reproductive diapause is a cessation of reproduction that marks adult diapause (Hodek, 2012). It is a prevalent photoperiodic regulation in insects, with both males and females entering diapause in many species. During diapause, females have small ovaries with oocytes containing little or no yolk,



while the development of the male accessory glands is typically suppressed. Mating behavior is largely suppressed during diapause, with many species typically mating in the spring after diapause ends (Nadeau et al., 2022). Hormonal regulation of adult diapause entails an intricate interaction of multiple hormones, particularly ecdysteroids and juvenile hormones (Ma et al., 2021a; 2021b). In addition to hormones, various other factors such as energy sensing, stress response, insulin-like signaling, and the TOR pathway can also affect the reproductive diapause of insects (Eustice et al., 2022). During immature stages, diapause significantly slows or stops development. This type of diapause may occur during the larval, nymphal, or pupal stages. Larval diapause is frequently observed in the life cycles of holometabolous insects, especially in lepidopteran, coleopteran, hymenopteran, and some dipteran species (Dittmer and Brucker, 2021). Nymphal diapause is well-studied in hemipteran species (Zhai et al., 2017). During pupal diapause, there are strong gene expression dynamics, revealing a preprogrammed transcriptional landscape that is active in the winter (Pruisscher et al., 2022).

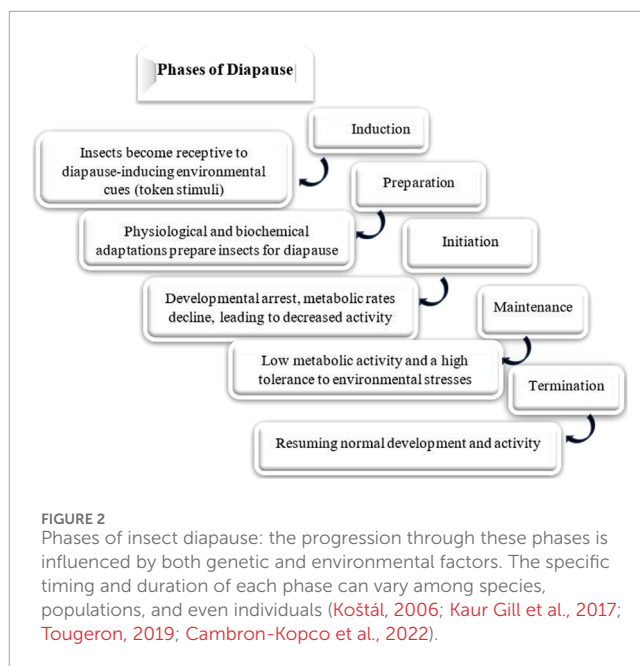
Ecophysiological phases of diapause

Diapause encompasses several ecophysiological phases: induction, preparation, initiation, maintenance, termination, and post-diapause, all regulated by exogenous and endogenous factors. These phases are marked by shifts in metabolic rates and physiological adaptations (Figure 2) (Košťál, 2006). The process of entering diapause begins with an insect responding to environmental signals, such as photoperiod, temperature, and food availability. This phase involves halting morphological development, changes in coloration or behavior, and secretion of specialized enzymes or hormones. Nutrient reserves, including lipids, proteins, and carbohydrates, are accumulated to sustain energy demands during diapause. Moreover, metabolism shifts from energy-intensive growth to glycolysis and gluconeogenesis, helping

conserve energy (Figures 3A,B) (Cambron-Kopco et al., 2022; Denlinger, 2023; Dong et al., 2019; Han and Bauce, 1998; Košťál, 2006; Košťál et al., 2017). The physiological mechanisms regulating nutrient homeostasis during diapause include pathways such as insulin signaling, AMP-activated protein kinase, and adipokinetic hormones (Hahn and Denlinger, 2007). While the biochemical pathways remain incompletely understood, nutrient storage directly influences diapause onset, duration, and post-diapause fitness (Batz and Armbruster, 2018; Short and Hahn, 2023). During diapause maintenance, insects experience metabolic depression and developmental arrest, relying on stored energy reserves, primarily lipids (Lehmann et al., 2016). Sensitivity to environmental cues increases as this phase progresses, signaling the approach of diapause termination (Košťál, 2006). Energy conservation is critical, with metabolic resources carefully managed to ensure survival and support post-diapause development. The use of stored nutrients, especially glycogen, also facilitates cryoprotectant production to mitigate the effects of low temperatures (Hahn and Denlinger, 2010). Genetic factors, metabolic processes, and environmental conditions influence diapause termination. However, it is often simply a consequence of the passage of time (Figure 4) (Robbins et al., 2010; Ragland et al., 2019; Poitou et al., 2020). The successful transition out of diapause depends on sufficient energy reserves to fuel post-diapause recovery and growth. The precise timing of diapause termination is key to optimizing survival and distribution (Arrese and Soulages, 2010; Hahn and Denlinger, 2010; 2007; Xu et al., 2021). Diapause termination in insects involves shifts in energy metabolism. They move from a state of metabolic depression to increased respiratory activity, which helps meet the higher energy demands for movement, feeding, and reproduction (Jiang et al., 2010; Dong et al., 2019; Karp, 2021). These changes involve elevated metabolic rates regulated by various hormones and enzymes that control energy production and utilization. Additionally, diapause termination is linked to resource allocation and morphogenesis, underscoring the importance of metabolic regulation during this phase. Proper coordination of these processes ensures a successful transition from dormancy to full physiological activity, allowing the insect to re-enter its life cycle and meet ecological challenges effectively (Jiang et al., 2010; Dong et al., 2019; Karp, 2021).

Enzyme activity during diapause

The biochemical processes that enable insect diapause represent a sophisticated strategy that underscores the complexity of diapause and offers insights into its broader ecological and evolutionary significance (Hahn and Denlinger, 2010). Enzymes, proteins that serve as catalysts, play a vital role in maintaining cellular processes and functions (Piumetti and Illanes, 2022). During diapause, the activity of certain enzymes including those involved in glycogen and lipid metabolism, and protein synthesis, is known to be altered to support the metabolic slowdown (Figures 5, 6) (Hahn and Denlinger, 2010). Some enzymes, especially those related to stress responses, remain active during diapause, helping insects survive harsh conditions. The specific enzymes involved in insect diapause vary depending on the insect species and their diapause strategy. Enzymes that play a role in insect



diapause can be classified according to their activity and the biological processes they regulate (Table 1). These enzymes facilitate metabolic adjustments, energy conservation, stress resistance, and other physiological changes essential for diapause. This review focuses on enzymatic pathways related to hormonal regulation, glycogen metabolism, cryoprotectant synthesis, and oxidative stress during diapause.

Hormones, diapause, and regulatory enzymes

The initiation and regulation of diapause are controlled by complex hormonal and enzymatic processes. The production and breakdown of hormones linked to insect diapause require the involvement of multiple enzymes. Understanding these hormonal processes and the related enzymes is crucial for understanding how insects adjust to seasonal changes, and could provide insights into how diapause is initiated and sustained. The primary hormones involved in diapause regulation are prothoracicotropic hormones (PTTHs), juvenile hormones (JHs), diapause hormones (DHs), and ecdysteroids (Renfree and Shaw, 2000; Denlinger, 2002; Hand et al., 2016; Harsimran et al., 2017).

Juvenile hormones

Juvenile hormones (JHs) are sesquiterpenoid hormones produced by the corpora allata, critically regulating insect development, reproduction, and diapause. During diapause, JH levels are typically suppressed, leading to the arrest of reproductive and developmental processes, particularly in species undergoing adult diapause (JH level is usually high during larval diapause). This suppression is mediated by the enhanced activity of JH-degrading enzymes, including juvenile hormone esterase (JHE) (Figure 7) (Table 2) and juvenile hormone epoxide (JHEH) hydrolase (Huttilz, 2022). For example, in *Coccinella septempunctata*, increased JHE and JHEH activity correlates with ovarian dormancy and suppressed reproductive behavior (Li et al., 2022). Similarly, in *Ostrinia nubilalis*, JHE is the key enzyme controlling JH catabolism

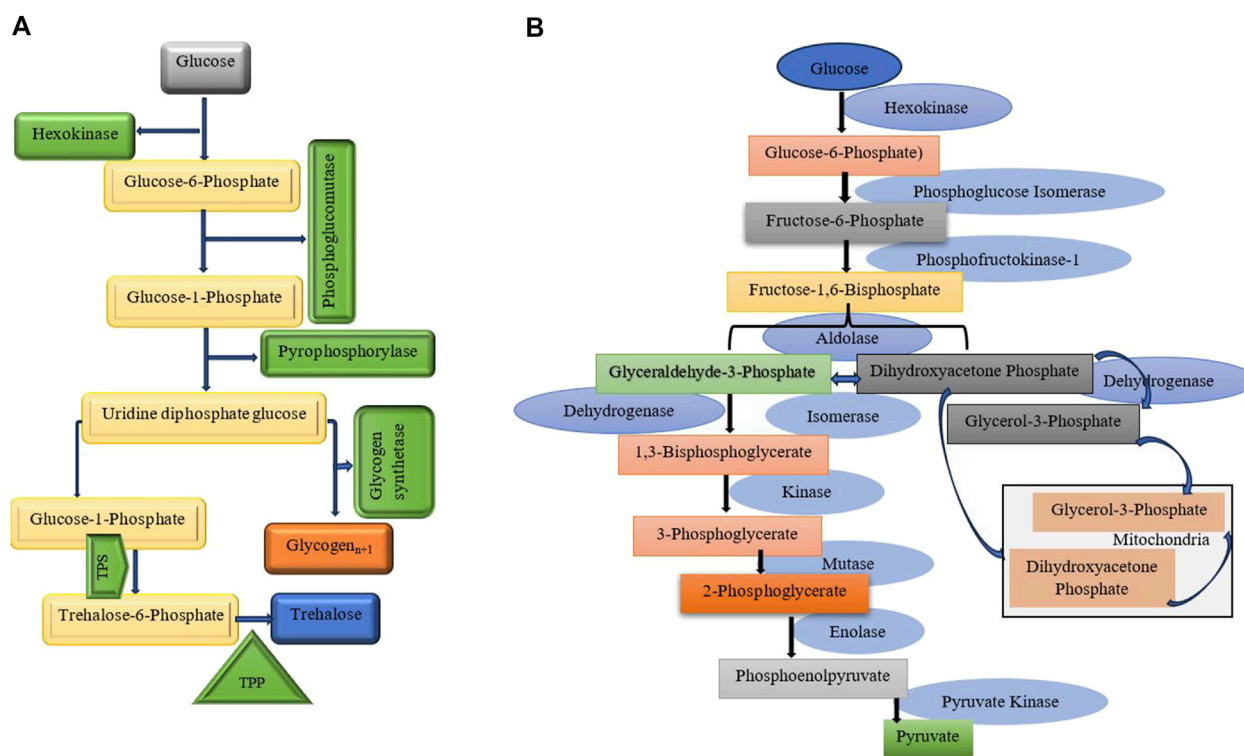
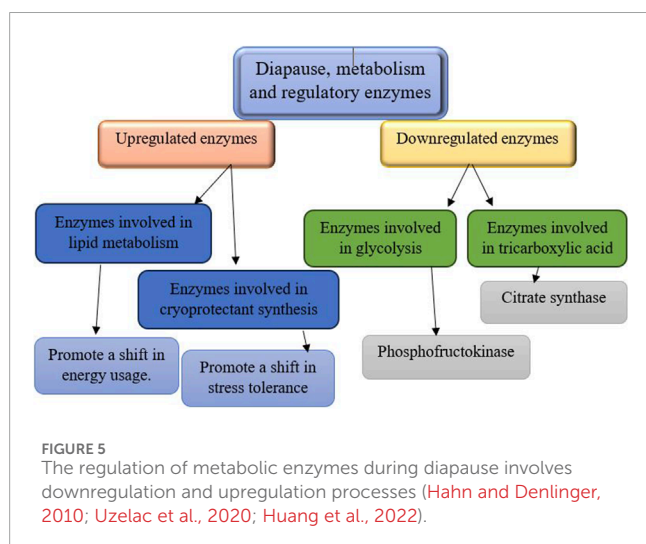
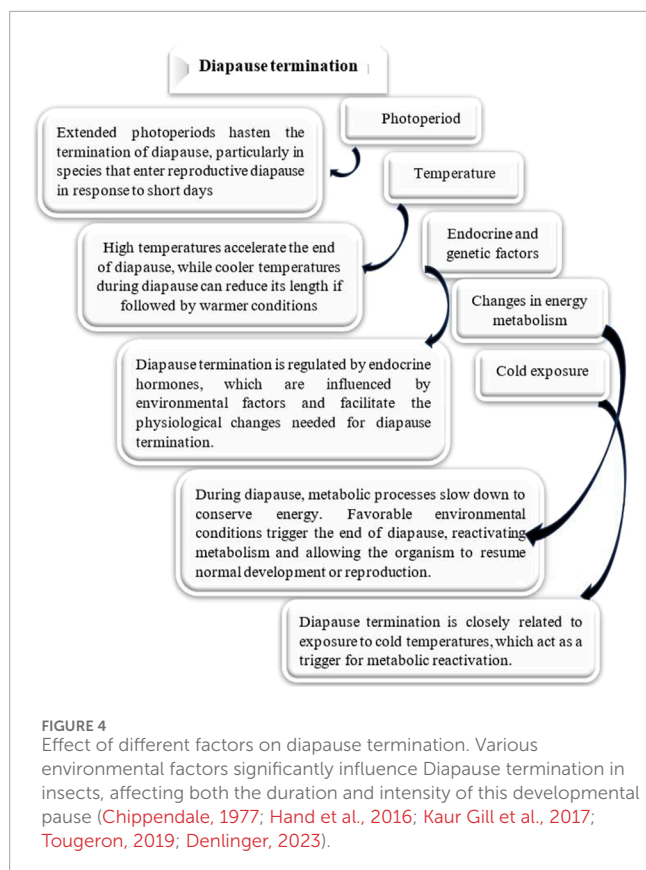


FIGURE 3

(A) The key aspects of glycogen and trehalose metabolism, their connections, and the enzymes involved. Trehalose synthesis and cryoprotectant production pathways are highlighted. It involves two key enzymes: Trehalose-6-phosphate synthase (TPS): Which catalyzes the formation of trehalose-6-phosphate from glucose-6-phosphate and UDP-glucose. Trehalose-6-phosphate phosphatase (TPP): Converts trehalose-6-phosphate into trehalose by removing the phosphate group (Silljé et al., 1999; Badaruddin et al., 2013; Seo et al., 2018). (B) This diagram illustrates glycolysis, a vital metabolic pathway that converts glucose into pyruvate, producing ATP. The process includes ten enzymatic steps, regulated by three key enzymes that manage its flow (Kunieda et al., 2006; Harris and Harper, 2015).

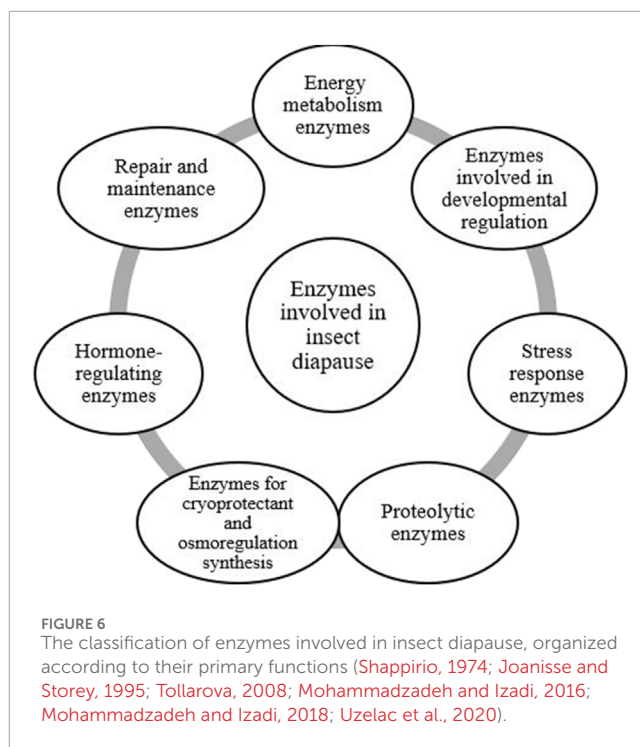
(Bean et al., 1982), whereas, in *Sesamia nonagrioides*, the decline in JH levels is more dependent on reduced biosynthesis than enzymatic degradation (Mane and Chippendale, 1981), illustrating species-specific regulatory mechanisms. At the molecular level, diapause-associated shifts in JH signaling involve changes in the expression of genes encoding JHE and JHEH. Upregulation of these genes during the early diapause phase supports the maintenance of metabolic suppression and developmental arrest. Notably, silencing these genes disrupts diapause by sustaining elevated JH levels, promoting reproductive processes such as ovarian maturation (Noriega, 2014; Zhang et al., 2022). The data, however, indicate that JHE is not essential for the transition between larval development, diapause, and metamorphosis in the Mediterranean corn borer, *S. nonagrioides* (Schafellner et al., 2008). Juvenile hormone biosynthesis, rather than the JH degradation pathway, may determine the decrease in JH levels in some diapausing insects (Gao et al., 2022). Moreover, JH signaling plays a crucial role in regulating reproductive diapause. This adult diapause mainly occurs when genes responsible for producing JH-binding proteins, JH esterase, JH acid methyltransferase (JHAMT), JH epoxide hydrolase, and fatty acid synthase are suppressed (Ma et al., 2021a). JHAMT is an enzyme found in insects that plays a role in the production of JH. In the final stages of this process, JHAMT transfers a methyl group from a compound called S-adenosyl-L-methionine

to either farnesoic acid (FA) or JH acid (JHA) (Li et al., 2013). During the nymphal diapause of *Laodelphax striatellus* (Hemiptera: Delphacidae) the gene JHAMT was upregulated, whereas, the gene cytochrome P₄₅₀ monooxygenase (CYP314A1, Shd) was downregulated (Zhai et al., 2017). During the adult emergence in the Eri silkworm, *Samia cynthia ricini*, two enzymes, 3-hydroxy-3-methylglutaryl CoA reductase, and JHAMT, are involved in the JH synthesis pathway (Sheng et al., 2008). Recent studies have highlighted interactions between JH and other hormonal pathways during diapause. For instance, JH cross-talks with insulin-like peptides (ILPs) and ecdysteroids to coordinate metabolic conservation and stress tolerance (Karpova et al., 2013; Gijbels et al., 2019). Despite advancements, gaps remain in understanding how environmental cues modulate JH signaling, particularly the mechanisms integrating photoperiod and temperature with JH biosynthesis and degradation. Future research should focus on elucidating how environmental and genetic factors collaboratively regulate the JH pathway. Identifying the upstream regulators of JHE and JHEH expression, as well as exploring their interactions with other enzymes in the JH signaling cascade, could provide valuable insights into the initiation and maintenance of diapause. However, this enzymatic suppression of JH offers a target for disrupting diapause in pest species or extending dormancy in beneficial insects.



Diapause hormone (DH)

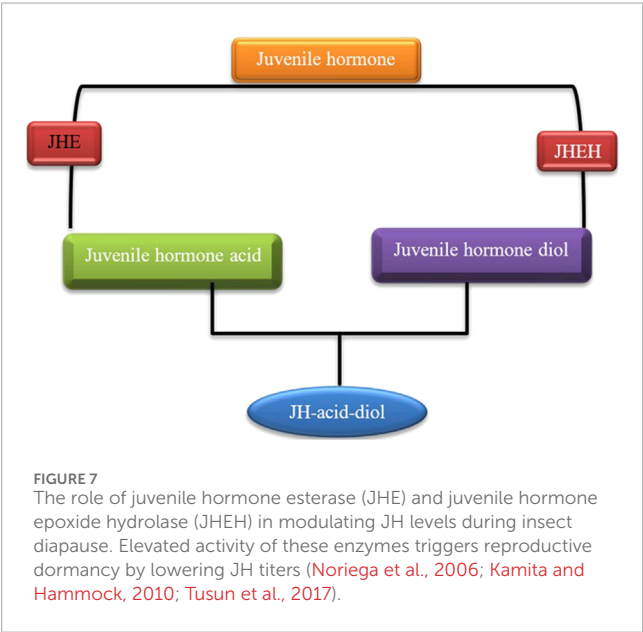
In *Bombyx mori*, embryonic diapause is intricately regulated by the diapause hormone (DH), a neuropeptide released from the subesophageal ganglion, which orchestrates the onset, continuation, and termination of the dormant state. Environmental cues trigger shifts in hormonal and enzymatic pathways, with DH playing a central role. Specifically, DH enhances trehalase activity in developing ovaries, leading to a buildup of glycogen in mature



eggs, a process known as hyperglycogenism that is essential for initiating diapause (Table 3) (Yamashita, 1996; Denlinger et al., 2012; Jiang et al., 2019; Chen L. et al., 2022). A study found that both diapausing and non-diapausing eggs contain the enzyme esterase A, but this enzyme is inactive in non-diapausing eggs. In diapausing eggs, especially those that have been chilled, there is a surge in esterase A activity right before glycogen begins to reappear. This increase closely correlates with the onset of hatching, indicating that the enzyme plays a crucial role in ending diapause rather than in later developmental stages (Kai and Nishi, 1976). Research into gene expression patterns has revealed that certain enzymes, such as glycogen phosphorylase, phosphofructokinase, sorbitol dehydrogenase-2, and glucose-6-phosphate dehydrogenase, show distinct activity profiles in diapausing versus non-diapausing eggs. For example, the glycogen phosphorylase gene remains continuously active in non-diapause eggs, while in diapause eggs, its activity is high during the early phase but decreases later on. Similar patterns of change are observed with the other metabolic genes, indicating a carefully regulated energy metabolism during diapause (Saravanakumar et al., 2008). Comparative examples further illustrate the diversity of diapause hormone's role in diapause. In *Helicoverpa* moths, higher levels of DH in non-diapausing pupae rapidly terminate diapause (Zhang et al., 2015), whereas, in *Drosophila melanogaster*, DH stimulates trehalase activity to promote the conversion of glycogen into glycerol and sorbitol, compounds that function as cryoprotectants to safeguard embryos during dormancy (Horie et al., 2000). Together, these enzyme-hormonal interactions underscore the complex molecular mechanisms that ensure the survival of diapausing eggs while allowing development to resume when environmental conditions improve.

TABLE 1 The classification of enzymes involved in insect diapause is organized according to their primary functions.

Main category	Primary function	Subcategory	Function	Examples
Energy metabolism enzymes	Regulation of the shift in energy production and storage during diapause	Glycolytic enzymes	Breakdown of glucose	Hexokinase, phosphofructokinase
		Gluconeogenic enzymes	Glucose synthesis	Glucose-6-phosphatase, fructose-1,6-bisphosphatase
		Lipid metabolism enzymes	Mobilizing and storing lipids	Lipase, Acyl-CoA synthetase
		Oxidative phosphorylation enzymes	Regulate mitochondrial energy production	Cytochrome c oxidase, ATP synthase
Stress response enzymes	Maintenance of cellular integrity under environmental stress during diapause	Antioxidant enzymes	Mitigate oxidative damage caused by reactive oxygen species	Superoxide dismutase, catalase, glutathione peroxidase
		Cryoprotectant-related enzymes	Facilitate the production of cryoprotectants	Aldose reductase (glycerol synthesis), trehalase (trehalose synthesis and breakdown)
		Ion-regulating enzymes	Maintaining ion gradients	Na ⁺ /K ⁺ -ATPase
Proteolytic enzymes	Regulate protein turnover to manage cellular repair and energy redistribution	Proteases	Break down proteins into amino acids for recycling or energy	Cathepsins, serine proteases
Hormone-regulating enzymes	Control hormonal pathways that regulate diapause	Juvenile hormone regulatory enzymes	Control juvenile hormone levels	Juvenile hormone esterase, juvenile hormone epoxide hydrolase
		Ecdysteroid-related enzymes	Involved in the production or breakdown of ecdysteroids	Ecdysone 20-monooxygenase



Ecdysteroid hormones

Ecdysteroids, particularly 20-hydroxyecdysone (20E), are the principal hormones regulating molting, metamorphosis, and diapause in insects. During larval and pupal diapause, ecdysteroid

levels are tightly regulated to maintain developmental arrest. The biosynthesis and metabolism of ecdysteroids are tightly regulated by different enzymes (Table 4), such as those encoded by the Halloween genes. These genes code for cytochrome P₄₅₀ enzymes in the ecdysteroidogenic pathway, which is responsible for the biosynthesis of ecdysone from cholesterol (Gilbert et al., 2002; Gu et al., 2021). During the larval stages, ecdysone, which is the precursor of 20E, is produced in the prothoracic glands (PGs) (Figures 8A,B). In adult stages, it is mainly produced in the ovaries of females. 20E binds to the intracellular ecdysone receptor (EcR), which then leads to the formation of a receptor heterodimer. This heterodimer triggers a signaling cascade that regulates processes such as molting, metamorphosis, and reproduction (Lafont et al., 2012; Guo et al., 2021). Ecdysteroids are typically linked to the diapause of larvae and pupae. During this period, elevated JH in the hemolymph inhibits the activation of the brain-prothoracic gland axis, thereby preventing the release of ecdysteroids necessary for larval growth and pupation. In the absence of ecdysteroids, the larva is unable to initiate the next molt (Watson et al., 1987; Lonard et al., 1996; Gu et al., 1997). The failure of the PG to release ecdysteroids may result from either the brain's inability to secrete PTTH or the prothoracic glands' insensitivity to PTTH (Figure 9) (Mizoguchi et al., 2015; Nardiello et al., 2019). PTTH is a key neuropeptide that activates enzymes necessary for insect ecdysone biosynthesis (Figure 8A) (Denlinger, 2002; Denlinger et al., 2012; Nardiello et al., 2019). Several insect species are known to suppress

TABLE 2 Enzymes play a role in the metabolism of juvenile hormones during insect diapause.

Regulatory enzyme	Function	References
Juvenile hormone esterases (JHEs)	Metabolizing JH through ester bond hydrolysis	Zhang et al. (2022)
Juvenile hormone epoxide hydrolase	Inactivation of JH through hydrolysis of the epoxide functional group	Tusun et al. (2017)
Juvenile hormone acid methyltransferase	Converts JH acids or inactive precursors to active JH at the final step of the JH biosynthesis pathway	Shinoda and Itoyama (2003)
3-hydroxy-3-methylglutaryl CoA (HMG-CoA) reductase	Catalyzes the conversion of HMG-CoA to mevalonate at the JH biosynthesis pathway	Wang et al. (2023)
Cytochrome P450 monooxygenase	Regulating juvenile hormone biosynthesis	Guo et al. (2024)

TABLE 3 Enzymes play a role in the metabolism of diapause hormone during insect (*Bombyx mori*) diapause.

Regulatory enzyme	Function	References
Trehalase	A glycoside hydrolase catalyzes the conversion of trehalose to glucose	Terra et al. (2019)
Esterase A	Hydrolyze the compounds that contain ester, amide, and thioester bonds	Ding et al. (2022)
Glycogen phosphorylase	Catalyzes the initial reaction of glycogen degradation, converting glycogen to glucose-1-phosphate	Livanova et al. (2002)
Phosphofructokinase	In glycolysis, catalyzes the phosphorylation of fructose-6-phosphate	Wegener and Krause (2002)
Glucose-6-phosphate dehydrogenase	Participates in the pentose phosphate pathway	Bhardwaj (2013)

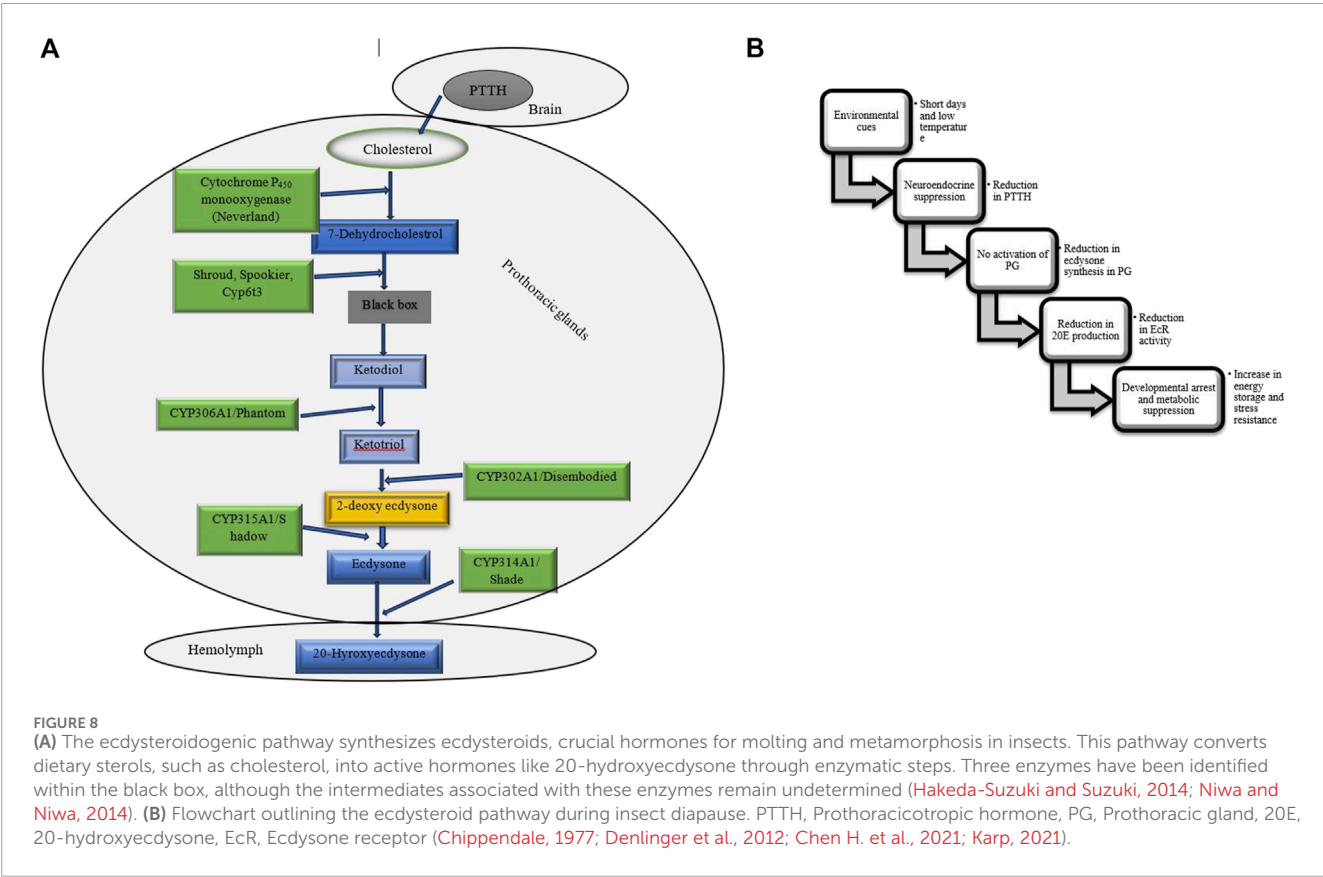
PTTH and ecdysteroids during diapause. The well-known examples are: *B. mori* (Hua et al., 1999) *Chilo suppressalis* (Zhu et al., 2016), *Manduca sexta* (Watson et al., 1996), and *Heliothis virescens* (Scieuzo et al., 2018). *Pieris napi* butterflies demonstrate coordinated suppression of PTTH and ecdysteroids during diapause, reinforcing their critical role in developmental arrest (Süess et al., 2022). The reduced expression of genes responsible for ecdysteroidogenic enzymes inhibits the production of ecdysteroids, which helps to maintain developmental arrest during diapause. For example, in the cabbage armyworm, *Mamestra brassicae*, pupae that are destined for diapause exhibit a significant decrease in the expression of these enzymes. This reduction leads to a suppression of 20-hydroxyecdysone biosynthesis. However, this suppression is reversed when diapause ends, allowing development to resume (Ogihara et al., 2017). Temporal changes in gene expression related to ecdysteroid biosynthesis and downstream signaling may be different between diapause-detained and non-diapause-distained specimens. In non-diapausing eggs of *B. mori*, 20E is synthesized both from maternal conjugated ecdysteroids and via *de novo* biosynthesis. In contrast, diapausing eggs do not undergo these metabolic processes, reflecting a distinct regulatory mechanism during diapause (Gu et al., 2021). Additionally, ecdysteroid-phosphate phosphatase (EPPase) (Sonobe and Yamada, 2004), and ecdysone 20-monooxygenase (Zhou et al., 2022) influence the induction and termination of diapause. However, it is important to understand how ecdysteroids, diapause, and their regulatory enzymes interact to comprehend insect development, physiology, and their ability to adapt to changing environments. An increase

in the activity of these enzymes signals the end of diapause and the resumption of growth (Niwa and Niwa, 2014). The two proteins, ultraspiracle protein (USP) and ecdysone receptor (EcR) form a complex with ecdysone. This complex binds directly to ecdysone response elements, leading to specific gene expression. For example, in the flesh fly, *Sarcophaga crassipalpis*, upregulation of USP leads to the initiation of adult development that marks the end of pupal diapause. Therefore, the expression of both proteins is crucial for receiving the ecdysteroid signal and analyzing their expression patterns is essential for understanding their role in regulating diapause ((Rinehart et al., 2001). Moreover, results highlighted the significant roles of ecdysone-signaling during the early embryogenesis of *Blattella germanica* (Cruz et al., 2023). In the cricket species *Allonemobius socius*, proteins involved in ecdysteroid synthesis and signaling, such as CYP₄₅₀, AKR, and RACK1, are consistently upregulated during the pre-diapause phase, followed by significant downregulation later during diapause. This pattern suggests that elevated levels of ecdysone may facilitate the onset of diapause (Reynolds and Hand, 2009).

The circadian clock, which controls daily rhythms in physiology and behavior, plays a crucial role in the regulation of diapause. Two core components of the circadian clock in insects are Period (PER) and Timeless (TIM) (Figure 10). These proteins operate within a negative feedback loop that modulates the expression of other clock genes, such as Clock (CLK) and Cycle (CYC) (Fyie et al., 2024; Goto and Nagata, 2022; Ikeno et al., 2010). The interaction among these genes establishes rhythmic patterns of gene expression that influence various physiological processes.

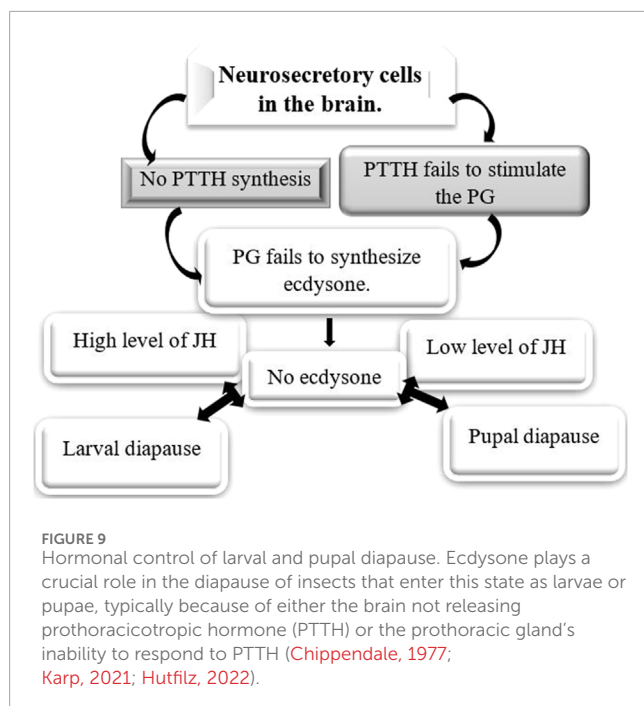
TABLE 4 Enzymes play a role in the metabolism of ecdysteroid hormones during insect diapause.

Regulatory enzyme	Function	References
Cytochrome P ₄₅₀ monooxygenases	Perform oxidation and reduction reactions	Danielson (2002)
Ecdysteroid biosynthetic enzymes	Regulating ecdysone biosynthesis in prothoracic glands	Niwa and Niwa (2014), Kamiyama and Niwa (2022)
Ecdysone 20-hydroxylase (Ecdysone 20-monooxygenase)	Catalyzes the chemical reaction that converts ecdysone into 20-hydroxyecdysone	Rauschenbach et al. (2008)
Ecdysteroid-phosphate phosphatase	Converts phosphate esters into active ecdysteroids	Yamada and Sonobe (2003)



PER accumulates during the night, and when it reaches a certain threshold, it moves into the nucleus, where it dimerizes with TIM. Together, they inhibit the activity of CLK and CYC, which reduces the transcription of their associated genes as well as other clock-controlled genes. Similar to PER, TIM also accumulates in response to light-dark cycles and plays an important role in stabilizing the PER protein. The formation of the PER-TIM complex is essential for maintaining circadian rhythms and is involved in photoperiodic signaling that can trigger diapause (Fyie et al., 2024; Goto and Nagata, 2022; Ikeno et al., 2010). The expression of the PER and TIM genes is influenced by photoperiodic cues, which are essential for initiating diapause in many insects. Shorter day lengths, indicative of autumn, trigger an increased expression of these clock genes, leading to physiological changes that promote diapause. For example, studies have demonstrated that silencing the Clock gene

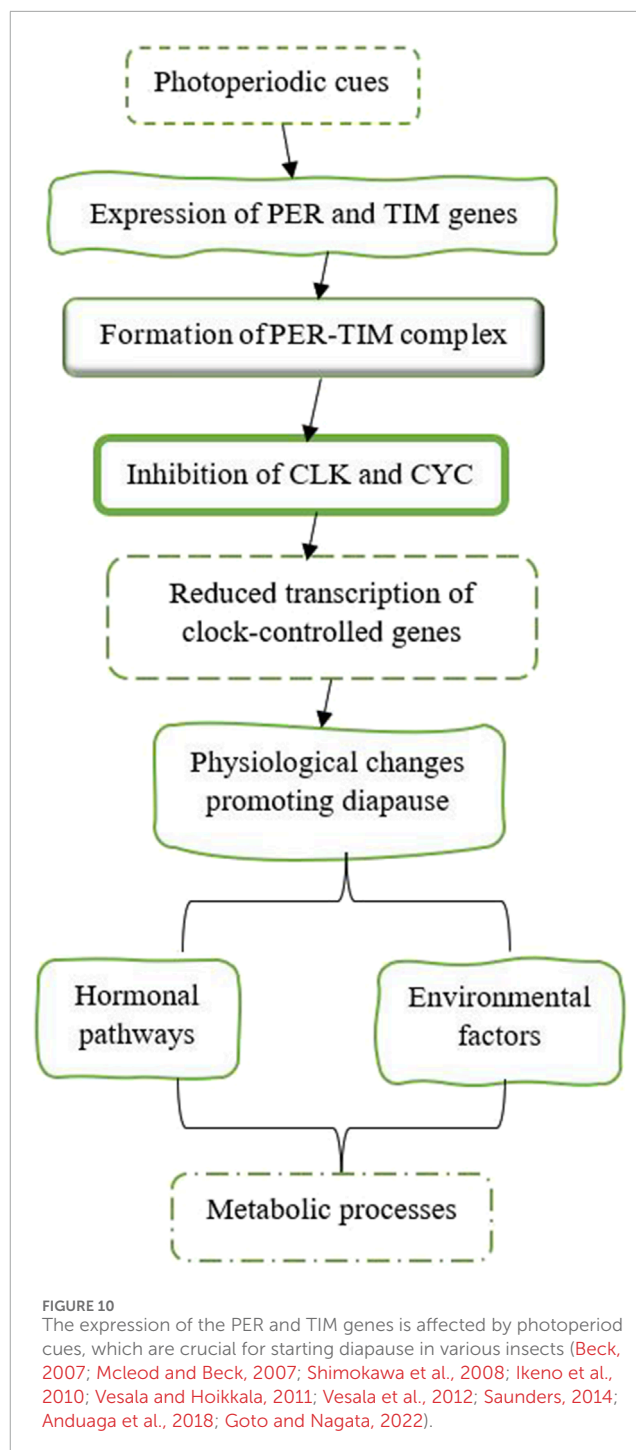
disrupts normal diapause responses in crickets, highlighting its role in sensing photoperiod and regulating reproductive behaviors associated with diapause (Goto and Nagata, 2022). In larvae of the sugar beet moth, *Scrobipalpa ocellatella*, destined for diapause, short-day conditions resulted in increased levels of the PER and TIM genes. These elevated gene levels decreased the amount of PTTH in both the brain and hemolymph. This reduction in PTTH then led to lower levels of 20E and triggered the induction of diapause (Ahmadi et al., 2021). Research has shown that the genes PER and TIM are involved in the temperature-dependent induction of diapause. In species such as *B. mori*, mutations in these clock genes can impair their ability to enter diapause when exposed to different temperature conditions. This indicates that the circadian clock combines both photoperiodic and temperature signals to regulate diapause (Homma et al., 2022). The activity of



the proteins PER and TIM is closely associated with hormonal pathways that regulate metabolism during diapause. By influencing hormonal pathways and metabolic processes, PER and TIM help determine when an insect enters or exits diapause, thereby ensuring its survival during adverse conditions. For instance, fluctuations in JH levels can interact with circadian clock mechanisms, influencing an insect's decision to enter or exit diapause (Ikeno et al., 2010). Understanding this relationship offers valuable insights into how insects adapt their life cycles in response to changing environments. Maintaining circadian rhythms during diapause is essential for properly timing metabolic processes. Disruptions to these rhythms, caused by environmental factors like artificial light at night (ALAN), can interfere with the onset of diapause by altering the expression patterns of clock genes such as PER and TIM (Fyie et al., 2024).

Prothoracicotropic hormone (PTTH)

Proper regulation of prothoracicotropic hormone (PTTH) is crucial for determining whether an insect resumes development or enters diapause. PTTH functions as a developmental trigger after diapause by being released into the hemolymph before the activation of the prothoracic glands, which then synthesize the necessary ecdysteroids for metamorphosis. In other words, timely PTTH release signals the end of diapause and initiates the subsequent developmental processes (Denlinger, 2002; Denlinger et al., 2012; Yamada et al., 2016). For example, the larvae of the cabbage army moth, *M. brassicae*, destined for diapause have lower levels of PTTH in their blood and reduced PTTH gene expression several days before they pupate. This suggests that the diapause program is already established in PTTH neurons during the middle to final stage of the larvae's development (Mizoguchi et al., 2013). Co-regulation of diapause by PTTH and ecdysone has also been reported in *Helicoverpa armigera* (Hou and Xu, 2007) and



P. napi (Süess et al., 2022). However, no information about the enzyme activity and its impacts on PTTH metabolism during diapause is available.

Insulin-like peptides (ILPs)

Insulin-like peptides (ILPs) are multifunctional hormones that play a crucial role in regulating metabolic pathways in insects, particularly in glycolysis, through complex signaling networks (Fernandez and Torres-Alemán, 2012). This interaction is essential for various physiological processes, including growth, reproduction,

and energy balance. ILPs are encoded by multigene families and are expressed in several tissues, such as the brain, midgut, salivary glands, and fat body. Their expression is often specific to certain tissues and developmental stages, allowing for precise control of metabolism throughout different life stages of insects (Brown et al., 2008; Kawabe et al., 2019; Chowański et al., 2021). When secreted, ILPs act as hormones that bind to insulin receptors (IRs) and activate intracellular signaling pathways. ILPs activate phosphoinositide 3-kinase (PI3K) and protein kinase B (Akt), which leads to the phosphorylation and inhibition of glycogen synthase kinase-3 (GSK-3). This process enhances glycogen breakdown and increases glucose availability for glycolysis. Additionally, ILPs promote the expression of key glycolytic enzymes, such as hexokinase, phosphofructokinase, and pyruvate kinase, thereby accelerating glycolysis and ATP production (Chowański et al., 2021; Weger and Rittschof, 2024). In *D. melanogaster*, insulin-like peptides (ILPs) increase the expression of Glut1-like glucose transporters, which facilitates glucose uptake into cells and supports glycolysis (Kauffman and DiAngelo, 2024). Reduced ILPs signaling is associated with diapause induction, as it shifts metabolism from anabolic to energy-conserving pathways. During periods of high ILPs signaling (the fed state), insects prioritize glycolysis for rapid energy production. Conversely, during diapause or starvation (low ILPs signaling), metabolism shifts toward lipid oxidation and gluconeogenesis to conserve carbohydrate reserves (Wu and Brown, 2006; Chowański et al., 2021; Weger and Rittschof, 2024). In the mosquito, *Culex pipiens* and the fruit fly, *D. melanogaster*, the levels of two specific insulin-like peptides, ILP-1 and ILP-5, decrease during diapause. This highlights their role in promoting lipid storage and enhancing stress resistance during this adaptive physiological state (Sim and Denlinger, 2009). The insulin/insulin-like growth factor signaling (IIS) pathway is essential for regulating carbohydrate and lipid metabolism, and plays a pivotal role in the regulation of diapause (Sim and Denlinger, 2013). In *C. pipiens* IIS signaling opposes diapause (Sim and Denlinger, 2013). Glucagon- and insulin-like signaling are vital in the physiological changes observed in *D. melanogaster* during reproductive diapause (Kubrak et al., 2014). Trehalose accumulation is also linked to the IIS pathway (Li et al., 2021). For instance, in *Drosophila*, ILPs also regulate trehalose metabolism, ensuring a steady supply of glucose for glycolysis. The enzyme trehalase, which converts trehalose into glucose, is regulated by the IIS pathway that links nutrient levels to essentially biological processes. In the Chinese oak silkworm, *Antheraea pernyi*, bovine insulin can initiate the end of diapause by increasing trehalose breakdown during the diapause termination phase. This indicates a regulatory mechanism that connects hormonal signals with trehalose metabolism during diapause (Li et al., 2021). The expression of insulin pathway genes in the solitary bee, *Megachile rotundata*, is significantly influenced by overwintering conditions during diapause. Bees that overwinter under fluctuating temperatures show different insulin signaling profiles compared to those kept at constant temperatures, suggesting that environmental conditions modulate insulin signaling during diapause (Cambron et al., 2021). In *B. mori*, ILPs influence glycolysis during metamorphosis, optimizing carbohydrate utilization to meet developmental energy demands (Chowański et al., 2021). Insulin-like growth factor signaling is a crucial regulatory pathway in insect diapause. It influences energy metabolism, stress resistance,

and developmental decisions allowing insects to survive harsh environmental conditions.

Allatostatins and allatotropins

Allatostatins (ASTs) are a family of neuropeptides that primarily inhibit the synthesis of juvenile hormone (JH). By inhibiting JH synthesis, allatostatins help regulate developmental processes during diapause. Allatotropins are another class of neuropeptides that stimulate the production of JH (Sheng et al., 2007). Insect diapause is tightly regulated by JH levels, which are influenced by allatotropin and allatostatin neuropeptides. In *C. pipiens*, suppression of allatotropin is critical for inducing reproductive diapause. Experimental knockdown of allatotropin mimics diapause-like states by halting ovarian development, reversible with JH application (Kang et al., 2014). The balance between allatotropin and allatostatin activity is central to regulating diapause through their control of JH levels, affecting both metabolic suppression and developmental arrest. In addition to the previously mentioned hormones, other hormones such as hypertrehalosemic hormones (HTHs) and adipokinetic hormones (AKHs) play a role in mobilizing lipids and carbohydrates from the insect's fat bodies during intense physical activities. These hormones, along with their regulatory enzymes, may also be involved in insect diapause; however, there is currently no available information on this topic.

Carbohydrates, diapause, and regulatory enzymes

Diapause is characterized by metabolic flexibility in response to environmental temperature changes (Uzelac et al., 2020). Carbohydrates are essential for energy storage and metabolic adjustments for maintaining and terminating diapause. Additionally, they serve as cryoprotectants, helping to survive during diapause. Regulating enzyme activity during diapause is essential for energy balance (Table 5). Research shows that glycolysis and gluconeogenesis enzymes (Figure 3B) are closely controlled through allosteric modifications and gene expression changes, allowing the organism to adjust energy use and storage during dormancy (Weber et al., 1967; Kageyama and Ohnishi, 1971; Ishii et al., 2004). Trehalose and glycogen are the key sugars of insects, playing crucial roles in energy metabolism and ecological protection (Guo et al., 2015). The conversion between glycogen and trehalose has been demonstrated in various diapausing species, such as the pistachio seed wasp, *Eurytoma plotnikovi* (Mohammadzadeh et al., 2017), the pistachio white leaf borer, *Ocneria terebinthina* (Behroozi et al., 2012), the almond wasp, *Eurytoma amygdali* (Khanmohamadi et al., 2016), the Sunn pest, *Eurygaster integriceps* (Hasanvand et al., 2020), the silkworm, *Philosamia cynthia pryeri* (Hayakawa and Chino, 1981), and four *Drosophila* species (Kimura et al., 1992). This conversion is often accompanied by changes in enzyme activities. Trehalose synthases are crucial enzymes for converting trehalose into glycogen (Figure 3A). Among them, trehalose-6-phosphate synthase is a vital enzyme involved in trehalose synthesis (Pan et al., 2008; Zhang et al., 2023). For example, in *Lissorhoptrus oryzophilus*, trehalose-6-phosphate synthase improves cold tolerance by facilitating rapid cold hardening through trehalose accumulation (Zhang et al., 2023). The expression of trehalose-6-phosphate synthase, glycogen synthase, and glycogen phosphorylase in *Aphidius gifuensis* was inhibited

during diapause maintenance. The suppression of trehalose-6-phosphate synthase expression indicates a decreased synthesis of trehalose, which may help avoid unnecessary energy expenditure. Additionally, the downregulation of glycogen synthase implies a shift away from active glycogen storage processes, which is consistent with the metabolic stasis characteristic of diapause. By reducing the expression of glycogen phosphorylase, glycogen degradation is minimized, indicating that glycogen may play a significant role in development after diapause (Zhang et al., 2020). Increased trehalase activity during diapause termination helps lower trehalose levels, facilitating the transition out of diapause. In simpler terms, reduced trehalose levels are necessary to end diapause (Guo et al., 2015). Glycogen can be rapidly converted into dextrose or trehalose for energy and transported to other tissues for glycolytic fuel (Arrese and Soulagès, 2010). Glycogenesis and glycogenolysis are regulated by two key enzymes glycogen synthase and glycogen phosphorylase, respectively (Figures 3A,B). Enzymes like phosphofructokinase, phosphoglucosylase, and pyruvate kinase regulate glycolysis, controlling both glycogen and trehalose metabolism in insects, while glucose-6-phosphatase dehydrogenase, phosphoglucosylase, and phosphoenolpyruvate carboxykinase play a role in gluconeogenesis, ensuring a balance of energy production and utilization (Pan et al., 2020). Phosphoenolpyruvate carboxykinase (PEPCK) is an enzyme belonging to the lyase family, playing a crucial role in the metabolic pathway of gluconeogenesis (Yang J. et al., 2009). It catalyzes the conversion of oxaloacetate into phosphoenolpyruvate and carbon dioxide. The rate-limiting step of gluconeogenesis is PEPCK, which is generally recognized as the first committed step in this pathway (Martins da Silva et al., 2023). Research has shown that PEPCK activity can be upregulated in diapausing insects, facilitating gluconeogenesis and enabling the mobilization of stored lipids and carbohydrates as needed. For example, in the flesh fly, *Sarcophaga bullata*, two isoforms of PEPCK show different expression patterns throughout development and in response to environmental stresses such as cold and starvation. This indicates that specific isoforms may be preferentially activated during diapause to meet metabolic needs (Roncalli et al., 2018; Martins da Silva et al., 2023). In pupae of the cotton bollworm, *H. armigera*, destined for diapause, low pyruvate levels in the brains are linked to three enzymes: pyruvate kinase (PK), phosphoenolpyruvate carboxykinase (PEPCK), and phosphoglycerate mutase (PGAM) (Wang et al., 2018). In addition to the previously mentioned enzymes, the activities of leucine aminopeptidase and alkaline phosphatase, both of which are associated with glucose metabolism, decrease during diapause. Furthermore, lactate dehydrogenase and glyceraldehyde-3-phosphate dehydrogenase exhibit complete activity loss by the late diapause stage. These findings suggest that the glycolytic pathway is disrupted during diapause (Sluss et al., 1975).

Metabolism, diapause, and regulatory enzymes

A hallmark of diapause is the dramatic reduction in metabolism, orchestrated by an array of molecular mechanisms that mirror those observed in proliferating cells. This metabolic slowdown is driven by comprehensive regulatory processes, including transcriptional, post-transcriptional, and post-translational modifications, that modulate gene expression, mRNA and protein accumulation, and protein function. In tandem, shifts in biochemical pathways and metabolic

products enhance the organism's stress tolerance, ensuring survival during adverse conditions (Hahn and Denlinger, 2007; MacRae, 2010; Huang et al., 2022). Energy expenditure during diapause varies across insect species and is influenced by factors such as diapause duration, body size, and environmental conditions. Energy expenditure during diapause initially shows low metabolic activity as energy is conserved. Over time, metabolic rates gradually increase, reflecting the utilization of stored energy to maintain essential metabolic functions (Hahn and Denlinger, 2007; Hahn and Denlinger, 2010). For example, studies on various beetle species have shown that their metabolic intensity increases as they advance through diapause, leading to more rapid use of energy reserves (Lehmann et al., 2020a). The study examined the relationship between metabolic rate and temperature in dormant willow leaf beetles, *Chrysomela aeneicollis*, and found that the metabolic rate increased as diapause progressed. Additionally, acclimating the beetles to variable conditions affected both the intensity of their metabolism and their sensitivity to temperature changes (Roberts and Williams, 2022). Enzymes involved in fatty acid synthesis and triacylglycerol storage play a pivotal role in the initiation phase of diapause. Once diapause is established, metabolic pathways such as fatty acid biosynthesis, oxidative phosphorylation, and carbohydrate metabolism, along with their regulatory enzymes, are often downregulated to conserve energy (Zhang et al., 2019). β -Oxidation is the catabolic process that breaks down fatty acids to produce acetyl-CoA, NADH, and FADH₂. The key enzymes in β -oxidation are acyl-CoA dehydrogenase, enoyl-CoA hydratase, hydroxyacyl-CoA dehydrogenase, and ketoacyl-CoA thiolase (Tables 6, 7). The activity of these enzymes can be affected by hormonal changes and the insect's physiological state, ensuring energy mobilization meets the insect's metabolic needs during dormancy (Wanders et al., 1999). For instance, in *C. pipiens*, fatty acid synthase is upregulated during early diapause, whereas genes involved in β -oxidation and energy generation are downregulated (Sim and Denlinger, 2009). Moreover, enzymes involved in fatty acid synthesis are suppressed during the overwintering of the mosquito, *A. albopictus* (Poelchau et al., 2013). Insects that undergo diapause may show reduced oxidative metabolism, characterized by decreased citrate synthase activity and lower levels of total glutathione and lipid peroxidation (Moreira et al., 2012). Additionally, to enhance metabolic activity before diapause, telomerase activity might be upregulated (Koubová et al., 2019). The relationship between diapause and cold tolerance is essential for regulating metabolic enzyme activity in various insect species. For instance, in the European corn borer, *O. nubilalis*, enzyme activity aligns with temperature changes, demonstrating these insects' adaptive responses to their environment. Research also shows that during diapause, specific enzymes such as glucose-6-phosphate dehydrogenase, lactate dehydrogenase, and aldose reductase become more active, which aids in the synthesis of protective metabolites, whereas, in some species diapause is marked by reduced activity of energy-intensive enzymes like ATPases and phosphofructokinase, reflecting a general metabolic slowdown (Uzelac et al., 2020; Moreira et al., 2021). Moreover, the activity of certain other enzymes may vary during diapause. For instance, in diapause-destined pupae of *H. armigera*, low glycogen synthase kinase 3 β (GSK3 β) activity is caused by elevated serine/threonine protein kinase activity, leading to diapause initiation (Song et al., 2023). In diapausing larvae of the sunflower caterpillar,

TABLE 5 Enzymes play a role in the metabolism of carbohydrates during insect diapause.

Regulatory enzyme	Function	References
Trehalose-6-phosphate synthase	Catalyzes the synthesis of trehalose 6-phosphate	Fichtner et al. (2020), Chen X. et al., 2021
Glycogen synthase	The key enzyme in the conversion of glucose into glycogen (glycogenesis)	Buschiazzo et al. (2004)
Glycogen phosphorylase	Catalyzes the rate-limiting step in glycogenolysis by releasing glucose-1-phosphate from the terminal alpha-1,4-glycosidic bond	BhagavanN (2002)
Trehalose-6-phosphate phosphatase	Hydrolyses the trehalose 6-phosphate into trehalose and phosphate	Kerbler et al. (2023)
Trehalase	A glycoside hydrolase catalyzes the conversion of trehalose to glucose	Terra et al. (2019)
Phosphofructokinase	In glycolysis, phosphofructokinase catalyzes the phosphorylation of fructose-6-phosphate (F6P) using ATP as a phosphate donor to form fructose-1,6-diphosphate and ADP.	Gheshlaghi et al. (2009)
Phosphoglucumutase	In glycolysis, catalyzes the interconversion of glucose 1-phosphate (G-1-P) and glucose 6-phosphate (G-6-P)	Brolin and Berne (1970)
Pyruvate kinase	In glycolysis, converts glucose into ATP	van Dijk et al. (2023)
Glucose-6-phosphate dehydrogenase	Participates in the pentose phosphate pathway by catalyzing D-glucose 6-phosphate into 6-phospho-D-gluconic-1,5-lactone	Thomas et al. (1991)
Phosphoenolpyruvate carboxykinase	In gluconeogenesis, catalyzes the conversion of oxaloacetate into phosphoenolpyruvate	Méndez-Lucas et al. (2014)
Aldose reductase	Initiates the NADPH-dependent conversion of glucose to sorbitol in the polyol pathway of glucose metabolism	Attar et al. (2013)
Polyol dehydrogenase	Catalyzes a two-step process converting glucose to fructose. Glucose is first reduced to sorbitol and then oxidized to fructose	Bonnefont-Rousselot (2002)
Ketose reductase	A NAD-dependent polyol dehydrogenase catalyzes the NADH-dependent reduction of fructose to sorbitol	Doehlert (1987)
Fructose-1,6-bisphosphatase	a key enzyme in glycolysis that catalyzes the hydrolysis of D-fructose 1,6-bisphosphate to D-fructose 6-phosphate and inorganic phosphate	Cui and Tcherkez (2021)
Glyceraldehyde-3-phosphatase	a crucial glycolytic enzyme that facilitates the reversible conversion of glyceraldehyde-3-phosphate into 1,3-diphosphoglycerate	Perez-Casal and Potter (2016)

Homoeosoma ellectellum, the oxidative metabolism and peroxide-detoxifying enzymes are downregulated, while glutathione transferase and isocitric dehydrogenase are upregulated (Moreira et al., 2021). The study revealed that cytochrome oxidase serves as the main terminal oxidase during the diapause of *Cecropia*, *Cynthia*, *Promethea*, and *Polyphemus* silkworm pupae (Kurland and Schneiderman, 1959).

Metabolic flexibility

Insects display remarkable metabolic flexibility during diapause, allowing them to manage their energy reserves effectively (Figure 11). They can sense their energy levels and adjust their

metabolic pathways accordingly (Hahn and Denlinger, 2010; Lehmann et al., 2016). For instance, aerobic processes are suppressed, as indicated by the reduced activity of enzymes associated with the Krebs cycle, while anaerobic pathways become more prominent. In the wheat midge, *Sitodiplosis mosellana* (Diptera: Cecidomyiidae), reduced activity of the citric acid cycle and increased production of functional metabolites likely contribute to maintaining low metabolic activity and cold tolerance during diapause (Huang et al., 2022). Research shows that the transition to anaerobic metabolism is marked by an increase in enzymes that enhance glycolysis and lactate production. Key

TABLE 6 Enzymes play a role in the metabolism of lipids during insect diapause.

Regulatory enzyme	Function	References
Acyl-CoA dehydrogenase	Creates a double bond between the second and third carbons down from the CoA group on acyl-CoA and in the process produces an FADH ₂	Swigoňová et al. (2009)
Enoyl-CoA hydratase	Hydrates the double bond between the second and third carbons on 2-trans/cis-enoyl-CoA	Bennett et al. (2020)
Hydroxy acyl-CoA dehydrogenase	catalyzes the NAD ⁺ dependent dehydrogenation of 3-hydroxy acyl-CoA to 3-ketoacyl-CoA in the β -oxidation of fatty acids	Galcheva et al. (2018)
Ketoacyl-CoA thiolase	Catalyzes the reversible hemolytic cleavage of 3-ketoacyl-CoA into acyl-CoA and acetyl-CoA	Fox et al. (2014)
Fatty acid synthase	Multi-enzyme polypeptides that catalyze fatty acid synthesis (the synthesis of palmitate from acetyl-CoA and malonyl-CoA, in the presence of NADPH.	Fox et al. (2014)
Citrate synthase	This enzyme catalyzes the formation of citrate from acetyl CoA and oxaloacetate in the Krebs cycle	Huang et al. (2020)
Telomerase	The synthesis of a telomere involves a reverse transcriptase called telomerase, which acts as an RNA-dependent DNA polymerase	Shay and Wright (2019)
Lactate dehydrogenase	Catalyzes the reversible conversion of lactate into pyruvate	Kantor et al. (2001)
Alanine aminotransferase	Catalyzes the transfer of an amino group from L-alanine to α -ketoglutarate, resulting in a reversible transamination reaction that produces pyruvate and L-glutamate	Yang et al. (2009b)
Aspartate aminotransferase	This enzyme catalyzes the conversion of aspartate and α -ketoglutarate into oxaloacetate and glutamate	Kirsch et al. (1984)
Cytochrome c oxidase	catalyzes the four-electron reduction of oxygen molecules to water and utilizes the chemical energy to transport four protons across cell membranes	Ishigami et al. (2023)
Glycogen synthase kinase 3 β	A kinase that phosphorylates several substrates and plays a crucial role in various cellular signaling pathways	Beurel et al. (2015)
ATPases	A group of enzymes catalyzes the synthesis of ATP from ADP.	Hisabori (2020)
Peroxide-detoxifying enzymes	Catalyzing the conversion of hydrogen peroxide to water (peroxiredoxins, glutathione peroxidases, and catalase)	Stancill and Corbett (2023)
Glutathione transferase	This enzyme catalyzes the conjugation of reduced glutathione with substrates	Lin and Gerson (2014)
Isocitrate dehydrogenase	Catalyzes the oxidative decarboxylation of isocitrate to α -ketoglutarate in Krebs's cycle, during which NAD ⁺ is reduced to NADH or NADP ⁺ to NADPH	Liu et al. (2024)

enzymes involved in this process include lactate dehydrogenase (LDH), phosphofructokinase (PFK), and pyruvate kinase (PK). These enzymatic adaptations are essential for maintaining energy production during hypoxia or metabolic stress (Rodas et al., 2000). Studies on the diapausing larvae of the European corn borer, *O.*

nubilalis, have revealed elevated lactate dehydrogenase activity levels at near-freezing temperatures. This indicates a shift towards anaerobic metabolism, enabling insects to produce energy without relying on oxygen, especially when oxygen availability is limited due to cold conditions (Uzelac et al., 2020). Diapausing pupae of the

TABLE 7 The four enzymes are crucial for the β -oxidation process, breaking fatty acids into acetyl-CoA molecules for energy production.

Enzyme	Function	Activity during diapause	Key products	References
Acyl-CoA dehydrogenase	Catalyzes the oxidation of acyl-CoA to trans-2-enoyl-CoA, producing FADH2	Exhibit altered expression levels during diapause preparation and maintenance. Upregulation during unfavorable conditions may enhance the insect's ability to utilize stored fats efficiently	Trans-2-enoyl-CoA, FADH2	Liu et al. (2016), Tan et al. (2017), Zhang et al. (2019), Lehmann et al. (2020b), Xiang et al. (2021), Yang et al. (2023)
Enoyl-CoA hydratase	Adds a water molecule to trans-2-enoyl-CoA, forming L-3-hydroxyacyl-CoA	The physiological requirements influence the expression levels during diapause. The activity at the end of diapause enhances the effective transformation of fatty acids into energy	L-3-hydroxyacyl-CoA	
Hydroxyacyl-CoA dehydrogenase	Oxidizes L-3-hydroxyacyl-CoA to 3-ketoacyl-CoA, generating NADH in the process	Differentially expressed genes involved in fatty acid metabolism are essential for lipid accumulation during the preparation phase for diapause	3-ketoacyl-CoA, NADH	
Ketoacyl-CoA thiolase	Cleaves 3-ketoacyl-CoA to yield acetyl-CoA and acyl-CoA, allowing the cycle to continue	Differentially expressed in response to the physiological requirements of diapause	Acetyl-CoA, acyl-CoA	

flesh fly, *Sarcophaga* sp. utilizes both aerobic lipid catabolism and anaerobic glycolysis to meet their energy demands (Chen C. et al., 2021). The metabolic switch from aerobic to anaerobic processes during insect diapause is a complex adaptation that helps these organisms survive harsh environments while efficiently managing their energy reserves (Lehmann et al., 2016; Uzelac et al., 2020).

Cryoprotectants, diapause, and regulatory enzymes

Cryoprotectants protect living cells and tissues from damage caused by freezing temperatures (Elliott et al., 2017; Jaiswal and Vagga, 2022; Chen et al., 2023). Insects have developed different mechanisms to survive in cold environments, including producing and accumulating cryoprotectants. The capacity of insects to accumulate these cryoprotectants changes during diapause development and involves various regulatory enzymes (Storey and Storey, 1991; Hahn and Denlinger, 2007). It was previously thought that insects accumulate cryoprotectants mainly from their internal macromolecular reserves during cold acclimation. However, the research indicates that food intake is essential for providing the materials necessary to create cryoprotectants, challenging the notion that these compounds mainly originate from the insect's internal reserves (Moos et al., 2022). Moreover, cold-acclimated *Chymomyza costata* (Diptera: Drosophilidae) larvae use amino acids from their food to produce proline, a key cryoprotectant and also convert internal reserves of glutamine. Various enzymes (Table 5) play a crucial role in regulating the metabolic pathways that lead to the accumulation of insect cryoprotectants. The interaction between glycogen breakdown, sugar metabolism, and amino acid conversion is essential for producing effective cryoprotectants like trehalose

and glycerol (Wang et al., 2016). Trehalose-6-phosphate synthase, glycogen phosphorylase, phosphofructokinase, aldose reductase, polyol dehydrogenase, ketose reductase, and glucose-6-phosphate dehydrogenase are among the most important of them (Yocum et al., 2009; Kim et al., 2017; Smolinski et al., 2019; Song et al., 2023). The activity of these enzymes may increase in the early phase of diapause but stabilize or decrease in the late phase. However, cold treatment affects enzyme activity differently based on the diapause phase, with some enzymes showing increased activity and others decreasing (Košťál et al., 2004). Cold acclimation involves significant physiological changes, including increased trehalose-6-phosphate synthase activity and related metabolic pathways. This increase is associated with the production of trehalose, an essential cryoprotectant that helps improve ion and water balance during exposure to cold temperatures. This balance is crucial for maintaining cellular integrity and function under stress conditions (Zhang et al., 2023). A study on the effects of cold acclimation during diapause showed that the activity of specific metabolic enzymes remains in dynamic equilibrium and is synchronized with external factors like low temperatures. This adaptation allows the organism to adjust its metabolism in response to environmental changes, directing it toward producing protective compounds such as glycerol and alanine (Uzelac et al., 2020). For instance, in *Trichogramma dendrolimi*, decreasing temperatures led to increased enzyme activity and trehalose accumulation (Guo et al., 2015). Three enzymes, aldose reductase, ketose reductase, and polyol dehydrogenase, were examined in adult female linden bugs, *Pyrrhocoris apterus*. High enzyme activity during female diapause indicates a strong ability to synthesize and store polyol cryoprotectants (Tollarova, 2008).

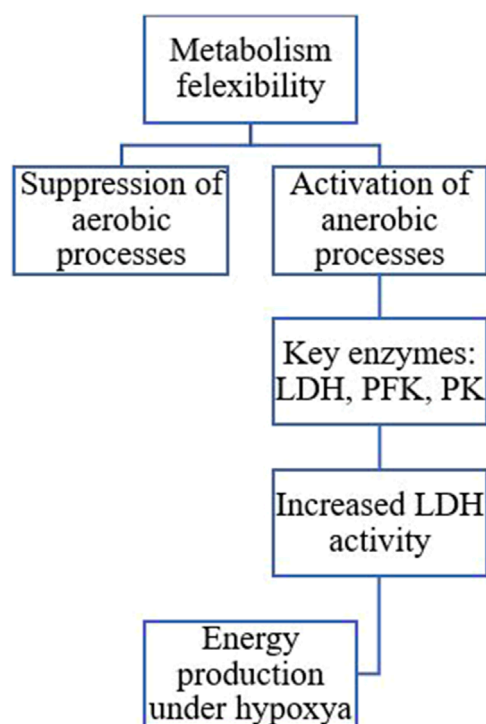


FIGURE 11

The transition to anaerobic metabolism is marked by increased enzymes that enhance glycolysis and lactate production. Key enzymes involved in this process include lactate dehydrogenase (LDH), phosphofructokinase (PFK), and pyruvate kinase (PK) (Hahn and Denlinger, 2007; Hahn and Denlinger, 2010; Sinclair, 2015; Uzelac et al., 2020; Chen X. et al., 2021).

Low temperatures cumulatively enhance glycerol production in the larvae of the rice stem borer, *C. suppressalis*, during various diapause development phases. This glycerol accumulation results from the activation of glycogen phosphorylase, inhibition of fructose-1,6-bisphosphatase, and activation of enzymes linked to glycerol synthesis, particularly glyceraldehyde-3-phosphatase (Table 8) and polyol dehydrogenase with glyceraldehyde activity (Li et al., 2002). However, cold hardiness is often different from the diapause program and may be triggered by the low temperatures of winter, rather than by the diapause program (Khanmohamadi et al., 2016).

Antioxidant enzymes and diapause

During diapause, insects enter a dormant state characterized by low metabolic activity and diminished antioxidant defenses. To counteract the resulting increase in oxidative stress, antioxidant enzymes are often upregulated. This adjustment helps protect cellular components from damage. The dynamic regulation of these enzymes, through changes in their expression and activity, enables insects to adapt to the physiological challenges of dormancy (Table 8) (Moreira et al., 2021). Enzymes like superoxide dismutase, catalase, and peroxidases help scavenge harmful reactive oxygen species (ROS) and protect cells from damage during diapause (Moreira et al., 2021). Studies have shown that the activity of antioxidant enzymes can significantly differ between the diapausing and non-diapausing stages of different insect species.

For instance, in the European corn borer, *O. nubilalis*, diapausing larvae exhibited reduced activities of catalase and glutathione S-transferase (GST) compared to non-diapausing larvae, suggesting a different oxidative stress management strategy during dormancy (Jovanović-Galović et al., 2007). However, antioxidant enzyme levels alone cannot fully indicate oxidative stress. Levels of glutathione and the reduced to oxidized glutathione ratio (GSH:GSSG) are also key markers. Additionally, a significant increase in the activities of GST and isocitrate dehydrogenase-NADP⁺ during diapause, suggests a preparation for potential oxidative stress (Moreira et al., 2021). The research on the sunflower caterpillar, *Chlosyne lacinia*, reveals significant insights into the metabolic adaptations associated with diapause. The study found that diapausing larvae exhibit a decreased capacity to manage oxidative stress, primarily due to reduced activities of peroxide-decomposing antioxidant enzymes. This impairment is critical as it suggests that these larvae are less equipped to handle oxidative damage during this dormant phase. However, the elevated levels of glutathione transferase and isocitrate dehydrogenase-NADP⁺ in diapausing larvae indicate a preparatory response to potential oxidative stress. The upregulation of these enzymes suggests that, despite their reduced overall antioxidant capacity, the caterpillars are strategically enhancing specific pathways to mitigate oxidative damage during diapause in tropical environments. Overall, the findings highlight the intricate balance between metabolic suppression and antioxidant defense mechanisms in diapausing insects, contributing to our understanding of their survival strategies in fluctuating habitats (Moreira et al., 2021). In the European corn borer, *O. nubilalis*, the hexose monophosphate shunt is linked to the antioxidative defense system, which is crucial for maintaining redox balance during diapause (Stanic et al., 2004). In the silkworm, *Antheraea mylitta*, diapause-destined pupae showed lower levels of hydrogen peroxide and higher activities of catalase and superoxide dismutase, indicating a strategic antioxidant protection mechanism that supports dormancy and potentially extending lifespan (Sahoo et al., 2018). Diapause adaptation to oxidative stress entails a complex interaction between antioxidant enzyme activity and ROS levels. For example, lower levels of hydrogen peroxide in diapausing insects may indicate a reduced metabolic rate and lower oxidative stress, allowing for survival during unfavorable conditions (Khurshid et al., 2021).

Protease enzymes and diapause

Protease enzymes (Table 9) are involved in the degradation of proteins, essential for recycling amino acids and regulating metabolic processes during diapause. Changes in the abundance of proteolytic enzymes can indicate shifts in metabolic pathways that support survival under unfavorable conditions (Richard, 2017). Studies have shown that different proteolytic enzymes and protease inhibitors exhibit varying abundance patterns in diapausing versus non-diapausing insects. For example, in the parasitoid wasp, *Nasonia vitripennis* (Hymenoptera: Pteromalidae), proteomic analyses revealed changes in the abundance of enzymes related to protein synthesis and degradation during early diapause, suggesting a metabolic switch that prepares the insect for dormancy (Wolschin and Gadau, 2009). Increased activity of proteases in post-diapause can be associated with the rebuilding of tissues and preparation for development. In the fall webworm, *Hyphantria*

TABLE 8 Antioxidant enzymes and their function in insect diapause.

Regulatory enzyme	Function	References
Superoxide dismutase	Catalyzes the dismutation of superoxide anion to hydrogen peroxide and triplet oxygen	Deeth (2021)
Catalase	Hydrogen peroxide (H ₂ O ₂) is broken down into water and oxygen molecules, protecting (Singh and Kumar, 2019) cells against oxidative damage caused by reactive oxygen species	Singh and Kumar (2019)
Peroxidases	Enzymes that catalyze the oxidation of substrates using hydrogen peroxide or organic peroxides as oxidizing agents	Everse (2013)
Glutathione S-transferase	Catalyzing the conjugation of electrophilic substrates to glutathione to detoxify endogenous compounds	Sheehan et al. (2001)
Isocitrate dehydrogenase-NADP+	Catalyzing the oxidative decarboxylation of isocitrate to α -ketoglutarate, while reducing NAD(P) ⁺ to NAD(P)H	Reitman and Yan (2010)

cunea, diapause-destined larvae exhibit lower protease activity than non-diapause-destined larvae. This reduction in protease activity helps conserve protein reserves, which is crucial for surviving the diapause period when feeding is impossible (Zhao et al., 2021). The decrease in protease activity during diapause facilitates a transition from protein breakdown to accumulating energy reserves like lipids, essential for sustaining long-term survival during dormancy. In agreement, in the mosquito, *C. pipiens*, there is a significant metabolic shift characterized by the downregulation of genes related to digestive enzymes, including trypsin and a chymotrypsin-like protease (Robich and Denlinger, 2005). Proteases can affect fatty acid accumulation, vital for energy during dormancy. For instance, cathepsin L is key in regulating lipid storage; silencing its gene leads to reduced lipid accumulation (Chen J. et al., 2022). Elastase, an enzyme crucial for protein digestion and remodeling, shows varying activity during diapause, suggesting that proteolytic activity is vital for the survival and subsequent emergence of the diapausing insect (Zaobidna et al., 2014). A comparison of diapausing and non-diapausing insects revealed significant changes in the expression of proteins related to metabolism and cellular protection. These changes include the regulation of heat-shock proteins and enzymes involved in protein synthesis and degradation, indicating that proteolytic enzymes are crucial for the diapause mechanism and the maintenance of cellular integrity during this period (Chen et al., 2010). Heat shock increases are often linked to diapause preparation (Denlinger, 2002). Heat shock proteins play a crucial role in maintaining cell homeostasis, particularly in stress response, by interacting with substrate proteins. Their expression is induced under stress conditions, even when protein synthesis is inhibited. During diapause the regulation of heat shock protein genes occurs differently, allowing for continued protein production without general disruption (Rinehart et al., 2007; King and MacRae, 2015). Regarding enzymatic regulation, in diapausing strains of the spongy moth, *Lymantria dispar*, proteolytic enzymes like trypsin and chymotrypsin activity is lower than in non-diapausing strains. This suggests that the suppression of proteolytic activity may be a key factor in maintaining diapause, as enzyme activity is closely linked to the insect's developmental processes (Lee et al., 1997). One of the key enzymes involved in diapause is diapause-associated protein kinase (DAPK), which is responsible for phosphorylating and activating various proteins involved in diapause regulation. DAPK

activity is regulated by phosphorylation and dephosphorylation events, which are influenced by the hormonal signals mentioned earlier. When the body experiences low energy levels due to factors like hypoxia and metabolic stresses, AMP-activated protein kinase (AMPK) is activated. This helps to turn on alternative pathways for producing ATP, ensuring enough energy to support the organism as overall energy production decreases during diapause. AMPK regulates cellular functions by phosphorylating metabolic enzymes and protein synthesis factors (Lu and Xu, 2010; MacRae, 2010; Gu et al., 2020).

Hormonal manipulation to disrupt diapause in pest species

Hormonal manipulation through juvenile hormone analogs, inhibitors, and neuropeptide interventions is an effective method for disrupting diapause in various pest species, offering new strategies for population management. In *Galeruca daurica*, the application of the juvenile hormone analog methoprene at the pre-diapause stage delayed diapause onset, inhibited lipid accumulation, and altered key metabolic gene expression, preventing adults from entering diapause (Ma et al., 2021). For *Aedes albopictus*, the insect growth regulator pyriproxyfen effectively terminated embryonic diapause when applied to newly deposited and fully embryonated eggs, resulting in high termination rates and significant mortality, which is promising for controlling overwintering mosquitoes (Suman et al., 2015). Research on *Helicoverpa zea* showed that agonists mimicking diapause hormone can terminate or prevent pupal diapause when given during the larval stage, while antagonists inhibit this termination. This technique can disrupt pest populations by forcing insects to remain active in unfavorable conditions, reducing their survival and reproduction (Zhang et al., 2011). Overall, hormonal manipulation offers a powerful tool for targeting diapause to enhance pest management strategies.

Conclusion

Enzyme-hormone interactions during diapause are essential for insect survival in adverse conditions. These interactions regulate the conversion and activation of ecdysteroids, preventing premature

TABLE 9 Proteolytic enzymes and their function in insect diapause.

Regulatory enzyme	Function	References
Trypsin	A serine protease cleaves long-chain protein molecules into smaller fragments	Rawlings and Barrett (1994)
Chymotrypsin	Hydrolyzes the peptide bonds of tryptophan, leucine, tyrosine, and phenylalanine residues	Cotten (2020a)
Cathepsin	A lysosomal cysteine proteinase that catalyzes the protein catabolism	Falke et al. (2024)
Elastase	A serine protease cleavages carboxyl groups on small hydrophobic amino acids, including glycine, alanine, and valine	Cotten (2020b)
Protein kinase	Catalyzes the transfer of a phosphate group from ATP to the serine or threonine residues of target proteins	Devang et al. (2021)

development. Additionally, they maintain the balance of juvenile hormone levels by managing the synthesis and degradation of relevant enzymes, thereby suppressing signals for growth and reproduction. Metabolic enzymes are also activated to produce cryoprotectants while keeping metabolic activity low. Together, these mechanisms create a stable physiological state that enables insects to endure until environmental cues indicate the appropriate time to resume development. Future research should aim to unravel the complex molecular interactions between hormones and enzymes. This understanding will enhance our knowledge of insect biology and guide the creation of innovative pest management strategies, as well as efforts to protect beneficial insect species. By manipulating the breakdown of juvenile hormones using inhibitors or analogs, we can disrupt the reproductive diapause of agricultural pests, making them more susceptible to adverse environmental conditions. Juvenile hormone esterase inhibitors can extend diapause in beneficial insects, such as pollinators, which helps them survive unseasonable climate changes. While diapause enhances resilience and can prolong lifespan, extended periods of dormancy pose significant risks for both individual insects and entire populations. One major concern is the reduction in reproductive capacity; prolonged dormancy can delay reproduction, resulting in fewer offspring when conditions eventually improve. Additionally, diapause is typically synchronized with the life cycles of host pests. If diapause lasts too long, it may lead to a mismatch between the emergence of beneficial insects and the availability of their prey or hosts, potentially reducing their effectiveness in controlling pests (Hoy, 1978; Bean et al., 2007; Meuti et al., 2024). Genetically engineering crop systems to disrupt hormone signaling specific to diapause could selectively target pest populations while preserving non-diapause species. Additionally, gaining insights into the synthesis of trehalose and glycerol could enhance cryopreservation techniques, aiding in the preservation of biological materials like pollinators and biological control agents. Inhibiting prothoracicotropic hormone or ecdysteroid production in overwintering pests may prolong diapause by delaying its termination and preventing reproduction. Disrupting the enzymes involved in cryoprotectant synthesis, particularly aldose reductase, which is essential for glycerol production, can make pest insects less tolerant to freezing temperatures. This may lead to higher mortality rates during their diapause phase. Conversely, by enhancing the cryoprotectant pathways in beneficial insects through genetic or environmental interventions, we could increase their resilience to

climate variability. This, in turn, would enhance their contributions to the ecosystem. Targeting enzymes related to glycolysis during diapause may cause energy depletion in pests, which can ultimately decrease their survival rates during winter. Additionally, monitoring environmental factors like photoperiod and temperature that affect hormonal and enzymatic pathways during diapause can improve pest forecasting models. Future research directions may include the following suggestions: Investigating CRISPR-based techniques for modifying diapause-related genes to enhance pest management and conservation efforts; Exploring the interactions between hormones, such as juvenile hormone, prothoracicotropic hormone, and insulin-like peptides, to identify new strategies for regulating diapause, and examining diapause in the context of extreme environmental conditions, such as drought or heat, to develop a comprehensive framework for climate adaptation.

Author contributions

HI: Methodology, Resources, Validation, Visualization, Writing–original draft, Writing–review and editing.

Funding

The author(s) declare that no financial support was received for the research, authorship, and/or publication of this article.

Conflict of interest

The author declares that the research was conducted in the absence of any commercial or financial relationships that could be construed as a potential conflict of interest.

Generative AI statement

The author(s) declare that no Generative AI was used in the creation of this manuscript.

Publisher's note

All claims expressed in this article are solely those of the authors and do not necessarily represent those of their affiliated

organizations, or those of the publisher, the editors and the reviewers. Any product that may be evaluated in this article, or claim that may be made by its manufacturer, is not guaranteed or endorsed by the publisher.

References

- Ahmadi, F., Mikani, A., and Moharrampour, S. (2021). Induction of diapause by clock proteins period and timeless via changes in PTTH and ecdysteroid titer in the sugar beet moth, *Scrobipalpa ocellatella* (Lepidoptera: Gelechiidae). *Arch. Insect Biochem. Physiol.* 107, e21790. doi:10.1002/arch.21790
- Anduaga, A. M., Nagy, D., Costa, R., Kyriacou, C. P., Martin, A., Nagy, D., et al. (2018). Diapause in *Drosophila melanogaster* – photoperiodicity, cold tolerance and metabolites. *J. Insect Physiol.* 105, 46–53. doi:10.1016/j.jinsphys.2018.01.003
- Arrese, E. L., and Soulages, J. L. (2010). Insect fat body: energy, metabolism, and regulation. *Annu. Rev. Entomol.* 55, 207–225. doi:10.1146/annurev-ento-112408-085356
- Attar, M., Brassard, J. A., Kim, A. S., Matsumoto, S., Ramos, M., and Vangyi, C. (2013). “Safety evaluation of ocular drugs,” in *A comprehensive guide to toxicology in preclinical drug development* (Amsterdam, Netherlands: Elsevier), 567–617. doi:10.1016/B978-0-12-387815-1.00024-1
- Badaruddin, M., Holcombe, L. J., Wilson, R. A., Wang, Z.-Y., Kershaw, M. J., and Talbot, N. J. (2013). Glycogen metabolic genes are involved in trehalose-6-phosphate synthase-mediated regulation of pathogenicity by the rice blast fungus *Magnaporthe oryzae*. *PLoS Pathog.* 9, e1003604. doi:10.1371/journal.ppat.1003604
- Batz, Z. A., and Armbruster, P. A. (2018). Diapause-associated changes in the lipid and metabolite profiles of the Asian tiger mosquito, *Aedes albopictus*. *J. Exp. Biol.* 221, jeb189480. doi:10.1242/jeb.189480
- Bean, D. W., Beck, S. D., and Goodman, W. G. (1982). Juvenile hormone esterases in diapause and nondiapause larvae of the European corn borer, *Ostrinia nubilalis*. *J. Insect Physiol.* 28, 485–492. doi:10.1016/0022-1910(82)90027-0
- Bean, D. W., Dudley, T. L., and Keller, J. C. (2007). Seasonal timing of diapause induction limits the effective range of *Diorhabda elongata deserticola* (Coleoptera: chrysomelidae) as a biological control agent for tamarisk. Available online at: <https://academic.oup.com/ee/article/36/1/15/491527>.
- Beck, S. D. (2007). Photoperiodic induction of diapause in an insect. *Biol. Bull.* 122, 1–12. doi:10.2307/1539316
- Behroozi, E., Izadi, H., Samih, M. A. A., and Moharrampour, S. (2012). Physiological strategy in overwintering larvae of pistachio white leaf borer, *Ocneria terebinthina* Strg. (Lepidoptera: lymantriidae) in Rafsanjan, Iran. *Ital. J. Zool.* 79, 44–49. doi:10.1080/11250003.2011.592152
- Bennett, M. J., Sheng, F., and Saada, A. (2020). Biochemical assays of TCA cycle and β -oxidation metabolites. *Methods Cell Biol.* 155, 83–120. doi:10.1016/bs.mcb.2019.11.021
- Beurel, E., Grieco, S. F., and Jope, R. S. (2015). Glycogen synthase kinase-3 (GSK3): regulation, actions, and diseases. *Pharmacol. Ther.* 148, 114–131. doi:10.1016/j.pharmthera.2014.11.016
- Bhagavan, N. V. (2002). “Carbohydrate metabolism II: gluconeogenesis, glycogen synthesis and breakdown, and alternative pathways,” in *Medical Biochemistry* (Amsterdam, Netherlands: Elsevier), 275–305. doi:10.1016/B978-012095440-7/50017-2
- Bhardwaj, S. B. (2013). “Alcohol and gastrointestinal tract function,” in *Bioactive food as dietary interventions for liver and gastrointestinal disease* (Amsterdam, Netherlands: Elsevier), 81–118. doi:10.1016/B978-0-12-397154-8.00015-4
- Bonnefont-Rousselot, D. (2002). Glucose and reactive oxygen species. *Curr. Opin. Clin. Nutr. Metab. Care* 5, 561–568. doi:10.1097/00075197-200209000-00016
- Brolin, S. E., and Berne, C. (1970). “The activity pattern of enzymes associated with glycogen metabolism in the islets of Langerhans,” in *The structure and metabolism of the pancreatic islets* (Amsterdam, Netherlands: Elsevier), 245–252. doi:10.1016/B978-0-08-015844-0.50031-6
- Brown, M. R., Clark, K. D., Gulia, M., Zhao, Z., Garczynski, S. F., Crim, J. W., et al. (2008). An insulin-like peptide regulates egg maturation and metabolism in the mosquito *Aedes aegypti*. *PNAS* 105, 5716–5721. doi:10.1073/pnas.0800478105
- Buschiazio, A., Ugalde, J. E., Guerin, M. E., Shepard, W., Ugalde, R. A., and Alzari, P. M. (2004). Crystal structure of glycogen synthase: homologous enzymes catalyze glycogen synthesis and degradation. *EMBO J.* 23, 3196–3205. doi:10.1038/sj.emboj.7600324
- Cambron, L. D., Yocum, G. D., Yeater, K. M., and Greenlee, K. J. (2021). Overwintering conditions impact insulin pathway gene expression in diapausing *Megachile rotundata*. *Comp. Biochem. Physiol. A Mol. Integr. Physiol.* 256, 110937. doi:10.1016/j.cbpa.2021.110937
- Cambron-Kopco, L. D., Yocum, G. D., Yeater, K. M., and Greenlee, K. J. (2022). Timing of diapause initiation and overwintering conditions alter gene expression profiles in *Megachile rotundata*. *Front. Physiol.* 13, 844820. doi:10.3389/fphys.2022.844820
- Chen, C., Mahar, R., Merritt, M. E., Denlinger, D. L., and Hahn, D. A. (2021). ROS and hypoxia signaling regulate periodic metabolic arousal during insect dormancy to coordinate glucose, amino acid, and lipid metabolism. *PNAS* 118, e2017603118. doi:10.1073/pnas.2017603118
- Chen, H., Wu, G., Zhou, H., Dai, X., Steeghs, N. W. F., Dong, X., et al. (2021). Hormonal regulation of reproductive diapause that occurs in the year-round mass rearing of *Bombus terrestris* queens. *J. Proteome Res.* 20, 2240–2250. doi:10.1021/acs.jproteome.0c00776
- Chen, J., Guo, P., Li, Y., He, W., Chen, W., Shen, Z., et al. (2022). Cathepsin L contributes to reproductive diapause by regulating lipid storage and survival of *Coccinella septempunctata* (Linnaeus). *Int. J. Mol. Sci.* 24, 611. doi:10.3390/ijms24010611
- Chen, L., Ma, W., Wang, X., Niu, C., and Lei, C. (2010). Analysis of pupal head proteome and its alteration in diapausing pupae of *Helicoverpa armigera*. *J. Insect Physiol.* 56, 247–252. doi:10.1016/j.jinsphys.2009.10.008
- Chen, L., Zhang, Z., Chen, K., Yu, Y., Hu, B., Song, H., et al. (2022). Transcriptional dynamics induced by diapause hormone in the silkworm, *Bombyx mori*. *Biol. (Basel)* 11, 1313. doi:10.3390/biology11091313
- Chen, X., Abubakar, Y. S., Yang, C., Wang, X., Miao, P., Lin, M., et al. (2021). Trehalose phosphate synthase complex-mediated regulation of trehalose 6-phosphate homeostasis is critical for development and pathogenesis in *Magnaporthe oryzae*. *mSystems* 6, e0046221. doi:10.1128/mSystems.00462-21
- Chen, S.-Y., Zhao, R.-N., Li, Y., Li, H.-P., Xie, M.-H., Liu, J.-F., et al. (2023). Cold tolerance strategy and cryoprotectants of *Megachile dorsalis* in different temperature and time stresses. *Front. Physiol.* 13. doi:10.3389/fphys.2022.1118955
- Chippendale, G. M. (1977). Hormonal regulation of larval diapause. *Annu. Rev. Entomol.* 22, 121–138. doi:10.1146/annurev.en.22.010177.001005
- Chowanski, S., Walkowiak-Nowicka, K., Winkiel, M., Marciniak, P., Urbański, A., and Pacholska-Bogalska, J. (2021). Insulin-like peptides and cross-talk with other factors in the regulation of insect metabolism. *Front. Physiol.* 12, 701203. doi:10.3389/fphys.2021.701203
- Cotten, S. W. (2020a). “Evaluation of exocrine pancreatic function,” in *Contemporary practice in clinical chemistry* (Amsterdam, Netherlands: Elsevier), 573–585. doi:10.1016/B978-0-12-815499-1.00033-8
- Cotten, S. W. (2020b). “Evaluation of exocrine pancreatic function,” in *Contemporary practice in clinical chemistry* (Amsterdam, Netherlands: Elsevier), 573–585. doi:10.1016/B978-0-12-815499-1.00033-8
- Cruz, J., Maestro, O., Franch-Marro, X., and Martín, D. (2023). Nuclear receptors EcR-A/RXR and HR3 control early embryogenesis in the short-germ hemimetabolous insect *Blattella germanica*. *iScience* 26, 106548. doi:10.1016/j.isci.2023.106548
- Cui, J., and Tcherkez, G. (2021). Potassium dependency of enzymes in plant primary metabolism. *Plant Physiol. Biochem.* 166, 522–530. doi:10.1016/j.plaphy.2021.06.017
- Danielson, B. S. P. (2002). The cytochrome P450 superfamily: biochemistry, evolution and drug metabolism in humans. *Curr. Drug Metab.* 3, 561–597. doi:10.2174/1389200023337054
- Deeth, H. C. (2021). Heat-induced inactivation of enzymes in milk and dairy products. A review. *Int. Dairy J.* 121, 105104. doi:10.1016/j.idairyj.2021.105104
- Denlinger, D. L. (2002). Regulation of diapause. *Annu. Rev. Entomol.* 47, 93–122. doi:10.1146/annurev.ento.47.091201.145137
- Denlinger, D. L. (2022). *Insect diapause*. Cambridge University Press. doi:10.1017/9781108609364
- Denlinger, D. L. (2023). Insect diapause: from a rich history to an exciting future. *J. Exp. Biol.* 226, jeb245329. doi:10.1242/jeb.245329
- Denlinger, D. L., Yocum, G. D., and Rinehart, J. P. (2012). “Hormonal control of diapause,” in *Insect endocrinology* (Amsterdam, Netherlands: Elsevier), 430–463. doi:10.1016/B978-0-12-384749-2.10010-X
- Devang, N., Pani, A., and Rajanikant, G. K. (2021). Pseudokinases: prospects for expanding the therapeutic targets armamentarium. *Adv. Protein Chem. Struct. Biol.* 124, 121–185. doi:10.1016/bs.apcsb.2020.09.004

- Ding, Y., Nie, L., Yang, X.-C., Li, Y., Huo, Y.-Y., Li, Z., et al. (2022). Mechanism and structural insights into a novel esterase, E53, isolated from *Erythrobacter longus*. *Front. Microbiol.* 12, 798194. doi:10.3389/fmicb.2021.798194
- Dittmer, J., and Brucker, R. M. (2021). When your host shuts down: larval diapause impacts host-microbiome interactions in *Nasonia vitripennis*. *Microbiome* 9, 85. doi:10.1186/s40168-021-01037-6
- Doehlert, D. C. (1987). Ketose reductase activity in developing maize endosperm. *Plant Physiol.* 84, 830–834. doi:10.1104/pp.84.3.830
- Dong, Y.-C., Chen, Z.-Z., Clarke, A. R., and Niu, C.-Y. (2019). Changes in energy metabolism trigger pupal diapause transition of *Bactrocera minax* after 20-hydroxyecdysone application. *Front. Physiol.* 10, 1288. doi:10.3389/fphys.2019.01288
- Elliott, G. D., Wang, S., and Fuller, B. J. (2017). Cryoprotectants: a review of the actions and applications of cryoprotective solutes that modulate cell recovery from ultra-low temperatures. *Cryobiology* 76, 74–91. doi:10.1016/j.cryobiol.2017.04.004
- Eustice, M., Konzman, D., Reece, J. M., Ghosh, S., Alston, J., Hansen, T., et al. (2022). Nutrient sensing pathways regulating adult reproductive diapause in *C. elegans*. *PLoS One* 17, e0274076. doi:10.1371/journal.pone.0274076
- Everse, J. (2013). "Heme proteins," in *Encyclopedia of biological chemistry* (Amsterdam, Netherlands: Elsevier), 532–538. doi:10.1016/B978-0-12-378630-2.00015-3
- Falke, S., Lieske, J., Herrmann, A., Loboda, J., Karničar, K., Günther, S., et al. (2024). Structural elucidation and antiviral activity of covalent cathepsin L inhibitors. *J. Med. Chem.* 67, 7048–7067. doi:10.1021/acs.jmedchem.3c02351
- Fernandez, A. M., and Torres-Alemán, I. (2012). The many faces of insulin-like peptide signalling in the brain. *Nat. Rev. Neurosci.* 13, 225–239. doi:10.1038/nrn3209
- Fichtner, F., Olas, J. J., Feil, R., Watanabe, M., Krause, U., Hoefgen, R., et al. (2020). Functional features of trehalose-6-phosphate synthase1, an essential enzyme in Arabidopsis. *Plant Cell* 32, 1949–1972. doi:10.1105/tpc.19.00837
- Fox, A. R., Soto, G., Mozzicafreddo, M., Garcia, A. N., Cuccioloni, M., Angeletti, M., et al. (2014). Understanding the function of bacterial and eukaryotic thiolases II by integrating evolutionary and functional approaches. *Gene* 533, 5–10. doi:10.1016/j.gene.2013.09.096
- Fyfe, L. R., Westby, K. M., and Meuti, M. E. (2024). Light pollution disrupts circadian clock gene expression in two mosquito vectors during their overwintering dormancy. *Sci. Rep.* 14, 2398. doi:10.1038/s41598-024-52794-x
- Galcheva, S., Al-Khawaga, S., and Hussain, K. (2018). Diagnosis and management of hyperinsulinaemic hypoglycaemia. *Best. Pract. Res. Clin. Endocrinol. Metab.* 32, 551–573. doi:10.1016/j.beem.2018.05.014
- Gao, Q., Li, B., Tian, Z., De Loof, A., Wang, J., Wang, X., et al. (2022). Key role of juvenile hormone in controlling reproductive diapause in females of the Asian lady beetle *Harmonia axyridis*. *Pest Manag. Sci.* 78, 193–204. doi:10.1002/ps.6619
- Gheshlaghi, R., Scharer, J. M., Moo-Young, M., and Chou, C. P. (2009). Metabolic pathways of clostridia for producing butanol. *Biotechnol. Adv.* 27, 764–781. doi:10.1016/j.biotechadv.2009.06.002
- Gijbels, M., Lenaerts, C., Vanden Broeck, J., and Marchal, E. (2019). Juvenile hormone receptor Met is essential for ovarian maturation in the desert locust, *Schistocerca gregaria*. *Sci. Rep.* 9, 10797. doi:10.1038/s41598-019-47253-x
- Gilbert, L. I., Rybczynski, R., and Warren, J. T. (2002). Control and biochemical nature of the ecdysteroidogenic pathway. *Annu. Rev. Entomol.* 47, 883–916. doi:10.1146/annurev.ento.47.091201.145302
- Goto, S. G., and Nagata, M. (2022). The circadian clock gene (Clock) regulates photoperiodic time measurement and its downstream process determining maternal induction of embryonic diapause in a cricket. *Eur. J. Entomol.* 119, 12–22. doi:10.14411/eje.2022.002
- Gu, S., Chen, C., and Lin, P. (2021). Changes in expressions of ecdysteroidogenic enzyme and ecdysteroid signaling genes in relation to *Bombyx* embryonic development. *J. Exp. Zool. A Ecol. Integr. Physiol.* 335, 477–488. doi:10.1002/jez.2466
- Gu, S.-H., Chen, C.-H., Hsieh, H.-Y., and Lin, P.-L. (2020). Expression of protein kinase C in relation to the embryonic diapause process in the silkworm, *Bombyx mori*. *J. Insect Physiol.* 121, 104010. doi:10.1016/j.jinsphys.2019.104010
- Gu, S.-H., Chow, Y.-S., and Yin, C.-M. (1997). Involvement of juvenile hormone in regulation of prothoracicotropic hormone transduction during the early last larval instar of *Bombyx mori*. *Mol. Cell Endocrinol.* 127, 109–116. doi:10.1016/S0303-7207(96)03995-0
- Guo, Q., Hao, Y.-J., Li, Y., Zhang, Y.-J., Ren, S., Si, F.-L., et al. (2015). Gene cloning, characterization and expression and enzymatic activities related to trehalose metabolism during diapause of the onion maggot *Delia antiqua* (Diptera: anthomyiidae). *Gene* 565, 106–115. doi:10.1016/j.gene.2015.03.070
- Guo, S., Tian, Z., Wu, Q.-W., King-Jones, K., Liu, W., Zhu, F., et al. (2021). Steroid hormone ecdysone deficiency stimulates preparation for photoperiodic reproductive diapause. *PLoS Genet.* 17, e1009352. doi:10.1371/journal.pgen.1009352
- Guo, X., Hou, J., Zhang, W., Zhang, Y., Li, H., Cao, W., et al. (2024). A cytochrome P450 monooxygenase (CYP337B5) plays a key role in regulating juvenile hormone biosynthesis and degrading chlorantraniliprole in *Spodoptera frugiperda* (Lepidoptera: noctuidae). *J. Asia Pac Entomol.* 27, 102298. doi:10.1016/j.aspen.2024.102298
- Hahn, D. A., and Denlinger, D. L. (2007). Meeting the energetic demands of insect diapause: nutrient storage and utilization. *J. Insect Physiol.* 53, 760–773. doi:10.1016/j.jinsphys.2007.03.018
- Hahn, D. A., and Denlinger, D. L. (2010). Energetics of insect diapause. *Annu. Rev. Entomol.* 56, 103–121. doi:10.1146/annurev-ento-112408-085436
- Hakeda-Suzuki, S., and Suzuki, T. (2014). Cell surface control of the layer specific targeting in the Drosophila; visual system. *Genes Genet. Syst.* 89, 9–15. doi:10.1266/ggs.89.9
- Han, E. R. N., and Baue, E. (1998). Timing of diapause initiation, metabolic changes and overwintering survival of the spruce budworm, *Choristoneura fumiferana*. *Ecol. Entomol.* 23, 160–167. doi:10.1046/j.1365-2311.1998.00111.x
- Hand, S. C., Denlinger, D. L., Podrabsky, J. E., and Roy, R. (2016). Mechanisms of animal diapause: recent developments from nematodes, crustaceans, insects, and fish. *Am. J. Physiol. Regul. Integr. Comp. Physiol.* 310, R1193–R1211. doi:10.1152/ajpregu.00250.2015
- Harsimran, K. G., Gaurav, G., and Gurminder, C. (2017). Insect diapause: A review. *J. Agric. Sci. Technol.* A7, 454–473. doi:10.17265/2161-6256/2017.07.002
- Harris, R. A., and Harper, E. T. (2015). "Glycolytic pathway," in *Encyclopedia of life Sciences* (Hoboken, NJ: Wiley), 1–8. doi:10.1002/9780470015902.a0000619.pub3
- Hasanvand, H., Izadi, H., and Mohammadzadeh, M. (2020). Overwintering physiology and cold tolerance of the Sunn pest, *Eurygaster integriceps*, an emphasis on the role of cryoprotectants. *Front. Physiol.* 11, 321. doi:10.3389/fphys.2020.00321
- Hayakawa, Y., and Chino, H. (1981). Temperature-dependent interconversion between glycogen and trehalose in diapausing pupae of *Philosamia cynthia ricini* and *pryeri*. *Insect Biochem.* 11, 43–47. doi:10.1016/0020-1790(81)90039-1
- Hisabori, T. (2020). Regulation machineries of ATP synthase from phototroph, 1–26. doi:10.1016/bs.abr.2020.07.003
- Hodek, I. (2012). Adult diapause in coleoptera. *Psyche (Stuttg)* 2012, 1–10. doi:10.1155/2012/249081
- Homma, S., Murata, A., Ikegami, M., Kobayashi, M., Yamazaki, M., Ikeda, K., et al. (2022). Circadian clock genes regulate temperature-dependent diapause induction in silkworm *Bombyx mori*. *Front. Physiol.* 13, 863380. doi:10.3389/fphys.2022.863380
- Horie, Y., Kanda, T., and Mochida, Y. (2000). Sorbitol as an arrester of embryonic development in diapausing eggs of the silkworm, *Bombyx mori*. *J. Insect Physiol.* 46, 1009–1016. doi:10.1016/S0022-1910(99)00212-7
- Hou, C., and Xu, W. (2007). Synthesis dynamic and developmental profile of prothoracicotropic hormone between diapause- and nondiapause-destined individuals in *Helicoverpa armigera*. *Chin. Sci. Bul.* 52, 2095–2099. doi:10.1007/s11434-007-0310-1
- Hoy, M. A. (1978). Variability in diapause attributes of insects and mites: some evolutionary and practical implications. *Proc. Life Sci.*, 101–126. doi:10.1007/978-1-4615-6941-1_5
- Hua, Y.-J., Tanaka, Y., Nakamura, K., Sakakibara, M., Nagata, S., and Kataoka, H. (1999). Identification of a prothoracicostatic peptide in the larval brain of the silkworm, *Bombyx mori*. *J. Biol. Chem.* 274, 31169–31173. doi:10.1074/jbc.274.44.31169
- Huang, L., Wang, C., Xu, H., and Peng, G. (2020). Targeting citrate as a novel therapeutic strategy in cancer treatment. *Biochimica Biophysica Acta (BBA) - Rev. Cancer* 1873, 188332. doi:10.1016/j.bbcan.2019.188332
- Huang, Q., Ma, Q., Li, F., Zhu-Salzman, K., and Cheng, W. (2022). Metabolomics reveals changes in metabolite profiles among pre-diapause, diapause and post-diapause larvae of *Sitodiplosis mosellana* (Diptera: Cecidomyiidae). *Insects* 13, 339. doi:10.3390/insects13040339
- Hutflitz, C. (2022). Endocrine regulation of lifespan in insect diapause. *Front. Physiol.* 13, 825057. doi:10.3389/fphys.2022.825057
- Ikeno, T., Tanaka, S. I., Numata, H., and Goto, S. G. (2010). Photoperiodic diapause under the control of circadian clock genes in an insect. *BMC Biol.* 8, 116. doi:10.1186/1741-7007-8-116
- Ishigami, I., Sierra, R. G., Su, Z., Peck, A., Wang, C., Poitevin, F., et al. (2023). Structural insights into functional properties of the oxidized form of cytochrome c oxidase. *Nat. Commun.* 14, 5752. doi:10.1038/s41467-023-41533-x
- Ishii, S., Iizuka, K., Miller, B. C., and Uyeda, K. (2004). Carbohydrate response element binding protein directly promotes lipogenic enzyme gene transcription. *PNAS* 101, 15597–15602. doi:10.1073/pnas.0405238101
- Jaiswal, A. N., and Vagga, A. (2022). Cryopreservation: A review article. *Cureus.* doi:10.7759/cureus.31564
- Jiang, T., Chen, Y., Tan, Z., Li, J., Qian, P., Tang, S., et al. (2019). Expression analysis and functional identification of several genes related to diapause in *Bombyx mori*. *Dev. Growth Differ.* 61, 150–157. doi:10.1111/dgd.12589
- Jiang, X. F., Huang, S. H., Luo, L. Z., Liu, Y., and Zhang, L. (2010). Diapause termination, post-diapause development and reproduction in the beet webworm, *Loxostege sticticalis* (Lepidoptera: Pyralidae). *J. Insect Physiol.* 56, 1325–1331. doi:10.1016/j.jinsphys.2010.04.016
- Joannis, D. R., and Storey, K. B. (1995). Temperature acclimation and seasonal responses by enzymes in cold-hardy gall insects. *Arch. Insect Biochem. Physiol.* 28, 339–349. doi:10.1002/arch.940280404

- Jovanović-Galović, A., Blagojević, D. P., Grubor-Lajšić, G., Worland, M. R., and Spasić, M. B. (2007). Antioxidant defense in mitochondria during diapause and postdiapause development of European corn borer (*Ostrinia nubilalis*, Hubn.). *Arch. Insect Biochem. Physiol.* 64, 111–119. doi:10.1002/arch.20160
- Kageyama, T., and Ohnishi, E. (1971). Carbohydrate metabolism in the eggs of the silkworm, *bombyx mori*. I. absence of phosphofructokinase in the diapausing egg. *Dev. Growth Differ.* 13, 97–106. doi:10.1111/j.1440-169X.1971.00097.x
- Kai, H., and Nishi, K. (1976). Diapause development in *Bombyx* eggs in relation to 'esterase A' activity. *J. Insect Physiol.* 22, 1315–1320. doi:10.1016/0022-1910(76)90152-9
- Kamita, S. G., and Hammock, B. D. (2010). Juvenile hormone esterase: biochemistry and structure. *J. Pestic. Sci.* 35, 265–274. doi:10.1584/jpestics.R10-09
- Kamiyama, T., and Niwa, R. (2022). Transcriptional regulators of ecdysteroid biosynthetic enzymes and their roles in insect development. *Front. Physiol.* 13, 823418. doi:10.3389/fphys.2022.823418
- Kang, D. S., Denlinger, D. L., and Sim, C. (2014). Suppression of allatotropin simulates reproductive diapause in the mosquito *Culex pipiens*. *J. Insect Physiol.* 64, 48–53. doi:10.1016/j.jinsphys.2014.03.005
- Kantor, P. F., Lopaschuk, G. D., and Opie, L. H. (2001). "Myocardial energy metabolism," in *Heart physiology and pathophysiology* (Amsterdam, Netherlands: Elsevier), 543–569. doi:10.1016/B978-012656975-9/50034-1
- Karp, X. (2021). Hormonal regulation of diapause and development in nematodes, insects, and fishes. *Front. Ecol. Evol.* 9. doi:10.3389/fevo.2021.735924
- Karpova, E. K., Adonyeva, N. V., Faddeeva, N. V., Romanova, I. V., Gruntenko, N. E., and Rauschenbach, I. Y. (2013). Insulin affects reproduction and juvenile hormone metabolism under normal and stressful conditions in *Drosophila* females. *Dokl. Biochem. Biophys.* 452, 264–266. doi:10.1134/S1607672913050153
- Kauffman, M. R., and DiAngelo, J. R. (2024). Glut1 functions in insulin-producing neurons to regulate lipid and carbohydrate storage in *Drosophila*. *Biomolecules* 14, 1037. doi:10.3390/biom14081037
- Kaur Gill, H., Goyal, G., and Chahil, G. (2017). Insect diapause: a review. *J. Agric. Sci. Technol.* A 7. doi:10.17265/2161-6256/2017.07.002
- Kawabe, Y., Waterson, H., and Mizoguchi, A. (2019). Bombyxin (*Bombyx* insulin-like peptide) increases the respiration rate through facilitation of carbohydrate catabolism in *Bombyx mori*. *Front. Endocrinol. (Lausanne)* 10, 150. doi:10.3389/fendo.2019.00150
- Kerbler, S. M., Armijos-Jaramillo, V., Lunn, J. E., and Vicente, R. (2023). The trehalose 6-phosphate phosphatase family in plants. *Physiol. Plant* 175, e14096. doi:10.1111/pp.14096
- Khanmohamadi, F., Khajehali, J., and Izadi, H. (2016). Diapause and cold hardiness of the almond wasp, *Eurytoma amygdali* (Hymenoptera: eurytomidae), two independent phenomena. *J. Econ. Entomol.* 109, 1646–1650. doi:10.1093/jeet/tow150
- Khurshid, A., Inayat, R., Tamkeen, A., Ul Haq, I., Li, C., Boamah, S., et al. (2021). Antioxidant enzymes and heat-shock protein genes of green peach aphid (*Myzus persicae*) under short-time heat stress. *Front. Physiol.* 12, 805509. doi:10.3389/fphys.2021.805509
- Kim, M., Lee, S., Chun, Y. S., Na, J., Kwon, H., Kim, W., et al. (2017). Heat tolerance induction of the Indian meal moth (Lepidoptera: Pyralidae) is accompanied by upregulation of heat shock proteins and polyols. *Environ. Entomol.* 46, 1005–1011. doi:10.1093/ee/nvx112
- Kimura, M. T., Awasaki, T., Ohtsu, T., and Shimada, K. (1992). Seasonal changes in glycogen and trehalose content in relation to winter survival of four temperate species of *Drosophila*. *J. Insect Physiol.* 38, 871–875. doi:10.1016/0022-1910(92)90098-X
- King, A. M., and MacRae, T. H. (2015). Insect heat shock proteins during stress and diapause. *Annu. Rev. Entomol.* 60, 59–75. doi:10.1146/annurev-ento-011613-162107
- Kirsch, J. F., Eichele, G., Ford, G. C., Vincent, M. G., Jansonius, J. N., Gehring, H., et al. (1984). Mechanism of action of aspartate aminotransferase proposed on the basis of its spatial structure. *J. Mol. Biol.* 174, 497–525. doi:10.1016/0022-2836(84)90333-4
- Košťál, V. (2006). Eco-physiological phases of insect diapause. *J. Insect Physiol.* 52, 113–127. doi:10.1016/j.jinsphys.2005.09.008
- Košťál, V., Stetina, T., Poupardin, R., Korbelová, J., and A. W. B. (2017). Conceptual framework of the eco-physiological phases of insect diapause development justified by transcriptomic profiling. *PNAS* 114, 8532–8537. doi:10.1073/pnas.1707281114
- Košťál, V., Tamura, M., Tollarová, M., and Zahradníčková, H. (2004). Enzymatic capacity for accumulation of polyol cryoprotectants changes during diapause development in the adult red firebug, *Pyrrhocoris apterus*. *Physiol. Entomol.* 29, 344–355. doi:10.1111/j.0307-6962.2004.00396.x
- Koubová, J., Jehlík, T., Kodrik, D., Šabová, M., Šima, P., Sehadová, H., et al. (2019). Telomerase activity is upregulated in the fat bodies of pre-diapause bumblebee queens (*Bombus terrestris*). *Insect Biochem. Mol. Biol.* 115, 103241. doi:10.1016/j.ibmb.2019.103241
- Kubrak, O. I., Kučerová, L., Theopold, U., and Nüssel, D. R. (2014). The sleeping beauty: how reproductive diapause affects hormone signaling, metabolism, immune response and somatic maintenance in *Drosophila melanogaster*. *PLoS One* 9, e113051. doi:10.1371/journal.pone.0113051
- Kunieda, T., Fujiyuki, T., Kucharski, R., Foret, S., Ament, S. A., Toth, A. L., et al. (2006). Carbohydrate metabolism genes and pathways in insects: insights from the honey bee genome. *Insect Mol. Biol.* 15, 563–576. doi:10.1111/j.1365-2583.2006.00677.x
- Kurland, C. G., and Schneiderman, H. A. (1959). The respiratory enzymes of diapausing silkworm pupae: a new interpretation of carbon monoxide-insensitive respiration. *Biol. Bull.* 116, 136–161. doi:10.2307/1539163
- Lafont, R., Dauphin-Villemant, C., Warren, J. T., and Rees, H. (2012). "Ecdysteroid chemistry and biochemistry," in *Insect endocrinology* (Amsterdam, Netherlands: Elsevier), 106–176. doi:10.1016/B978-0-12-384749-2.10004-4
- Lebenzon, J. E., Denezis, P. W., Mohammad, L., Mathers, K. E., Turnbull, K. F., Staples, J. F., et al. (2022). Reversible mitophagy drives metabolic suppression in diapausing beetles. *PNAS* 119, e2201089119. doi:10.1073/pnas.2201089119
- Lee, K.-Y., Valaitis, A. P., and Denlinger, D. L. (1997). Further evidence that diapause in the gypsy moth, *Lymantria dispar*, is regulated by ecdysteroids: a comparison of diapause and nondiapause strains. *J. Insect Physiol.* 43, 897–903. doi:10.1016/S0022-1910(97)00054-1
- Lehmann, P., Pruischer, P., Posledovich, D., Carlsson, M., Kälälä, R., Tang, P., et al. (2016). Energy and lipid metabolism during direct and diapause development in a pierid butterfly. *J. Exp. Biol.* 219, 3049–3060. doi:10.1242/jeb.142687
- Lehmann, P., Westberg, M., Tang, P., Lindström, L., and Kälälä, R. (2020a). The diapause lipidomes of three closely related beetle species reveal mechanisms for tolerating energetic and cold stress in high-latitude seasonal environments. *Front. Physiol.* 11, 576617. doi:10.3389/fphys.2020.576617
- Lehmann, P., Westberg, M., Tang, P., Lindström, L., and Kälälä, R. (2020b). The diapause lipidomes of three closely related beetle species reveal mechanisms for tolerating energetic and cold stress in high-latitude seasonal environments. *Front. Physiol.* 11, 576617. doi:10.3389/fphys.2020.576617
- Li, W., Huang, Z. Y., Liu, F., Li, Z., Yan, L., Zhang, S., et al. (2013). Molecular cloning and characterization of juvenile hormone acid methyltransferase in the honey bee, *Apis mellifera*, and its differential expression during caste differentiation. *PLoS One* 8, e68544. doi:10.1371/journal.pone.0068544
- Li, Y.-N., Ren, X.-B., Liu, Z.-C., Ye, B., Zhao, Z.-J., Fan, Q., et al. (2021). Insulin-like peptide and FoxO mediate the trehalose catabolism enhancement during the diapause termination period in the Chinese oak silkworm (*Antheraea pernyi*). *Insects* 12, 784. doi:10.3390/insects12090784
- Li, Y.-P., Goto, M., Ding, L., and Tsumuki, H. (2002). Diapause development and acclimation regulating enzymes associated with glycerol synthesis in the Shonai ecotype of the rice stem borer larva, *Chilo suppressalis* walker. *J. Insect Physiol.* 48, 303–310. doi:10.1016/S0022-1910(01)00177-9
- Li, Y.-Y., Chen, J.-J., Liu, M.-Y., He, W.-W., Reynolds, J. A., Wang, Y.-N., et al. (2022). Enhanced degradation of juvenile hormone promotes reproductive diapause in the predatory ladybeetle *Coccinella septempunctata*. *Front. Physiol.* 13, 877153. doi:10.3389/fphys.2022.877153
- Lin, Y., and Gerson, S. L. (2014). "Clinical trials using IV-P140K-mgmt for gliomas," in *Gene therapy of cancer* (Amsterdam, Netherlands: Elsevier), 379–391. doi:10.1016/B978-0-12-394295-1.00026-3
- Liu, G., Cai, S., Hou, J., Zhao, D., Han, J., Zhou, J., et al. (2016). Enoyl-CoA hydratase mediates polyhydroxyalkanoate mobilization in *Haloflex mediterranei*. *Sci. Rep.* 6, 24015. doi:10.1038/srep24015
- Liu, Y., Li, T., Yang, C., and Deng, H. (2024). "Bacterial energy metabolism," in *Molecular medical microbiology* (Amsterdam, Netherlands: Elsevier), 177–200. doi:10.1016/B978-0-12-818619-0.00155-6
- Livanova, N. B., Chebotareva, N. A., Eronina, T. B., and Kurganov, B. I. (2002). Pyridoxal 5'-phosphate as a catalytic and conformational cofactor of muscle glycogen phosphorylase B. *Biochem. Mosc.* 67, 1089–1098. doi:10.1023/A:1020978825802
- Lonard, D. M., Bhaskaran, G., and Dahm, K. H. (1996). Control of prothoracic gland activity by juvenile hormone in fourth instar *Manduca sexta* larvae. *J. Insect Physiol.* 42, 205–213. doi:10.1016/0022-1910(95)00095-X
- Lu, Y.-X., and Xu, W.-H. (2010). Proteomic and phosphoproteomic analysis at diapause initiation in the cotton bollworm, *Helicoverpa armigera*. *J. Proteome Res.* 9, 5053–5064. doi:10.1021/pr100356t
- Ma, H.-Y., Li, Y.-Y., Li, L., Tan, Y., and Pang, B.-P. (2021a). Regulation of juvenile hormone on summer diapause of *Galeruca daurica* and its pathway analysis. *Insects* 12, 237. doi:10.3390/insects12030237
- Ma, H.-Y., Li, Y.-Y., Li, L., Tan, Y., and Pang, B.-P. (2021b). Juvenile hormone regulates the reproductive diapause through Methoprene-tolerant gene in *Galeruca daurica*. *Insect* 30 (4), 446–458. doi:10.1111/imb.12710
- MacRae, T. H. (2010). Gene expression, metabolic regulation and stress tolerance during diapause. *Cell Mol. Life Sci.* 67, 2405–2424. doi:10.1007/s00018-010-0311-0
- Mane, S. D., and Chippendale, G. M. (1981). Hydrolysis of juvenile hormone in diapausing and non-diapausing larvae of the southwestern corn borer, *Diatraea grandiosella*. *J. Comp. Physiol. B* 144, 205–214. doi:10.1007/BF00802759
- Martins da Silva, R., de Oliveira Daumas Filho, C. R., Calixto, C., Nascimento da Silva, J., Lopes, C., da Silva, V., Jr, I., et al. (2023). PEPCK and glucose metabolism homeostasis in arthropods. *Insect Biochem. Mol. Biol.* 160, 103986. doi:10.1016/j.ibmb.2023.103986

- McLeod, D. G. R., and Beck, S. D. (2007). Photoperiodic termination of diapause in an insect. *Biol. Bull.* 124, 84–96. doi:10.2307/1539570
- Méndez-Lucas, A., Hyrššová, P., Novellademunt, L., Viñals, F., and Perales, J. C. (2014). Mitochondrial phosphoenolpyruvate carboxykinase (PEPCK-M) is a pro-survival, endoplasmic reticulum (ER) stress response gene involved in tumor cell adaptation to nutrient availability. *J. Biol. Chem.* 289, 22090–22102. doi:10.1074/jbc.M114.566927
- Meuti, M. E., Fyfe, L. R., Fiorta, M., and Denlinger, D. L. (2024). Trade-offs between winter survival and reproduction in female insects. *Integr. Comp. Biol.* 64, 1667–1678. doi:10.1093/icb/icae027
- Mizoguchi, A., Kamimura, M., Kiuchi, M., and Kataoka, H. (2015). Positive feedback regulation of prothoracicotropic hormone secretion by ecdysteroid – a mechanism that determines the timing of metamorphosis. *Insect Biochem. Mol. Biol.* 58, 39–45. doi:10.1016/j.ibmb.2015.01.001
- Mizoguchi, A., Ohsumi, S., Kobayashi, K., Okamoto, N., Yamada, N., Tateishi, K., et al. (2013). Prothoracicotropic hormone acts as a neuroendocrine switch between pupal diapause and adult development. *PLoS One* 8, e60824. doi:10.1371/journal.pone.0060824
- Mohammadzadeh, M., Borzoui, E., and Izadi, H. (2017). Physiological and biochemical differences in diapausing and nondiapausing larvae of eurytoma plotnikovi (hymenoptera: eurytomidae). *Environ. Entomol.* 46, 1424–1431. doi:10.1093/ee/nvx128
- Mohammadzadeh, M., and Izadi, H. (2016). Enzyme activity, cold hardiness, and supercooling point in developmental stages of *Acrosternum arabicum* (Hemiptera: pentatomidae). *J. Insect Sci.* 16, 64. doi:10.1093/jisesa/iew045
- Mohammadzadeh, M., and Izadi, H. (2018). Cold acclimation of *Trogoderma granarium* Everts is tightly linked to regulation of enzyme activity, energy content and ion concentration. *Front. Physiol.* 30. doi:10.1101/296467
- Moos, M., Korbelová, J., Štětina, T., Opekar, S., Šimek, P., Grgac, R., et al. (2022). Cryoprotective metabolites are sourced from both external diet and internal macromolecular reserves during metabolic reprogramming for freeze tolerance in drosophilid fly, *Chymomyza costata*. *Metabolites* 12, 163. doi:10.3390/metabo12020163
- Moreira, D. C., Paula, D. P., and Hermes-Lima, M. (2012). “Redox metabolism during tropical diapause in a Lepidoptera larva,” in *Living in a seasonal world* (Berlin, Heidelberg: Springer), 399–409. doi:10.1007/978-3-642-28678-0_35
- Moreira, D. C., Paula, D. P., and Hermes-Lima, M. (2021). Changes in metabolism and antioxidant systems during tropical diapause in the sunflower caterpillar *Chlosyne lacinia* (Lepidoptera: nymphalidae). *Insect Biochem. Mol. Biol.* 134, 103581. doi:10.1016/j.ibmb.2021.103581
- Nadeau, E. A. W., Lecheta, M. C., Obrycki, J. J., and Teets, N. M. (2022). Transcriptional regulation of reproductive diapause in the convergent lady beetle, *Hippodamia convergens*. *Insects* 13, 343. doi:10.3390/insects13040343
- Nardiello, M., Salvia, R., Scala, A., Scieuzo, C., Bufo, S. A., Franco, A., et al. (2019). Ecdysteroidogenesis in *Heliothis virescens* (Lepidoptera: noctuidae): recombinant prothoracicotropic hormone and brain extract show comparable effects. *J. Insect Sci.* 19, 23. doi:10.1093/jisesa/iez057
- Niwa, R., and Niwa, Y. S. (2014). Enzymes for ecdysteroid biosynthesis: their biological functions in insects and beyond. *Biosci. Biotechnol. Biochem.* 78, 1283–1292. doi:10.1080/09168451.2014.942250
- Noriega, F., Riberiro, J., Koener, J., Valenzuela, J., Hernandezmartines, S., Pham, V., et al. (2006). Comparative genomics of insect juvenile hormone biosynthesis. *Insect Biochem. Mol. Biol.* 36, 1–16. doi:10.1016/j.ibmb.2006.01.013
- Noriega, F. G. (2014). Juvenile hormone biosynthesis in insects: what is new, what do we know, and what questions remain. *Int. Sch. Res. Not.* 2014, 967361–967416. doi:10.1155/2014/967361
- Ogihara, M. H., Ikeda, H., Yamada, N., Hikiba, J., Nakaoka, T., Fujimoto, Y., et al. (2017). Identification of ecdysteroidogenic enzyme genes and their expression during pupal diapause in the cabbage armyworm, *Mamestra brassicae*. *Insect Mol. Biol.* 26, 286–297. doi:10.1111/imb.12291
- Pan, B.-Y., Liu, Y.-K., Wu, H.-K., Pang, X.-Q., Wang, S.-G., Tang, B., et al. (2020). Role of phosphoglucomutase in regulating trehalose metabolism in *Nilaparvata lugens*. *3 Biotech.* 10, 61. doi:10.1007/s13205-020-2053-5
- Pan, Y., Carroll, J. D., Asano, N., Pastuszak, I., Edavana, V. K., and Elbein, A. D. (2008). Trehalose synthase converts glycogen to trehalose. *FEBS J.* 275, 3408–3420. doi:10.1111/j.1742-4658.2008.06491.x
- Perez-Casal, J., and Potter, A. A. (2016). Glyceradehyde-3-phosphate dehydrogenase as a suitable vaccine candidate for protection against bacterial and parasitic diseases. *Vaccine* 34, 1012–1017. doi:10.1016/j.vaccine.2015.11.072
- Piumetti, M., and Illanes, A. (2022). “Enzymes and their function,” in *Molecular dynamics and complexity in catalysis and biocatalysis* (Cham, Switzerland: Springer International Publishing), 23–53. doi:10.1007/978-3-030-88500-7_2
- Poelchau, M. F., Reynolds, J. A., Elisk, C. G., Denlinger, D. L., and Armbruster, P. A. (2013). Deep sequencing reveals complex mechanisms of diapause preparation in the invasive mosquito, *Aedes albopictus*. *Proc. Biol. Sci. B* 280, 20130143. doi:10.1098/rspb.2013.0143
- Poitou, L., Bras, A., Pineau, P., Lorme, P., Roques, A., Rousselet, J., et al. (2020). Diapause regulation in newly invaded environments: termination timing allows matching novel climatic constraints in the box tree moth, *Cydalima perspectalis* (Lepidoptera: Crambidae). *Insects* 11 (9), 629. doi:10.3390/insects11090629
- Pruisscher, P., Lehmann, P., Nylin, S., Gotthard, K., and Wheat, C. W. (2022). Extensive transcriptomic profiling of pupal diapause in a butterfly reveals a dynamic phenotype. *Mol. Ecol.* 31, 1269–1280. doi:10.1111/mec.16304
- Ragland, G. J., Armbruster, P. A., and Meuti, M. E. (2019). Evolutionary and functional genetics of insect diapause: a call for greater integration. *Curr. Opin. Insect Sci.* 36, 74–81. doi:10.1016/j.cois.2019.08.003
- Rauschenbach, I. Y., Gruntenko, N. E., Chentsova, N. A., Adonyeva, N. V., and Alekseev, A. A. (2008). Role of ecdysone 20-monooxygenase in regulation of 20-hydroxyecdysone levels by juvenile hormone and biogenic amines in *Drosophila*. *J. Comp. Physiol. B* 178, 27–32. doi:10.1007/s00360-007-0196-x
- Rawlings, N. D., and Barrett, A. J. (1994). Families of serine peptidases. *Methods Enzymol.* 244, 19–61. doi:10.1016/0076-6879(94)44004-2
- Reitman, Z. J., and Yan, H. (2010). Isocitrate dehydrogenase 1 and 2 mutations in cancer: alterations at a crossroads of cellular metabolism. *JNCI* 102, 932–941. doi:10.1093/jnci/djq187
- Renfree, M. B., and Shaw, G. (2000). Diapause. *Annu. Rev. Entomol.* 62, 353–375. doi:10.1146/annurev.physiol.62.1.353
- Reynolds, J. A., and Hand, S. C. (2009). Embryonic diapause highlighted by differential expression of mRNAs for ecdysteroidogenesis, transcription and lipid sparing in the cricket *Allonemobius socius*. *J. Exp. Biol.* 212, 2075–2084. doi:10.1242/jeb.027367
- Richard, M. W. (2017). Insecticide resistance and intracellular proteases. *Pest Manag. Sci.* 73, 2403–2412. doi:10.1002/ps.4646
- Rinehart, J. P., Cikra-Ireland, R. A., Flannagan, R. D., and Denlinger, D. L. (2001). Expression of ecdysone receptor is unaffected by pupal diapause in the flesh fly, *Sarcophaga crassipalpis*, while its dimerization partner, USP, is downregulated. *J. Insect Physiol.* 47, 915–921. doi:10.1016/S0022-1910(01)00064-6
- Rinehart, J. P., Li, A., Yocum, G. D., Robich, R. M., Hayward, S. A. L., and Denlinger, D. L. (2007). Up-regulation of heat shock proteins is essential for cold survival during insect diapause. *PNAS* 104, 11130–11137. doi:10.1073/pnas.0703538104
- Robbins, H. M., Van Stappen, G., Sorgeloos, P., Sung, Y. Y., MacRae, T. H., and Bossier, P. (2010). Diapause termination and development of encysted *Artemia* embryos: roles for nitric oxide and hydrogen peroxide. *J. Exp. Biol.* 213, 1464–1470. doi:10.1242/jeb.041772
- Roberts, K. T., and Williams, C. M. (2022). The impact of metabolic plasticity on winter energy use models. *J. Exp. Biol.* 225, jeb243422. doi:10.1242/jeb.243422
- Robich, R. M., and Denlinger, D. L. (2005). Diapause in the mosquito *Culex pipiens* evokes a metabolic switch from blood feeding to sugar gluttony. *PNAS* 102, 15912–15917. doi:10.1073/pnas.0507958102
- Rodas, G., Ventura, J. L., Cadefau, J. A., Cussó, R., and Parra, J. (2000). A short training programme for the rapid improvement of both aerobic and anaerobic metabolism. *Eur. J. Appl. Physiol.* 82, 480–486. doi:10.1007/s004210000223
- Roncalli, V., Cieslak, M. C., Castelfranco, A. M., Hopcroft, R. R., Hartline, D. K., and Lenz, P. H. (2021). Post-diapause transcriptomic restarts: insight from a high-latitude copepod. *BMC Genomics* 22, 409. doi:10.1186/s12864-021-07557-7
- Roncalli, V., Sommer, S. A., Cieslak, M. C., Clarke, C., Hopcroft, R. R., and Lenz, P. H. (2018). Physiological characterization of the emergence from diapause: a transcriptomics approach. *Sci. Rep.* 8, 12577. doi:10.1038/s41598-018-30873-0
- Sahoo, A., Dutta, A., Dandapat, J., and Samanta, L. (2018). Low H₂O₂ and enhanced oxidative resistance in the diapause-destined pupa of silkworm, *Antheraea mylitta* (Lepidoptera: saturniidae) suggest their possible involvement in dormancy and lifespan extension. *BMC Zool.* 3, 1. doi:10.1186/s40850-018-0027-4
- Saravanakumar, R., Ponnuel, K. M., and Qadri, S. M. H. (2008). Expression of metabolic enzyme genes and heat-shock protein genes during embryonic development in diapause and non-diapause egg of multivoltine silkworm *Bombyx mori*. *Biol. Bratisl.* 63, 737–744. doi:10.2478/s11756-008-0124-x
- Saunders, D. S. (2014). Insect photoperiodism: effects of temperature on the induction of insect diapause and diverse roles for the circadian system in the photoperiodic response. *Entomol. Sci.* 17, 25–40. doi:10.1111/ens.12059
- Schafellner, C., Eizaguirre, M., López, C., and Sehna, F. (2008). Juvenile hormone esterase activity in the pupating and diapausing larvae of *Sesamia nonagrioides*. *J. Insect Physiol.* 54, 916–921. doi:10.1016/j.jinsphys.2008.04.015
- Scieuzo, C., Nardiello, M., Salvia, R., Pezzi, M., Chicca, M., Leis, M., et al. (2018). Ecdysteroidogenesis and development in *Heliothis virescens* (Lepidoptera: noctuidae): focus on PTTH-stimulated pathways. *J. Insect Physiol.* 107, 57–67. doi:10.1016/j.jinsphys.2018.02.008
- Seo, Y., Kingsley, S., Walker, G., Mondoux, M. A., and Tissenbaum, H. A. (2018). Metabolic shift from glycogen to trehalose promotes lifespan and healthspan in *Caenorhabditis elegans*. *PNAS* 115, E2791–E2800. doi:10.1073/pnas.1714178115

- Shappirio, D. G. (1974). Comparative studies of oxidative enzyme systems in epidermis and fat body of diapausing and non-diapausing silkworms. *J. Insect Physiol.* 20, 291–300. doi:10.1016/0022-1910(74)90061-4
- Shay, J. W., and Wright, W. E. (2019). Telomeres and telomerase: three decades of progress. *Nat. Rev. Genet.* 20, 299–309. doi:10.1038/s41576-019-0099-1
- Sheehan, D., Meade, G., Foley, V. M., and Dowd, C. A. (2001). Structure, function and evolution of glutathione transferases: implications for classification of non-mammalian members of an ancient enzyme superfamily. *Biochem. J.* 360, 1–16. doi:10.1042/0264-6021:3600001
- Sheng, Z., Ma, L., Cao, M., Jiang, R., and Li, S. (2008). Juvenile hormone acid methyl transferase is a key regulatory enzyme for juvenile hormone synthesis in the Eri silkworm, *Samia cynthia ricini*. *Arch. Insect Biochem. Physiol.* 69, 143–154. doi:10.1002/arch.20268
- Sheng, Z., Ma, L., Cao, M.-X., Li, S., and Jiang, R.-J. (2007). Biochemical and molecular characterization of allatotropin and allatostatin from the Eri silkworm, *Samia cynthia ricini*. *Samia cynthia Ricini. Insect Biochem. Mol. Biol.* 37, 90–96. doi:10.1016/j.ibmb.2006.09.007
- Shimokawa, K., Numata, H., and Shiga, S. (2008). Neurons important for the photoperiodic control of diapause in the bean bug, *Riptortus pedestris*. *J. Comp. Physiol. A Neuroethol. Sens. Neural Behav. Physiol.* 194, 751–762. doi:10.1007/s00359-008-0346-y
- Shinoda, T., and Itoyama, K. (2003). Juvenile hormone acid methyltransferase: a key regulatory enzyme for insect metamorphosis. *PNAS* 100, 11986–11991. doi:10.1073/pnas.2134232100
- Short, C. A., and Hahn, D. A. (2023). Fat enough for the winter? Does nutritional status affect diapause? *J. Insect Physiol.* 145, 104488. doi:10.1016/j.jinsphys.2023.104488
- Silljé, H. H. W., Paalman, J. W. G., ter Schure, E. G., Olsthoorn, S. Q. B., Verkleij, A. J., Boonstra, J., et al. (1999). Function of trehalose and glycogen in cell cycle progression and cell viability in *Saccharomyces cerevisiae*. *J. Bacteriol.* 181, 396–400. doi:10.1128/JB.181.2.396-400.1999
- Sim, C., and Denlinger, D. L. (2009). Transcription profiling and regulation of fat metabolism genes in diapausing adults of the mosquito *Culex pipiens*. *Physiol. Genomics* 39, 202–209. doi:10.1152/physiolgenomics.00095.2009
- Sim, C., and Denlinger, D. L. (2013). Insulin signaling and the regulation of insect diapause. *Front. Physiol.* 4, 189. doi:10.3389/fphys.2013.00189
- Sinclair, B. J. (2015). Linking energetics and overwintering in temperate insects. *J. Therm. Biol.* 54, 5–11. doi:10.1016/j.jtherbio.2014.07.007
- Singh, P., and Kumar, S. (2019). “Microbial enzyme in food biotechnology,” in *Enzymes in food biotechnology* (Amsterdam, Netherlands: Elsevier), 19–28. doi:10.1016/B978-0-12-813280-7.00002-5
- Sluss, T. P., Sluss, E. S., Crowder, L. A., and Watson, T. F. (1975). Isozymes of diapause and non-diapause pink bollworm larvae, *Pectinophora gossypiella*. *Insect biochem.* 5, 183–193. doi:10.1016/0020-1790(75)90080-3
- Smolinski, M. B., Green, S. R., and Storey, K. B. (2019). Glucose-6-phosphate dehydrogenase is posttranslationally regulated in the larvae of the freeze-tolerant gall fly, *Eurosta solidaginis*, in response to freezing. *Arch. Insect Biochem. Physiol.* 102, e21618. doi:10.1002/arch.21618
- Song, Z., Tang, L., Liu, Z., and Wu, D. (2023). Low GSK3 β activity is required for insect diapause through responding to ROS/AKT signaling and down-regulation of Smad1/ECR/HR3 cascade. *Insect Biochem. Mol. Biol.* 154, 103909. doi:10.1016/j.ibmb.2023.103909
- Sonobe, H., and Yamada, R. (2004). Ecdysteroids during early embryonic development in silkworm *Bombyx mori*: metabolism and functions. *Zool. Sci.* 21, 503–516. doi:10.2108/zsj.21.503
- Stancill, J. S., and Corbett, J. A. (2023). Hydrogen peroxide detoxification through the peroxiredoxin/thioredoxin antioxidant system: a look at the pancreatic β -cell oxidant defense. *Vitam. Horm.* 121, 45–66. doi:10.1016/bs.vh.2022.11.001
- Stanic, B., Jovanovic-Galovic, A., Blagojevic, D. P., Grubor-Lajsic, G., Worland, R., and Spasic, M. B. (2004). Cold hardness in *Ostrinia nubilalis* (Lepidoptera: Pyralidae): glycerol content, hexose monophosphate shunt activity, and antioxidative defense system. *Eur. J. Entomol.* 101, 459–466. doi:10.14411/eje.2004.065
- Storey, K. B., and Storey, J. M. (1991). Biochemistry of cryoprotectants. *Insects A. T. Low Temp.*, 64–93. doi:10.1007/978-1-4757-0190-6_4
- Süss, P., Dirksen, H., Roberts, K. T., Gotthard, K., Nässel, D. R., Wheat, C. W., et al. (2022). Time- and temperature-dependent dynamics of prothoracicotropic hormone and ecdysone sensitivity co-regulate pupal diapause in the green-veined white butterfly *Pieris napi*. *Insect Biochem. Mol. Biol.* 149, 103833. doi:10.1016/j.ibmb.2022.103833
- Suman, D. S., Wang, Y., and Gaugler, R. (2015). The Insect growth regulator pyriproxyfen terminates egg diapause in the Asian tiger mosquito, *Aedes albopictus*. *PLoS One* 10, e0130499. doi:10.1371/journal.pone.0130499
- Swigoňová, Z., Mohsen, A.-W., and Vockley, J. (2009). Acyl-CoA dehydrogenases: dynamic history of protein family evolution. *J. Mol. Evol.* 69, 176–193. doi:10.1007/s00239-009-9263-0
- Tan, Q.-Q., Liu, W., Zhu, F., Lei, C.-L., and Wang, X.-P. (2017). Fatty acid synthase 2 contributes to diapause preparation in a beetle by regulating lipid accumulation and stress tolerance genes expression. *Sci. Rep.* 7, 40509. doi:10.1038/srep40509
- Terra, W. R., Barroso, I. G., Dias, R. O., and Ferreira, C. (2019). Molecular physiology of insect midgut. *Adv. Insect Phys.*, 117–163. doi:10.1016/bs.aiip.2019.01.004
- Thomas, D., Cherest, H., and Surdin-Kerjan, Y. (1991). Identification of the structural gene for glucose-6-phosphate dehydrogenase in yeast. Inactivation leads to a nutritional requirement for organic sulfur. *EMBO J.* 10, 547–553. doi:10.1002/j.1460-2075.1991.tb07981.x
- Tollarova, M. (2008). Seasonal activity-profiles of enzymes involved in cryoprotectant biosynthesis in *Pyrrhocoris apterus* (Heteroptera: pyrrhocoridae). *Eur. J. Entomol.* 105, 149–152. doi:10.14411/eje.2008.020
- Tougeron, K. (2019). Diapause research in insects: historical review and recent work perspectives. *Entomol. Exp. Appl.* 167, 27–36. doi:10.1111/eea.12753
- Tusun, A., Li, M., Liang, X., Yang, T., Yang, B., and Wang, G. (2017). Juvenile hormone epoxide hydrolase: a promising target for hemipteran pest management. *Sci. Rep.* 7, 789. doi:10.1038/s41598-017-00907-0
- Uzelac, I., Avramov, M., Čelić, T., Vukašinić, E., Gošić-Dono, S., Purać, J., et al. (2020). Effect of cold acclimation on selected metabolic enzymes during diapause in the European corn borer *Ostrinia nubilalis* (Hbn.). *Sci. Rep.* 10, 9085. doi:10.1038/s41598-020-65926-w
- van Dijk, M. J., de Wilde, J. R. A., Bartels, M., Kuo, K. H. M., Glenthøj, A., Rab, M. A. E., et al. (2023). Activation of pyruvate kinase as therapeutic option for rare hemolytic anemias: shedding new light on an old enzyme. *Blood Rev.* 61, 101103. doi:10.1016/j.blre.2023.101103
- Vesala, L., and Hoikkala, A. (2011). Effects of photoperiodically induced reproductive diapause and cold hardening on the cold tolerance of *Drosophila montana*. *J. Insect Physiol.* 57, 46–51. doi:10.1016/j.jinsphys.2010.09.007
- Vesala, L., Salminen, T. S., Kankare, M., and Hoikkala, A. (2012). Photoperiodic regulation of cold tolerance and expression levels of regucalcin gene in *Drosophila montana*. *J. Insect Physiol.* 58, 704–709. doi:10.1016/j.jinsphys.2012.02.004
- Wanders, R. J. A., Vreken, P., den Boer, M. E. J., Wijburg, F. A., Van Gennip, A. H., and IJlst, L. (1999). Disorders of mitochondrial fatty acyl-CoA beta-oxidation. *J. Inher. Metab. Dis.* 22, 442–487. doi:10.1023/A:1005504223140
- Wang, J., Zhang, R. R., Gao, Q. Q., Ma, M. Y., and Chen, H. (2016). Cold tolerance and silencing of three cold-tolerance genes of overwintering Chinese white pine larvae. *Sci. Rep.* 6, 1–17. doi:10.1038/srep34698
- Wang, S., Feng, Y., Lou, Y., Niu, J., Yin, C., Zhao, J., et al. (2023). 3-Hydroxy-3-methylglutaryl coenzyme A reductase genes from Glycine max regulate plant growth and isoprenoid biosynthesis. *Sci. Rep.* 13, 3902. doi:10.1038/s41598-023-30797-4
- Wang, T., Geng, S.-L., Guan, Y.-M., and Xu, W.-H. (2018). Deacetylation of metabolic enzymes by Sirt2 modulates pyruvate homeostasis to extend insect lifespan. *Aging* 10, 1053–1072. doi:10.18632/aging.101447
- Watson, R. D., Ackerman-Morris, S., Smith, W. A., Watson, C. J., and Bollenbacher, W. E. (1996). Involvement of microtubules in prothoracicotropic hormone-stimulated ecdysteroidogenesis by insect (*Manduca sexta*) prothoracic glands. *J. Exp. Zool.* 276, 63–69. doi:10.1002/(SICI)1097-010X(19960901)276:1<63::AID-JEZ7>3.0.CO;2-3
- Watson, R. D., Agui, N., Haire, M. E., and Bollenbacher, W. E. (1987). Juvenile hormone coordinates the regulation of the hemolymph ecdysteroid titer during pupal commitment in *Manduca sexta*. *Insect biochem.* 17, 955–959. doi:10.1016/0020-1790(87)90102-8
- Weber, G., Lea, M. A., Hird Convery, H. J., and Stamm, N. B. (1967). Regulation of gluconeogenesis and glycolysis: studies of mechanisms controlling enzyme activity. *Adv. Enzyme Regul.* 5, 257–300. doi:10.1016/0065-2571(67)90020-9
- Wegener, G., and Krause, U. (2002). Different modes of activating phosphofructokinase, a key regulatory enzyme of glycolysis, in working vertebrate muscle. *Biochem. Soc. Trans.* 30, 264–270. doi:10.1042/BST0300264
- Weger, A. A., and Rittschof, C. C. (2024). The diverse roles of insulin signaling in insect behavior. *Front. Insect Sci.* 4, 1360320. doi:10.3389/finsc.2024.1360320
- Wolschin, F., and Gadau, J. (2009). Deciphering proteomic signatures of early diapause in *Nasonia*. *PLoS One* 4, e6394. doi:10.1371/journal.pone.0006394
- Wu, Q., and Brown, M. R. (2006). Signaling and function of insulin-like peptides in insects. *Annu. Rev. Entomol.* 51, 1–24. doi:10.1146/annurev.ento.51.110104.151011
- Xiang, M., Zhang, H.-Z., Jing, X.-Y., Wang, M.-Q., Mao, J.-J., Li, Y.-Y., et al. (2021). Sequencing, expression, and functional analyses of four genes related to fatty acid biosynthesis during the diapause process in the female ladybird, *Coccinella septempunctata* L. *Front. Physiol.* 12, 706032. doi:10.3389/fphys.2021.706032
- Xu, R., Chen, Y.-H., Xia, J.-F., Zeng, T.-X., Li, Y.-H., and Zhu, J.-Y. (2021). Metabolic dynamics across prolonged diapause development in larvae of the sawfly, *Cephalcia chuxiongica* (Hymenoptera: pampiliidae). *J. Asia Pac. Entomol.* 24, 1–6. doi:10.1016/j.aspen.2021.04.015
- Yamada, N., Okamoto, N., Kataoka, H., and Mizoguchi, A. (2016). Endocrine mechanisms regulating post-diapause development in the cabbage armyworm, *Mamestra brassicae*. *PLoS One* 11, e0146619. doi:10.1371/journal.pone.0146619

- Yamada, R., and Sonobe, H. (2003). Purification, kinetic characterization, and molecular cloning of a novel enzyme ecdysteroid-phosphate phosphatase. *J. Biol. Chem.* 278, 26365–26373. doi:10.1074/jbc.M304158200
- Yamashita, O. (1996). Diapause hormone of the silkworm, *Bombyx mori*: structure, gene expression and function. *J. Insect Physiol.* 42, 669–679. doi:10.1016/0022-1910(96)00003-0
- Yang, G., Sun, S., He, J., Wang, Y., Ren, T., He, H., et al. (2023). Enoyl-CoA hydratase/3-hydroxyacyl CoA dehydrogenase is essential for the production of DHA in zebrafish. *J. Lipid Res.* 64, 100326. doi:10.1016/j.jlr.2022.100326
- Yang, J., Kalhan, S. C., and Hanson, R. W. (2009a). What is the metabolic role of phosphoenolpyruvate carboxykinase? *J. Biol. Chem.* 284, 27025–27029. doi:10.1074/jbc.R109.040543
- Yang, R.-Z., Park, S., Reagan, W. J., Goldstein, R., Zhong, S., Lawton, M., et al. (2009b). Alanine aminotransferase isoenzymes: molecular cloning and quantitative analysis of tissue expression in rats and serum elevation in liver toxicity. *Hepatology* 49, 598–607. doi:10.1002/hep.22657
- Yocum, G. D., Rinehart, J. P., and Larson, M. L. (2009). Down-regulation of gene expression between the diapause initiation and maintenance phases of the Colorado potato beetle, *Leptinotarsa decemlineata* (Coleoptera: chrysomelidae). *Eur. J. Entomol.* 106, 471–476. doi:10.14411/eje.2009.059
- Zaobidna, E. A., Dmochowska, K., Frączek, R., Dymczyk, E., and Żółtowska, K. (2014). The proteolytic activity of diapausing and newly hatched red mason bees (Osmia rufa: megachilidae). *J. Apic. Sci.* 58, 85–91. doi:10.2478/jas-2014-0008
- Zhai, Y., Zhang, Z., Gao, H., Chen, H., Sun, M., Zhang, W., et al. (2017). Hormone signaling regulates nymphal diapause in *Laodelphax striatellus* (Hemiptera: Delphacidae). *Sci. Rep.* 7, 13370. doi:10.1038/s41598-017-13879-y
- Zhang, C., Wei, D., Shi, G., Huang, X., Cheng, P., Liu, G., et al. (2019). Understanding the regulation of overwintering diapause molecular mechanisms in *Culex pipiens pallens* through comparative proteomics. *Sci. Rep.* 9, 6485. doi:10.1038/s41598-019-42961-w
- Zhang, H. Z., Wang, M. Q., Xie, Y. Q., Xiang, M., Li, P., Li, Y. Y., et al. (2020). Gene cloning and expression analysis of trehalose-6-phosphate synthase, glycogen synthase and glycogen phosphorylase reveal the glycometabolism in the diapause process of *Aphidius gifuensis*. *J. Asia Pac. Entomol.* 23, 641–645. doi:10.1016/j.aspen.2020.05.007
- Zhang, J., Qi, L., Chen, B., Li, H., Hu, L., Wang, Q., et al. (2023). Trehalose-6-phosphate synthase contributes to rapid cold hardening in the invasive insect *Lissorhoptrus oryzophilus* (Coleoptera: Curculionidae) by regulating trehalose metabolism. *Insects* 14, 903. doi:10.3390/insects14120903
- Zhang, Q., Nachman, R. J., and Denlinger, D. L. (2015). Diapause hormone in the Helicoverpa/Heliothis complex: a review of gene expression, peptide structure and activity, analog and antagonist development, and the receptor. *Pept. (N.Y.)* 72, 196–201. doi:10.1016/j.peptides.2015.05.005
- Zhang, Q., Nachman, R. J., Kaczmarek, K., Zabrocki, J., and Denlinger, D. L. (2011). Disruption of insect diapause using agonists and an antagonist of diapause hormone. *PNAS* 108, 16922–16926. doi:10.1073/pnas.1113863108
- Zhang, X., Li, S., and Liu, S. (2022). Juvenile hormone studies in *Drosophila melanogaster*. *Front. Physiol.* 12, 785320. doi:10.3389/fphys.2021.785320
- Zhao, L., Wang, W., Qiu, Y., and Torson, A. S. (2021). Physiological mechanisms of variable nutrient accumulation patterns between diapausing and non-diapausing fall webworm (Lepidoptera: arctiidae) pupae. *Environ. Entomol.* 50, 1158–1165. doi:10.1093/ee/nvab074
- Zhou, Z., Dou, W., Li, C., and Wang, J. (2022). CYP314A1-dependent 20-hydroxyecdysone biosynthesis is involved in regulating the development of pupal diapause and energy metabolism in the Chinese citrus fruit fly, *Bactrocera minax*. *Pest Manag. Sci.* 78, 3384–3393. doi:10.1002/ps.6966
- Zhu, J., Dong, Y.-C., Li, P., and Niu, C.-Y. (2016). The effect of silencing 20E biosynthesis relative genes by feeding bacterially expressed dsRNA on the larval development of Chilo suppressalis. *Sci. Rep.* 6, 28697. doi:10.1038/srep28697

Frontiers in Physiology

Understanding how an organism's components work together to maintain a healthy state

The second most-cited physiology journal, promoting a multidisciplinary approach to the physiology of living systems - from the subcellular and molecular domains to the intact organism and its interaction with the environment.

Discover the latest Research Topics

[See more →](#)

Frontiers

Avenue du Tribunal-Fédéral 34
1005 Lausanne, Switzerland
frontiersin.org

Contact us

+41 (0)21 510 17 00
frontiersin.org/about/contact

